UNIVERSITY
of
GLASGOW

Two-Dimensional Computational Fluid Dynamics Analysis of Wings In Ground Effect and Assessment on lift, drag and momentum coefficients resulting in a Three-Dimensional Turbulence model of efficiency and instability.

By
Elizabeth Ford
9504789

supervisor
Dr R.C McGREGOR

Vol. 1 of 2

POSTGRADUATE STUDIES (MSc)
Department of MECHANICAL ENGINEERING

DATE – JUNE 2001

To my parents George Ford and Elena Staromiraki who have taught and inspired me throughout my life. Thank you.

DECLARATION

Except where reference is made to others, this thesis presents the author's 'Elizabeth Ford' own work.

Abstract

The analysis of the following topic has been carried out using the following subdivisions, namely;

- **History of Wigs- involving the Database,**
- **The CFD analysis-involving the Gambit and Fluent 5 program, and**
- **The Experimental tests.**

Database: A database of WIG craft was comprised, this allowed statistical analysis of WIG characteristics to be carried out. With the use of specific attributes of previous WIG designs a new design could then be comprised.

CFD: Although difficult, it is vital to compare lift, drag and moment coefficients with both α (the angle of attack) as well as h/c (the height to chord ratio). For this reason, as well as the increase in WISE craft over the years it is believed of great importance to analyze these characteristics using numerical simulation techniques based on CFD programs. It is hoped to describe all forces exerted on wing profiles while analyzing all stages of take-off. The aim of this section was to analyze two different types of airfoil profiles using CFD. The NACA 0012 due to there being adequate information available on it, (it seemed logical to commence my CFD analysis on this profile) and the S-shaped profile, (which incorporates the Munk M6R2 over the upper portion and the CJ-5 over its lower portion). This was due to all new designs being based on this fairly new concept which has an increased effectiveness and has been proven to be of more use in surface effect vehicles. Details of the strategy behind the numerous input requirements of the Gambit program, such as the mesh generation process, the boundary conditions involved have been studied as well as the Fluent 5 program creation of solver input files and information on the running of solutions given prior to the solver outputs attained. Due to the involvement of five different angles of attack, namely 0,2,5,7.5 and 10 degrees varying with five different h/c values, namely 1.5,1,0.75,0.5 and 0.25, a positive or negative contribution to the aerodynamics involved around the airfoil could then be produced. Statistical analysis on the outcomes would then take place, resulting in effective results. Examples of the types of programs run are shown below, the LHS is NACA0012 over still water and the RHS for S-shaped over curved ground simulating waves. These are two cases from 150.

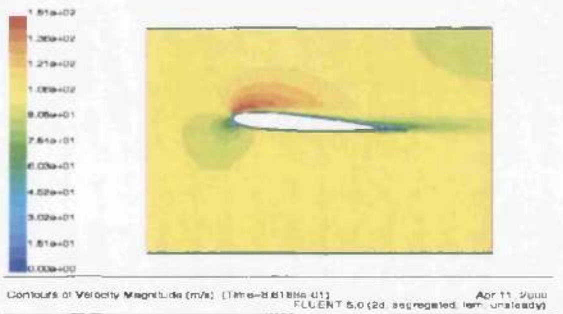

This thesis is intended to enlighten and persuade the readers requiring various types of information enticed to the W.I.S.E. field, to subsequently interrogate such enigmas in more detail and hence, aid in the development and construction of future W.I.S.E. designs.

CONTENTS PAGE

LIST OF FIGURES

Apologies for format alterations, computer error which could not be changed by the author.

LIST OF GRAPHS

6. series 2 is a=2 degrees angle of attack
7. series 3 is a=5 degrees angle of attack
8. series 4 is a=7.5 degrees angle of attack
9. series 5 is a=10 degrees angle of attack

111S1-5B[p.185] All Cm Values For S-shaped Aerofoil Over Curved Ground (Trough) where;

1.. series 1 is a=0 degrees angle of attack
2. series 2 is a=2 degrees angle of attack
3. series 3 is a=5 degrees angle of attack
4. series 4 is a=7.5 degrees angle of attack
5. series 5 is a=10 degrees angle of attack

112[p.186] All Cd Values of the Shaped Aerofoil at 0 degrees angle of Attack where;

1. series 1 is over ground
2. series 2 is over still water
3. series 3 is over peak
4. series 4 is over trough

1113[p.186] All Cd Values of the Shaped Aerofoil at 2 degrees angle of Attack where;

1. series 1 is over ground
2. series 2 is over still water
3. series 3 is over peak
4. series 4 is over trough

114[p.186] All Cd Values of the Shaped Aerofoil at 5 degrees angle of Attack where;

1. series 1 is over ground
2. series 2 is over still water
3. series 3 is over peak
4. series 4 is over trough

Due to human errors 115-116 do not exist.

117 [187] All Cl Values For 2 Degrees Angle of attack for S-shaped Aerofoil where;

1. series 1 is over ground
2. series 2 is over still water
3. series 3 is over peak
4. series 4 is over trough

LIST OF TABLES

ACKNOWLEDGEMENTS

I would like to thank my supervisor Dr. R. C. McGregor, from the Engineering Faculty at Glasgow University, for increasing my knowledge on the W.I.S.E. sector and pointing me in the right direction. I also thank my friends and family for showing their support and encouragement when it was most required.

This thesis is intended to increase the readers knowledge on the W.I.S.E. field, encouraging interrogation and ultimately aiding in the development and construction of future W.I.S.E. designs.

1.0 W.I.S.E TECHNICAL ADVANCES

1.1 GENERAL

In the process of this thesis, Wing-In-Surface Effect technical advances, analysis and design aspects (such as the constructional characteristics) are covered. The interactions relating these aspects of design are explored and interconnected through the structure of this thesis. The objective behind such investigations lies in their contribution towards determining the overall weight, the economic viability and, primarily, the performance of every craft.

WISE (Wing-In-Surface Effect) craft are high-speed vehicles, which are based on the advantageous aerodynamic phenomena present when in ground effect. This is especially the case, during their take-off procedure, which is made easier due to the great L/D (lift to drag ratio) present. The term 'Surface Effect' is adopted on account of its ability to describe all surfaces, whether ground or water.

In order for WISE craft to be introduced in the passenger-carrying field, the study of wing profiles is essential. This is mainly due to WISE craft being a unique concept, unlike present sea going transportation vehicles, which do not include the wing concept in their design characteristics.

Many methods have been used to study the aerodynamics of wings in ground effect such as the 'moving belt' technique, the 'boundary layer' method, the panel method and CFD simulation to name but a few. It has been incredibly difficult but highly important to compare the lift, drag and moment coefficients with both α (the angle of attack) as well as h/c (the height to chord ratio). For this reason it is imperative to analyse these characteristics using numerical simulation techniques based on CFD (Computational Fluid Dynamics) programmes.

A vast amount of research has already been carried out on the stability of WISE craft. It has been found that the centre of pressure, which is present on the underside of the wing, moves forward with reduction of the h/c ratio. This results in the nose of the craft moving upwards as the height between the wing and the surface decreases. This is why numerous WISE craft adopt a large tail plane concept resulting in an increase in stability. Unfortunately the tail planes do not increase the lift, but do however decrease the L/D ratio of the wings. This is a major disadvantage and is why Russia commenced study on the S shaped aerofoil. It was said that by giving the aerofoil an S shape at its ends its stability would increase.

Results on the S shaped aerofoil have been obtained through practical experience as well as by experiments involving the upper section of such wing profiles. It was believed that this project would provide numerical data on the subject by describing in detail the forces exerted on the wing profiles while analysing all stages of take-off.

The report will commence by contributing information on the history of WISE craft. This will then be followed by a database of all known W.I.S.E. craft, which was compiled during the study. Analysis of the database may be found in section 1.4 of the report. This was then followed with future conceptual designs in section 1.5. A discussion of these designs will ensue.

Inclusive family trees of multitudinous sea transportation vehicle types have been presented in Fig.5-7. This broad approach is to provide the reader with enough information to understand the reason for choosing the S-shaped aerofoil design as the skeleton for this project.

The comments made on the design of the S-shaped aerofoils exceptionally resourceful design (Section 4) are then reinforced with the use of a Computational Fluid Dynamics Program. The input file for FLUENT 5 was prepared on GAMBIT, a computer program that allowed efficient and effective construction of the models.[Ref.62 - 65 and Section4.3]

The aim of this project was to analyse two different types of aerofoil profiles using CFD analysis. The most basic shaped wing is known to be the NACA 0012. It seemed logical to commence CFD analysis on this profile due to there being adequate information available on it. The second was the S-shaped profile, which incorporates the Munk M6R2 over the upper portion and the CJ-5 over its lower portion. It was chosen due to all recent designs being based on this innovative concept. It has been proven to provide increased effectiveness in surface effect vehicles.

This thesis analyses a CFD problem involving wings in surface effect. The Computational Fluid Dynamics programme utilised is ; the GAMBIT and FLUENT 5 5 programmes.

A frequently used aerofoil section in wing-in-surface effect craft is the S-shaped aerofoil. Prior to commencing simulation of this aerofoil section over still water and then over uneven ground conditions, it was thought essential to verify the programme's capabilities by primarily modelling the NACA 0012 section over ground and then over still water. This was carried out in order to acquire solutions, which could be compared with existing results and hence validated.

The simulations of the NACA 0012 over still water were carried out in order to observe variations in lift, drag, momentum coefficients, turbulence, the effects of wave patterns at low altitudes of flight and the effects of low altitude flight on the water surface.

Following this introduction, which includes background information on aerofoil sections and describes the CFD Fluent programme, it goes on to analyse aerofoil sections studied during the analysis [Sections 2.10, 2.11, 2.19 and 2.20]. It gives details of the strategy behind the numerous input requirements of Gambit, such as the mesh generation process, the boundary conditions involved, the Fluent 5 programme creation of solver input files and information on the running of solutions given prior to the solver outputs being attained [Section 4].

Due to the involvement of five different angles of attack, namely 0, 2, 5, 7.5 and 10 degrees varying with five different h/c values, namely 1.5, 1, 0.75, 0.5 and 0.25, it was possible to show positive or negative contribution to the aerodynamics involved around the aerofoil [Section 5].

It may be that if more information, however vague and general, was available to the public that more people would be intrigued by W.I.S.E. craft and wish to study them in greater detail. Perhaps, even, construct a passenger liner for commercial use.

1.2 OBJECTIVES OF STUDY

The original concept of W.I.S.E. creation was for this class of craft to attain characteristic qualities not yet acquired by conventional air and sea craft[Section 2].

Although there are some ships capable of accomplishing relatively high speeds, there is still a requirement for them to travel at even higher speed and in a smoother and safer manner, resulting in greater efficiency as a means of transport.

Aircraft on the other hand do have the speed required but lack the ability to travel close to the sea surface. It is in this area that W.I.S.E. craft are fundamentally suited, permitting the gap in transport to be filled effectively [Fig.3 - 4].

Ultimately, if W.I.S.E. craft were to be sufficiently modified in the future, incorporating characteristic capabilities not adopted by other craft as yet, they would be greeted positively by all sectors including the military, passenger and cargo [Ref;8, 12, 15, 18, 26, 43, 44, 44, 46, 49, 51, 80,- 102, 127, 131, 156 - 182].

For reasons discussed further on in this thesis my interest was drawn to the outstanding design of the S-shaped aerofoil (which incorporates the Munk M6R2 over the upper portion and the CJ-5 over the lower portion). Although complicated due to its asymmetrical configuration, it was apparent that it would become very interesting to work on such a project and find as much information as possible involving wing designs. However, there is limited availability of specific data, due to the security and confidentiality of many national and military organisations.

Section 5 has further analysed the effects an S-shaped aerofoil would have on the efficiency of a WISE craft especially when flown at the advised altitudes and angles of attack. The results indicate that this design should, therefore, be taken into consideration for the future, since it would be capable of aiding the take-off, cruise and landing and stability procedures of all WISE craft.

A frequently used aerofoil section for wing-in-surface effect craft is the S-shaped aerofoil. Prior to commencing simulation of this aerofoil section it was deemed essential to verify the 'FLUENT' programme's capabilities by modelling the NACA 0012 section over ground and then over still water. This was carried out in order to acquire solutions, which were compared with existing results and then validated.

The simulations of the NACA 0012 over still water were carried out in order to observe variations in lift, drag, momentum coefficients, turbulence, the effects of wave patterns at low altitudes of flight and the effects of low altitudes of flight on the water surface.

As well as containing an introduction to the problem, this section of the thesis includes background information on aerofoils, describes the CFD FLUENT programme and analyses aerofoil sections studied during the analysis. It provides details of the strategy behind the numerous input requirements of the GAMBIT programme, such as the mesh generation process, the boundary conditions involved, the FLUENT 5 programme creation of solver input files and information on the running of solutions given prior to the solver outputs being attained.

Due to the involvement of five different angles of attack, namely 0, 2, 5, 7.5 and 10 degrees varying with five different h/c values, namely 1.5, 1, 0.75, 0.5 and 0.25 , it was possible to show positive or negative contribution to the aerodynamics involved around the aerofoil.

It is believed that if more information on this subject was available to the public, even if vague and general, that a greater number of people would in fact be intrigued by W.I.S.E. craft and wish to study them in greater detail, if not construct a passenger liner for commercial use.

What is Ground Effect?

As described above, ground effect increases lift. The air cushion is created by high pressure that builds up under the wing when the ground is approached. When the ground distance becomes very small the air can even stagnate under the wing, this gives the highest possible pressure, so called ram pressure.

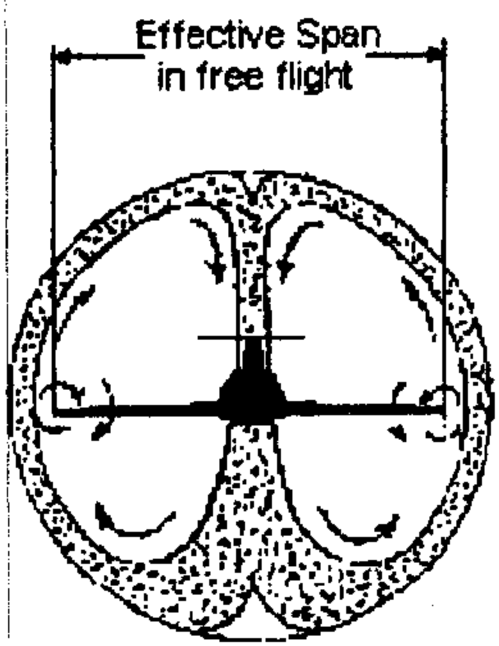

Fig. 1

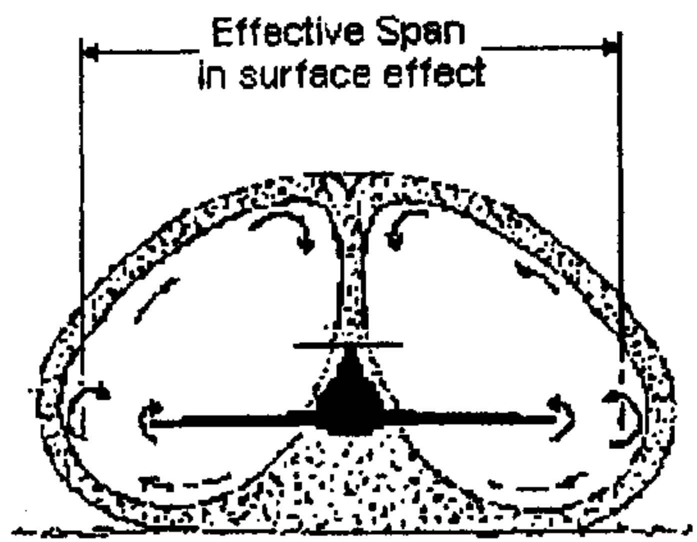

Fig. 2

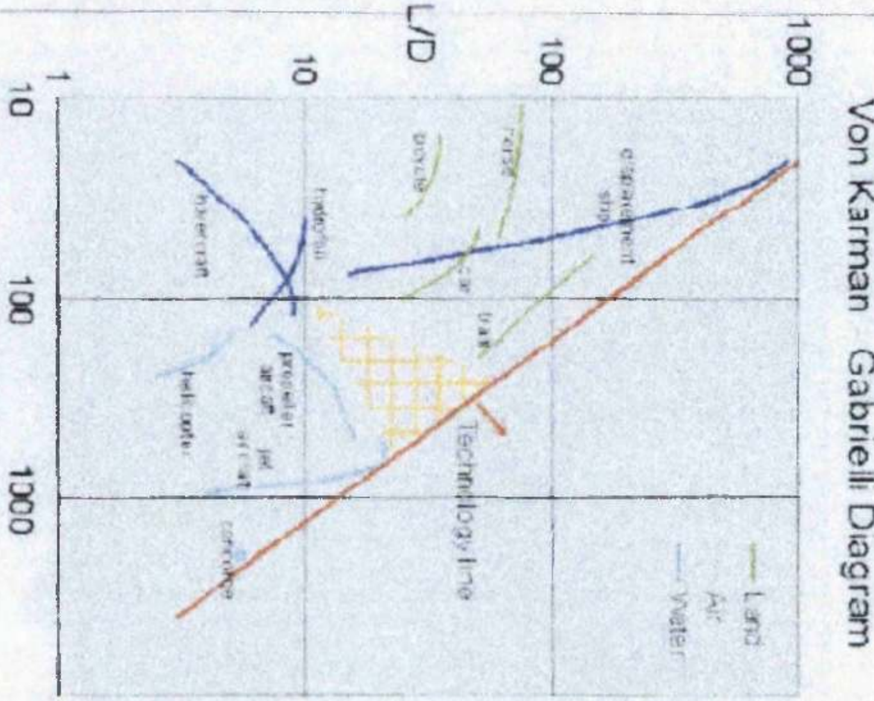

Von Karman Gabrielli Diagram
L/D
V [km/h]
Technology line
Land
Air
Water
1000
100
10
1
10
100
1000

Fig. 3

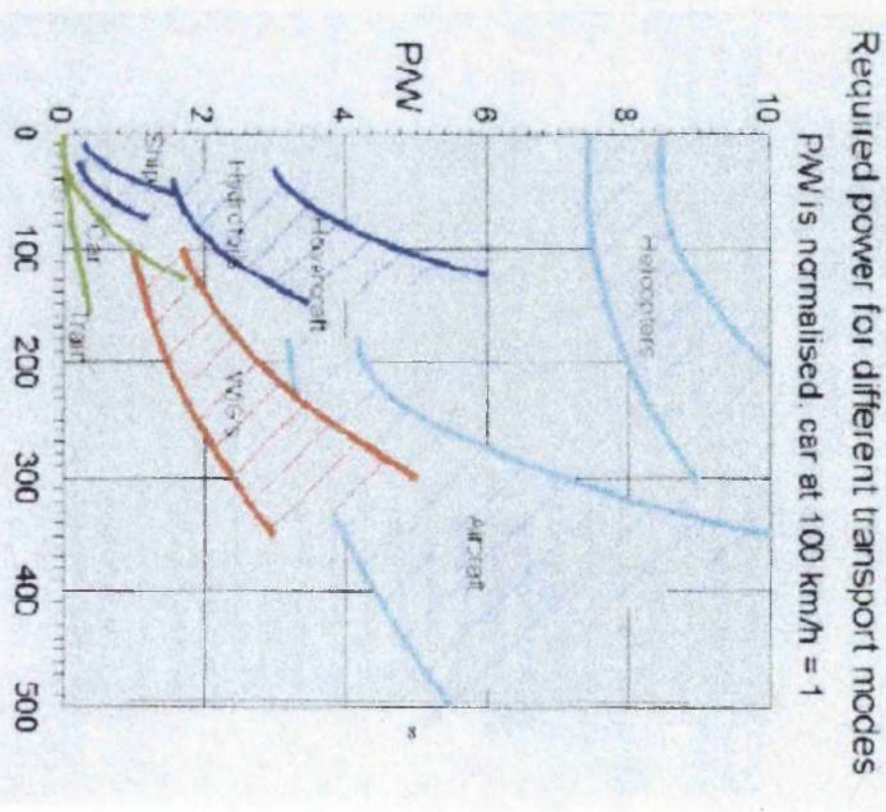

Required power for different transport modes
P/W is normalised, car at 100 km/h = 1
P/W
V [km/h]
Helicopters
Aircraft
Hovercraft
Hydrofoils
Ship
Car
Train
WIG's
0
100
200
300
400
500
2
4
6
8
10

Fig. 4

1.3 HISTORY OF W.I.S.E

"Those involved in design can never quite agree as to just where the design process begins. The designer thinks it starts with a new aeroplane concept. The sizing specialist knows that nothing can begin until an initial estimate of the weight is made. The customer, civilian or military, feel that the design begins with requirements. They are all correct."

(quotation by Daniel P.Raymer
From Aircraft Design: A Conceptual Approach p.3)

The fabrication of Wing-In-Surface Effect vehicles has undergone abundant investigation. In consideration of previously acquired knowledge, gathered from its historical background, it was noted, with some surprise that they are not accounted for in the transportation system (for example the Von Karmen transportation diagramme in Fig 3 - 4) as a means of transport. In addition to this, it may also be said that, their general characteristic configuration and technical requirements have not yet been fully established.

In the not too distant future, the use of W.I.S.E. vessels may be extensively broadened to accommodate transportation, sea rescue missions and air carriers, as well as sea launch vessels for space vehicles. Due to technological advances, which may be expected to take place, it could be assumed that transatlantic transportation could be made possible. However, for such applications of W.I.S.E. craft, they would require to be of a large size and weigh up to several thousands tons [Section 1.5 and Ref.42, 99, 185, 188].

Although these are futuristic conceptual advances, conclusions concerning current configuration and design may be made. For this reason it is imperative that the history of such craft is first discussed.

It is a well-known fact that every aircraft in existence undergoes a ground effect or cushioning phenomena of an air pressure build up. This is experienced, primarily, during both the take-off and landing stages.

Numerous experiments have been carried out using various design concepts of such craft all over the world. However, the majority of the work has been a specialisation of Germany, USA, Australia (who are using W.I.S.E. type vehicles as sea taxis of a limited capacity), China and Russia (where an extremely large amount of investigation was carried out) [Section 3.5].

The Russian design was named the Ekranoplan or nizkolet. (N.B. 'Ekran' is Russian for 'screen' or 'ground'.) This type of craft, however, is also known as an 'acopter' (Greek for "curved wing"), a power augmented ram-in-ground effect (PARWIG) a wing-ship and a ram-wing craft among many others.

The most famous Russian Ekranoplans are the "Caspian Sea Monsters". According to the internet "Russian Aviation Page" on the "Caspian Sea Monsters" :- "It is believed that Russia is far ahead of the West with air-cushion vehicle technology and with W.I.S.E. in particular".

Although, different countries commenced their studies of W.I.S.E. vehicles independent of each other in the 1960's, the actual concept of "Surface Effect" was adopted in the 1920's.

In the 1960's the designs of such craft varied tremendously and numerous concepts were theorised. The three countries which focused and advanced their theories during this period were the U.S.S.R, the U.S.A. and Japan.

The Alexeyev Central Hydrofoil Design Bureau undertook the implementation of a significant design. All their efforts in creating a high speed W.I.S.E. paid off when an incredibly large, 550 tonne, heavy lift military Ekranoplan was produced. It had the capability of flying over any smooth terrain.

They adopted a number of vector thrusting methods such as the use of Power Augmented Rams (P.A.R. W.I.G.'S) in order to achieve both a pressure circulation below the wings and an air cushion which aided in the take off and landing stages. The same engines are used during cruising flight and for lift. However, due to having to keep the nose down in order to stay in ground effect, difficulty was often encountered and stability lost, resulting in accidents where the Ekranoplan flipped over[Section 2.2]

This secret military extravaganza was uncloaked when an unknown vessel was detected by satellite on the Caspian Sea, giving such vehicles the name of "Caspian Sea Monster". These W.I.S.E.s have a reduced induced drag as long as they fly at an altitude similar to the chord line of the wings. Their stay in ground effect enhances their characteristics due to a reduction of fuel requirements, making them more economical to fly than a conventional aeroplane. The larger the distance it flies the more money on fuel may be saved. Hence, although the majority of W.I.S.E. craft are used for A.S.W. (Anti submarine warfare), rescue schemes, sealift, amphibious assault and coastal defence, they would be ideal passenger and cargo carrying vehicles in places such as:-

* The following places are quoted from the Internet "W.I.G. Page" on 'the efficiency of W.I.G. vehicles.

1.	Sheltered seas	Baltic, Mediterranean
2.	Large lakes	U.S.A. Russia
3.	Sheltered coastal areas	Australia
4.	Archipelagos	Japan, Philippines and Indonesia

It should be mentioned that the Lun was the ekranoplan which was given the nickname the "Caspian Sea Monster". In 1989 it was engaged in a search for the Komsomolets submarine, which had been involved in a disastrous nuclear accident.

The Alexeyev Central Hydrofoil Design Bureau was known for its tremendous efforts in designing such prototype craft. There were numerous constructions achieved of which ten became well known. One was the Orlyonok and the other was the Lun. These two designs were the most advanced in their time and were said to have been close to operational standards. Plans of the Orlyonok design may be found at the end of this section.

However, [Ref.34], the following section discusses the characteristic features of W.I.S.E. vehicles. It is believed that this information will enable the reader to gain qualitative information on all aspects of W.I.S.E. craft. It is therefore advised that the above reference should be referred to for further information, if required by the reader.

In addition to aerodynamic means of reducing the resistance and the load on the hull of the W.I.S.E. vehicle, hydrodynamic devices in the form of water skis are used. These are placed under the hull and act as a shock absorber. The possibility of using hydrofoils is being studied [Appendix A for Examples]

In evaluating the conditions of operation of a W.I.S.E. vehicle airframe with a complete set of take-off devices, one may note that the loads acting on the airframe of a W.I.S.E. vehicle are greater than the loads acting on the airframe of an aircraft. Thus, the weight of the hull of the W.I.S.E. craft is greater than the weight of corresponding designs of aircraft. An additional factor, which increases the weight of the hull, is the need to include corrosion protection under marine conditions.

The main method discussed in this paper, is the introduction of a compound wing configuration, which increases the dimensions of the W.I.S.E. craft. Estimates and studies show that for a flight weight on the order of 1000-1500 tonnes it is realistic to achieve a good aerodynamic quality. An even larger value is obtained in studies to improve the systems, which create an air stream under the wing during take-off. It is obvious that a system associated with the conversion of the kinetic energy of the engine stream into static pressure is, in principle, unsuitable in terms of energy. Thus, the search for new designs, which use special blowers and non-traditional designs of flexible enclosures should continue. At present the low economy and load ratio do not permit the W.I.S.E. craft to successfully compete with aeroplanes in solving the traditional transport problems. They will become promising when specific properties of W.I.S.E. craft, such as the amphibiousness, increased seaworthiness on take-off & the possibility of remaining afloat in the sea for a prolonged period, begin to play a decisive role. This makes it possible to see the W.I.S.E. craft as an effective component of rescue systems, as well as its use as a platform for equipment during oceanographic and geographic studies. Moreover, the difference between the technical and economic factors of the aeroplane and W.I.S.E. craft are reduced when one reduces the distance of the flight.

Analysing all marine transportation, it should be noted that a range of speeds from 0-60 knots is covered by displacement ships and ships with dynamic support principles. Today's W.I.S.E. craft reach speeds of 200 knots and above. The creation of new marine craft which use either the ground effect or hybrid support schemes to cover that practically important range of speeds is promising.

Due to their economical fuel consumption, these craft would be best suited for commercial use on long haul routes such as Europe / Australia / Japan or possibly even internal flights inside the U.S.S.R.

[Ref. 99] Even though ACV's and W.I.S.E.'s have had several conferences dedicated to them, they have several common qualities, which automatically distinguish them from other maritime transportation craft. Nevertheless, they all adopt a quality, which results in their advantageous characteristics with respect to hydrodynamic lift and aerodynamic drag. These qualities become significant at higher speeds.

Both Air Cushion vehicles and Wing-In-Ground Effect Craft fly in the 'air' side of the air-to-water boundary using the air cushion or the ground effect as a method of sustaining a specific height above the water surface, which produces aerodynamic lift.

Development would be required in four areas, namely: Structural materials, power plants, propulsion systems and Control vertical & in azimuth. These are discussed but not in detail in this paper.

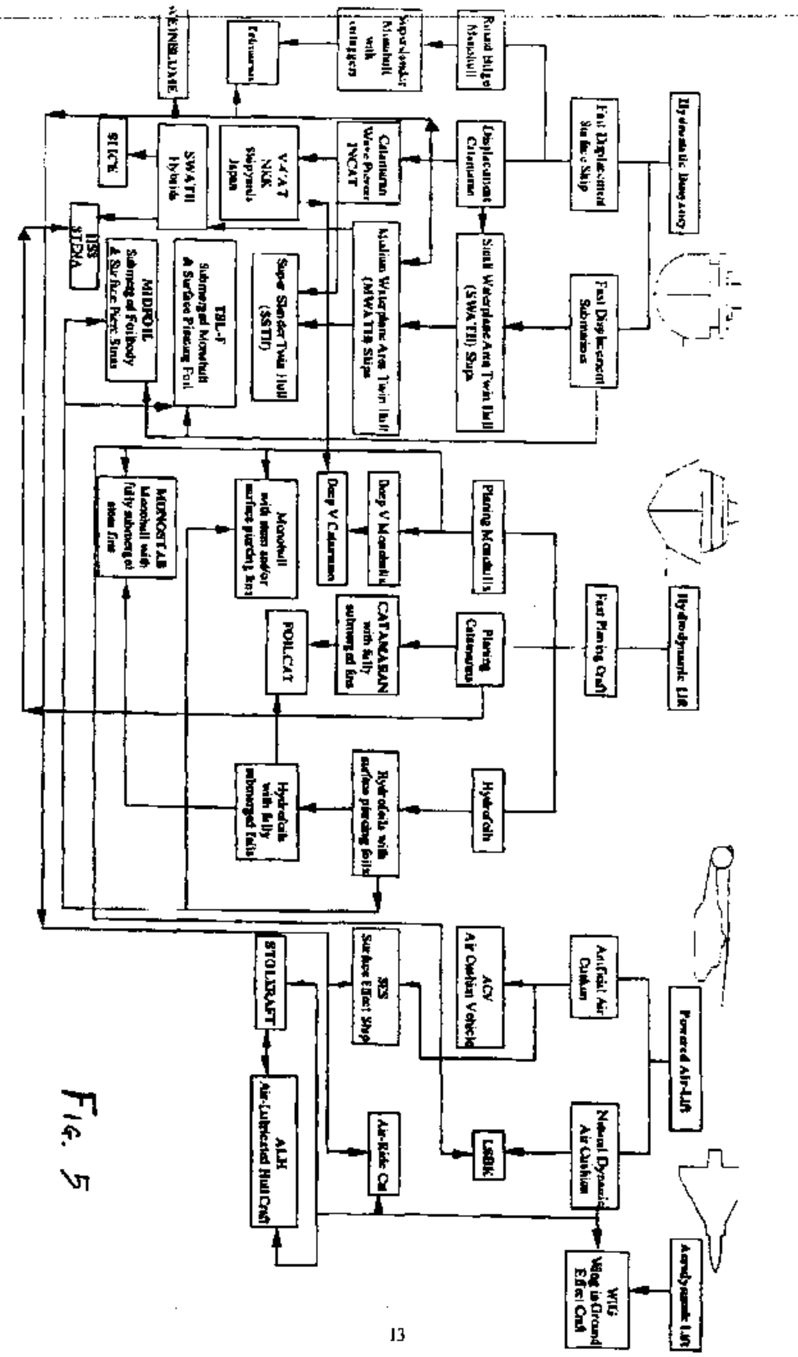

ADVANCED MARINE VEHICLES
Basic Types and Hybrids

Fig. 5

13

Fig. 6

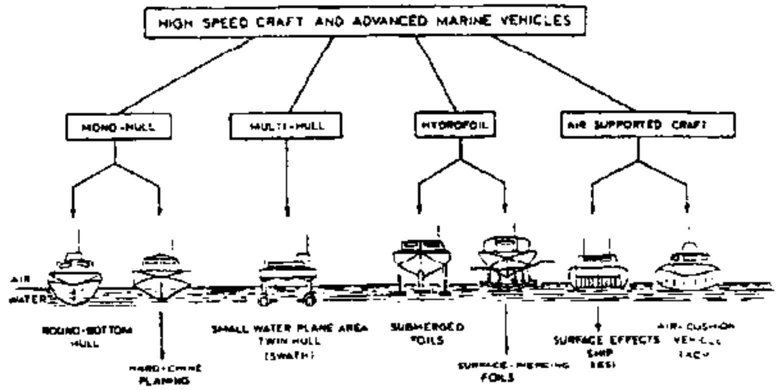
HIGH SPEED CRAFT AND ADVANCED MARINE VEHICLES
MONO-HULL
MULTI-HULL
HYDROFOIL
AIR SUPPORTED CRAFT
AIR
WATER
ROUND-BOTTOM HULL
HARD-CHINE PLANING
SMALL WATER PLANE AREA TWIN HULL (SWATH)
SUBMERGED FOILS
SURFACE-PIERCING FOILS
SURFACE EFFECTS SHIP (SES)
AIR-CUSHION VEHICLE (ACV)

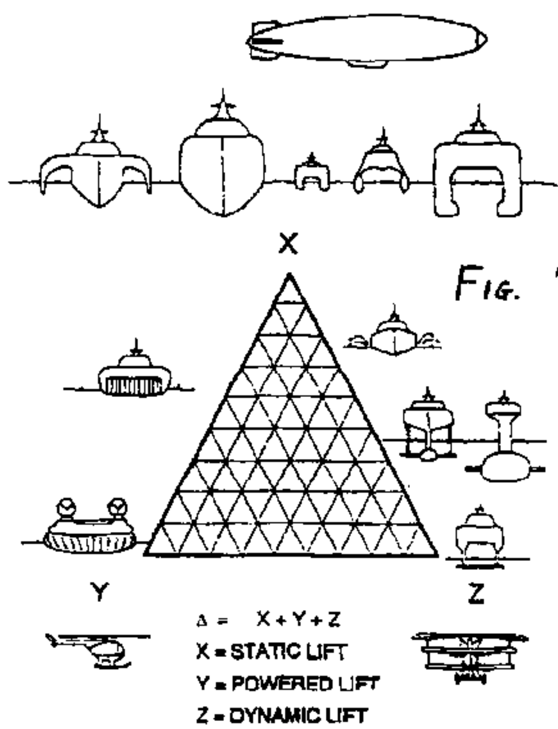
X
Y
Z
Δ = X + Y + Z
X = STATIC LIFT
Y = POWERED LIFT
Z = DYNAMIC LIFT

Fig. 7

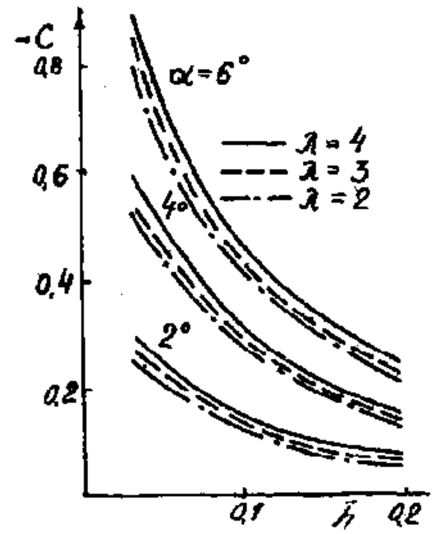

~~Fig.~~ Aerodynamical wings characteristics of ecranoplan.

GRAPH. 1

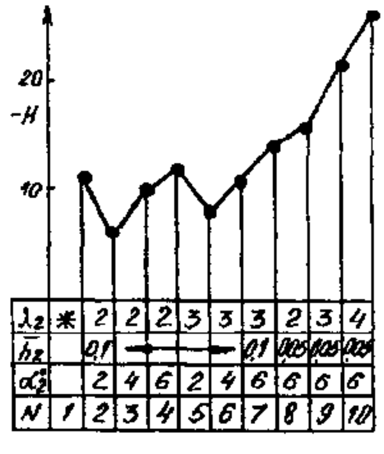

$\lambda_1 = 2 \div 4$; $\bar{h}_1 = 0.05 \div 0.2$; $\alpha_1 = 2°$;

$* \ \lambda_1 = \lambda_2$; $\bar{h}_1 = \bar{h}_2$; $\alpha_1 = \alpha_2$

~~Fig.~~ Dependence of H on main parameters of ecranoplan.

GRAPH. 2

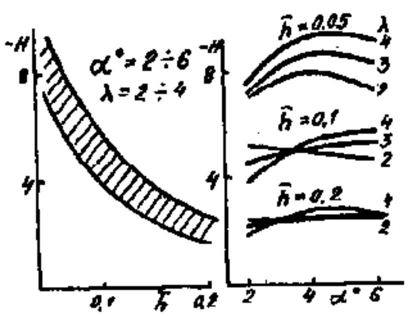

$\lambda_1 = \lambda_2$; $\alpha_1 = \alpha_2$; $b_1 = b_2$;

$\bar{h}_1 = \bar{h}_2$, $\bar{l}_1 = 0.5$

~~Fig.~~ Stability characteristics of ekranoplan with identical forward and after wing.

GRAPH. 3

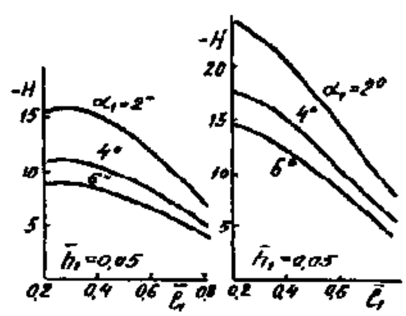

N8 $\bar{h}_2 = 0.05$ N10 $\bar{h}_2 = 0.05$

$\lambda_2 = 2$; $\alpha_2 = 6°$ $\lambda_2 = 4$, $\alpha_2 = 6°$

~~Fig.~~ Dependes of H on mass center of position ecranoplan.

GRAPH. 4

FIG. 8

Impression of the Skate 50-seat amphibious hoverferry

FIG. 9

Artist's impression of an Orion type sidewall craft

FIG. 10

The Soviet giant wing-in-ground-effect machine has similar lines to the craft depicted above, it is believed. The main power plants (1) are thought to be gas-turbines rather than turboprops as shown, and the booster gas turbines (2) to accelerate the craft through hump to cruising speed are likely to have been moved to a forward position.

FIG. 11

Impression of a new catamaran-hulled Ekranoplan research craft now under development in the Soviet Union. Designed for high speed long distance passenger services along the main Soviet rivers, it rides on a dynamic air cushion formed between its wings and the supporting surface below. Seats are provided for forty passengers in each of the twin hulls. Top speed is likely to be between 150-200 knots

A90.150 Orlyonok

FIG. 12

Photo: A. Belyaev

Lun

FIG. 13

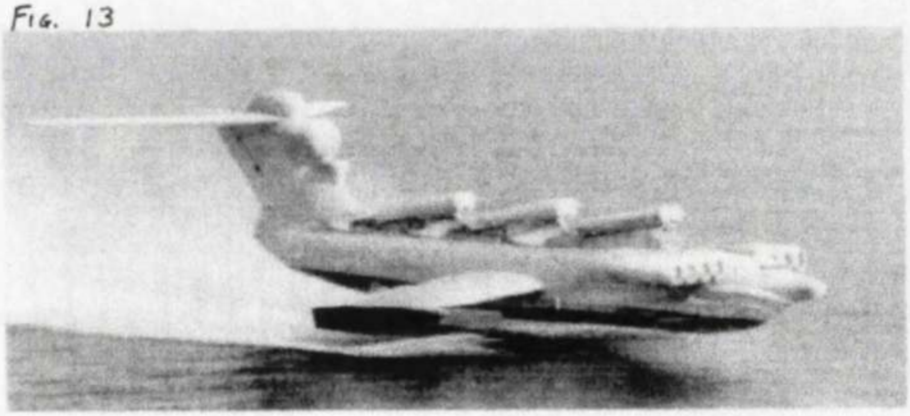

Photo: A. Belyaev

1.4 W.I.S.E DATABASE

Co. Name	Sukhoi OKB	Sukhoi OKB	C.L.S.T.
W.I.G. Name	S-90-200	S-90-8	ESKA 1
Date	1992	1992	1975
Status	not yet built	not yet built	built
Length m	40	11.7	7.55
Width m	61	15.1	6.9
Height m	11.85	3.5	2.5
Span, folded m			
Tailplane Span		9.3	
Wing Area Centre Section mE2	757.16	48.2	
Centre Section Area mE2	502	36.6	
Outerwing Panel Area mE2	250	11.6	
Aileron Area mE2		1.31	
Tailplane Area mE2		11	
Control Surf's. Area mE2	31.59	2.86	
Outer Faperon Area mE2	28.52		
Wing Leading Edge -			
Forward Sweep Angle degrees	1	-1	
Tailplane area mE2	69.86		
Tailplane incidence degrees	33	30	
Tailplane anhedral degrees	-2		
Type of tail unit		Vee (450 outside)	
Wing Aspect Ratio		5	
Dihedral		100	
Wing loading (at take-off			
weight) kg/mE2	35.08 lb/ft2	15.71 lb/ft2	
Powerplant	2x NK-1 2MK turboprops or	M-601 turboprop engine with	One 22 kW M63
	turbofans at rear of centre	four-bladed variable pitch co-	motorcycle engine
	wing section along symmetry	axial propeller on a pylon on	
	with fourblade co-axial variable-	centre of symmetry (front)	
	pitch propellers		
Engine Rating K.W	15,000 h.p.	551	22
Sp. Power (at take-off			
weight) K.W / kg	.227 hp/kg	.2 hp/kg	
Thrust Rating kg	15,000		
Empty Weight kg			
Max. Take-off Weight	132,000	3,700	450
Payload kg	20,000	273	
Fuel Weight kg	58,000	500	
Max. Range km	7995.2	477.98	350
Take-off Speed km/h			
Max Speed km/h	470	300	
Cruise Speed km/h	380	200	110
No. Passengers	220	6	0
No. Crew	2	2	2
Max. Flight Alt. M	1499.6	1499.6	10
Cruise alt. M	6.6-18	4.9-6.6	0.3 - 1.5
Ground Effect Alt. M	6.6-18	4.9-6.6	0.3 - 1.5
No. of fuselage	2	2	1
Take-off aids	static air cussion below centre	static air cussion below centre	Curved Wing design with
	wing by retractable flexible skirt.	wing	added floats and high
	A cruise engine for static pressur-		speed take-off by the use
	isation for take-off and landing		of RAM.
Materials Used	fuselages are of segmented	fuselages are of segmented	
	rubber-fabric shells on their	rubber-fabric shells on their	
	bottom surfaces	bottom surfaces	
Funct's & Modifications	high comfirt passenger liner	high speed passanger craft	Used as an experimental
	over water surfaces, has a plus	for short haul routes. It's	high speed rescue
	shaped wing, capability to fly at	feaures are for high speed	and liaison craft for
	low alt. Over water, snow, swamp	comfortand cost effectiveness.	inland Russia.
	grass and meduim flight alt.		
Internet add.	http://www.aero.cst.nihon-u.ac.jp	hhttp://www.aero.cst.nihon-u.ac.jp/	http://www.io.tudelft.nl/-

Co. Name	C.L.S.T.	C.L.S.T.	C.L.S.T.	OIIMF
W.I.G. Name	ESKA 4	E-120	ES-2	OIIMF-1
Date		1971		1963
Status	not built	built	built	built
Length m				5
Width m				3.2
Height m				
Span, folded m				
Tailplane Span				
Wing Area Centre Section mE2				
Centre Section Area mE2				
Outerwing Panel Area mE2				
Aileron Area mE2				
Tailplane Area mE2				
Control Surf's. Area mE2				
Outer Faperon Area mE2				
Wing Leading Edge - Forward Sweep Angle degrees				
Tailplane area mE2				
Tailplane incidence degrees				
Tailplane anhedral degrees				
Type of tail unit				
Wing Aspect Ratio				
Dihedral				
Wing loading (at take-off weight) kg/mE2				
Powerplant				A 13 kW engine
Engine Rating K.W				13
Sp. Power (at take-off weight) K.W / kg				
Thrust Rating kg				
Empty Weight kg				
Max. Take-off Weight				
Payload kg				
Fuel Weight kg				
Max. Range km				
Take-off Speed km/h				
Max Speed km/h				
Cruise Speed km/h				
No. Passengers	2	0	1	0
No. Crew	2	1	1	1
Max. Flight Alt. M				
Cruise alt. M				
Ground Effect Alt. M				
No. of fuselage	1	1	1	1
Take-off aids	An engine located at the tail	Its circular shape and engine.	light weight, curved wing design and engine located at the front.	
Materials Used			Made of Aluminium not certain about wing material used.	
Funct's & Modifications			A Blanik glider which had been converted into a WIG possibly for test purposes for ESKA.	Used as a WIG research craft.
Internet add.	http://www.io.tudelft.nl/-twaio/edwin/html/cclst.htm	http://www.io.tudelft.nl/-twaio/edwin/html/cclst.htm	http://www.io.tudelft.nl/-twaio/edwin/html/cclst.htm	http://www.io.tudelft.nl/-twaio/edwin/html/coiimf.htm

Co. Name	OIIMF	George Hennebutte	CSSRC	CSSRC
W.I.G. Name	OIIMF-2	PSI-575	Ram WIG 902	XTW-1
Date	1965		1983	
Status	built	built	built	built
Length m	5	5.7	9.55	
Width m	3.2	10	5.8	
Height m		1.7		
Span, folded m				
Tailplane Span				
Wing Area Centre Section mE2				
Centre Section Area mE2				
Outerwing Panel Area mE2				
Aileron Area mE2				
Tailplane Area mE2				
Control Surf's. Area mE2				
Outer Faperon Area mE2				
Wing Leading Edge -				
Forward Sweep Angle degrees				
Tailplane area mE2				
Tailplane incidence degrees				
Tailplane anhedral degrees				
Type of tail unit				
Wing Aspect Ratio				
Dihedral				
Wing loading (at take-off				
weight) kg/mE2				
Powerplant	Two 13 kW engines	A 37 kW twin rotor	Two HS350 kW	Two HS350 kW
	driving 1.2 m propeller	wankel engine, the RFE	aircraft piston engines	aircraft piston engines
		SG85 with a three	with fixed pitch prop-	with fixed pitch prop-
		bladed ducted fan	ellers	ellers
Engine Rating K.W	6 k	37	30	30
Sp. Power (at take-off				
weight) K.W / kg				
Thrust Rating kg				
Empty Weight kg	370			
Max. Take-off Weight	450		385	950
Payload kg		250	105	
Fuel Weight kg				
Max. Range km		450 km		
Take-off Speed km/h				
Max Speed km/h				
Cruise Speed km/h	100	140	120	130
No. Passengers		2	0	2
No. Crew		1	1	2
Max. Flight Alt. M			0.5	
Cruise alt. M			under 0.5	
Ground Effect Alt. M			under 0.5 m	
No. of fuselage	1	1	1	1
Take-off aids		light weight, curved wing	Two engines	Two engines
		design.	equires a short take-off	
			length of 150 m.	
Materials Used		Made of rubber. The		
		hull of laminated kevlar		
		wing tip floats of		
		polyurethane.		
Funct's & Modifications	A research craft		A CSSRC test vehicle.	Incorporates a re-
	buit by students			tractable under carriage
	of the Institute.			for slipway handling.
				A development of the 90:
Internet add.	ttp://www.io.tudelft.n	http://www.io.tudelft.nl/	http://www.io.tudelft.nl/	http://www.io.tudelft.nl/
	twaio/edwin/html/com	waio/edwin/html/chenn	waio/edwin/html/ccssr	waio/edwin/html/ccssrc
	.htm	.htm	.htm	.htm

Co. Name	CSSRC	F.F & AFD GmbH	F.F & AFD GmbH	F.F & AFD GmbH
W.I.G. Name	XTW-2	Airfisch 1	Airfisch 2	Airfisch 3
Date	1990	1987	after Airfisch 1.	1990
Status	built	built	built	built
Length m	18.5			9.9
Width m	12.72 m			7.5
Height m	5.14 m			
Span, folded m				5.9
Tailplane Span				
Wing Area Centre Section mE2				
Centre Section Area mE2				
Outerwing Panel Area mE2				
Aileron Area mE2				
Tailplane Area mE2				
Control Surf's. Area mE2				
Outer Faperon Area mE2				
Wing Leading Edge - Forward Sweep Angle degrees				
Tailplane area mE2				
Tailplane incidence degrees				
Tailplane anhedral degrees				
Type of tail unit				
Wing Aspect Ratio				
Dihedral				
Wing loading (at take-off weight) kg/mE2				
Powerplant	Two wing mounted 448 kW IO-540 K1B5 piston engines which drive two propellers.			Two cylinder BMW 60 kW boxer engine driving a geared six bladed ducted prop.
Engine Rating K.W	896			129
Sp. Power (at take-off weight) K.W / kg				
Thrust Rating kg				
Empty Weight kg				425
Max. Take-off Weight	3600			650
Payload kg	1200			190
Fuel Weight kg				35
Max. Range km	900			370
Take-off Speed km/h				70
Max Speed km/h				
Cruise Speed km/h	150			120
No. Passengers	14	0	0	1
No. Crew	2	1	1	1
Max. Flight Alt. M	30			4.5
Cruise alt. M	1			1
Ground Effect Alt. M				1
No. of fuselage	1	1	1	1
Take-off aids	The lower halves of the propellers may provide some PAR thrust at take-off.	an airodynamic curved ring desing. However, unable to carry out free flight.		
Materials Used			Made of light composite and metal construction.	
Funct's & Modifications	Is a further development of the 902 and the XTW-1	Derived from Lippisch's design to reduce purchase and opperational cost.	Development of the Airfisch 1 with a lower aspect ratio wing to improve harbour maneouvering.	Development of other Airfisch designs. Has enhanced harbour manoeuvering electrical controlled folded winglets and retractable water scew.
Internet add.	http://www.io.tudelft.nl/-twaio/edwin/html/ccssrc.htm	http://www.io.tudelft.nl/-twaio/edwin/html/cff.htm	http://www.io.tudelft.nl/-twaio/edwin/html/cff.htm	http://www.io.tudelft.nl/-twaio/edwin/html/cff.htm

Co. Name	F.F & AFD GmbH	F.F & AFD GmbH	F.F & AFD GmbH	F.F & AFD GmbH
W.I.G. Name	Airfisch 4 & 5	Airfisch 8	HW-2VT Hoverwing	HW80 Hoverwing
Date		1990's	1997	
Status	built	built	built	
Length m	10.86		10.63	
Width m	8.5		10.62	
Height m			2.5	
Span, folded m	6.9			
Tailplane Span				
Wing Area Centre Section mE2				
Centre Section Area mE2				
Outerwing Panel Area mE2				
Aileron Area mE2				
Tailplane Area mE2				
Control Surf's. Area mE2				
Outer Faperon Area mE2				
Wing Leading Edge -				
Forward Sweep Angle degrees				
Tailplane area mE2				
Tailplane Incidence degrees				
Tailplane anhedral degrees				
Type of tail unit				
Wing Aspect Ratio				
Dihedral				
Wing loading (at take-off				
weight) kg/mE2				
Powerplant			An 80 kW Hirth F30	
			engine driving a prop.	
			and a 1kW auxiliry	
			water drive.	
Engine Rating K.W			81	
Sp. Power (at take-off				
weight) K.W / kg				
Thrust Rating kg				
Empty Weight kg				
Max. Take-off Weight			900	
Payload kg			175	
Fuel Weight kg				
Max. Range km			200	800
Take-off Speed km/h				
Max Speed km/h			130	
Cruise Speed km/h			100	180
No. Passengers		8	0	80
No. Crew		1 or 2	1	1 or 2
Max. Flight Alt. M			5	
Cruise alt. M			under 0.75	
Ground Effect Alt. M				
No. of fuselage	1	1	1	1
Take-off aids			A static air cushion	
			under the hull and	
			hydrodynamic forces	
Materials Used				
Funct's & Modifications		Aimed for commercial	Used to reduce take-	Aimed to opperate
		use in 1999 as a sea	off drag without PAR	in the Baltic sea.
		taxi in sheltered areas	and hydrofoils. Used	
			as a model for the	
			HW-80	
Internet add.	http://www.io.tudelft.nl/	http://www.io.tudelft.nl/	http://www.io.tudelft.nl/	http://www.io.tudelft.nl/-
	twaio/edwin/html/cff	twaio/edwin/html/cff	twaio/edwin/html/cff	twaio/edwin/html/cff
	.htm	.htm	.htm	.htm

Co. Name	J.S.E Alexeive C.H.D.B	J.S.E Alexeive C.H.D.B	J.S.E Alexeive C.H.D.B	J.S.E Alexeive C.H.D.B
W.I.G. Name	SM-1	SM-2 & SM-2P	SM-2P7	SM-3
Date	1961	1962	1964	after the SM-2P7
Status	built	built	built	built
Length m	20	20	19.4	14.5
Width m	10.3	11.5	19.5	8.9
Height m	1.53	1.5	1.54	1.3
Span, folded m				
Tailplane Span				
Wing Area Centre Section mE2				
Centre Section Area mE2				
Outerwing Panel Area mE2				
Aileron Area mE2				
Tailplane Area mE2				
Control Surf's. Area mE2				
Outer Faperon Area mE2				
Wing Leading Edge - Forward Sweep Angle degrees				
Tailplane area mE2				
Tailplane incidence degrees				
Tailplane anhedral degrees				
Type of tail unit				
Wing Aspect Ratio				
Dihedral				
Wing loading (at take-off weight) kg/mE2				
Powerplant	One turbojet engine.	One turbojet engine.	The turbojet engine was mounted inside the fuselage and the air intake was in the nose.	One turbojet engine.
Engine Rating K.W				
Sp. Power (at take-off weight) K.W / kg				
Thrust Rating kg				
Empty Weight kg				
Max. Take-off Weight	2830	3200	6300	3400
Payload kg				
Fuel Weight kg				
Max. Range km				
Take-off Speed km/h				
Max Speed km/h				
Cruise Speed km/h	170-270	160-270	130-270	140-180
No. Passengers	2	2		0
No. Crew	1	1		1
Max. Flight Alt. M				
Cruise alt. M				
Ground Effect Alt. M				
No. of fuselage	1	1	1	1
Take-off aids			Take-off speed was reduced by blowing under the wing, thus providing a static air cushion.	
Materials Used				
Funct's & Modifications	Their first full scale WIG vehicle. Not Successful due to extreamly high take-off speed. Crashed in 1962.	The SM-2 was a tandem craft. It was rebuilt with a rectangular wing and a high T-tail.(SM-2P)	Was the first vehicle to use PAR	Very low aspect ratio wing with endplates and large horizontal stbiliser. Was a test vehicle for very long chord design. Was very unstable.
Internet add.	http://www.io.tudelft.nl/-twaio/edwin/html/cchdb.htm	http://www.io.tudelft.nl/-twaio/edwin/html/cchdb.htm	http://www.io.tudelft.nl/-twaio/edwin/html/cchdb.htm	http://www.io.tudelft.nl/twaio/edwin/html/cchdb.htm

Co. Name	J.S.E Alexeive C.H.D.B	J.S.E Alexeive C.H.D.B	J.S.E Alexeive C.H.D.B	J.S.E Alexeive C.H.D.B
W.I.G. Name	SM-4	SM-5	SM-6	SM-8
Date	after the SM-3	1963	1972	1967
Status	built	built	built	built
Length m	20	18	31	18.48
Width m	15.7	19.4	14.8	19.4
Height m	1.96	1.52	7.85	1.52
Span, folded m				
Tailplane Span				
Wing Area Centre Section mE2				
Centre Section Area mE2				
Outerwing Panel Area mE2				
Aileron Area mE2				
Tailplane Area mE2				
Control Surf's. Area mE2				
Outer Faperon Area mE2				
Wing Leading Edge - Forward Sweep Angle degrees				
Tailplane area mE2				
Tailplane Incidence degrees				
Tailplane anhedral degrees				
Type of tail unit				
Wing Aspect Ratio				
Dihedral				
Wing loading (at take-off weight) kg/mE2				
Powerplant	Two turbojet engines. One forward for PAR thrust & one aft for cruise thrust.	Two mounted PAR nozzles.	One turboprop cruise engine and two AI-25 turbofans or turbojets for PAR power & acceleration	One turbojet or turbofan mounted at the top of the fuselage.Exhaust is directed to 8 forward mounted nozzles which blow under the wings.
Engine Rating K.W				
Sp. Power (at take-off weight) K.W / kg				
Thrust Rating kg				
Empty Weight kg				
Max. Take-off Weight	4800	7300	26925	8100
Payload kg				
Fuel Weight kg				
Max. Range km			700	120
Take-off Speed km/h				
Max Speed km/h				
Cruise Speed km/h	140-230	140-230	350	220
No. Passengers	0		20	
No. Crew	2	1	1	1
Max. Flight Alt. M				
Cruise alt. M				
Ground Effect Alt. M				
No. of fuselage	1	1	1	1
Take-off aids				
Materials Used				
Funct's & Modifications	Development of SM-2P7 Used as a trainer with engines internally moun-ted in fuselage.	The first KM 1/4 scale prototype. A spray wall protected the internal engine against spray ingnition. It crashed in 64	A small predecessor of the Orlyonok for water ice & land. In the 80's it was used as a trainer.	A 1/4 scale of the KM The first to incorporate a tail-plane with dihedral as in the KM The air intake of the engine is protected by a spray screen.
Internet add.	http://www.io.tudelft.nl/-twaio/edwin/html/cchdb.htm	http://www.io.tudelft.nl/-twaio/edwin/html/cchdb.htm	http://www.io.tudelft.nl/-twaio/edwin/html/cchdb.htm	http://www.io.tudelft.nl/-twaio/edwin/html/cchdb.htm

Co. Name	J.S.E Alexeive C.H.D.B.	J.S.E Alexeive C.H.D.B.	J.S.E Alexeive C.H.D.B.	J.S.E Alexeive C.H.D.B.
W.I.G. Name	SM-9	SM-10	SM-11	KM
Date	1977	1985	1985	1963
Status	built	built	built	built
Length m	11.4	11.43	6.95	92-106
Width m	9.85	7.63	9.94	32-40
Height m	2.57	3.32	1.91	22
Span, folded m				
Tailplane Span				
Wing Area Centre Section mE2				
Centre Section Area mE2				
Outerwing Panel Area mE2				
Aileron Area mE2				
Tailplane Area mE2				
Control Surf's. Area mE2				
Outer Faperon Area mE2				
Wing Leading Edge - Forward Sweep Angle degrees				
Tailplane area mE2				
Tailplane Incidence degrees				
Tailplane anhedral degrees				
Type of tail unit				
Wing Aspect Ratio				
Dihedral				
Wing loading (at take-off weight) kg/mE2				
Powerplant				8 turbojets mounted at the front of the fuselage. The exhausts could be deflected to create PAR under wings. 2 more turbojets mounted on the fin for extra thrust for acceleration.
Engine Rating K.W				
Sp. Power (at take-off weight) K.W / kg				
Thrust Rating kg				13208.6
Empty Weight kg				548665.3
Max. Take-off Weight	1750	2200	600	502943-548665
Payload kg				
Fuel Weight kg				
Max. Range km		300		1500 (at v = 400)
Take-off Speed km/h				
Max Speed km/h				
Cruise Speed km/h	120	120	110	430
No. Passengers	0			
No. Crew	1		1	1
Max. Flight Alt. M				
Cruise alt. M				
Ground Effect Alt. M				
No. of fuselage	1	1	1	1
Take-off aids				
Materials Used				
Funct's & Modifications	An aspect ratio of 5 to improve L/D quality. Also different wing designs had been tested to improve the stability of the craft.	The prototype of the Volga-2.	Together with the SM-9 & SM-11 it was used to improve the L/D quality of Ekranoplans.	It was the largest ever built of its kind,was tested for different wing designs.Has a large T-tail with dihedral and a mid-wing.
Internet add.	http://www.io.tudelft.nl/-twaio/edwin/html/cchdb.htm	http://www.io.tudelft.nl/-twaio/edwin/html/cchdb.htm	http://www.io.tudelft.nl/-twaio/edwin/html/cchdb.htm	http://www.io.tudelft.nl/-twaio/edwin/html/cchdb.htm

Co. Name	J.S.E Alexeive C.H.D.B	J.S.E Alexeive C.H.D.B.	J.S.E Alexeive C.H.D.B.	J.S.E Alexeive C.H.D.B.
W.I.G. Name	A 90.150 Orlyonok	Lun	Spasatel	UT
Date	1973	1970	1990	
Status	built	built	nearly finished	built
Length m	58	73.8	73	
Width m	31.5	44	45	
Height m	16	16	20	
Span, folded m				
Tailplane Span				
Wing Area Centre Section mE2				
Centre Section Area mE2				
Outerwing Panel Area mE2				
Aileron Area mE2				
Tailplane Area mE2				
Control Surf's. Area mE2				
Outer Faperon Area mE2				
Wing Leading Edge -				
Forward Sweep Angle degrees				
Tailplane area mE2				
Tailplane incidence degrees				
Tailplane anhedral degrees				
Type of tail unit				
Wing Aspect Ratio				
Dihedral				
Wing loading (at take-off				
weight) kg/mE2				
Powerplant	One Kunetsov NK-12MK	Eight NK-87 turbofan		Czech engine, with no
	11000kW turboprop high	engines four on each side		PAR
	at the fin for cruise thrust	of the fuselage aft of cockpit		
	& two NK-8-4K turbofans			
	of10.5 ton thrust for PAR,			
	take-off, accelerating &			
	landing.			
Engine Rating K.W				
Sp. Power (at take-off				
weight) K.W / kg				
Thrust Rating kg				
Empty Weight kg				
Max. Take-off Weight	110-125 tons	380-400 tons	390 ton	
Payload kg	15-28 tons			
Fuel Weight kg	15 ton			
Max. Range km	2000km (at 400 km/h)	3000 km	3000 km (at 400 km/h)	
Take-off Speed km/h				
Max Speed km/h				
Cruise Speed km/h	400 km/h	450-550 km/h	550 km/h	
No. Passengers	100-150	400	150 sitting or 500 standing	
No. Crew				
Max. Flight Alt. M		3000 m		
Cruise alt. M		1-4 m		
Ground Effect Alt. M				
No. of fuselage	1	1	1	1
Take-off aids	At trailing edge of wings a			
	5 section flap/aileron is fitted			
	and on leading edges, close to			
	wing tips are take-off screens			
	Two hydroskis are fitted on			
	the underside of fuselage			
	one at front and one at C.G.			
Materials Used				
Funct's & Modifications	As troops transport & assault	As a missile launching	Designed to locate & rescue	Is a small trainer
	vehicles. 4 were built, one was	strike craft. Similar to KM,	people at sea from ships,	
	used for static tests.	but has a lower wing, is	aircraft or oil rigs & platforms	
		smaller,has no fin mounted		
		engines.		
		Also used for search & rescue		
Internet add.	http://www.io.tudelft.nl/-	http://www.io.tudelft.nl/-	http://www.io.tudelft.nl/-	http://www.io.tudelft.nl/-
	twaio/edwin/html/cchdb	twaio/edwin/html/cchdb	twaio/edwin/html/cchdb	twaio/edwin/html/cchdb
	.htm	.htm	.htm	.htm

Co. Name	J.S.E Alexeive C.H.D.B.	J.S.E Alexeive C.H.D.B.	J.S.E Alexeive C.H.D.B.	Beriev
W.I.G. Name	Volga-2	Strizh PE-201 (Marlet)	Raketa 2	Be-`
Date				1961
Status	built	built	not built	built
Length m	11.43 m	11.40 m	34.8 m	
Width m	7.63 m	6.60 m	19.8 m	
Height m	3.32 m		10.0 m	
Span, folded m				
Tailplane Span				
Wing Area Centre Section mE2				
Centre Section Area mE2				
Outerwing Panel Area mE2				
Aileron Area mE2				
Tailplane Area mE2				
Control Surf's. Area mE2				
Outer Faperon Area mE2				
Wing Leading Edge -				
Forward Sweep Angle degrees				
Tailplane area mE2				
Tailplane incidence degrees				
Tailplane anhedral degrees				
Type of tail unit				
Wing Aspect Ratio				
Dihedral				
Wing loading (at take-off				
weight) kg/mE2				
Powerplant	Two VAZ-413 rotary engines	PAR WIG craft with two	Three 1785 kW turboprop	An RU-19 turbojet on the
	of 95 kW each	engines on wings, extended	engines, two for take-off &	back of the wing.
		shafts drive the props which	one for cruise.	
		blow under wings for propulssio		
		as well as lift		
Engine Rating K.W	190 kw			
Sp. Power (at take-off				
weight) K.W / kg				
Thrust Rating kg				
Empty Weight kg				
Max. Take-off Weight	2700 kg	1630 kg	33 t	
Payload kg	800 kg	more than 1 t		
Fuel Weight kg				
Max. Range km	500 km	1,500 km	800 km	
Take-off Speed km/h				
Max Speed km/h				
Cruise Speed km/h	120 km/h	220 km/h	180 km/h	
No. Passengers	8	1	90	
No. Crew	1 or 2	1	1 or 2	
Max. Flight Alt. M	0.5 m			
Cruise alt. M				
Ground Effect Alt. M				
No. of fuselage	1	1	1	1
Take-off aids				Two floats with a very
				small aspect ratio wing
				inbetween & small wings
				extending from the floats
				&surface piercing hydrofoils
				also on the floats.
Materials Used	The flexible design is of			
	light alloy.			
Funct's & Modifications	Is a PAR-WIG vehicle as	Used as anavy pilot trainer	Similar to Volga 2 but has	A small test craft for
	economic as existing	With dual control cockpits	third engine on the fin. It's a	exploring stability &
	hydrofoils. It has balloon		design of the Design Bureau	control of the VVA-14
	typestructures for amphi-		for larger WIGs for inland	It's design also includes
	bious qualities.		waterways.	landing gear.
	Can cimb a 10% gradient			
	to land. Stable design.			
Internet add.	http://www.io.tudelft.nl/-	http://www.io.tudelft.nl/-	http://www.io.tudelft.nl/-	http://www.io.tudelft.nl/-
	twaio/edwin/html/cchdb	twaio/edwin/html/cchdb	twaio/edwin/html/cchdb	twaio/edwin/html/cberiev
	.htm	.htm	.htm	.htm

Co. Name	Beriev	Beriev	Amficon	Amficon
W.I.G. Name	VVA-14	VVA-14M1P	NVA-3	NVA-30P
Date	1972	1976		
Status	built	built	not built	not built
Length m	28.12 m	26 m	11.6 m	16.5 m
Width m	30 m	30 m	10 m	15 m
Height m				
Span, folded m				
Tailplane Span				
Wing Area Centre Section mE2				
Centre Section Area mE2				
Outerwing Panel Area mE2				
Aileron Area mE2				
Tailplane Area mE2				
Control Surf's. Area mE2				
Outer Faperon Area mE2				
Wing Leading Edge -				
Forward Sweep Angle degrees				
Tailplane area mE2				
Tailplane Incidence degrees				
Tailplane anhedral degrees				
Type of tail unit				
Wing Aspect Ratio				
Dihedral				
Wing loading (at take-off				
weight) kg/mE2				
Powerplant	Two D-30 M turbofans	Two D-30 M turbofans	Two 50 hp engines &	Twin 1900 kW turbo-
	above trailing edge of	above trailing edge of	a single 150 hp engine	props on fins & The
	central wing	central wing & two at	for fan	lifting fan also 1900 kW
		the nose for PAR take-off		
Engine Rating K.W				
Sp. Power (at take-off				
weight) K.W / kg				
Thrust Rating kg				
Empty Weight kg				
Max. Take-off Weight	36-52 tons	52 t	3 t	30 ton
Payload kg			1.2 t	12 ton
Fuel Weight kg				
Max. Range km	2450 km	2450 km		
Take-off Speed km/h				
Max Speed km/h				
Cruise Speed km/h	360-760 km/h	760 km/h	200 km/h	250 km/h
No. Passengers			4	70
No. Crew	2	1 or 2	1 or 2	1 or 2
Max. Flight Alt. M				
Cruise alt. M	10 km	10 km		
Ground Effect Alt. M				
No. of fuselage	1	1	1	1
Take-off aids	Was later fitted with	Was later fitted with rigid		A big fan inside the
	inflatable pontoons	pontoons		twin shaped fuselage
				Powered by a separate
				engine.
Materials Used				
Funct's & Modifications	Ground effect is just a	Is the VVA-14 re-designed	Considered as a acale	
	take-off aid		model for larger craft.	
	Used for anti-submarine			
	warfare. Had borrowed land-			
	ing gear from the Tu-22.			
Internet add.	http://www.io.tudelft.nl/-	http://www.io.tudelft.nl/-	http://www.io.tudelft.nl/-	http://www.io.tudelft.nl/-
	twaio/edwin/html/cberiev	twaio/edwin/html/camfikor	twaio/edwin/html/camfikor	waio/edwin/html/camfikon
	.htm	.htm	.htm	.htm

Co. Name	Amficon	Amficon	BOTEC I.GmbH	BOTEC I.GmbH
W.I.G. Name	NVA-60P	NVA-120GP	TAB VII Jorg 1	TAF VIII-1 Jorg 2
Date			1974	1976
Status	not built	not built	built	built
Length m	25.5 m	35 m	6.20 m	8.30 m
Width m	33.4 m	42 m	4.10 m	3.28 m
Height m			1.55 m	1.75 m
Span, folded m				
Tailplane Span				
Wing Area Centre Section mE2				
Centre Section Area mE2				
Outerwing Panel Area mE2				
Aileron Area mE2				
Tailplane Area mE2				
Control Surf's. Area mE2				
Outer Faperon Area mE2				
Wing Leading Edge -				
Forward Sweep Angle degrees				
Tailplane area mE2				
Tailplane Incidence degrees				
Tailplane anhedral degrees				
Type of tail unit				
Wing Aspect Ratio				
Dihedral				
Wing loading (at take-off				
weight) kg/mE2				
Powerplant	Twin 36 kW turbofans	Twin 60 kN turbofans	1000cc 48 kW Fiat	
	on fuselage a lift fan is	on fuselage & lift fan	engine driving a	
	powered by a 5200kW	is a 5200 kW gasturbine	pisher propeller	
	gasturbine.			
Engine Rating K.W				
Sp. Power (at take-off				
weight) K.W / kg				
Thrust Rating kg				
Empty Weight kg				
Max. Take-off Weight	60 ton	120 ton	700 kg	740 kg
Payload kg	27 ton	60 ton	265 kg	200 kg
Fuel Weight kg				
Max. Range km			200 km	200 km
Take-off Speed km/h				
Max Speed km/h				
Cruise Speed km/h	280 km/h	350 km/h	110 km/h	125 km/h
No. Passengers	200		1	1
No. Crew	1 or 2		1	1
Max. Flight Alt. M				
Cruise alt. M				
Ground Effect Alt. M				
No. of fuselage	1	1	1	1
Take-off aids				
Materials Used				Made of Aluminium
Funct's & Modifications			Is a flair boat. The first	It is an improved Jorg 1
			of a series of experimental	
			tandem wing craft.	
Internet add.	http://www.io.tudelft.nl/-	http://www.io.tudelft.nl/-	http://www.io.tudelft.nl/-	http://www.io.tudelft.nl/
	twaio/edwin/html/camfikor	twaio/edwin/html/camfikor	twaio/edwin/html/cjoerg	twaio/edwin/html/cjoerg
	.htm	.htm	.htm	.htm

Co. Name	BOTEC.I.GmbH	BOTEC.I.GmbH	BOTEC.I.GmbH	BOTEC.I.GmbH
W.I.G. Name	TAF VIII-2 Jorg4	TAF VIII-3 Jorg 6	TAF VIII-5	TAF VIII-7 Jorg 2
Date	1981	1991		
Status	built	built	built	not yet built
Length m	8.30 m	14.00 m	19.90 m	45.60 m
Width m	3.28 m	5.85 m	8.50 m	16.6 m
Height m	1.75 m	3.30 m	4.65 m	9.00 m
Span, folded m				
Tailplane Span				
Wing Area Centre Section mE2				
Centre Section Area mE2				
Outerwing Panel Area mE2				
Aileron Area mE2				
Tailplane Area mE2				
Control Surf's. Area mE2				
Outer Faperon Area mE2				
Wing Leading Edge - Forward Sweep Angle degrees				
Tailplane area mE2				
Tailplane Incidence degrees				
Tailplane anhedral degrees				
Type of tail unit				
Wing Aspect Ratio				
Dihedral				
Wing loading (at take-off weight) kg/mE2				
Powerplant	A 2.3 L 147 kW BMW engine with fixed pitch propeller	A 6.81 V8 engine of 380kW.	MTU 8 cylinder turbo diesel engine	Two gas turbine engines of 4250 kW each
Engine Rating K.W				
Sp. Power (at take-off weight) K.W / kg				
Thrust Rating kg				
Empty Weight kg				
Max. Take-off Weight	740 kg	3150 kg	8000 kg	60 ton
Payload kg	200 kg		1500 kg	14 ton
Fuel Weight kg				
Max. Range km	200 km	400 km	500 km	1000 km
Take-off Speed km/h				
Max Speed km/h				
Cruise Speed km/h	125 km/h	150 km/h	185 km/h	200 km/h
No. Passengers	4 to 6	7	14	113
No. Crew				2
Max. Flight Alt. M				
Cruise alt. M		0.4	0.3-1	1.25 m
Ground Effect Alt. M		0.4	0.3-1	1.25 m
No. of fuselage	1	1	1	1
Take-off aids				
Materials Used	Made of Aluminium			
Funct's & Modifications	Is an aluminiu tandem wing flarboat. Better than the GFRP Jorg 3 which could not withstand impact loads from floating objects.	Only for inland waters Due to go for series production	Built for a customer in the Middle East.	
Internet add.	http://www.io.tudelft.nl/-twaio/edwin/html/cjoerg.htm	http://www.io.tudelft.nl/-twaio/edwin/html/cjoerg.htm	http://www.io.tudelft.nl/-twaio/edwin/html/cjoerg.htm	http://www.io.tudelft.nl/-twaio/edwin/html/cjoerg.htm

Co. Name	J.S.E Alexeive C.H.D.B	J.S.E Alexeive C.H.D.B	TsAGI + MiG	Pasific Teq. Dev/ment Moscow
W.I.G. Name	Utka (Duck)	Dingo	Mig-TA4 (Finder)	Amphistar
Date				
Status	built	built	built	built
Length m				10.4 m
Width m				
Height m				
Span, folded m				
Tailplane Span				
Wing Area Centre Section mE2				
Centre Section Area mE2				
Outerwing Panel Area mE2				
Alleron Area mE2				
Tailplane Area mE2				
Control Surf's. Area mE2				
Outer Faperon Area mE2				
Wing Leading Edge -				
Forward Sweep Angle degrees				
Tailplane area mE2				
Tailplane Incidence degrees				
Tailplane anhedral degrees				
Type of tail unit				
Wing Aspect Ratio				
Dihedral				
Wing loading (at take-off				
weight) kg/mE2				
Powerplant	Tail mounted main	Main: P&W PT6	Teledyne IO-550C &	2 tilt-rotor Subaru powered
	engine with single prop.	Lift: TBA-200	Nelson N-63CP	props (220hp)
	Two lift engine in nose.			
Engine Rating K.W				
Sp. Power (at take-off				
weight) K.W / kg				
Thrust Rating kg				
Empty Weight kg				
Max. Take-off Weight	20 tons	3.6 tons		
Payload kg		0.84 tons		
Fuel Weight kg				
Max. Range km		850 km		
Take-off Speed km/h				
Max Speed km/h				
Cruise Speed km/h	350 km/h	275 km/h		80 m/h
No. Passengers	15-20	2	2	5
No. Crew		2	2	1
Max. Flight Alt. M				
Cruise alt. M				
Ground Effect Alt. M				
No. of fuselage	1	1	1	1
Take-off aids				
Materials Used				
Funct's & Modifications	Light transport.	General Aviation	General Aviation	Multipurpose amphibian, leisure
				Similar to Volga 2.
Internet add.	http://www.io.tudelft.nl/-	Russion Aviation Page	Russion Aviation Page	Russion Aviation Page
	twaio/edwin/html/cjoerg			
	.htm			

GRAPHS ATTAINED FROM DATABASE

GRAPH 5

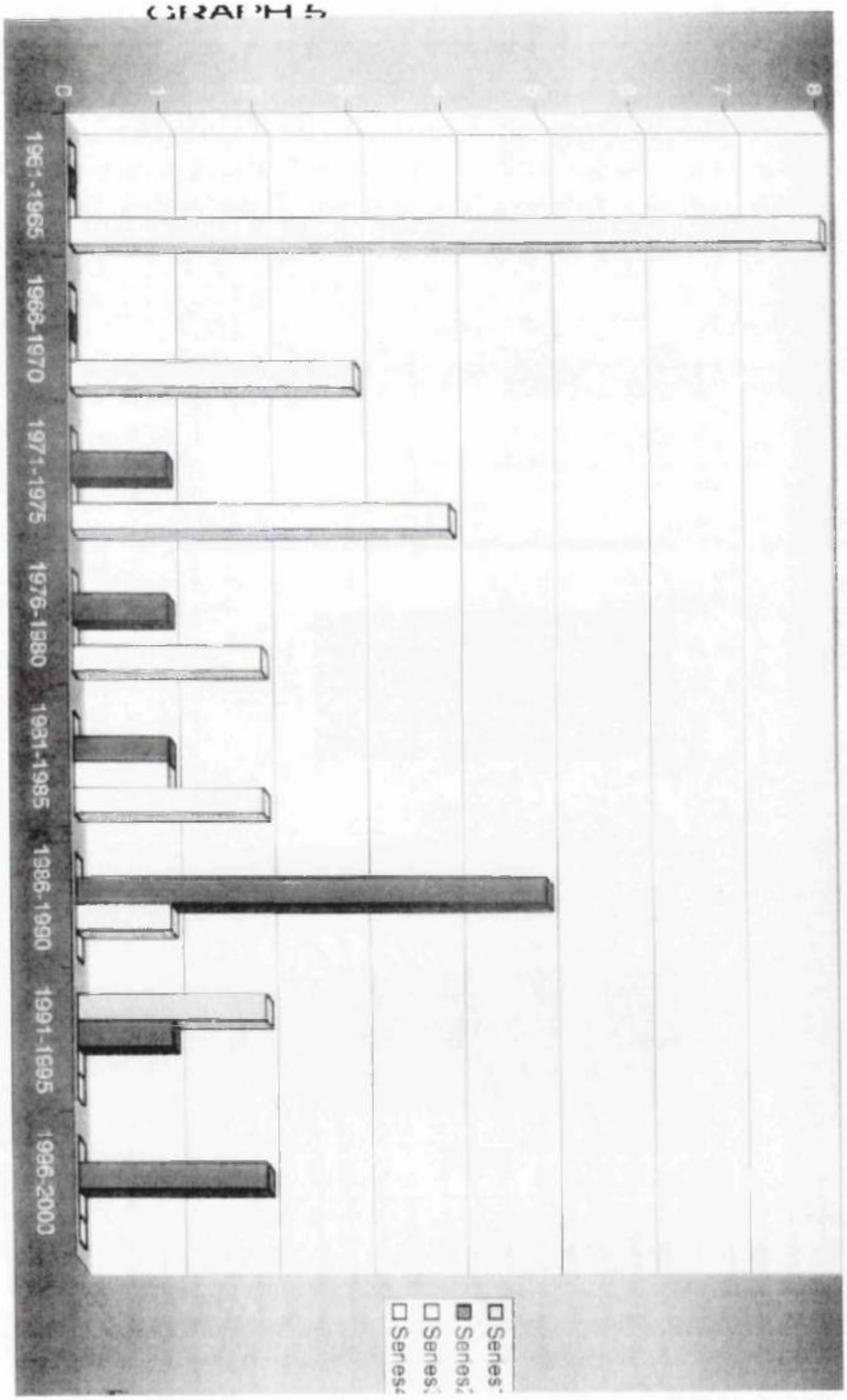
0
1
2
3
4
5
6
7
8
1961-1965
1966-1970
1971-1975
1976-1980
1981-1985
1986-1990
1991-1995
1996-2000
Series

GRAPH 6

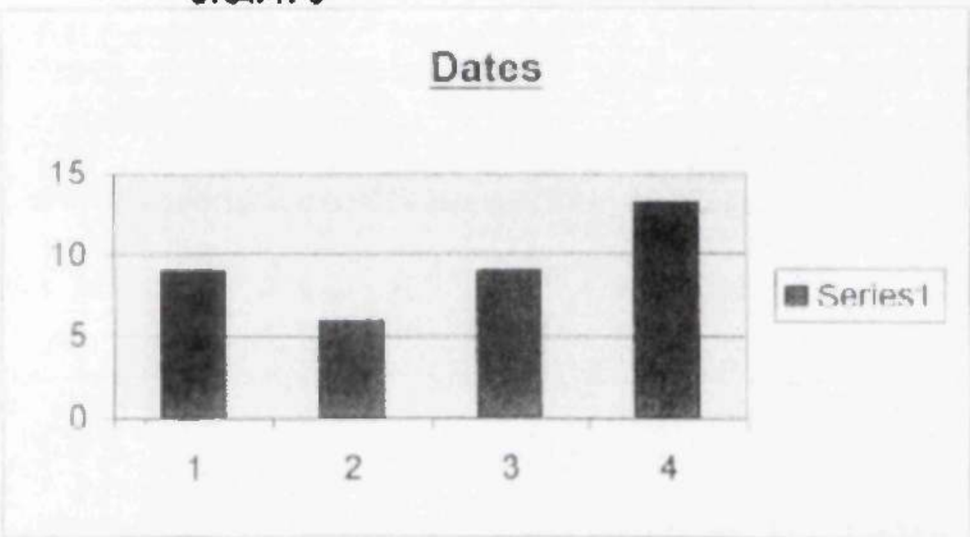

GRAPH 7

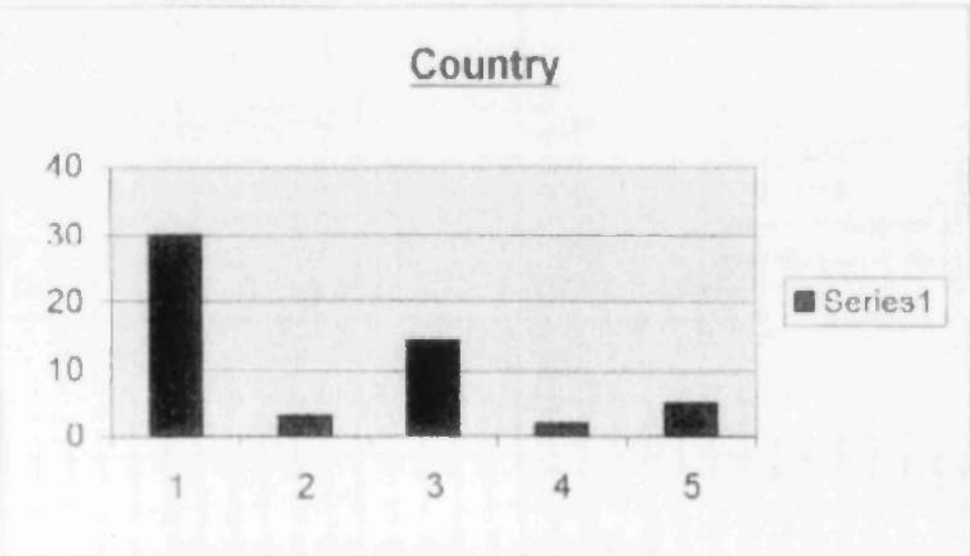

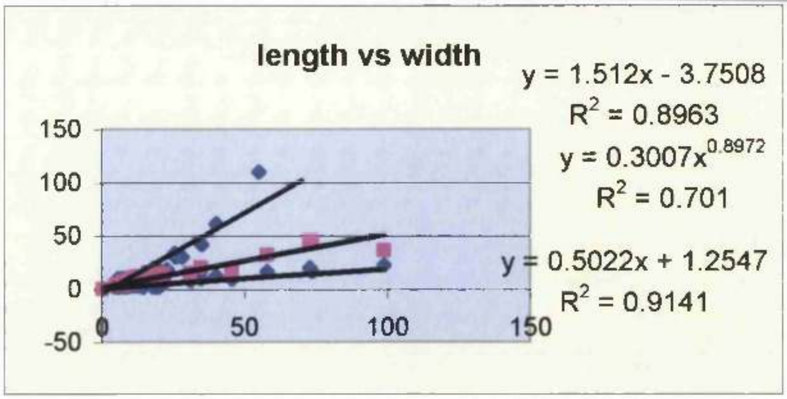

GRAPH 8

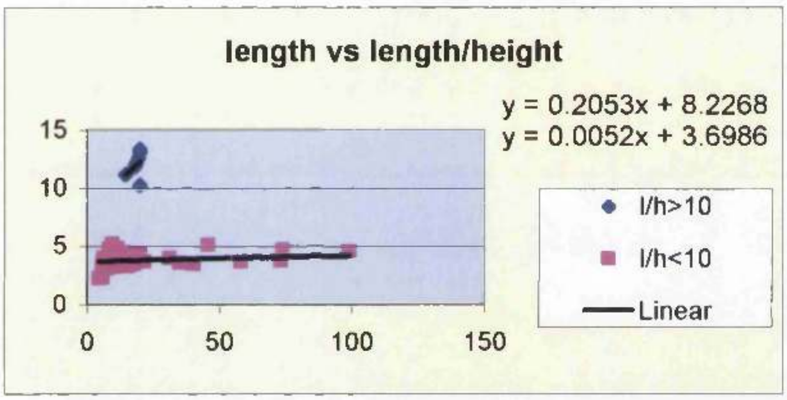

GRAPH 9

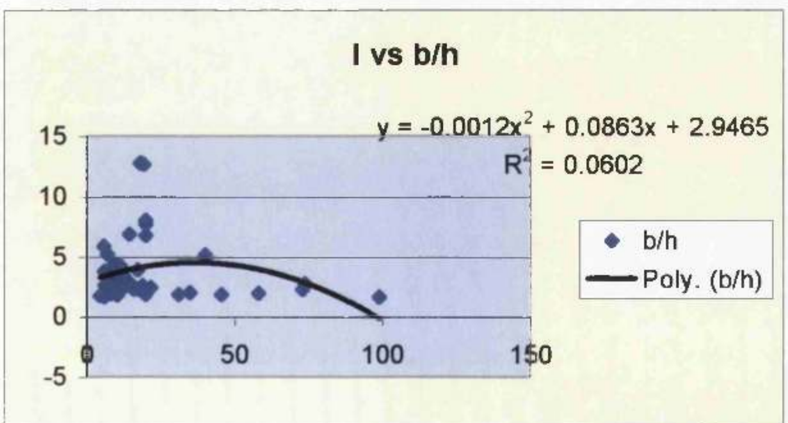

GRAPH 10

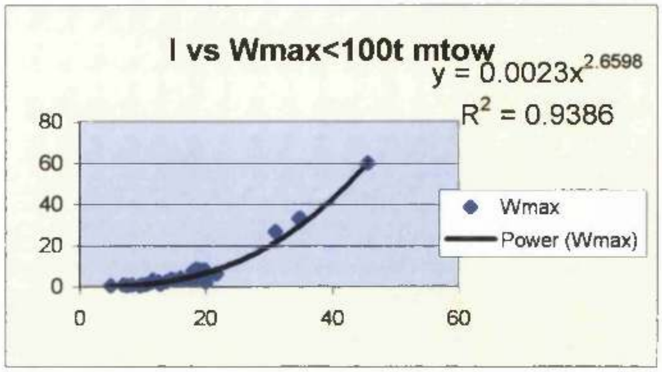

GRAPH 11

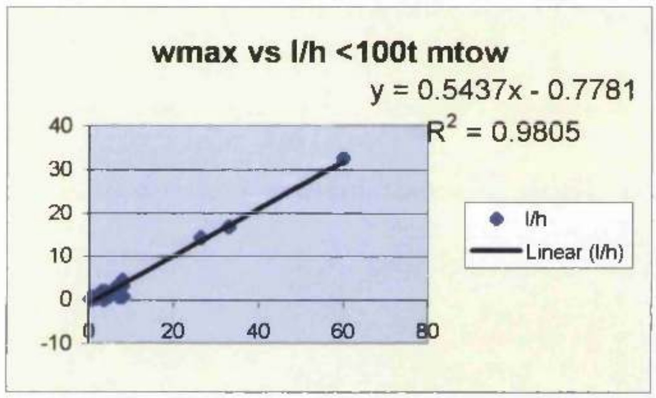

GRAPH 12

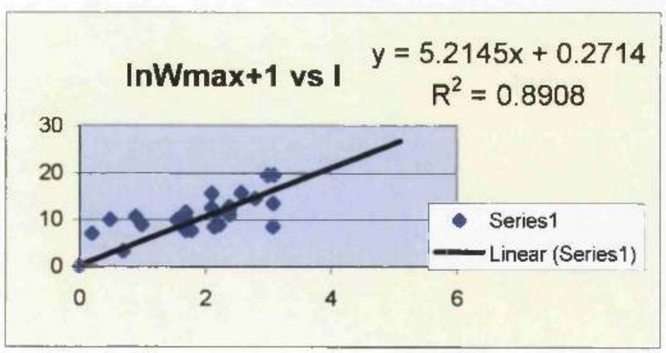

GRAPH 13

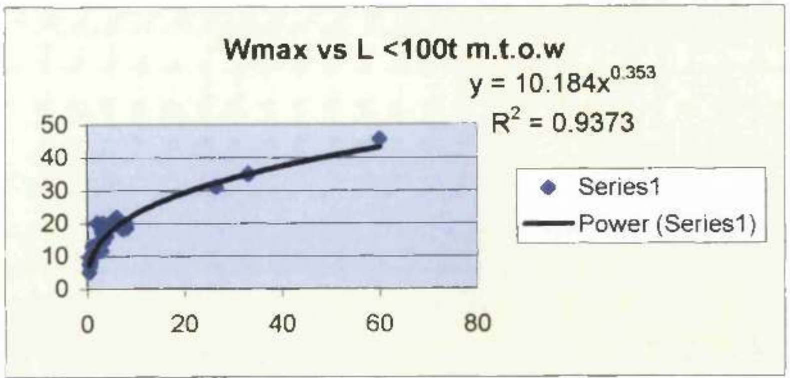

GRAPH 14

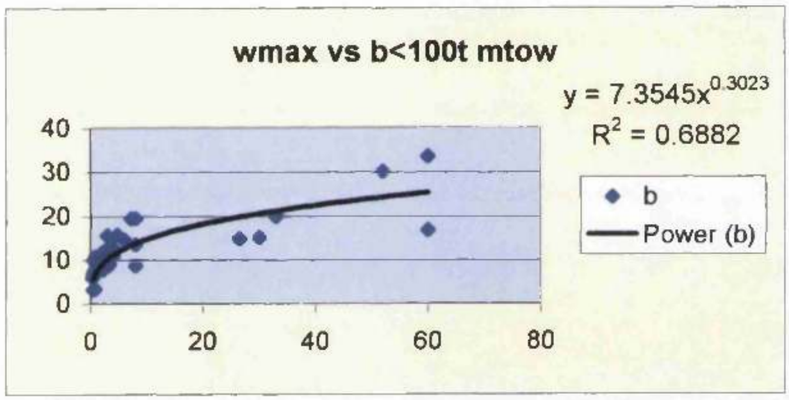

GRAPH 15

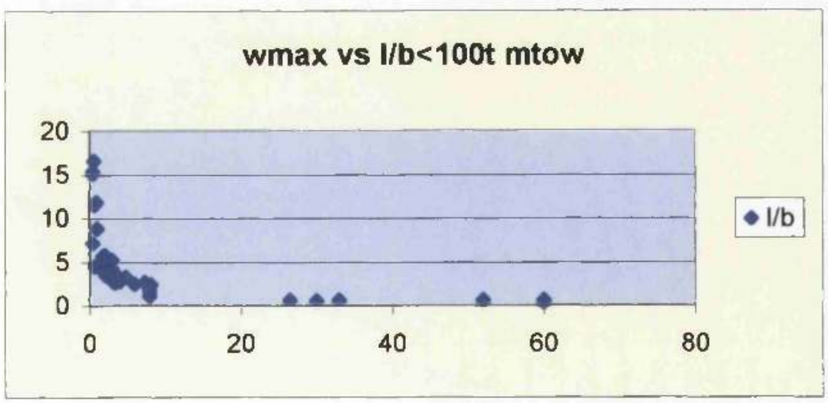

GRAPH 16

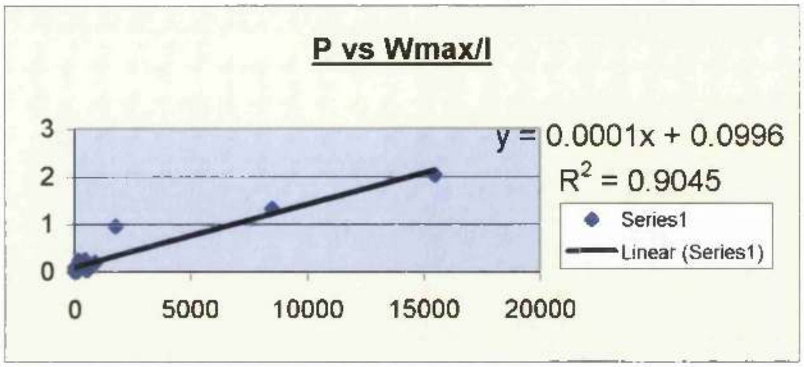

GRAPH 17

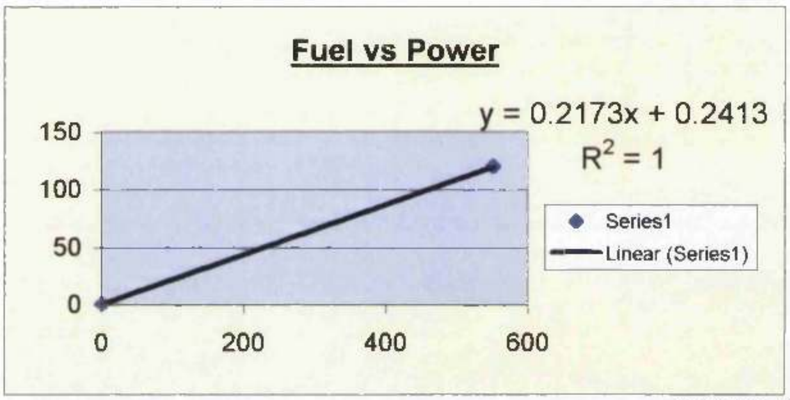

GRAPH 18

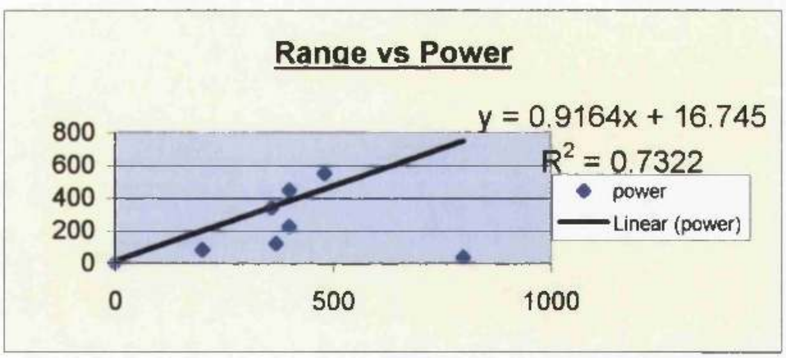

GRAPH 19

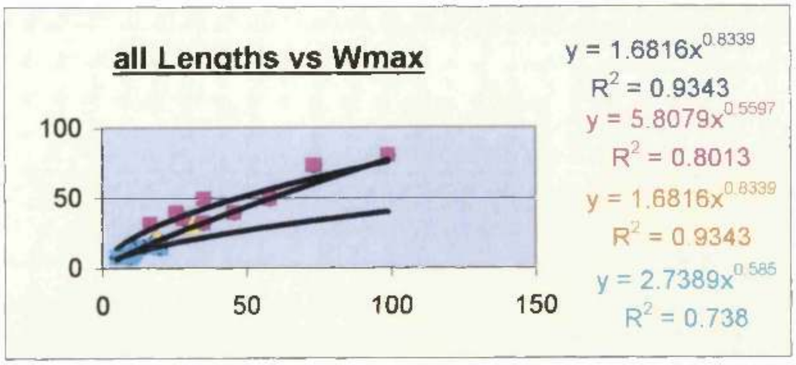

GRAPH 20

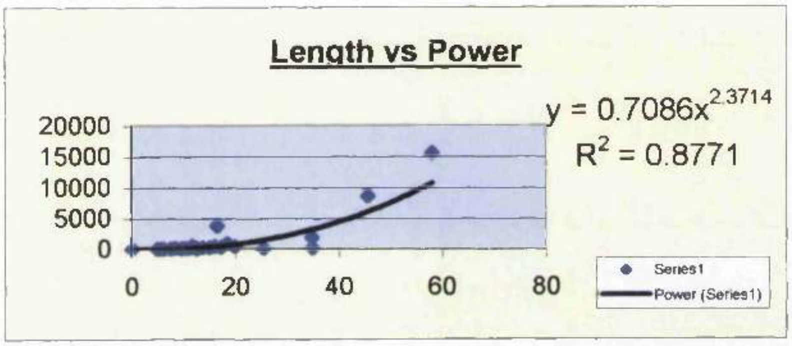

GRAPH 21

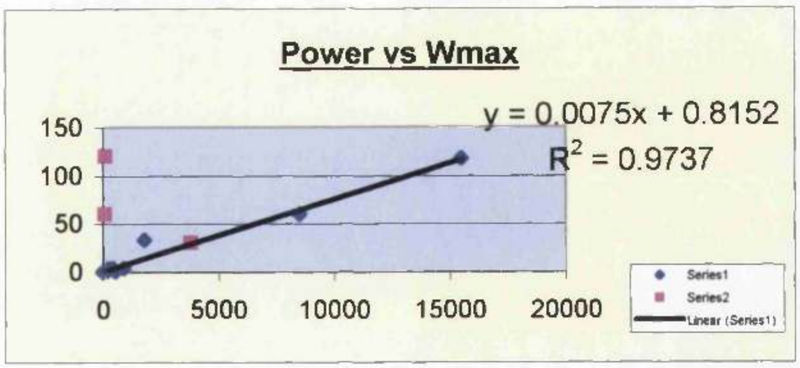

GRAPH 22

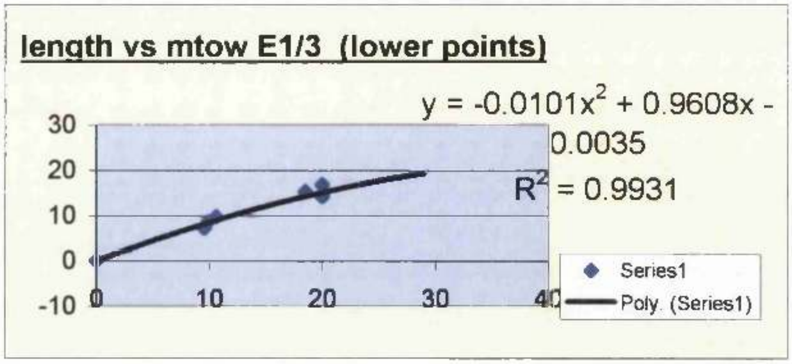

GRAPH 23

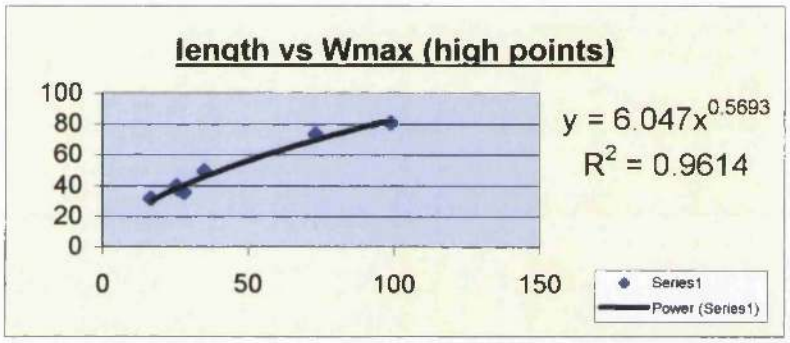

GRAPH 24

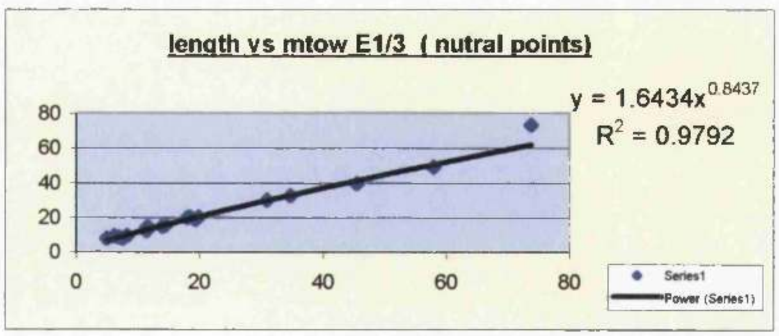

GRAPH 25

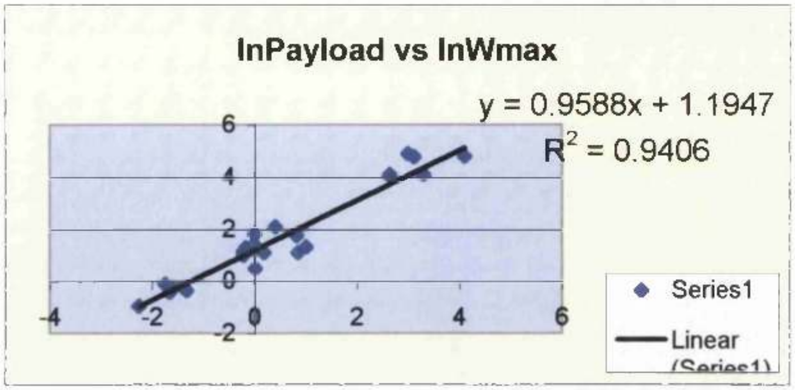

GRAPH 26

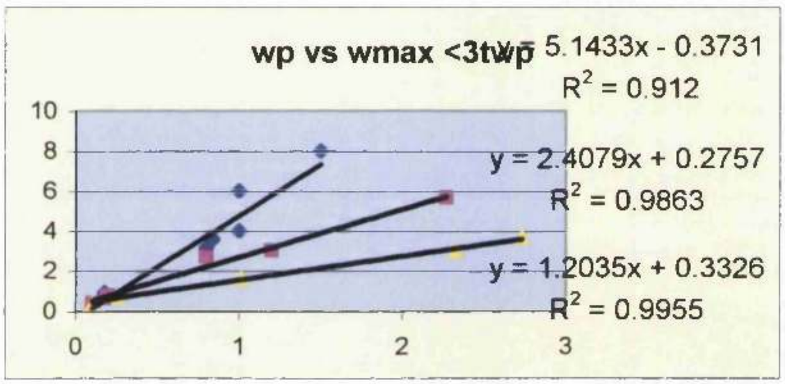

GRAPH 27

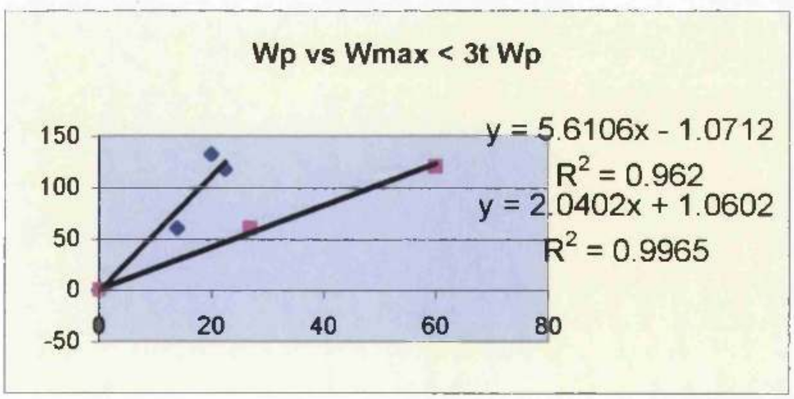

GRAPH 28

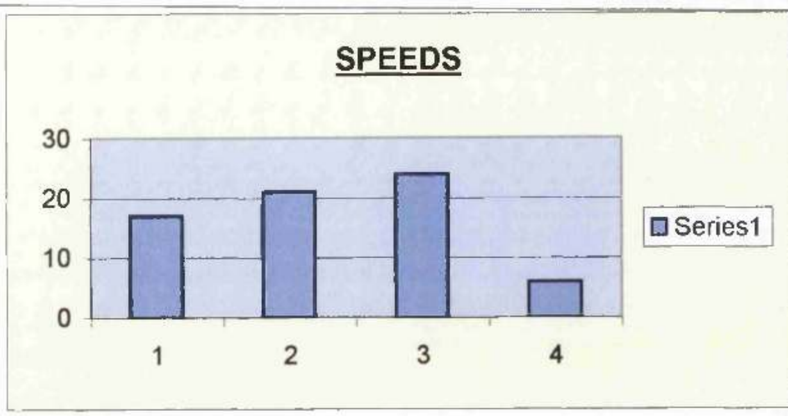

GRAPH 29

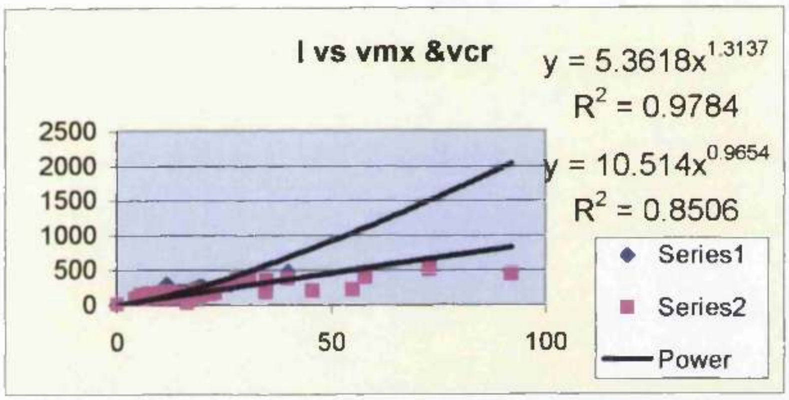

GRAPH 30

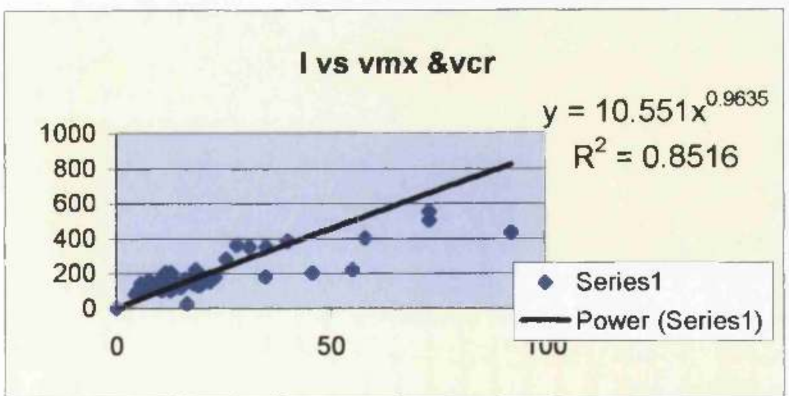

GRAPH 31

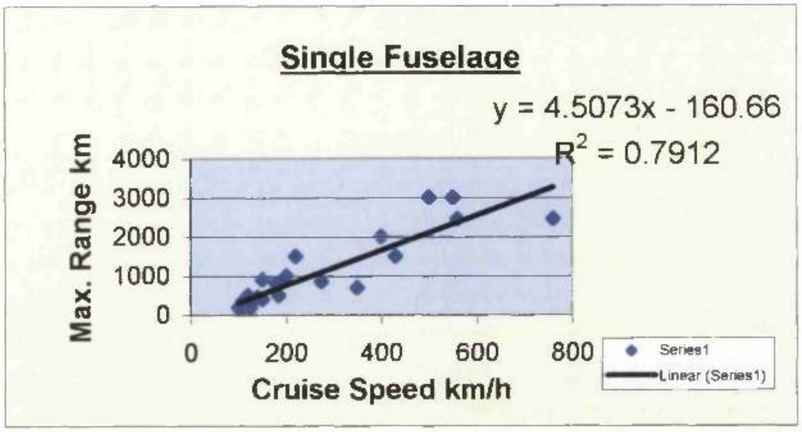

GRAPH 32

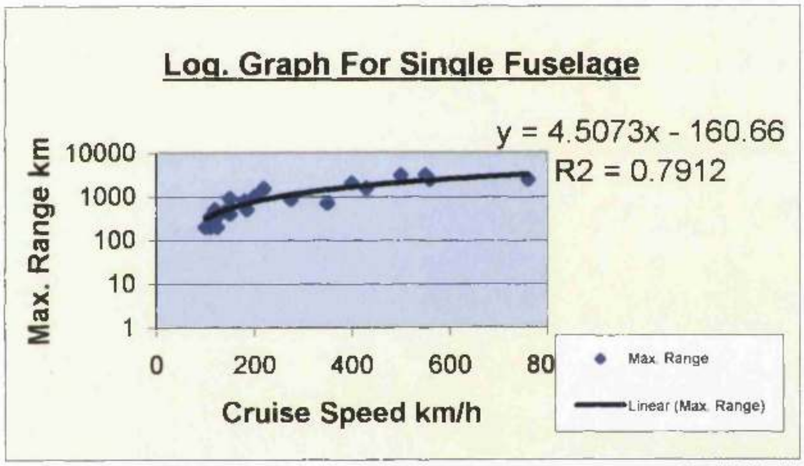

GRAPH 33

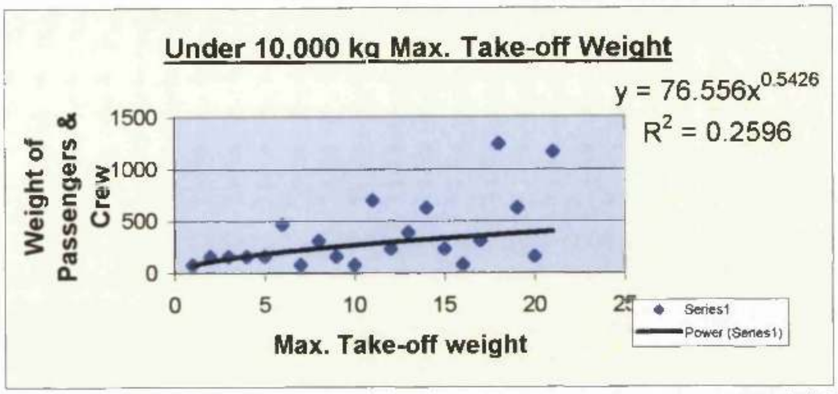

GRAPH 34

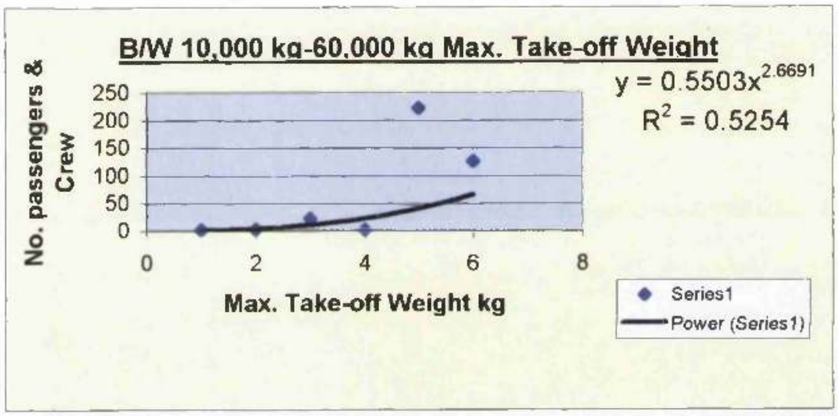

GRAPH 35

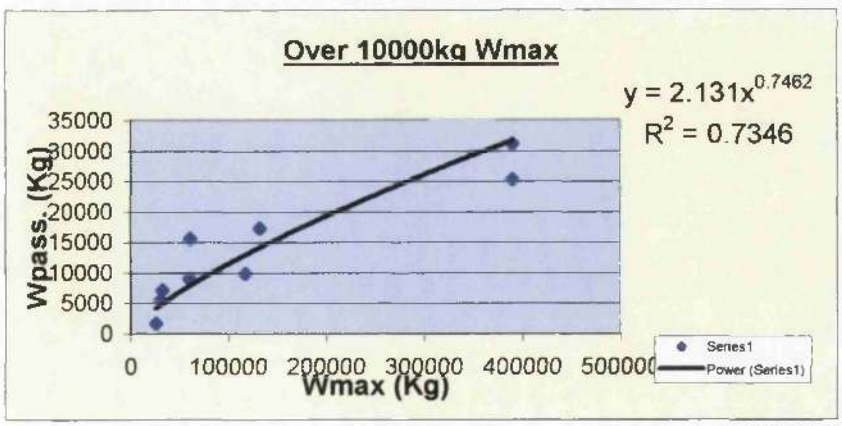

GRAPH 36

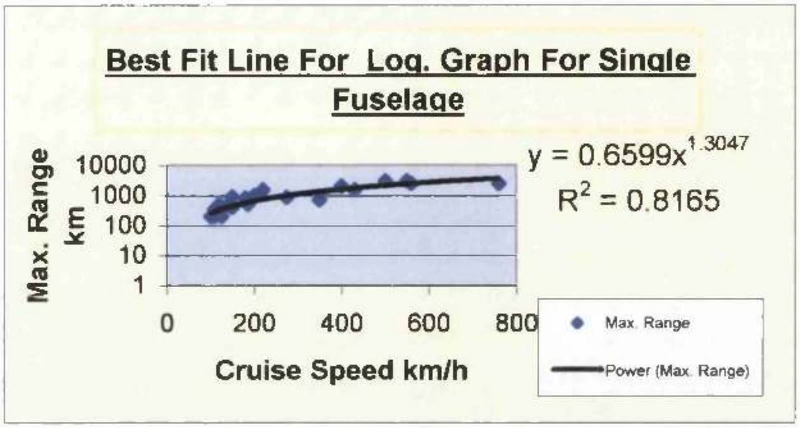

GRAPH 37

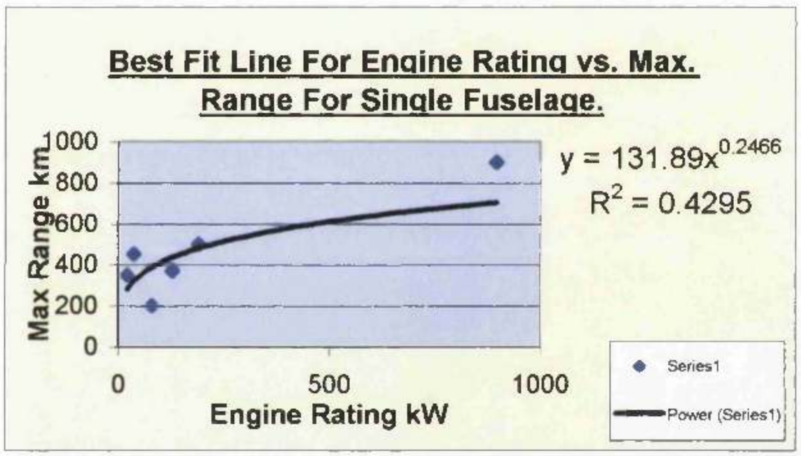

GRAPH 38

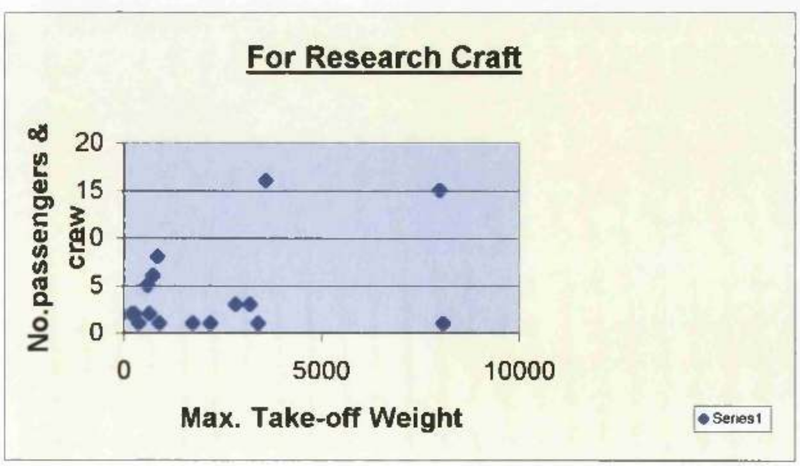

GRAPH 39

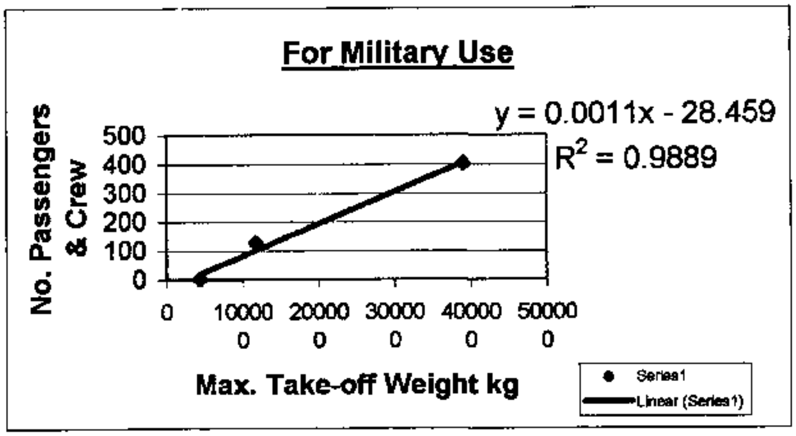

GRAPH 40

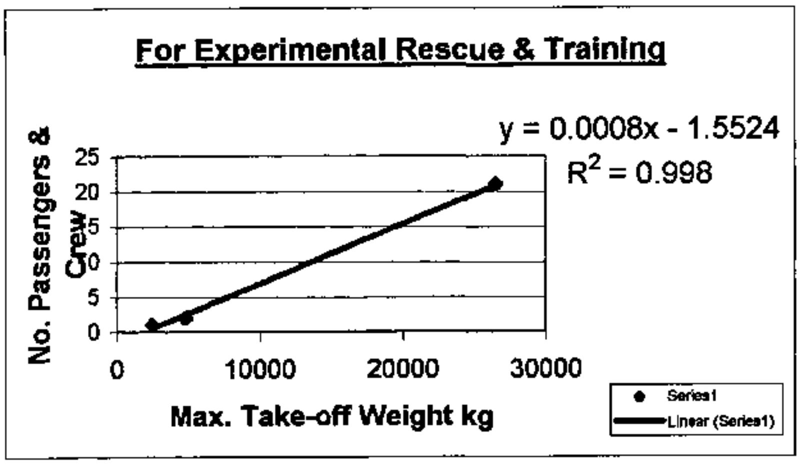

GRAPH 41

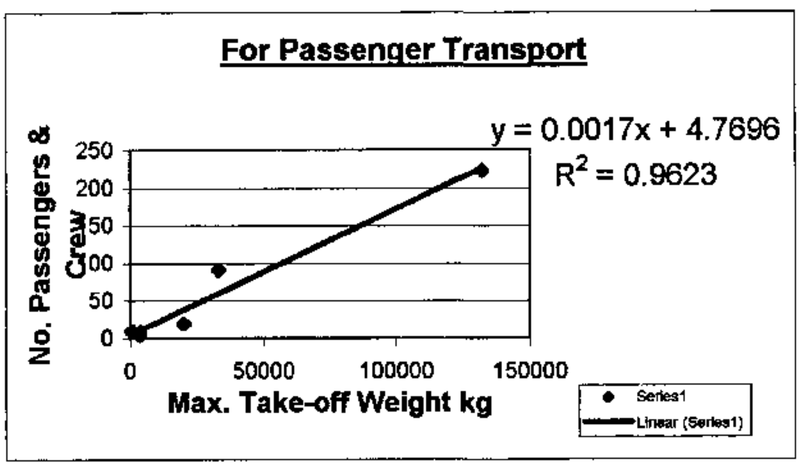

GRAPH 42

[Ref. 49] However, at the turn of the century C. Ader, performed experiments involving wings in ground effect for the French government. Unfortunately, after an unsuccessful demonstration of his Avion -3, financial support was withdrawn in 1897. Nevertheless, he persisted with his work and patented the concept in England in 1904.

During the development and testing of their early manned gliders in 1900, the Wright brothers frequently flew in ground effect often reaching an astonishing distance of one foot above ground level.

Wing-In -Ground Effect has been acknowledged and studied since the initialisation of aviation. The finest early representation of ground effect involved the Dornier DO-X seaplane. The DO-X seaplane was a large (56 ton) aircraft constructed by the Dornier Co., Germany, in 1929, which was in service in 1930-31. The DO-X employed ground effect in order to increase its payload and range during flights.

In 1932 a Finnish engineer, Toivo Kaario, also carried out experiments on a high-speed snow sleigh. In 1935 he developed the first successful RAM-Wing-Ground Effect vehicle. More details on this vehicle and on other experimental vehicles are contained in the next section of this paper.

Pages 49 - 59 in section 1.3.1 below are examples of WISE craft add need only be referd to if additional information is required by the reader on specific characteristics of designs.

1.3.1 EXPERIMENTAL WING-IN-SURFACE EFFECT VEHICLES

The initial triumphant developments of W.I.S.E. vehicles took place in Sweden, Finland and Northern U.S.A, where vehicles capable of skimming over snow covered ground, swamps, marshes and open water were investigated. Russia also commenced its development of vehicles in order to offer high-speed transportation to undeveloped sections of the country. These experimental vehicles are described in the following paragraphs.

***North European developments*:**

As discussed earlier, the first successful W.I.S.E. vehicle was an experimental, RAM wing, snow sled developed by TOIVO KAARIO in Finland in 1935.

Powered by a 16 HP engine

Carried one man over the snow

Travelled up to 12 knots.

In 1962, he developed the Aerosani no. 8

Capable of transporting two passengers

Travelled at 43 knots.

During the late 1930's, I. Troeng of Sweden researched and developed concepts involving both a 3 ton and a 500 kg water born Wing-In-Ground Effect vehicle, they were based on the "lying wing" principle and used a hydroski located aft for stability. Unfortunately, government funds ceased together with further developments when the vehicles became unstable during tests. The Aeroboat is shown in fig 2 and its known Characteristics are also listed. Once more, the reader is advised to refer to this report for further information if required.

Dr W. R. Bertelson of Neponset, Illinois, developed a series of Ram wing vehicles in the late 1950`s and early 60`s. The vehicles were designed to aid him in visiting his home bound parents in his rural medical practice. The GEM-3 is described below and in more detail in the report discussed.

A four seat vehicle

Capable of speeds up to 95 knots

Capable of travelling over snow or water

Dr. Bertelson is still developing Air Cushion vehicles but has discarded the ram-wing concept in favour of a gimballed, ducted fan that helps to control the lift of the craft.

In1963 the Kawasaki group of Japan commenced testing the KAG 3 catamaran waterborne craft. However due to it being powered by an outboard marine engine it was not capable of leaving the water surface. Due to their developments facing further problems, the project was eventually abandoned.

According to [Ref. 134], "Simulation on the behaviour of Wing-In-Surface Effect Ships", a W.I.S.E. vehicle is faster than any other marine vehicle as summarised by Hooker and Terry (1992) and Rozhdestvensky and Synitsin (1993). W.I.S.E.s are based on the same concept as a super high-speed vehicle for commuter use, as proposed by Kubo of Japan, where demand for high-speed marine vehicles stems from the need to improve the domestic transportation system. The Techno-superliner (TSL) is expected to take the role of a commercial cargo transport service to the Tokyo Metropolitan area in place of road vehicles.

With close reference now to the Date Bar Chart on page provided, it may be noted that the Russians commenced their construction on W.I.S.E. craft in the early 1960's and rapidly decreased the number constructed before increasing once more up till 1975. From this time, their numbers decreased once again and then attained a steady output for the next decade.

A list of these craft has been made available below:

Be-1, built in 1961, a test craft,
SM-1, built in 1961, a research craft, crashed in 1962,
SM-2, built in 1962, a research craft, for research on tandem design,
OMIIF-1, built in 1963, a research craft,
SM-5, built in 1963, a research craft, the prototype of the KM,
KM, built in 1963, a research craft, used to test various wing designs.
SM-2P1, built in 1964, a research craft for PAR

Although not inserted in the graph due to their exact dates not being given, the SM-3 and the SM-4 were probably built after the SM-2 and before the SM-5 and should be noted at this point.

It should be noted that all the craft in the above list were either research craft or used for testing purposes. In addition to this it should also be noted that no other countries built W.I.S.E. craft during this time span. (That is none that have not been mentioned in the graph constructed. If their were others, then they will either be mentioned in the section below, or have not been known about, by myself, as yet).

There were an additional three craft built by the Germans between 1966-70 which, similar to the above, were once again research craft, one of them was the SM-8, which was a 1/4 scale model of the KM.

As noted previously, although the numbers were less during the following five year period, five craft were built by the Russians and one by the Germans. Those built by the Russians during this time span are listed below:

E-120, built in 1971, probably a research craft,
SM-6, built in 1972, a predecessor of the Orlyonok, probably also used as a research craft,
VVA-14, built in 1972, used for anti-submarine warfare,
A-90-150
Orlyonok, built in 1973, used for troops transport and assault vehicle,
ESKA-1, built in 1975, used as an experimental rescue and liaisons craft.

As may be seen from the given information, significant progress had been achieved and the fewer craft produced were of more use and more successful. The majority of them were now of some use to the military rather than just being used for research.

Between 1976-80 two craft were constructed by the Russians and one by the Germans. The two Russian craft are listed below:

VVA-14M1P, built in 1976, a redesign of the VVA-14, used for anti-submarine warfare,
SM-9, built in 1977, used as a research craft.

Although yet another research craft was constructed, progress was once again made on an existing design, the VVA-14, resulting in higher efficiency and performance.

During the span of 1981-85, four craft were constructed, two by the Russians, one by the Germans and one by the Americans. The Russian W.I.S.E. craft are listed below:

SM-10, built 1985, used as a prototype of the Volga-2
SM-11, built in 1985, used as a research craft.

As may be noted, during this period, only two craft were constructed and were both used as research craft.

Between 1971-1975,the Germans produced a low, but steady output before shooting up in the number of W.I.S.E.'s constructed between 1986-1990. The Germans faced a rapid decrease in their numbers between 1990-91, which could have been affected by a decrease in their economic status as well as by the fall of the Berlin wall. However, it is encouraging to see that they have managed to increase these figures in this last decade.

Two of the craft constructed by the Germans are listed below:

TAFVII-1 Jorg 2, built in 1977, used as a research craft,
TAFVIII-2 Jorg 2, built in 1981, also used as a research craft.

As may be noted, due to this being the start of the German constructions of W.I.S.E. craft, the two, which were built, were both research craft.

During the five-year span between 1986-1990, five W.I.S.E. craft were constructed by the Germans and one by the Americans. The German craft are listed below:

Airfisch-1, built in 1987, used as a research craft as a cost-effective design,

Airfisch-2, built in 1988, used as a research craft, a re-design of the Airfisch-1,

Airfisch-3, built in 1990, used as a research craft and had increased harbour manoeuvrability,

Airfisch-8, built in 1990, aimed for commercial use,

Spasatel, built in 1990, used as a rescue craft.

As may be observed above, the Germans showed an incredible amount of progress in their constructions of W.I.S.E. craft and moved from research craft to rescue craft and finally to commercially aimed craft.

However, this incredible success was not continued and only three craft were built in the following decade. Two of which were used for research purposes and the other (The TAFVIII3-Jorg 6) which was used for inland waters.

By this time, the Chinese had also commenced construction of W.I.S.E. craft. However they merely continued their constructions for a decade before ceasing. Their construction period spanned from 1981 to 1990. They managed to construct two W.I.S.E. craft. They are listed below:

Ram WIG 902, built in 1981, used as a research craft

XTW-2, built in 1990, used as a research and rescue craft.

The Americans had proposed two W.I.S.E. craft designs between 1991-95. They were the

S-90-200, and the S-90-8.

However, neither have been constructed as yet.

The energy crisis of the 1970's brought about a renewed interest in W.I.S.E. technology because this technology had the promise of providing cost efficient craft to serve as large, long distance cargo transports (passenger service no longer being a viable role). Several new conceptual craft were proposed. To date, programmes to develop these craft have not been funded.

Meanwhile, a new generation of experimental craft, having the emphasis on ram-wing and par-wing concepts, has been constructed and tested.

In 1963, Dr. Alexander M. Lippisch tested his first "ramwing-in-ground effect vehicle" the X-112.
In 1964 Dr. Lippischs dynamic air-cushion vehicle was described by Gunston and proved to exercise an approximate 30% reduction of drag during flight when the speed was four times the original value. The speed varied from 10 m.p.h. to 40.m.p.h. proving that flying at high speeds in ground effect actually reduced the amount of drag created and it, therefore, became a craft of higher efficiency suitable for travelling long distances.

The following is explained better by Dr. Lippischs results, plotted on a graph, showing drag as a function of speed. This may be found on page 2 of the proceedings of the Twenty-First Century Flying Ships by the University of New South Wales, Australia 1995. Pictures of his designs may be found on page 38 of the same paper.

This design was tested in order to examine the stability problems. Further developments were undertaken in 1967 and the X-113 was then constructed. It could operate not only in ground effect but also could achieve a height of 100m. In ground effect it required 1/3 of the power it was supplied with and flew at its optimum performance at a height of half the wingspan [Ref. 91].

In 1963, the Kawasaki Corporation in Japan built a waterborne ground effect craft, a catamaran powered by an outboard marine engine, designated KAG-3. In 1964-66, the SM-5 and SM-8 were built and tested.

Less known W.I.G vehicles were developed in the former Soviet Union in the 1960's. Their designs were based on the Lippisch Antonov-2 as well as a Blanik glider. These soon developed into the Volga-2, which was designed by the S.D.P.P. design bureau. During tests it was noted that this craft exhibited extraordinary pitch stability.

It was then apparent that this advantageous characteristic was the result of an S-shaped wing. Although this type of wing is still in the process of being researched all around the globe, its success has resulted in a recent production model of the Volga-2 and high hopes for the future.

In the seventies the Russian Ekranoplan program continued and led to the most successful Ekranoplan so far, The 125 ton A-90.150, Orlyonok.

In 1973, another new development was the tandem W.I.G vehicle, the German Jorg. Also in Germany at about the same time, an aviation company called Rhein Flugzeugboch (RFB) bought Lippisch's patents and developed them. The largest Ekranoplan produced was the six seat X-114 that was also tested by the German military.

μ sky as a high-speed boat
by Syozo Kubo, Toshio Matsuoka and Teetuya Kawamura
From: 4th Pacific congress marine sciences technology
1990 1 I 220-7
Title: Development of a wing-in-ground effect marine craft, μ sky, as a high-speed boat.

It may be stated that ACV is a good method of transportation over water. We must remember the fact that ACV has its speed limit. ACV is lifted up from the surface by its air cushion. When its cruising speed exceeds the design limit air will be lost from the air cushion. This will result in loss of efficiency and stability. In practice, when the cruising speed goes below the design limit, variations in flight altitude occur resulting in a similar loss of efficiency and stability[Section 2.8.3]

1.5 W.I.S.E. FORECASTING

Despite their having no immediate pre-eminence over existing craft, they do present admirable possibilities for the near future. Consequently, there is a necessity for them to undergo change. Current propositions for their designs, are competing within the aircraft realm. Nonetheless, there is barely any optimism for them ever being as proficient as aircraft. W.I.S.E. craft, therefore, ought to compete with ships and hence, fill the gap in the Von Carmen-Gabrielli transportation graph located at the end of Section 1.3.

It has been proposed that in divergence to the first generation W.I.S.E. designs, the second generation be of two-mode capability. They are either to work as ships [Ref 21, 28, 40, 60], close to the sea surface, or like aircraft further from it. This new generation will consequently be fulfilling its chosen problem/solution requirements [Ref. 49, 52, 160].

Due to them taking-off from and landing on the sea, it is imperative that they embody ship attributes enabling them to accomplish their task. Thus they incorporate the indispensable use of an acicular bow, a common characteristic of ships, as well as large wing areas performing the function of acquiring a sufficient air cushion to elevate the craft high above the sea surface[Appendix A]

[Ref. 75 - 79, 107]. In relation to future W.I.S.E.s designs, they will possess a unique arrangement, which although physically different to customary ships, will enable them to transform in to a prevalent instrument of marine transport. The new conception of W.I.S.E. craft will not only own marine aptitudes but over and above these credentials, they will attain a higher standard of safety than any conventional aircraft. This places them in an incomparable situation.

Miscellaneous W.I.S.E. designs will be contrived in the future [9, 88, 133, 152, 185]., principally substituting for inefficient air travel over a short distance. The larger designs would compete with long haul flights and ships. This would be due to their competence in providing transmarine flights, creating economical and exceptional methods of transportation for passengers and cargo.

Returning to the S-90-200, the focal point of this project, it may be said that, despite it not yet having been put into production, it is a second-generation W.I.S.E. craft. Nevertheless, its futuristic plans do not end there. Its evolution will later develop, resulting in a super heavy weight W.I.S.E. similar to the 750 tons Ekranoplan of the 1970s.

The 750 tons ekranoplan, which may be found in the Krylov Shipbuilding Research Institute, has the ability to perform transatlantic flights, the principal objective of W.I.S.E. designs. It had a payload of 250-300 tons, travelled at a speed of 25 km/h, at a height no more than 3-5 meters above sea level. With new designs being aimed towards fulfilling these specifications, immense research is focused on providing new successful concepts, which would ultimately solve existing problems.

NATO is currently discussing a task force of future W.I.S.E. craft. The discussion is concerned with the use of W.I.S.E. craft in environmentally catastrophic incidences at sea, such as oil spills, and rescue operations. Simultaneously, consideration is being given to providing a new means of shuttle launch from super heavy W.I.S.E. craft. This would ultimately resolve some environmental threats.

Hydaer

FIG. 14

Hydaer Technical Data	
Length	55 m
Width (span)	110 m
Cruise speed	220 km/h

S-90-200

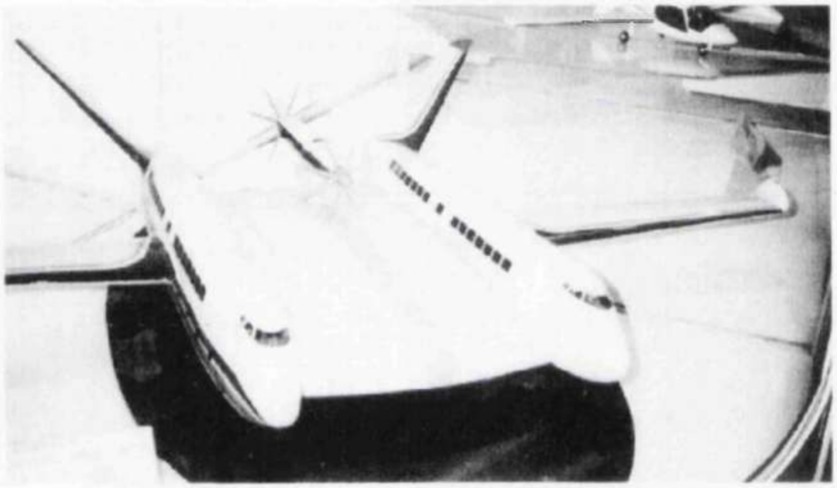

FIF. 15

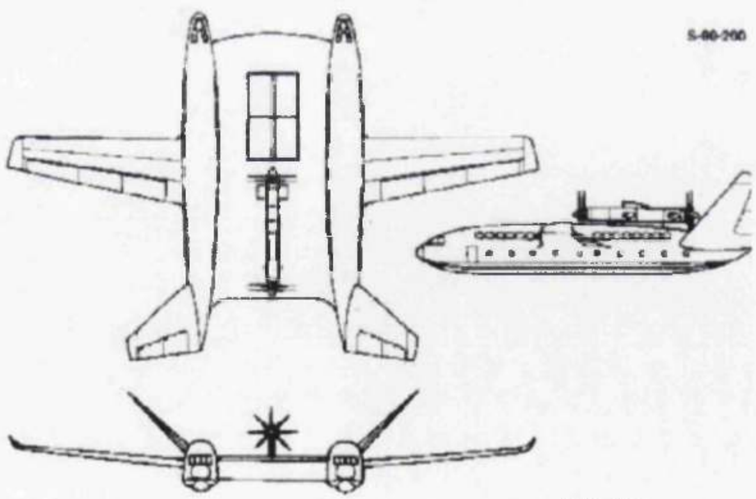

FIG. 16

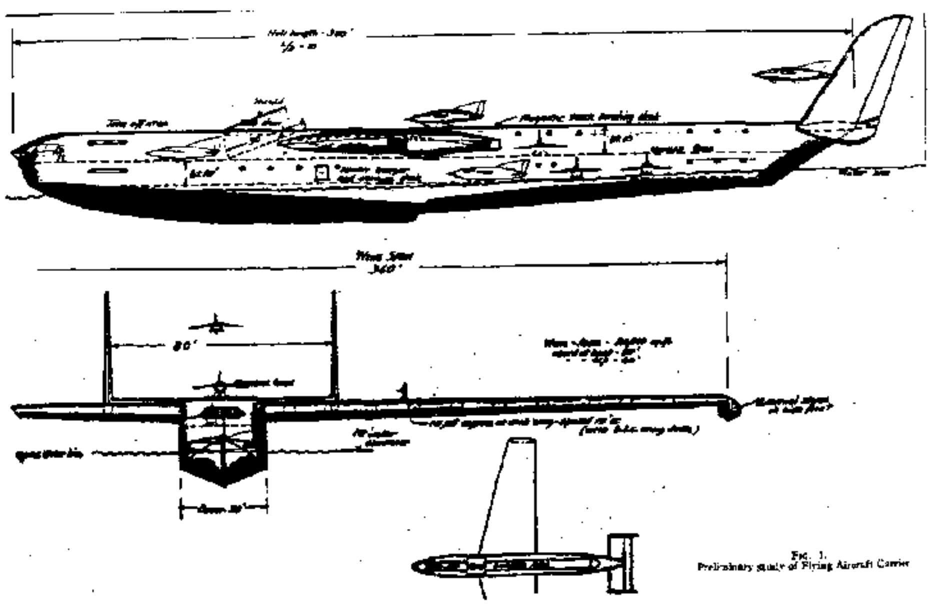

FIG. 17

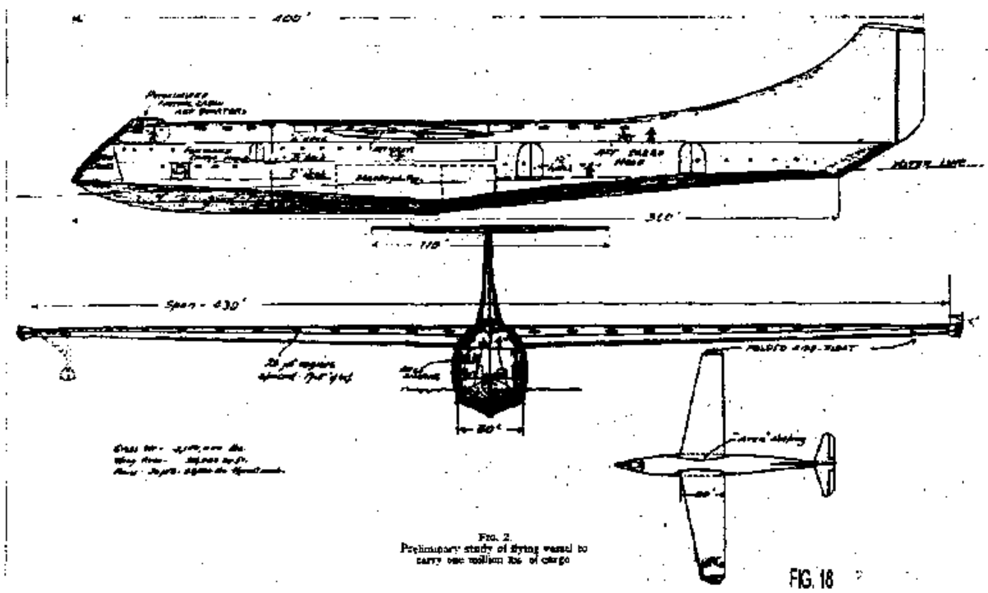

FIG. 18

2.0 CERTAIN W.I.S.E. DESIGN ASPECTS

2.1 Aircraft Disadvantages:

Aircraft are expensive

Aircraft control requires a high degree of skill and training.

Maintenance of aircraft is intricate and costly.

Accidents tend to become catastrophic.

Airfield maintenance is expensive and difficult to monitor.

2.2 Characteristics of W.I.S.E.'s:

In the theory of the aircraft wing, one knows that surface effect increases lift and reduces drag.

W.I.S.E.'s are craft which can fly at only 10% of their aerodynamic dimensions, which is generally wing span or chord length due to the design preference for large chord lengths. They can only travel on a small layer adjacent to the surface. Its movement is restricted in a two dimensional layer. From another point of view, this limitation is not always a demerit. Due to its restricted motion many mechanisms of the W.I.S.E. may be simplified. Its engine is, for example, simpler than an aircraft's. It may be as simple as a car engine. There is also no need for a pressurised cabin.

By simple mechanisms we will be able to construct a W.I.S.E. at reasonable cost. Its maintenance will be relatively simple and again at a low cost.

Operational running costs of a W.I.S.E. are also lower than for an aircraft. A wing-in-ground effect has better efficiency than that at a high altitude. This means better and cheaper fuel consumption. The cost of the pilot training is much lower. And the maintenance costs are also lower.The quasi 2-D motion of the W.I.S.E. is also easier to control than the 3-D motion of aircraft; the motion resembles that of a car or a boat.
[For Desing Spects of WISE craft Refer to Ref. 11, 20, 27, 29, 36, 53, 77, 107, 142, 175].

2.3 Classification of W.I.S.E.s:

2.3.1 Flying Boat Type

A craft of this type has a hull, main wing and tail units separately, just like an ordinary flying boat. This type is suitable for a high-speed craft, because the wing area is relatively small. We can design the main wing without a serious interaction between other elements of the craft. The type is thus suited to a large high performance craft.

2.3.2 Lippisch Wing Type

This type has a special wing, the so-called "Lippisch Wing", whose plan form is an inverted triangle with a negative dihedral angle. The inventor of this wing was Alexander Lippisch, the famous designer of sail plane and aircraft, especially the inventor of the delta wing. A very high performance was reported on the aerodynamic characteristics ~~of the wing. An experimental craft was first constructed~~ in the USA. Development of this type of craft has continued in West Germany and in the USSR. CLST has been continuing their effort on developing W.I.S.E.s of this type in China

2.3.3 Tandem Wing Type.

This type has two wings, the front wing and the rear wing. It has no horizontal tail wing. Gunter Jorg, who was a designer of vertical take-off and landing aircraft in West Germany, has investigated this type.

2.3.4. Ram Wing Type.

This type has a big wing extended from the nose to tail of the craft. This is the simplest type of W.I.S.E.. It has relatively large wing area. Thus it is suitable for a slow craft. One of the famous W.I.S.E.'s of the ram wing type is RAMESES-I, which was developed in the USA in 1975. This craft can even today, satisfy our requirements except for its pitching stability. The problem of W.I.S.E. of ram wing type from the time of the first

W.I.S.E. by Kaario. Many experimental crafts including RAMESES-I, have been abandoned due to the difficult problem of controlling the pitching motion. This is a real problem for W.I.S.E. craft in practical use.

When one considers a craft of this class, one should keep in mind that more severe requirements will be imposed on developers. One of them will be the economic efficiency; one must have knowledge about performance of the W.I.S.E. wing. This suggests to us that systematic data on wing sections must be piled up just as the data of wing sections of aircraft has been accumulated. It is not so easy to obtain such data in short periods of time. Numerical simulations will help us to find an optimum configuration of a W.I.S.E., if one can develop a suitable method of simulation.
The other one difficult problem will be to decide the operational limits and to improve the ability to operate over rough water and in different sea states.

One can disregard many of the W.I.S.E. operational problems. These problems are thought to be unavoidable in a machine of revolutionary new characteristics. They will be solved step by step by the efforts of persons dealing with each individual problem in detail.

2.4 CURRENT W.I.S.E. ACHIEVEMENTS

2.4.1 Primary credentials

Capable of achieving extreme aerodynamic efficiency when flying in ground effect.

Due to its advantageous amphibious characteristics it proved to have a higher degree of safety when compared to conventional craft.
Evidence supporting the capability of W.I.S.E. landing and taking off from water has been made available.
The PAR WIG concept has been found to offer an increase in hydrodynamic efficiency.
They acquire an ability to ascend to cruising altitude with less energy than conventional aircraft.
Reduce their weight by not requiring a pressurised cabin.
Due to them becoming cheaper to run as their size increases, either additional passengers may be carried or each passenger may have additional space resulting in travel of increased comfort.

2.4.2 Disadvantages.

Although W.I.S.E. craft do have their advantages, similar to all transport vehicles, they unfortunately also have disadvantages, they may be found below.

Due to the immense power required for adequate PAR effect, the weight of the machinery adopted for such tasks increases the overall weight of the craft, reducing the aerodynamic efficiency and stability.
Their immense noise pollution,
The high take-off speed required
The costs involved with their construction,
W.I.S.E. crafts increase in efficiency as their size increases.

The safety problems caused by their requirement to fly at the lowest possible altitudes for fuel efficiency. This may prove to be incredibly dangerous when the waters are not calm.

Their inability to fit into existing regulations,

Their deficiencies when flying over rough waters are additional reasons, which cause dissatisfaction,

2.5 W.I.S.E. Efficiency.

2.5.1 Aerodynamic Efficiency

The aerodynamic efficiency of W.I.S.E. vehicles is primarily due to their capability of travelling in close proximity to a horizontally parallel smooth surface. When these, relatively new, concepts are compared to other existing methods of transportation, it may be noted that they corroborate a high lift to drag ratio conjointly with a slow speed as contrasted to conventional craft of a similar size. However, they do have a similar efficiency to any modern heavy aircraft flying along the same path.

The fact that W.I.S.E. craft require shorter and wider wing designs is an additional reason for prohibiting the mounting of PAR equipment on top of the actual wing areas to blow the air directly under the wing. It is for this reason that W.I.S.E. craft are not as efficient as conventional craft. It is possible that new ideas may be put forward in the future, resulting in highly competitive W.I.S.E. concepts

2.5.2 Time Effective

W.I.S.E. vehicles are known to travel at great speeds unlike ships. If the average speed of a conventional ship was to be 36 km/h and an average W.I.S.E., (not a super heavy weight), travelled at 500 km/h, then it could be stated that a W.I.S.E. craft travelled 14 times further in one day, than a ship.

2.5.3 Fuel Efficiency

There are two similar theories involved when considering the fuel efficiency of W.I.S.E. craft. One refers to the Von Karman - Gabrielli diagram shown at the end of this section. With regard to this diagram, it is stated that any vehicles close to the technology line are 'fuel efficient'. This is primarily due to the fact that it is theorised that as higher technology is adopted, these technological advances bring about a reduction in fuel consumption.

However, this is contrasted with the fuel efficiency diagram observed at the end of this section by the E.A.Aframeev ship building Research Institute. They state that even though first generation WIG craft did have incredibly high fuel efficiency, "the second generation Ekranoplans may have a fuel efficiency closer to that of a conventional air craft. This would be due to the simultaneous increase of weight efficiency and more effective use of the "ground" effect. [Ref. 40].

2.6 Effective Design

In order for a W.I.S.E. craft to have an effective design and consequently fulfil all Product Design Specifications, it must have a primary design requirement. This must deal with the craft's ability to fly above a specific wave height. This in turn determines their capability of landing and taking-off from that sea surface. It is true that, in this respect, W.I.S.E. craft do have extreme similarities with conventional hydroplanes and therefore may adopt their advantageous characteristic capabilities in overcoming similar problems.

2.7 Power Requirements

Although one could say that due to the W.I.S.E.s low fuel consumption, relatively similar engines would be required such as those used for conventional aircraft designs. It is the taking off procedure, which incorporates the majority of the predicaments involved. Due to the immense power required for take-off, a vast amount of thrust generated by an incredibly powerful power plant would be imperative.

2.8.0 Skirt Drag.

2.8.1 Introduction

Due to the S-90-200s utilisation of a skirt enclosing the static pressure below the centre wing section, it is believed that the following section is of relevance in explaining the reason for retracting the skirt during flight.

The section is a brief description on skirt drag during the early stages of take-off, if further information is required on this section please refer to the "International conference papers on Hovering Craft Hydrofoils Advanced Transit Systems Amsterdam 5-8 November1998 page 169" The following data is based on this paper.

4.8.2 ACV Skirt Drag

The skirt drag of the common ACV, when travelling over water. R. Murao, Dr Eng. from the Ship Research Institute, Ministry of Transport, Japan, has proved that, for such a craft over calm water, the skirt drag is determined by both the Froude number and the cushion pressure which has been shown in the diagram provided. In ACV the skirt plays a significant role in the hydrodynamic drag component but is difficult to measure directly.

2.8.3 Utilisation of ACV Techniques.

[Ref. 165, 166, 178, 180]. Through the course of the succeeding section, it may be noted that characteristics of W.I.S.E. craft, primarily resembling ships and then air craft, is bridged by adopting ACV attributes. It may be of assistance for the reader to refer to the illustrations in this sub-section. They are shown to clarify the connection between W.I.S.E. and ACV craft [Ref. 91].

In addition to this, according to [Ref.157] W.I.S.E.s have the advantage of being capable of lift-off from water surfaces. They create water runways in order to achieve their required speed for take-off. It is preferable for a W.I.S.E. craft to have a high wing loading when a high speed is utilised. This is only the case, however, when the appropriate height-to-chord ratio, angle of attack and stability are present. It is also the case that three times the cruising power is required for the take-off procedure. This is in order to overcome what is termed the 'hydrodynamic humpdrag'.

In order for a W.I.S.E. craft to avoid the high drag, produced by the dense water during the early stages of take off, it must lift-off from the sea surface. This is achieved by building an air pressure below the wing areas. Although this may be achieved with the use of PAR mechanisms, a more efficient and effective way of accomplishing its task is to adopt a skirt design, surrounding the edges of the centre wing panel. This modifies the dynamic pressure to static pressure, aiding W.I.S.E. lift-off procedures.

Studies on the X-113, using an air cushion, have been carried out by the Fischer Flugmechanic Company. Hanno Fischer developed the 'hoverwing-technology' in order to increase the vehicle's efficiency and decrease its power requirements at take-off. The Fischer company also investigated the use of hydrofoils on the X-114 WIG craft. These caused a static air cushion to build up between the floats, aiding take-off. Once in cruise mode, the vehicle would operate using a dynamic pressure build up, resulting in a high lift to drag ratio. Due to the difference in water and air density being 800:1, it may be stated that the drag reduces as the distance from the water surface increases.

The main advantage gained by solving such a problem in this manner is that both aerodynamic and hydrodynamic problems, such as hydrodynamic drag, are overcome.

An excellent breakthrough was achieved by the Fischer Flugmechanic (FF), when it developed the Hoverwing - Technology" aimed at reducing the lift-off power required for W.I.S.E. craft. Later, the "Hoverwing 80" was developed. It had the ability to transport 80 passengers at a speed of 100 knots.

The Hoverwing Technology uses a small portion of the propeller slipstream to create a static air cushion between the floats. This is similar to the concept adopted for the S-90-200, which may be found in the database provided in section 1.

In this example, the air is trapped under the centre section of the craft raising it efficiently above the water surface. The displacement of the Hoverwings floats was reduced by 80 %, increasing its efficiency and ultimately reducing the power it would require. A close achievement could easily be attained by other craft choosing to adopt this method

The Thrust-to-weight ratio diagram provided clearly exhibits the prerequisites of all transport media. A seaplane or a very fast boat demand high thrust for cruise. Unfortunately, W.I.S.E.s can only take-off at a zero angle of attack. For this reason designs in general accomplish a 1:4 ratio of thrust-to-weight. However, the use of Hoverwing technology a 1:6.5 can be achieved. The future prospects of such technology indicate that a capability for W.I.S.E.s to achieve a 1:8 ratio is imminent.

The figure at the end of this section shows the relationship between different types of transport technology up to now. With the use of this diagram, it may be seen that the Hoverwing Technology is the bridge between the W.I.S.E. and the ACV.

Various marine vehicles adopt different methods in order to produce a static air build up aiding in the reduction of drag. However, these vehicles, unlike W.I.S.E.s, do not leave the surface of the water. For this reason, it may be stated that W.I.S.E.s could easily compete with such craft due to their overall efficiency.

The retractable hydrofoils of the X-114H improved the seagoing ability during rough sea circumstances compared to theX-114, which did not incorporate hydrofoils. However, the drag at lower hump-speed could not be reduced. The power –augmentation as tested on the Airfisch-3PA, showed improvement in take-off drag. Nevertheless, it automatically became a more complex, hence more costly, design. A suitable and appropriate take-off mechanism should be chosen only after careful consideration of both its characteristic and economic requirements.

[Ref. 157] by Hanno Fischer, states that the hoverwing is the link between the displacement vessel and the helicopter, while also being the link between hydrofoils and aircraft. It is for this reason that it may be stated that the hoverwing technology is the link between ACV and W.I.S.E.

Although there is an apparent advantage in using a static air cushion, which, results in a smoother take-off and landing procedure, there is a disadvantage to this design configuration when catamaran floats are included. The reason for this is due to the requirement of a certain volume of air being present. This is in opposition to the high speed planning requirements.

Nevertheless, this was improved upon by the Versuchsalt für Biennenschiffbau e V (VBV) in Germany. In addition to this aerodynamic data may be obtained using a tool developed by FF called the 'circuit test' which is described further in the reference by Fischer, the reader is urged to refer to this paper for further information if required.

2.8.3.1 Conclusion

It may be concluded, that a static air cushion through the use of Hoverwing Technology, reduces the take off drag considerably, so as to achieve similar outcomes as an SES. Once take off has taken place, the skirt would be retracted allowing the static air pressure build up to change into dynamic air pressure, this result will greatly aid the craft in achieving ground effect.

Although, a skirt is included in the design of the S-90-200, it is imperative that the skirt retracts during flight. Reasons for this have previously been discussed. Never the less, during the take-off stage when the skirt is down, skirt drag is inevitable. For this reason, skirt drag has been discussed separately later in the report.

W.I.S.E.'s have the potential to fill the high-speed gap remaining between aircraft and other sea going transportation methods, however this would require the planning of routes, sheltered terminals and other various aspects relevant to the subject.

Wing-In-Surface Effect vehicles must complete each voyage with no intermission in order to be efficient. An emergency landing or a take-off is hazardous when in open sea conditions, except when a very calm sea state is present. Nevertheless, commercial aircraft achieve this non-stop voyage requirement with a very high degree of reliability.

In addition to this, it is also hazardous for such vehicles to fly round ships and other obstacles. This has been proven to be a problem for Air Cushion vehicles and the latest generation of High Speed Craft, due to there being a constraint on route planning, which necessitates long distances for turn-round time. However, it must be noted that these distances must be kept to a minimum in order for such vehicles to be competitive with air travel. Terminal points should be conveniently situated both for passengers and for cargo in order to provide an advantage over Flying boats which have more restrictions placed on their terminal location.

[Ref. 97] Nevertheless, early commercialisation of W.I.S.E. vehicles could establish an enduring market dominance with powerful W.I.S.E. designs, company planning and operation. The focus must lie in choosing its base for operations. This entails finding a suitable market and route where people require transport at both ends.

Airfisch 1

Photo: Fischer Flugmechanik

FIG. 19

flight and therefore registered as a boat instead of an aircraft. This is also the main difference with the X-112, X-113 and X-114. In 1987 the first prototype, the Airfisch 1 was completed. The concept was proven during countless test flights on Lake Baldeney in Germany.

Airfisch 2

FIG. 20

FIG. 21

SeaWing International

FIG. 22A

FIG. 22B

FIG. 22C

Top: Dr. Alexander Lippisch's new X-113 Am Aerofoil boat during demonstrations on Lake Constance. One of the first full-scale wing-in-ground-effect machines to be built outside the Soviet Union, it takes off and begins to skim above the surface at 31 mph (50 km/h)
Centre: Seen in this photograph are the anhedral delta wing and the dihedral tips outboard of the two wing floats. Power for the craft is supplied by a single 40 hp Nelson H63-CP engine
Bottom: X-113Am taxying across Lake Constance. Although the craft normally flies at heights up to 5 ft (1.52 m), it has attained an altitude of 328 ft (100 m) during flight tests out of ground effect

FIG. 23A

ESKA 1

The ESKA 1 is a two-seat Lippisch type ram wing vehicle, which is employed as an experimental, high speed rescue and liaison craft on Russian inland waterways. It is powered by a 22 kW M63 motorcycle engine. The maximum flying height is about 10 m, but the cruise height is 0.3 to 1.5 m, depending on the wave height.

The ESKA first flew in 1973 and four had been built by 1975. Different variants were being developed, but unfortunately no more information is available. It is assumed that these developments were abandoned in favour of the other Ekranoplan concepts. The letters ESKA are a Russian abbreviation for Ekranoplan Amphibious Lifeboat.

ESKA 1 Technical Data	
Length	7.55 m
Width (span)	6.90 m
Height	2.50 m
Max. take-off weight	450 kg
Range	350 km
Cruise speed	110 km/h

FIG. 23B

ESKA 4

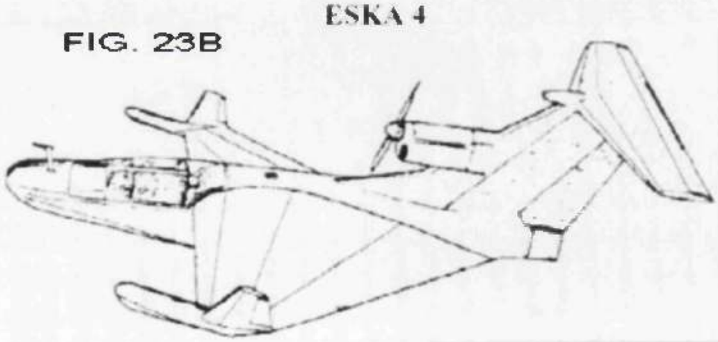

2.8.4 The High Autoplane Maritime

The first design, adopted the use of foils, the second hydroskis and the third an inflatable parasol delta wing to increase dynamic lift. This later design became triumphant and was chosen for extensive examination. It became the first of its kind and implemented the use of inflatable catamaran hulls.

Trials initiated in 1971, the craft's astonishing success determined by its new design. The normal outboard motor was discarded and in its place a raised air propeller was incorporated. This characteristic may also be observed in the S-90-200 design to be found at the end of this report titled S-90-200. It is used to elevate the craft by utilising the thrust gained. This provides the means of overcoming obstructing obstacles and waves.

Once this reached an acceptable level, the ram-wing design could be amended for improved efficiency. In 1973, the normally outboard wing surfaces were located inboard on the prototype. This was to prevent damage being incurred during flight. This craft was a 1/3-scale model of the Hennebutte Autoplane Maritime ram-wing ACV.

FIG. 24A

-third scale dynamic model of a Hennebutte Autoplane Maritime ram-wing ACV. The proto-, which was due to start its trials in the late summer of 1973, has its lifting surfaces inboard of the twin hulls to reduce the possibility of damage

FIG. 24B

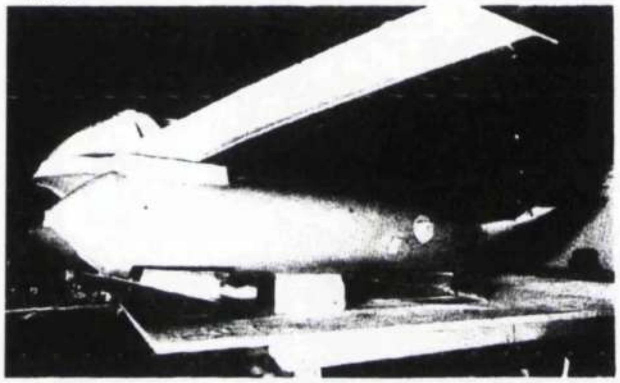

se-up of the Autoplane Maritime model showing the inflatable hulls and the planing foils beneath. Foils of this type are a feature of the Hennebutte series of high speed dinghies

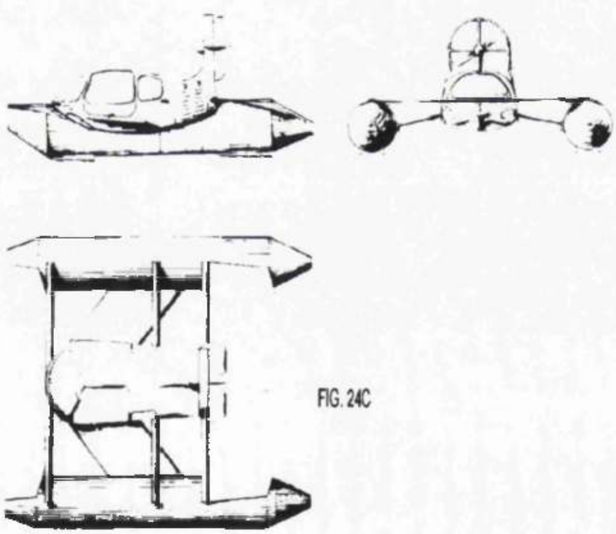

FIG. 24C

General arrangement of the HGH 77 Autoplane Maritime

2.9 DESIGN OF W.I.S.E. VEHICLES

[Section 1 - 2.8]Due to the evolutionary change in society there is a requirement for easy transportation methods which are feasible, consume minimum customer time and are available at reasonable cost. Marine transportation, in particular has been developed, to a great extent, in providing solutions to such needs. However, air travel still remains an alternative solution which, although it costs more, consumes the least time and takes into account the great comfort of the passengers, even when travelling in 'economy' class.

As previously stated, WISE (Wing-In-Surface Effect) vehicles fill the gap in transportation between air and sea travel. For this reason, as stated in [Ref. 14];

A W.I.S.E. vehicle is a participating nomination for future super high speed marine craft which would prove itself to be of a higher efficiency than air vehicles due to its ability of sustaining ground effect flight. During cruise, W.I.S.E.s fly by using dynamic lift caused by the pressure build up on the wing sections. This is caused by the close proximity of the boundary to the vehicle, namely ground or surface effect. It is for this reason that numerous conceptual configurations of W.I.S.E. craft have been developed over the years. Nevertheless, the safety, economy and impact loads caused by waves are topics which, must be thought of with care.

Prior to commencing the primary stage of design, evaluation of the weight, performance and stability must take place. Some of the characteristic design specifications which have to be considered according to reference (above) are;

The size and design of the main wing for adequate surface effect,
The size and design of the tails for longitudinal stability
The size and design of the fuselage(s) for attaining hydrodynamic efficiency.

In addition to this, analysis took place in the form of a research project by the Ship Research Institute of Japan on the safety of WISES. Due to a computer aided design

(CAD) system for W.I.S.E. vehicles having communal characteristics to that of airplanes, such as aerodynamics caused by ground effect and hydrodynamics, the direct operating costs (DOC) of W.I.S.E. craft were evaluated using those methods normally allocated to air vehicles.

In order for one to design a W.I.S.E. vehicle, it is necessary to simulate either by means of a mathematical configuration or a model craft, the boundary representing either a solid or a fluid surface [Ref. 16]

Two and Three Dimensional algorithms and results are presented, where the stability, increase in lift and maximum lift of the design process is discussed. The corroboration is achieved through wind tunnel measurements at wing sections. Various wing designs are demonstrated. The control which the geometrical parameters have on the aerodynamic characteristics, flight stability and overall performance is presented. The means in which this takes place involves the initial design of a wing configuration for an 80 seat craft.

As a means of achieving a W.I.S.E. design, it is essential to use dependable computational models in order to forecast the aerodynamics involved. Stability is responsive to lift and lift coefficients, drag, drag coefficients and momentum. It is for this reason that those are the parameters investigated in this report through the use of Computational Fluid Dynamics. A precise result for the aerodynamics is attained using the Navier-Stokes-Solver, while an alternative approach involves Potential Theory.

As stated in the later section as well as in this reference, aircraft methods and results should and have been used as a guide and a starting point in order to attain effective ground effect results.

2.10 WING CALCULATION AND DESIGN

It was thought that the following could not be said in a better way than [Ref. 16];

The vortex lattice method

This technique adopts the use of vortices on the camber line of the wing. The strength of the vortices is obtained using the normal condition on the camber line and the Kutta condition at the trailing edge (as boundary condition). The centre plane is treated as a symmetry plane which ultimately decreases the size of the resulting equation. The ground is modelled as a stream plane
The influence of the ground is accounted by the mirror image method.

Mirrored image method

Schlichting (1985) investigated the influence of the exact position of the forces on the wing. The free vortices are assumed to be in the direction of the onset flow. The forces are computed at the place of the vortices with the corresponding local velocity using the formula of Kutta - Joukowski.
$F = v \times \Gamma$

Even for unconventional wings and wing configurations the numerical convergence of this method is proven. With the vortex lattice method, a quick and reliable algorithm is available. The effect of geometrical changes to the aerodynamic characteristics could be estimated easily.

2.10.1 SURFACE DISTRIBUTION OF VORTICES

The surface distribution method is based on the Potential theory. The singularities are vortices on the surface of the wing. Green's theorem states that the use of closed vortex rings of invariable strength is comparable to a dipole distribution on the exterior.

The pressure distribution on the surface is attained using the Bernoulli equation with local velocities. The force and moment coefficients are found through the integration of the pressure distribution. While the lift and moment coefficients show a good accuracy the drag coefficient could not be computed accurately enough. This is mainly due to the finite number of panels in the region of the suction peak, which could not be sufficiently resolved [Ref. 16].

2.10.2 CONCLUSION

The study illustrates that these Potential computing models are a feasible means of designing and developing a wing-in-surface effect vehicle. Depending on the chosen optimising function, profiles may be developed. The impact of alterations in the wing geometry may be calculated using the vortex lattice technique. Furthermore, adopting the surface distribution approach may help to develop a more precise wing.

By interrogating the constructed database it became relatively easy to process all given information from previous designs. This formed a convenient starting point for this new design and provides an approximate means of checking a proposed solution.

For W.I.S.E. craft validated designs are rare. However the many available conceptual designs provide another source of this type of information. The distinct trends exhibited in the database suggest that this information is of significant value. The database constructed aided in the development of a new design and it, therefore, may be stated that it will be of use to future designers.

2.11 Wing Aspect Ratio

An additional paper which included various informative and detailed information was [Ref. 14], which discussed the following points:

Although, higher drag is induced while the proximity between the aerofoil section and the surface decreases, comparatively high lift is attained.

As the wing loading factor increases, the fuel costs also have a tendency to increase when the height is kept constant.

A lower loading factor, less than $300kg/m^2$, is preferred when there is a lower cruising height involved due to greater surface effects.

The lighter wing loading factor is preferred in order to attain a lower landing speed.

A loading factor of less than $300kg/m^2$, seems to be required in order that the W.I.S.E.s of this size may possess seaworthiness in up to 3m. wave height.

A small aspect ratio wing can be used for WISES, unlike aircraft, because a relatively high lift due to the surface effect can be achieved for small aspect ratios.

A high aspect ratio wing is preferred.

Considering the risk of contact with water in the heel condition and the accumulative lift due to PAR effects, the smaller aspect ratios are considered better.

If the aspect ratio is 3, good efficiency is expected in the case of a 3m cruising height but less efficiency for a 6m height. For this reason an aspect ratio of 4 was chosen in the latter mentioned paper.

As stated in [Ref. no.6 from Ref.14], a cambered and thin wing section is suitable for the wing-in-surface effect.

2.11.1 THE FORCES ON A LOW ASPECT RATIO WING

A model wing was tested with the ground plate and using the image technique to compare the results from the two methods. [Ref. 23] shows the variations of the lift coefficient, Cl, and the pitching moment coefficient, Cm, (about the quarter chord) with height of the trailing edge, h_{TE}, and incidence, α. The correlation proposed by Sullivan is also shown (please refer to Owden in References), which suggested that for positions above the line a method to remove the boundary layer should be used.

ENGINE AND PROPELLER CHARACTERISTICS

Design of a new engine is too expensive considering the small size of the WISES market. The reciprocal engine has a relatively low power to weight ratio, and is impossible to mount on the larger W.I.S.E. craft. The turbojet engine has a reduced efficiency at low altitudes. A turboprop was selected for the design of that paper [Ref14]. The required horsepower is defined as sufficient to overcome the hump resistance and to enable take-off.

According to [Ref.no5 from Ref. 14], even at the hump speed, the WISES should have 0.1g-0.2g acceleration in order to take-off safely.

2.12.1 Tail Wings.

Due to limited data on tail wing designs for W.I.S.E. craft, in that paper[Ref.no5 from Ref. 14], examinations of practical stability using the DTACOM method from reference no.7 was carried out.

A large vertical tail area is desirable for WISES to have stability in lateral wind

They must also have suitable manoeuvrability, considering the small allowance for the bank angle when turning.

2.12.2 Other items

Hydrodynamic performance and stability which shifts forward.

The same engine horsepower as for a seaplane is required to overcome the hump in the resistance curve and to obtain the take-off speed

A W.I.S.E., which flies close to the surface, takes advantage of the extra lift present. Also, it should overcome the longitudinal instability.

Not necessary to have a high aspect ratio wing due to the ground effect.

Pressurisation of the cabin and the landing gear are not required.

Less fuel is used since they do not have to climb to high altitude.
However, drag due to external configuration and extra weight due to the reinforced fuselage design is included for hydrodynamic performance and water impact forces.

Efficiency of jet engines decreases as they operate at sea level, and treatment is required to prevent the harmful effects of salt-water spray.
Ducted propellers could be used to improve the efficiency and reduce the noise as well as to protect from spray.

According to [Ref.14], the following points were found to be of importance and have therefore been mentioned below:

For W.I.S.E.s designs with larger wings, higher drag is induced but at the same time relatively high lift is obtained due to the surface effect.
As wing loading factor is increased so is the fuel cost, when at constant height.
A lower loading factor less than 300kg/m2, is preferred when there is a lower cruising height involved due to the surface effect being greater than at higher cruising heights.
The lighter wing loading factor is preferred to attain a lower landing speed.

2.13 PARALLEL WINGS

According to reference no.68, which discusses a W.I.S.E. design and uses parallel wings, the following points were of interest and are mentioned below:

The sole, negative, Delta wing - Ram - Air Wing - has been replaced by two big identical parallel wings in a tandem arrangement, positioned in one trace.
-By this, better efficiency of the wings has been achieved.
-Stability has been improved, since both wings are moving in the same medium.(Surface Effect)
-Tandem construction allows an elongated boat construction, the harmful (injurious) total - resistance was reduced.

The wings have been combined by two end-discs and this formed a kind of channelled stream vehicle.
-This resulted in better usage of Ground Effect (higher efficiency) and
-an increased static stability of the craft in rougher sea conditions, during landing in wave conditions and in cornering flight.

In addition to the above information, the paper also discusses other aspects of design such as the engine, the fact that elastic aerofoil wings are used, the flaps and other points of relevance, the reader is advised to refer to this paper for further information if required.

Conclusion

The trend in navigation is towards faster, hydrodynamically improved ships or gliders. This is occurring - but increasing pollution of sea and rivers by obstacles, such as sunken ships or drifting shoals, has to be considered and taken seriously. For aerofoils, flairing in G.E., there is less danger of this sort, which is mainly limited to take-off and landing routes. Areas near harbours are easier to survey and may be secured at reasonable cost.

2.14 POWER-AUGMENTED-RAM

[Ref: 33, 43, 46, 58, 89, 120, 121, 132, 150, 159, 170, 173, 174].It is anticipated that a W.I.S.E. craft will become a super high-speed vehicle in the near future, owing its efficiency to its exceptional ability of attaining a high lift to drag ratio when operating at low altitudes. Unfortunately, a disadvantage that has been analysed in previous years and is continuing to evolve is its lack of ability to perform an optimum take-off and landing procedure when the air speed is low. It is therefore not feasible for many of the numerous designs to progress into the construction phase due to this problem. Furthermore, due to the extraordinary power required for take-off and landing, in order to overcome both the drag and the loads presented during these procedures from wave action, the structure of the vehicle must be of very high strength. The result is an increase in weight, in addition to the extra weight of the high powered engines needed for take off.

The search for a feasible solution to this problem results in the use of aiding mechanisms such as an air cushion below the centre wing areas or the use of power-augmented ram (PAR). The PAR concept incorporates the use of propulsors that are mounted in front of the wing to produce a high lift at low speeds. The advantageous characteristics of this concept entail its ability to take-off and land at low speeds. Reducing the speed at take-off or landing produces a safer atmosphere due to decreased loads caused by wave action.

Between the years of 1975 and 1978, the David W. Taylor Naval Ship Research and Development Centre was analysing the aerodynamics of PAR-WIGs through experimental techniques. The tests were performed with zero forward speed as well as with a feasible airspeed, over a solid surface and over water in various sea states. They also predicted the static lift and drag performance using two-dimensional incompressible potential theory.

Lately, experimental investigation and theoretical analyses, which take forward speed into consideration, have been conducted in Japan. Although no-flow computation has been carried out, CFD simulation for two-dimensional PAR-WIGs has not been analysed. These studies were carried out by Hirata, who has been involved in numerous W.I.S.E. papers many of which are quoted both in the references and in the bibliography of this report.

The paper discussed in this section presents a study on the aerodynamics of three-dimensional PAR WIG configurations using CFD as well as experimental techniques. The Navier-Stokes solver used is based on the MUSCL-type third-order accurate upwind differencing, finite volume, pseudo-compressibility method with an algebraic turbulence model to close the system of equations. A multi-block grid approach was introduced and, in order to better comprehend the PAR effect, the following two boundary conditions were imposed on the ground.

The velocity is equal to the uniform flow and
The no-slip condition.

Solutions involving a variety of trailing edge heights are compared with experimental data and the aerodynamic characteristics are discussed. The reader is urged to refer to this article for further information due to its extensive discussion of different aspects of the procedures involved as well as additional information on PAR WIG vehicles.

2.15 ENGINE CHARACTERISTICS

Although it is two engine aircraft that fly over the Atlantic, four engines will probably be chosen for the New Large aircraft for several reasons. First, every plane must be able to climb from take-off with one engine totally disabled. For a two-engine plane this requires twice as much thrust available as that used in take-off. This would cause problems, such as a decrease in the cabin height and an increase in the hull size. It is the trend, for reasons explained later to make the new engines bigger and heavier for the same thrust than the ones they replace.

2.16 SIZING OF THE WING

Referring to the change in lift of an aircraft according to its angle of attack it may be seen that the lift rises almost in proportion to the angle of incidence until around the peak, beyond which it falls rapidly. The rapid drop in lift is due to a stall, which occurs when the boundary layers separate from the upper surface of the wing. Due to the danger this presents in a craft flying near the ground, it is important that this never takes place. The flight speed must therefore be high enough for lift to equal to the aircraft weight at a value of lift coefficient that is well away from the stalling value.

2.17 LIFT, DRAG, FUEL CONSUMPTION AND RANGE

Civil aircraft must lift as much as possible with minimum drag. Reducing the drag for the same lift allows the aircraft to use less fuel and travel a greater distance. To achieve this the quantity to be optimised is the product of flight speed and lift/drag ratios, VL/D. For steady, level flight, at small angles of attack, as for cruise, the following applies:
Lift = weight and drag = thrust of the engine.

In order to estimate the range, one requires to relate the fuel used to the thrust, which is the fuel flow rate divided by thrust.Fortunately, it may be said that, the aircraft is at an advantage if it can reach its optimum speed as soon as possible, allowing it to work efficiently and effectively. For W.I.S.E. craft this is done considerably faster which is an advantage. Please refer to 'Jet propulsion, a simple guide to the aerodynamic and thermodynamic design and performance of jet engines' by Nicolas Cumpsty Chapter 2.

2.18 THE TURBOJET AND THE TURBOFAN

To make efficient use of high temperature ratios and pressure ratios of the engine a bypass stream is normally used. Modern subsonic civil aircraft engines normally have bypass ratios of five or more.

The temperature of the gas entering the turbine is as high as the metal and the cooling arrangements will allow. At most operating conditions it is close to, or above, the melting temperature of the turbine material. During cruise the turbine entry temperature is typically about 250K lower than at take-off; this is desirable in order to prolong the life of the turbine but it also keeps the non-dimensional turbine inlet temperature T4/T2 nearly constant.

The highest temperature ratio is encountered at top of climb and at this condition the non-dimensional variables in the engine, such as pressure ratio and non-dimensional rotational speed, will be greatest.

The pressure ratios now employed are sufficiently high that the temperature of the gas leaving the compressor is as near to the limit as is possible with current materials.

With a turbine inlet temperature for initial cruise (at 31000 ft) of 1450 K it is sensible to take an overall pressure ratio of 40 and use this as the design condition. This may be divided into 1.6 for the core flow through the fan and 25 in the core itself. A pressure ratio of 40 for cruise would give a pressure ratio of about 45 at maximum climb and nearly this at take-off.

There are aspects of the engine that require some understanding of the way gases flow when the pressure changes are a substantial fraction of their absolute pressure, because there are then significant variations in density. This occurs when the flow velocities are a substantial fraction of the local sonic velocity, and such is the case throughout most parts of the engine.

2.19 STABILITY AND CONTROL

[Ref. 149, 167] Common aircraft are designed to take-off and land with the use of wheels. In the take-off stages, it is noted that the aircraft's reaction is to pitch-up. In order to avoid stalling due to high angles of attack and due to the fact that all W.I.S.E. vehicles must take-off at a zero angle of attack, the pilot is required to pitch the nose slightly down keeping a minimum angle of attack until off the water. When the craft is climbing after take-off, the crafts initial reaction is once again to pitch up, this must be controlled with care until straight and level flight can be attained at the required altitude.

Unlike aeroplanes, W.I.S.E.s acquire an air cushion below the craft at approximately the centre of the cushioning area, which may be calculated by using the crafts half-mean chord of the wings. For W.I.S.E.s, this position must also be its centre of gravity.

However, it should be noted that not all W.I.S.E.s have as big a problem with longitudinal stability as others do . Lippisch's proof of the reversed delta wing proved to be advantageous in this respect. In addition to this, the S-shaped camber line has been under great investigation and has, in fact, proven to be the most stable. This type of wing has already proven its success through the production of the Volga-2 and the Hydrowing.

For this reason, as well as for better lift and reduced economical expenses the S-90-200 is designed as it is.

The "stabilisers" of any aircraft whether conventional or ground effect, determine the crafts ability to fly either in or out of ground effect but not both.

Tailplanes and elevators counter the pitching motions of any craft and move the centre of gravity slightly backwards returning the craft to level flight. For this reason W.I.Gs have a larger tailplane than common aircraft, in order to handle efficiently the quick and large changes in angle of attack required, not only when clearing obstacles but primarily for the hard and powerful take-off procedures.

It should also be noted that one of the theories currently available, associated with W.I.S.E. stability, states that the stability varies according to the size of W.I.S.E. designed. For example, a craft of large dimensions will self stabilise, considering it is of a super heavy nature (weighing between 800-1500 tons). Considering the fact that future plans for W.I.S.E. craft tend towards them being of a large nature, a section is included in this report on the optimisation of W.I.S.E. craft tending toward Large Scale W.I.S.E. designs. Please refer to this section for further information on this topic.

In the S-90-200 design, the two fuselages may be compared to catamaran aerofoils. In both cases aerodynamic lift is produced. For this reason it was advisable to research other similar ideas which have already been adopted by the Australians.

They have produced sea taxi W.I.S.E. craft of a limited capacity, which adopt curved wing designs.

The use of curved wings, increases the stability of such craft and therefore reduces roll. Nonetheless, if the wings were highly curved, as to submerse greatly prior to take-off, additional drag would become a big problem. A picture shown at the end of this section, made available from the internet clearly indicates the Australian designs. For this reason, it is advisable that if the wings were to be curved, only a small curve should be present, allowing the wings to partially aid with the roll stability of the craft in flight, as well as aid with accomplishing sufficient lift at take-off.

In this project, by using the same properties as the initial S-90-200 concept (indicating that currently available materials would be used), it became apparent that the current structure, if altered at the wings, could cope with such a change. The lesser-curved wings would be preferred, due to them involving fewer stresses than the highly curved wings.

This design should therefore be taken into consideration for the future, since it would be capable of aiding the take-off procedure for all W.I.S.E. craft, as well as aiding with their stability.

In order to aid future research in this subject, the following section, although not adopted in this report, contributes effective information for calculating the following:-

The choice of elements used resulting in full stability of the craft at its maximum speed.
The determination of the stability as it accelerates or decelerates.
The stability of the craft when fully constructed and loaded.

$$H = (\Delta M/\Delta\alpha)(1/Dl)$$
$$= l_1(1+ l_1)\{(1\ {}^{+}C1\ l1lb1)1/\alpha 1-[1+C2(1+ l_1)\ lb1(1+ l_1/-p\ l_1)^{1/2}]1/\alpha_2\}$$

where:-

H	full longitudinal metacentric height of the object
M	the total mass of the object
$\Delta\alpha$	increment of the angle of attack
D	object weight
l	distance between the centres of pressure of the hydrofoils
l_1	arm of lifting force of the back hydrofoil relating to the mass centre
lb1 = l/ b1	characteristic of the object lengthening relative to the chord of back wing.

The above is analysed further in the NATO conference papers held between 5-8 October 1998. The paper concerning the above is titled "Longitudinal Stability of Ekranoplans and Hydrofoils, written by V.I.Korolyov from the Institute of Hydrodynamics of Ukraine National Academy of Sciences.

Furthermore, the same institute has also carried out tests on the Hydrodynamics of W.I.S.E. wings. The generated hydrodynamic characteristics of the wing can then be used to design the W.I.S.E.. These tests have taken place on calm and wavy water surfaces and are of great relevance for the stability and control of such craft.

If further analysis was to be made on this field, using a scaled down model of the S-90-200 rather than a single wing, a more accurate result on the workings of such craft could be developed. Although not analysed further in this report, the paper concerning this may be found in the same set of conference papers as the above and is titled "Hydrodynamical Characteristics Of An Ekranoplan Wing Flying Near The Wavy Sea Surface" by V.G.Byelinskyy and P.I.Zinchuk [Ref. 79]

With regard to [Ref.78], the word "Ground effect" has been accepted as a technical term by the aerodynamicists. The word is however, not suitable to express an aerodynamic effect of a wing flaring always at a low altitude above a SEA SURFACE. therefore the present authors want to call it "Surface Effect". The term "WIG" will be changed to "WISE" (wing-in-surface effect).

It is known well that a number of experimental WISE crafts have been developed from the time of Kaario (1935, see OLILLA 1980). There will be many reasons. The present authors, as well as their co-workers, are attempting to establish a production model of WISE craft. We will introduce our prototype of WISE craft "MARINE SLIDER; μ sky-2"[Ref. 8], (for μ sky-1 refer to [Ref. 48]).

We can disregard many other serious problems related to W.I.S.E. operation. The authors think that these problems are unavoidable in a machine of revolutionary new characteristics. These will be solved step by step by the efforts of those persons dealing with the individual problems [Ref. 149, 167].

2.20 INFLUENCE OF PAR IN GROUND EFFECT

This section discusses some of the theoretical methods and data used in the design and performance analysis of craft using wings operating in surface effect, W.I.S.E.. These W.I.S.E. craft derive improved lift to drag ratios as a result of the decreased induced drag losses from the reduction of down wash velocity due to the ground effect and increased due to ram either from the forward motion or directly from power. The existing theoretical methods are given and are used to predict performance for comparison with tests. The comparison shows that the lift drag ratios measured especially at low ground clearances are better than had been theoretically predicted. Possible procedures for improving the comparison are given. Using the conservative theoretical methods, the size and performance of competitive water-based craft are determined. The fundamental design problems of the W.I.S.E. configuration are discussed and the need for power augmentation of the ram flow, PAR, is given. Using the PAR-WIG concept, practical high performance craft can be developed.

High performance advanced air vehicles with a capability of a high cruising range and a relatively high cruising speed are needed for a variety of strategic missions. These craft should be capable of water takeoff and landing and be water based as in any future conflict, land bases and large airfields may not be available. While there are several types of craft that can operate from water, none of these can fulfil the speed, range and payload requirements needed. To satisfy the high performance requirements several investigators, both in this country and abroad, have suggested the use of wing-in -ground effect craft or their derivatives. These are known as W.I.S.E. craft. When the power is used to augment the free air ram lift they are termed PAR-WIG craft. Due to the high lift to drag ratios possible with rather compact low aspect ratio wings operating close to the ground, it appears that the W.I.S.E. or PAR-W.I.S.E. type craft may be suitable for meeting the requirements. With high lift to drag ratios and a high respective cruise speed it should be possible to accomplish the desired mission with good transport efficiency and high productivity.

With regard to the data table provided it may be seen that several countries have demonstrated successfully that Lippisch craft have been flown in and out of ground effect with satisfactory stability and good values of lift to drag ratio. In spite of the Lippisch success and the fact that the concept has been considered for many years, there have been numerous failures and there has been little progress in developing operational W.I.S.E. craft. Because of the promise of the possibility of a highly useful advance craft the available technology and characteristics of the W.I.S.E. and PAR-WIG concept are relied on to establish any operational and performance advantages and /or disadvantages with respect to other transport systems. Further it is desirable to determine just what makes the system good and what might be the technical risks for development.

[Ref: 33, 43, 46, 58, 89, 120 - 121, 132, 150, 159, 162, 165, 170, 173, 174].

3.0 METHODS OF ANALYSIS

3.1 FEATURES OF WISE MOTION

A W.I.S.E. craft operates near the ground deriving its lift both as a result of the usual circulation effects and from a pressure increase on the lower surface of the wing. This pressure increase is due to the conversion of the dynamic pressure of the forward motion to static pressure. This pressure increase is caused by the restriction of the airflow due to the closeness of the trailing edge and the wing end plates to the surface. [Ref 181]

3.1.1 Ground Effect

Changes in wing resistance near the ground are important for the more accurate determination of the conditions in the taking off and landing of an airplane. It has been found** that the wing resistance diminishes on approaching the ground, while the lift increases somewhat, thereby making the lift-drag ratio more favorable. A convenient method will be shown here which makes it possible to determine the polar curve of an airplane at short distances from the ground by a simple short calculation, when the polar curve is known for flight in unlimited space. The satisfactory agreement between experiment and calculation is determined by the results of two experiments with models.

The features of W.I.S.E.s motion are investigated by means of a mathematical model and simulations of motion. Principally almost all the features of W.I.S.E.s are related to the nature of the surface effect on wings. Using a model of the so-called Lippisch type WISES with an inverse delta main wing, aerodynamic forces and moments are measured in a towing tank and a wind tunnel. The aerodynamic measurements, theoretical or empirical estimation of the derivatives in the surface effect are applied.

3.1.2 ANALYSIS OF WISES RESPONSE TO THE ELEVATOR

In order to investigate the general characteristics of WISES, simulations with the linear and non-linear models are carried out. Typical results of the response due to the elevator and shown from figs.4-7 of Ref 181. The difference in the response of the non-linear and linear models shows the effects of the non-linear aerodynamic characteristics on the motions, which are due to the surface effect and produced by relatively large motions. They are remarkable in the damping of unstable motions. Therefore the unstable range of altitude estimated by the linear stability analysis is wider than that for the non-linear model. An example of responses induced by the non-linearity due to the surface effect are clearly seen in fig. 5. Typical non-linear behaviour of the W.I.S.E.s motion is seen for the less stable W.I.S.E.s with a small tail. In fig. 6. Time histories of impulsive response of W.I.S.E.s with a tail of VTR* = 0.8 are shown. Fig 7 shows examples of trajectories of the impulsive response in a phase plane. It can be said that the W.I.S.E. craft is locally unstable but is stable in the global sense for these conditions.

3.1.3 CONCLUSION

Basic dynamic characteristics of WISES were clarified by the simulation of the response to the elevator. The non-linear nature of the aerodynamic derivatives with the height, induced by the surface effect, brought drastic changes in the motion characteristics.
In a certain range of cruising altitude from the sea, the WISES showed longitudinal instability. The effects of the position of the centre of gravity and the tail volume ratios of the WISES on the characteristics were also examined.
By means of a suitable feed back system designed as an optimal regulator, the WISES maintained stable cruising in gusts, and a height change manoeuvre was achieved by the alteration of the reference height for the regulator.
The results of a series of tests for the reference height and the feed back method allowed the performance and limitations of the closed loop WISES system to be examined. Abrupt changes of height for collision avoidance required the combination of elevator control and thruster control.
Simulation of WISES behaviour in a realistic operating condition offers useful information for their safety assessment. Further investigation under various conditions will be required for the full assessment of safety.

The paper [Ref.104] discusses mathematical models of the aerodynamics of wing-in-ground effect vehicles in close proximity to the ground.

3.2 FLOW COMPUTATION FOR THREE-DIMENSIONAL WING-IN-GROUND EFFECT USING MULTI-BLOCK METHOD TECHNIQUE

[Ref. 61] A W.I.S.E. craft is expected to be one of the promising super-high speed craft in the next generation. A W.I.S.E. is characterised by a high lift to drag ratio and a backward shift of aerodynamic centre in close proximity to the ground, hence estimating their features accurately is very important in the design and safety evaluation.
In the present investigation, flows around a three-dimensional wing with end plates in ground effect are computed by the Navier -Stokes solver. Because of the geometric complexity of the configuration, a multi-block technique is used. In order to clarify the aerodynamic interactions between the wing and the ground, two boundary conditions on the ground are considered in this case 1) velocity is equal to the uniform flow and case 2) no slip condition. They correspond to an actual condition and a wind tunnel condition with a ground effect plate respectively. The results were compared with experimental data and the aerodynamic characteristics in ground effect are discussed.

3.3 EXPERIMENTAL

Two experiments were carried out in the Gottingen laboratory on a monoplane model of 134 cm span, with fuselage and elevator, whereby the air forces were measured once in unlimited space and once near the ground. It is evident that this curve fully agrees with the measured values of the lift coefficients up to about $c_a=1$. For very large lift values, we obtain deviation for which no satisfactory explanation can yet be given. [Ref. 137]

Motions of Wing -in -ground Effect Ships (WISES) are investigated by means of stability analysis and computer simulation. Characteristics of WISES with a simple feed back control are examined for cruising at a constant altitude and for height change manoeuvres. Impulsive gusts and varying gusts with turbulence are used as disturbances. Application of the simulation results for safety assessments is discussed. Only longitudinal motions are considered for Simplicity and because of the poor accuracy of predictions of the lateral aerodynamic derivatives.

In Japan demand for high speed marine vehicles stems from a need for improvement in the domestic transportation system. The Techno-Superliner (TSL) is expected to take the role of a commercial cargo transport service to the Tokyo metropolitan area in place of road vehicles. A W.I.S.E. concept enables use of a faster ship than the TSL or any other conventional high speed ship as summarised by Hooker and Terry (1992), and Rozhdestvensky and Synitsin.(1993). WISES based on the same concept are considered as candidates for a super high speed vehicle for commuter use in the future as proposed by Kubo (1993) plane and possesses the properties and nature of both.

WISES is a hybrid of a ship and an aeroplane and possesses the properties and nature of both.

Because W.I.S.E.s is a new and entirely different type of ship running at extremely high speed, a thorough safety assessment based on a rational method is required. It is known that ground effect/surface effect on a wing includes longitudinal stability, so proper understanding of the motion characteristics and suitable design control system for WISES are key aspects of safety.

A research [Ref. 57] project on WISES is being carried out in the Ship Research institute. The objective of the project is to perform a feasibility study on WISES for commercial use and to establish a foundation for the safety regulations of WISES as already introduced by Fuwa et al. (1993).

[Ref. 23] There is generally no boundary layer on the ground, for motion of a vehicle at low ground clearances without any atmospheric disturbances. An accurate experimental representation of such a flow field in a wind tunnel is difficult due to the existence of a boundary layer on the surface representing the ground that alters the "ram-wing" features. This boundary layer can not be ignored in many applications including automobiles, racing vehicles and Wises, the latter of which is the concern of this paper.

The exact extent to which the boundary layer (or lack of it) affects experimental results for Wises applications is not clear at present but the required experimental range for wises is greater than that for conventional aircraft. This is because the minimum height at which information is required is near to zero as the current designs are generally for landing/take-off from water. However, it has been reported that the boundary layer altered the measured lift coefficients on an aspect ratio 6 model by 33% at a moderate ground height of 20% of the span (equiv. 120% of the mean cord). The importance of such effects is clear when we consider that the static and dynamic stability of the craft is directly dependent upon the lift and drag pitching moment derivatives with both incidence and height.

In order to determine the regions where the boundary layer will affect the lift coefficients. Turner compared lift coefficients for a relatively high aspect ratio wing using a flat plate and a belt. The height to span ratio at the point where the methods started to disagree showed a linear correlation with lift coefficients according to equation 1, indicating when to remove the boundary layer. (Where h is the wing reference height, b is the span, Cl is the lift coefficient and AR is the aspect ratio)

$$[(h/b) / Cl] < 0.05. \quad AR = 6$$

Sullivan also analysed the phenomenological flow features in ground effect and came to a similar conclusion which included the effect of aspect ratio given by equation 2

$$[(h/b) / Cl] < 1/AR\pi$$

In addition, a minimum length of ground plate of 1 or 2 spans forward of the model was suggested based on the relative size of flow features. This minimum length will impose restrictions on the minimum height at which measurements can be made due to the boundary layer on the plate in front of the model.

Some resent Wises designs have used power-augmented ram (PAR) where the engine exhaust is directed under the wings to provide additional lift. This is particularly useful during take-off and landing as it allows slower and hence safer speeds but the influence of the boundary layer during experiments is unclear.

Turner also tested a tilt rotor configuration where the majority of the lift came from the power plants and not from aerodynamic factors. It was found that the moving belt technique was not required in this case. In the case of PAR the aerodynamic lift is greatly affected by the flow from the power plants and hence the boundary layer should be removed, if possible, when indicated by equation 2.

Previous studies have attempted to resolve the boundary layer problem in a number of ways, all of which involve either complex and expensive equipment or approximations to the flow field.

Fink and Lastinger used two similar models, which were placed to form an image system with symmetry plane representing the ground. This is a very simple arrangement and possesses good access for flow visualisation. The mean velocity field will be adequately represented. However, if flow separation is present this will not be the case. The turbulence field is unlikely to be well represented and investigation of PAR effect is not possible, due to the difficulty of ensuring symmetry of effects from the engines. In addition the method had the added expense and difficulty of making two identical models and supports, which also increases the blockage in the tunnel, hence reducing the range of available model sizes.

Katzoff and Sweberg attempted to improve on the image technique by introducing a thin plate between the models. Its leading edge was downstream of the leading edges of the wings. This was in an attempt to better simulate the turbulence field in the region of the ground. The subsequent boundary layer on the plate will be small but may separate at some position behind the wing particularly if negative incidences are investigated. In addition, the pressure field needs to be known before the plate can be positioned. This required longer experimentation periods.

Undoubtedly, the best method was that described by Turner which involved removing the boundary layer from the tunnel floor by suction and then introducing a moving belt which was run at the same speed as the reference velocity. The effectiveness of this technique was found to be relatively insensitive to the belt speed, so precise speed control was not necessary. In addition the mean and turbulent flow field were well simulated with little necessary increase in tunnel blockage, and Par investigations were possible . The applicable speed range is dependent on the maximum speed of the belt and the technique requires possibly expensive and complicated equipment particularly for large tunnels with regard to removing the initial boundary layer.

The current work was carried out to provide a simple, cheap and accurate alternative to the above method.

[Ref;1-6, 10-14, 16-17, 23-28, 43-44, 4857, 90, 109, 174, 190, 191 are but some]

3.4 THEORETICAL ANALYSIS

A derivation then took place. The derivation for the relevant design parameters assumes that changes in quantities are isentropic and quasi-static allowing the use of mean values. It is proposed that the real velocities in the boundary layer, U and the boundary layer height at the slot, h_s, can be expressed by the equivalent constant velocity,U_θ and height, h_θ, such that the total momentum and mass flow rate of both the real and equivalent boundary layers are the same, ρ is the density, y is the ordinary perpendicular to the plate and L is the slot length. In this way we obtain several equations which lead to the following equation: [p.s. if extra information is required on the following please refer to Sowden and Hori, from the Aeronautical Journal June/July 1996]

Then, using Newton's second law, Bernouli's equation and simplifying by using other physics assumptions we finally get:

ρLhsUs = ρL integral Udy + ρLhcU$_{\text{infinity}}$ (note: from hs to zero).

The computation methods based on theory are outlined in this reference and below. They are used for recalculation and design of profiles, wings and wing configurations.

The flow is non-viscous, non-rotational,

The fluid is incompressible and stationary,

The potential function satisfies the Laplace Equation (the reader is urged to refer to this reference for further information if required)

The disturbance potential has to satisfy the following boundary conditions:

Vanishing in infinity- where the disturbance potential tends to zero as the sum of the $x^2 + y^2 + z^2$ tends to infinity.

Normal condition, there is no flow through the body's surface.

- If lifting bodies are computed, the Kutta condition is applied in this paper as γ (trailing edge) = 0

Wing-In-Ground Effect vehicles are generally unstable where various pitching motions are concerned. For this reason, when designing a W.I.S.E., moving closer to the ground, one has to face the demand for natural height stability. The decisive factors involved in the pitching stability may be found in this reference on page 599, where it is stated that Staufenbeil (1976) introduced the parameter Fm as criterion for static height stability. Where: Fm = (CMh/CLh) / (CMa/Cla) and where height stability is proofed if Fm<1 or (CMh/CLh) < (CMa/CLa). Where CMh/CLh equals the shift of the centre of lift due to change of the height, while CMa/CLa is the shift due to change of the angle of attack.

As recommended in this reference, in order to attain profiles adapted for surface effect, an initial stage involving theoretical investigations should be performed. One method is using potential flow methods, where one may acquire effective results for numerous wing profiles at various distances from the boundary. Three methods, based on the ideas of Martensen (1959), Hess and Smith (1972) and Oellers (1962) were tested in this reference. In all these techniques surface effect is represented using the mirror image process.

The method of Martensen and Oellers is based on finding the stream function, which, initially, generates a streamline shaped in a manner similar to the contour of the profile. Martensen uses the normal condition to find unknown singularities, while Oellers uses the equation for the whole stream function, which is constant on the profile. The Kutta condition is used in both methods.

The Hess and Smith technique is based on a distribution of sources and a vortex line on the profile contour. The Kutta condition is used to determine the strength of the vortices. The strength of the sources may be found if the normal condition is applied.
The methods of Oellers, Hess and Smith are not adequate for thin profiles, Martensen showed the best results. It is for this reason that Martensen's technique was adopted in the paper discussed, which, should be referred to by the reader for further information if required.

The reason behind this paper being of importance was due to its general informative manner of representing and describing the design process as well as its discussion of S shaped aerofoils, a profile that has been chosen to be under investigation in this report. In the previously mentioned paper, the contour of the profile was created using the four digit NACA algorithm, where S shaped profiles may be created using two superimposed profiles. With the use of this paper, one may carry out an optimisation of the profile by giving a certain range for the parameters like chord and thickness.
The optimising criteria are the stability characteristics at various heights and angles of attack, the increase of lift when decreasing the height to chord ratio and the maximum lift of a profile when at its maximum angle of attack and lowest height. It was for this reason that numerous angles of attack and height/chord values were chosen for analysis when carrying out the CFD process.

In this paper, for every combination of the parameters, in the optimising process, the appropriate profile was computed, followed by the flow calculation with the Martensen method for a given number of heights and angles of attack. According to the resulting lift and moment coefficients the stability figures Fm are determined.

[Ref:1, 5, 29-31, 81, 181-182]

3.5 NUMERICAL CALCULATIONS

The polar curve for unlimited space is converted in the present case, with the aid of L. Prandtl's wing theory and the multi-plane theory. According to this theory, the air from about the wing can be calculated on the assumption that the lift is distributed over the wing span in the form of half an ellipse, which is accurate enough for most practical cases. In this connection, we will utilize the theoretical consideration that a vortex band goes out from the trailing edge of each wing. The axes of the elementary vortices of this band are nearly parallel to the direction of flight and the width of the band is equal to the wing span. The added disturbing velocity resulting from this vortex band at any point is the integral of the disturbing velocities produced by the individual elementary vortices, whereby the former are calculated according to the Biot-Savart law. If a wing is in an airflow which is disturbed by a second wing, only the vertical component of the disturbing velocity comes into consideration for the induced drag of the first wing, since the inflow direction and therewith the induced drag are changed by the vertical components of the disturbing velocity at the place of the supporting line. The vertical velocities, in the vertical plane passing through the middle of the chord, were calculated and graphically represented in fig.1, for a series of distances from the supporting line, by K Pohlhausen, at the suggestion of L. Prandtl, on the assumption that the lift is distributed in half an ellipse over the wing span.

In order to investigate the change in the resistance near the ground, we utilize the principle of reflection. We replace the surface of the ground by wing 1' reflected by the ground [Ref 137. Fig 2] and calculate (by a method analogous to that for calculating the drag of a multiplane from the drag of a monoplane) in what manner the airflow about wing 1 will be affected by its image. We denote the distance from the ground by h/2. Wing 1 is now on the pressure side of wing 1'. We already recognize qualitatively that the disturbing velocity due to 1' on wing 1 is directed upward. The resulting direction of flow on wing 1, which is found by the geometric addition of the original direction of the velocity v and the vertical velocity w_{11}' due to wing 1', and whose direction is indicated by v', is therefore, as we see, deflected downward somewhat less than in the undisturbed condition. The induced drag near the ground must therefore be smaller than at a higher altitude, since there is decreasing distance between wing 1 and its image 1'.

3.6 POTENTIAL FLOW INVESTIGATION ON GROUND EFFECT BY IMAGE METHODS

APPENDICIES D - G

Potential Flows in Ground Effect

There are several approaches to this issue. They are

(a) flow past a cylinder at various heights
  (i) without circulation
  (ii) with circulation
(b) flow past a source sink pair aligned into the flow for a range of heights
(c) flow past an oblique series of vortices approximating flat plat at incidence
(d) flow past a doublet - vortex model of a foil where the doublet size varies in such a way to match the projected foil blockage for an angle of attack corresponding to the vortex strength
(e) analyse the foil itself.

The approaches have advantages and disadvantages as set out in the table below

	Model	**Variables**	**Advantages**	**Disadvantages**
a(i)	cylinder	h/a	complete image pattern	h/a>1
a(ii)	spinning cylinder	h/a.,circulation	complete image pattern, models lift	h/a>1 link to incidence imprecise
b	Rankine Oval	h/c. t/c	indicative of camber	only 0 deg c and t vary
c	flat plate at incidence	no of vortices a, h/c	accuracy can be improved	line rough no use at zero and no thickness, camber needs calibration
d	variable cylinder and vortex	h/c, t/c,	lowest level with all features, provides a form drag model	
e	foil	h/c, t/c, camber	full solution, allows advanced turbulent / viscous flow models to be used	requires CFD. most rime consuming

Potential

Stream - Lines With Wake

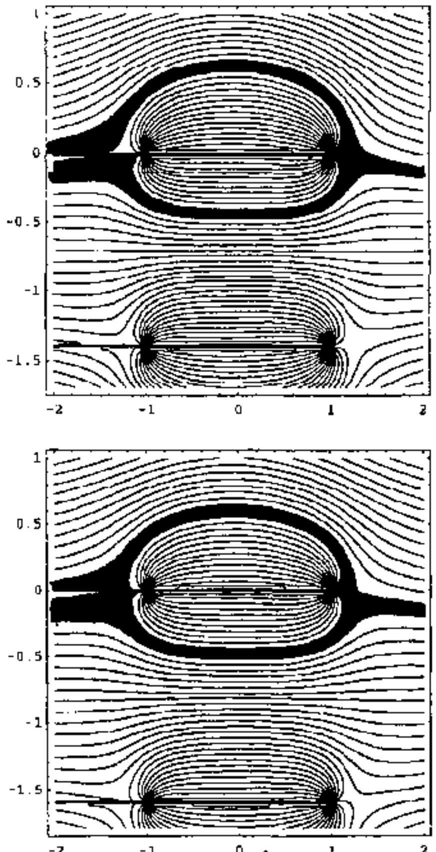

FIG.25 above

Stream Lines Without Wake

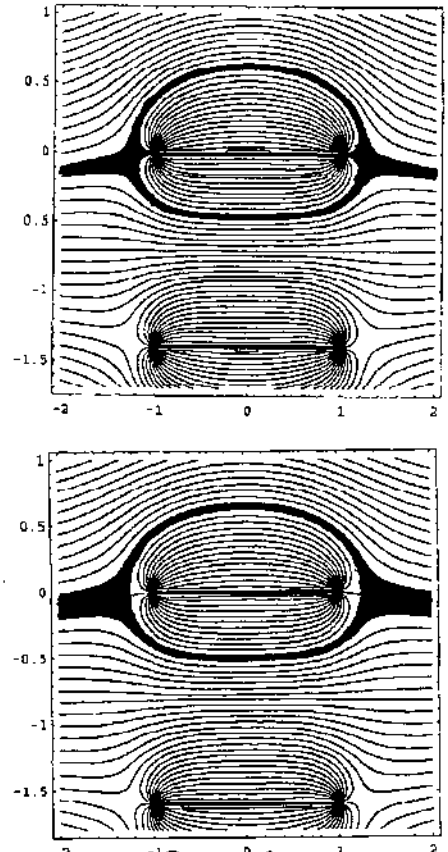

FIG.26 above

Discussion:

The following are a series of runs, which produced a representation of a closed shape parallel to the water surface. These pictures illustrate that the width and the camber of the body change from a large camber when near the water surface to no camber when in the air.

The bottom right hand picture shows the 'zero stream - line' producing a slight Rankine Oval. The difference between this picture and the bottom left hand illustration is that the latter allows 10% of the fluid to escape, representing a wake.

It will be seen later that although this does not have a substantial change on the lift it does on the drag. Appendix 'A' shows different conditions of source strength. The stronger the source strength, the thicker the resulting bodies.

Top Right
Length of Body = 2.4
Max. Point = 0.62
Min. Point = -0.48
Thickness = 1.10

Bottom Right
Length of Body = 2.45
Max. Point = 0.65
Min. Point = -0.5
Thickness = 1.05

POTENTIAL

Source Lift Without Wake

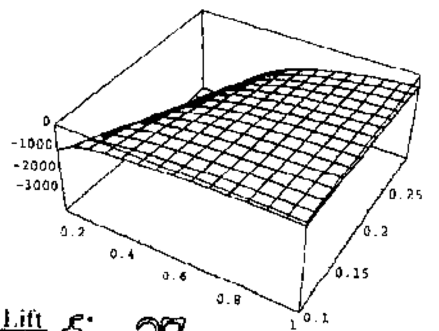

Lift fig.27

Sink Lift Without Wake

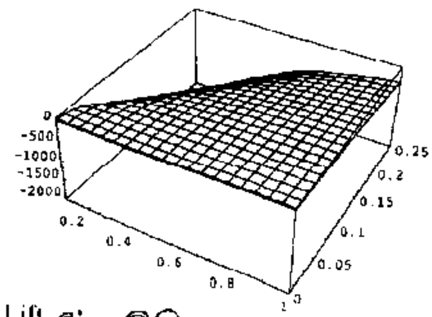

Lift fig.28

Source Drag Without Wake

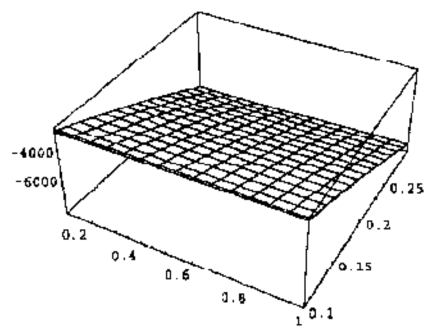

Drag fig.29

Sink Drag Without Wake

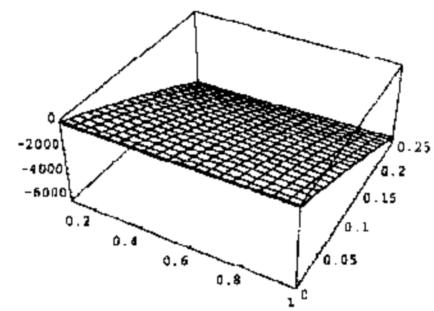

Drag fig.30

Discussion:

Sink Lift Without Wake - **the variation with sink strength is quite weak. When further from the water surface one notices only a slight curve. But as the surface is approached the change in lift with sink strength increases quite dramatically. The results with high sink strength and low altitude gives a very sizeable contribution to lift. With high being clse to 1 and low close to 0.2. With low sink strength the dependance on 'h' is quite small.**

Source Lift Without Wake - **With low source strength (close to 0.2), dependance on 'h' is appreciably more significant. For higher flight dependance on source strength the results are fairly similar to 'sink lift without wake'.**

Drag - **Although the Drag illustrations seems to be similar, the source drag without Wake has a higher drag than** Sink Drag Without Wake

Source Lift Without Wake - **With low source strength (close to 0.2), dependance on 'h' is**

Potential

Source With Wake

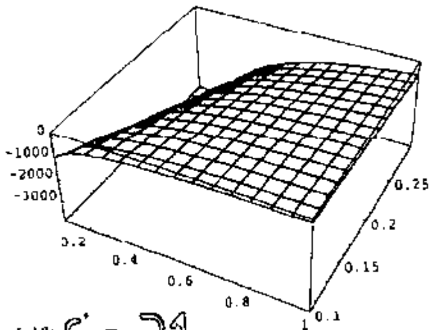

Lift fig. 31

Sink With Wake

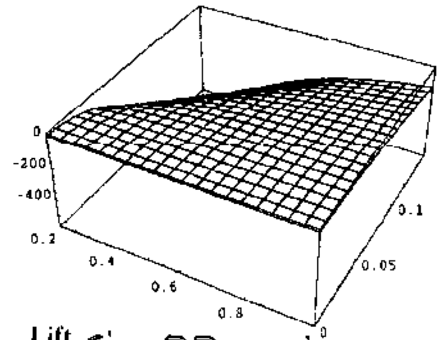

Lift fig. 33

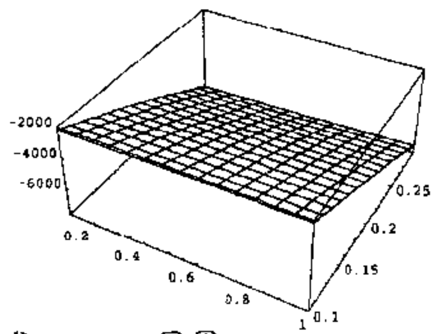

Drag fig. 32

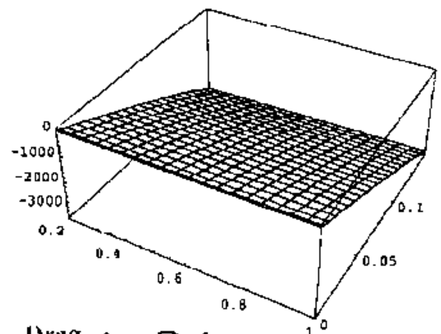

Drag fig. 34

Discussion:

Sink Lift Without Wake - **As the surface is approached the change in lift with sink strength increases, although one may assume at first glance that this Sink Lift |without Wake is similar to that on the previous page, one then notices that the sink strength this time reaches a value of 0.15 and not 0.25, resulting in an overall reduced lift with high sink strength. However, once again, with low sink strength the dependence on 'h' is small.**

Source Lift Without Wake - **With low source strength close to 0.2), dependence on ' h' is quite significant. For higher flight dependence on source strength the results are not as similar to that on the previous page when comparing to 'sink lift without wake', due the value of sink strength reaching 0.1.**

Drag - **Although the Drag illustrations seems to be similar, the source drag with Wake has a higher drag** Sink Drag Withl Wake

Formulae: -

Stream Function Without Wake Producing Lift and Drag

```
NSolve[
U (1 + s (1 / Abs [z - c] - 1 / Abs [z - c + 2 h I] - 1 / Abs [ z + c + 2hI] ) ) = = c - 1,
{x, y} ]
Nsolve [ D [ (u z - u s ( Log[z - c ] Log [z + c] + Log [z - c + 2hI] - Log [z + c +
2hI])), x] = = 0,{x, y}]
Nsolve [ D [ (u z - u s ( Log[z - c ] Log [z + c] + Log [z - c + 2hI] - Log [z + c +
2hI])), x] = = 0,{x, y}]
```

Stream Function With Wake producing Lift and Drag

```
Plot 3D [ Im[Residue[
(D[ (u z - u s ( Log[z - c ] Log [z + c] + Log [z - c + 2hI] - Log [z + c + 2hI])), x] ^2,
{r, c}] ] , {h, 0.1, 1}, {s, 0.1, 0.3}]
(D[ (u z - u s ( Log[z - c ] Log [z + c] + Log [z - c + 2hI] - Log [z + c + 2hI])), x] ^2,
{r, c}] ] , {h, 0.1, 1}, {s, 0.1, 0.3}] , {h, 0.1,1,0.1}], {s,0.1,0.1,0.1}]
```

Source and Sink Without Wake Producing Lift and Drag

```
(D[(u z - u s (Log[z - c] - 0.9 Log[z + c] + Log[z - c + 2 h I] - 0.9 Log[z + c + 2 h I])),
   x]) ^ 2
, {r, c}]], {h, 0.1, 1}, {s, 0.1, 0.3}]
Plot3D[Re[Residue[
  (D[(u z - u s (Log[z - c] - 0.9 Log[z + c] + Log[z - c + 2 h I] - 0.9 Log[z + c + 2 h ])),
   x]) ^ 2
```

Source and Sink With Wake Producing Lift and Drag

```
In[107]:= u = 100

Plot3D[Im[%80], {h, 0.2, 1}, {s, 0, 0.15}, PlotPoints → 20]
Plot3D[Re[%80], {h, 0.2, 1}, {s, 0, 0.15}, PlotPoints → 20]
```

A fig.35 **WITHOUT WAKE** B fig.36

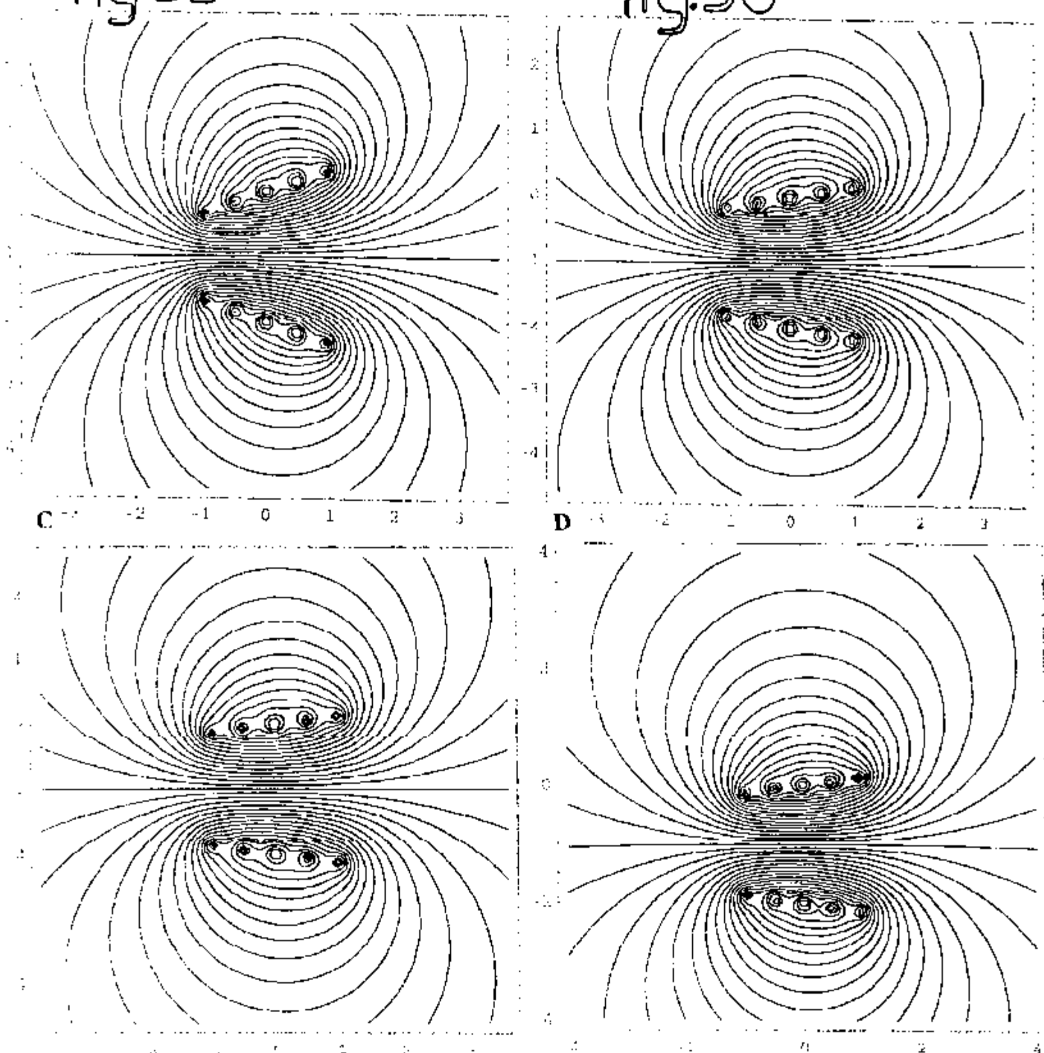

C D

fig. 37 fig. 38

fig.38 WITH WAKE fig.39

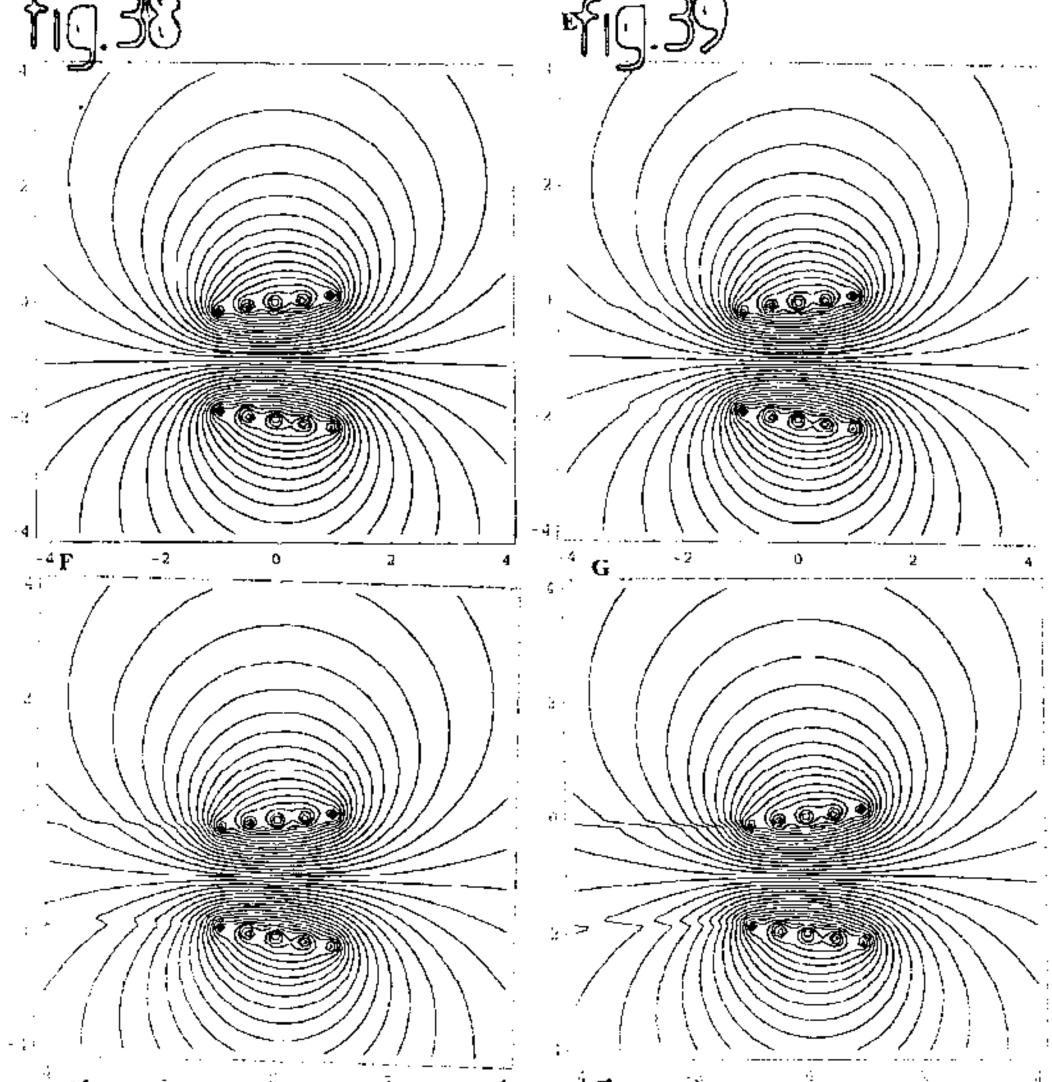

fig.40 fig.41

A

```
a = Pi / 9
h = 1
v = 8
v = 2 Pi c u a / 5

ContourPlot[Im[(u (z + I v Log[z] - I v Log[z + 2 h I]
+ I v Log[z + c / 2 (Cos[a] + I Sin[a])] - I v Log[z + 2 h I + c / 2 (Cos[a] - I Sin[a])]
+ I v Log[z + c (Cos[a] + I Sin[a])] - I v Log[z + 2 h I + (Cos[a] - I Sin[a])]
+ I v Log[z - c / 2 (Cos[a] + I Sin[a])] - I v Log[z + 2 h I - c / 2 (Cos[a] - I Sin[a])]
+ I v Log[z - c (Cos[a] + I Sin[a])] - I v Log[z + 2 h I - c (Cos[a] - I Sin[a])]))],
{x, -3.6 h, 3.6 h}, {y, -4.6 h, 2.6 h},
Contours → 41, PlotPoints → 80, ContourShading → False]
```

Out (32) = 1 , Out (34) = 1 , Out (35) = 40 π^2 / 9 , Out (31) = P / 9

B

```
a = Pi / 18
h = 1
v = 8
c = 1
v = 2 Pi c u a / 5

+ I v Log[z + c / 2 (Cos[a] + I Sin[a])] - I v Log[z + 2 h I + c / 2 (Cos[a] - I Sin[a])]
+ I v Log[z + c (Cos[a] + I Sin[a])] - I v Log[z + 2 h I + (Cos[a] - I Sin[a])]
+ I v Log[z - c / 2 (Cos[a] + I Sin[a])] - I v Log[z + 2 h I - c / 2 (Cos[a] - I Sin[a])]
+ I v Log[z - c (Cos[a] + I Sin[a])] - I v Log[z + 2 h I - c (Cos[a] - I Sin[a])]))],
{x, -3.6 h, 3.6 h}, {y, -4.6 h, 2.6 h},
Contours → 41, PlotPoints → 80, ContourShading → False]
```

π^2 / 9

Out (38) = π / 18 , Out (39) = 1 , Out (40) = 8 , Out (41) = 1 , Out (42) = 20 π^2 / 9

C

```
a = Pi / 24
h = 1
v = 8
c = 1
v = 2 Pi c u a / 5

ContourPlot[Im[(u (z + I v Log[z] - I v Log[z + 2 h I]
+ I v Log[z + c / 2 (Cos[a] + I Sin[a])] - I v Log[z + 2 h I + c / 2 (Cos[a] - I Sin[a])]
+ I v Log[z + c (Cos[a] + I Sin[a])] - I v Log[z + 2 h I + (Cos[a] - I Sin[a])]
+ I v Log[z - c / 2 (Cos[a] + I Sin[a])] - I v Log[z + 2 h I - c / 2 (Cos[a] - I Sin[a])]
+ I v Log[z - c (Cos[a] + I Sin[a])] - I v Log[z + ? h I - c (Cos[a] - I Sin[a])]))],
{x, -3.6 h, 3.6 h}, {y, -4.6 h, 2.6 h},
Contours → 41, PlotPoints → 80, ContourShading → False]
```

Out [44]= $\frac{\pi}{24}$ Out [45]= 1 Out [46]= 8 Out [47]= 1 Out [48] $\frac{5\pi}{3}$

```
a = Pi / 24
h = 1
v = 8
c = 1
u = 100
v = 2 Pi c u a / 5

ContourPlot[Im[(u (z + I v Log[z] - I v Log[z + 2 h I]
+ I v Log[z + c / 2 (Cos[a] + I Sin[a])] - I v Log[z + 2 h I + c / 2 (Cos[a] - I Sin[a])]
+ I v Log[z + c (Cos[a] + I Sin[a])] - I v Log[z + 2 h I + (Cos[a] - I Sin[a])]
+ I v Log[z - c / 2 (Cos[a] + I Sin[a])] - I v Log[z + 2 h I - c / 2 (Cos[a] - I Sin[a])]
+ I v Log[z - c (Cos[a] + I Sin[a])] - I v Log[z + 2 h I - c (Cos[a] - I Sin[a])]))],
{x, -4 h, 4 h}, {y, -4 h, 4 h}, Contours → 41, PlotPoints → 80, ContourShading → False]
```

D

Out (63) = π/24 , Out (64) = 1 , Out (65) = 8 , Out (66) = 1 , Out (67) = 100 , Out (68) = 5 π^2 / 3

```
a = Pi / 24
v = 8
s = 0.2
c = 1
u = 100
v = 2 Pi c u a / 5

ContourPlot[Im[(u (z + I v Log[z] - I v Log[z + 2 h I]
+ I v Log[z + c / 2 (Cos[a] + I Sin[a])] - I v Log[z + 2 h I + c / 2 (Cos[a] - I Sin[a])]
+ I (v + I s) Log[z + c (Cos[a] + I Sin[a])] -
I (v + I s) Log[z + 2 h I + (Cos[a] - I π2 / 24  π2 / 24
+ I v Log[z - c / 2 (Cos[a] + I Sin[a])] - I v Log[z + 2 h I - c / 2 (Cos[a] - I Sin[a])]
+ I v Log[z - c (Cos[a]  π Sin[a])] - I v Log[z + 2 h I - c (Cos[a] - I Sin[a])]))],
{x, -4 h, 4 h}, {y, -4 h, 4 h  Contours → 41, PlotPoints → 80, ContourShading → False]
```

E

Out (70) = π / 24 , Out (71) = 1 , Out (72) = 8 , Out (73) = 0.2 , Out (74) = 1 , Out (75) = 100 , Out (76) = 5 π^2 / 24

```
a = Pi / 24
h = 1
v = 8
s = 0.5
u = 100

ContourPlot[Im[(u (z + I v Log[z] - I v Log[z + 2 h I]
+ I v Log[z + c / 2 (Cos[a] + I Sin[a])] - I v Log[z + 2 h I + c / 2 (Cos[a] - I Sin[a])]
+ I (v + I s) Log[z + c (Cos[a] + I Sin[a])] -  I (v + I s) Log[z + 2 h I + (Cos[a] - I Sin[a])]
+ I v Log[z - c / 2 (Cos[a] + I Sin[a])] - I v Log[z + 2 h I - c / 2 (Cos[a] - I Sin[a])]
+ I v Log[z - c (Cos[a] + I Sin[a])] - I v Log[z + 2 h I - c (Cos[a] - I Sin[a])]))],
{x, -4 h, 4 h}, {y, -4 h, 4 h}, Contours → 41, PlotPoints → 80, ContourShading → False]
```

F

Out (87) = π / 24 , Out (88) = 1 , Out (89) = 8 , Out (90) = 0.5 , Out (91) = 1 , Out (92) = 100 , Out (93) = 5 π^2 / 3

```
a = Pi / 24
h = 1
v = 8
s = 1
c = 1
u = 100
v = 2 Pi c u a / 5
ContourPlot[Im[(u (z + I v Log[z] - I v Log[z + 2 h I]
+ I v Log[z + c / 2 (Cos[a] + I Sin[a])] - I v Log[z + 2 h I + c / 2 (Cos[a] - I Sin[a])]
+ I (v + I s) Log[z + c (Cos[a] + I Sin[a])] -
I (v + I s) Log[z + 2 h I + (Cos[a] - I Sin[a])]
+ I v Log[z - c / 2 (Cos[a] + I Sin[a])] - I v Log[z + 2 h I - c / 2 (Cos[a] - I Sin[a])]
+ I v Log[z - c (Cos[a] + I Sin[a])] - I v Log[z + 2 h I - c (Cos[a] - I Sin[a])]))],

{x, -4 h, 4 h}, {y, -4 h, 4 h}, Contours → 41, PlotPoints → 80,
ContourShading → False]
```

$\frac{\pi}{24}$

1

8

1

1

100

$\frac{5\,\pi^2}{3}$

Potential Flow About Idealised Foil

.POTENTIAL FLOW ABOUT IDEALISED FOIL

The function which shows behaviour at an angle of attack is f2 below

In[8]:= $\mathbf{a / 2 \int_{-1}^{1} (1 - X)\ (x - X) / \sqrt{(1 - X^2)}\ dX}$

Out[8]= $\frac{1}{2}\, a\, \pi \left(\frac{1}{2} + x\right)$

Substituting this value in the formula for the circulation density gives γ2

In[21]:= $\mathbf{a / Pi \sqrt{\frac{(1 - x)}{(1 + x)}} \int_{-1}^{1} \sqrt{\frac{(1 + X)}{(1 - X)}}\ \frac{(X + 1/2)}{(X - x)}\ dX}$

This integration is in general complex and is given below in full

Out[21]=

$$\Bigg(i\, a \sqrt{\frac{1-x}{1+x}} \Bigg(3 \sqrt{-1+x}\ \sqrt{1+x}\ \mathrm{Log}\left[-\frac{i}{\sqrt{2}}\right] + 2 \sqrt{-1+x}\ x \sqrt{1+x}\ \mathrm{Log}\left[-\frac{i}{\sqrt{2}}\right] - 3 \sqrt{-1+x}\ \sqrt{1+x}$$

$$\mathrm{Log}\left[\frac{i}{\sqrt{2}}\right] - 2 \sqrt{-1+x}\ x \sqrt{1+x}\ \mathrm{Log}\left[\frac{i}{\sqrt{2}}\right] + \mathrm{Log}\left[-\frac{4 i}{\sqrt{-1+x}\ (1+x)^{3/2}\ (1+2x)}\right] +$$

$$3\, x\, \mathrm{Log}\left[-\frac{4 i}{\sqrt{-1+x}\ (1+x)^{3/2}\ (1+2x)}\right] + 2 x^2\, \mathrm{Log}\left[-\frac{4 i}{\sqrt{-1+x}\ (1+x)^{3/2}\ (1+2x)}\right] -$$

$$\mathrm{Log}\left[\frac{4 i}{\sqrt{-1+x}\ \sqrt{1+x}\ (1+3x+2x^2)}\right] - 3\, x\, \mathrm{Log}\left[\frac{4 i}{\sqrt{-1+x}\ \sqrt{1+x}\ (1+3x+2x^2)}\right] -$$

$$2 x^2\, \mathrm{Log}\left[\frac{4 i}{\sqrt{-1+x}\ \sqrt{1+x}\ (1+3x+2x^2)}\right]\Bigg)\Bigg) \Big/ \left(2 \pi \sqrt{-1+x}\ \sqrt{1+x}\right)$$

Tidying this expression up gives

In[22]:=

Simplify[%9]

Out[22]=

$$-\Bigg(i\, a \sqrt{\frac{1-x}{1+x}}$$

$$\Big(-i\, \pi \sqrt{-1+x}\ \sqrt{1+x}\ (3+2x) + (1+3x+2x^2)\, \mathrm{Log}\left[\frac{4 i}{\sqrt{-1+x}\ (1+x)^{3/2}\ (1+2x)}\right] -$$

$$(1+3x+2x^2)\, \mathrm{Log}\left[-\frac{4 i}{\sqrt{-1+x}\ \sqrt{1+x}\ (1+3x+2x^2)}\right]\Big)\Bigg) \Big/ \left(4 \pi \sqrt{-1+x}\ \sqrt{1+x}\right)$$

Putting an angle of 20 degrees for illustration. The Imaginary values are seen to be always positive, whereas the Real part produces the anticipated result for γ2 but with some extra terms. Integrating over the chord will give the lift coefficient, which to first order correction for Brown Poroximity gives Cl = 2 πa (1 + 1 / ((4h ^ 2)). If this truncation is not made the integration gives the complex result below.

In (24) : - = , a = Pi / 9 , Out (24) = Pi / 9

In[32]:= **Plot[{Re[%22], Im[%22]}, {x, -1, 1}]**

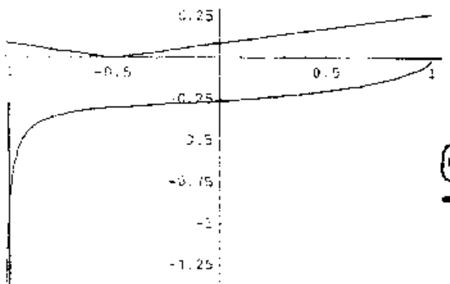

Graph43

Out[32]= - Graphics -

In[33]:=

$$\int_{-1}^{1} \%22\, dx$$

Integrating over the chord will give the lift coefficient,

which too first order correction for Brown porcximity gives Cl = 2 πα (1 + 1 / (4 h ^ 2)).

If this truncation is not made the integration gives the complex result below.

Out[33]= $-\frac{1}{72}\, i\, (-5 - 4\, i\, \pi)\, \pi$

$$-\frac{1}{72}\, i\, (-5 - 4\, i\, 9\, \alpha)\, \pi$$

In[35]:= **Re[%33]**

Out[35]= $-\frac{\pi^2}{18}$

$$-\frac{\alpha\pi}{2}$$

which is the coefficient of the first correction term. There is also an Imaginary part, which is 5 / 8 α

In[36]:= **Im[%33]**

Out[36]= $\frac{5\,\pi}{72}$

In[37]:= $\int_{-h}^{h} \%22\, dx$

The general result integrating between (-h) and (+h) is very complicated.

Out[37]= $- i\, \sqrt{1-h}\, \sqrt{\frac{-1-h}{-1+h}}\, \sqrt{1+h}\, \pi + 2\, i\, \sqrt{1-h}\, \sqrt{\frac{-1-h}{-1+h}}\, h\, \sqrt{1+h}\, \pi -$

$2\, i\, \sqrt{1-h}\, \sqrt{\frac{-1-h}{-1+h}}\, h^3\, \sqrt{1+h}\, \pi + i\, \sqrt{1-h}\, \sqrt{\frac{-1-h}{-1+h}}\, h^4\, \sqrt{1+h}\, \pi +$

$$i\sqrt{1-h}\sqrt{\frac{1-h}{1+h}}\sqrt{1+h}\,\pi+2\,i\sqrt{1-h}\,h\sqrt{\frac{1-h}{1+h}}\sqrt{1+h}\,\pi-$$

$$2\,i\sqrt{1-h}\,h^3\sqrt{\frac{1-h}{1+h}}\sqrt{1+h}\,\pi-i\sqrt{1-h}\,h^4\sqrt{\frac{1-h}{1+h}}\sqrt{1+h}\,\pi+$$

$$\sqrt{\frac{-1-h}{-1+h}}\,h\sqrt{-1-2h-h^2}\,\mathrm{Log}\Big[\frac{4\,i}{\sqrt{-1-h}\sqrt{1-h}\,(-1+h)\,(-1+2h)}\Big]-$$

$$3\sqrt{\frac{-1-h}{-1+h}}\,h^2\sqrt{-1-2h-h^2}\,\mathrm{Log}\Big[\frac{4\,i}{\sqrt{-1-h}\sqrt{1-h}\,(-1+h)\,(-1+2h)}\Big]+$$

$$3\sqrt{\frac{-1-h}{-1+h}}\,h^3\sqrt{-1-2h-h^2}\,\mathrm{Log}\Big[\frac{4\,i}{\sqrt{-1-h}\sqrt{1-h}\,(-1+h)\,(-1+2h)}\Big]-$$

$$\sqrt{\frac{-1-h}{-1+h}}\,h^4\sqrt{-1-2h-h^2}\,\mathrm{Log}\Big[\frac{4\,i}{\sqrt{-1-h}\sqrt{1-h}\,(-1+h)\,(-1+2h)}\Big]+$$

$$\sqrt{-1+h}\,h\sqrt{\frac{1-h}{1+h}}\sqrt{1+h}\sqrt{1-h^2}\,\mathrm{Log}\Big[\frac{4\,i}{\sqrt{-1+h}\,(1+h)^{3/2}\,(1+2h)}\Big]+$$

$$2\sqrt{-1+h}\,h^2\sqrt{\frac{1-h}{1+h}}\sqrt{1+h}\sqrt{1-h^2}\,\mathrm{Log}\Big[\frac{4\,i}{\sqrt{-1+h}\,(1+h)^{3/2}\,(1+2h)}\Big]+$$

$$\sqrt{-1+h}\,h^3\sqrt{\frac{1-h}{1+h}}\sqrt{1+h}\sqrt{1-h^2}\,\mathrm{Log}\Big[\frac{4\,i}{\sqrt{-1+h}\,(1+h)^{3/2}\,(1+2h)}\Big]-$$

$$\sqrt{\frac{-1-h}{-1+h}}\,h\sqrt{-1-2h-h^2}\,\mathrm{Log}\Big[-\frac{4\,i}{\sqrt{-1-h}\sqrt{1-h}\,(1-3h+2h^2)}\Big]+$$

$$3\sqrt{\frac{-1-h}{-1+h}}\,h^2\sqrt{-1-2h-h^2}\,\mathrm{Log}\Big[-\frac{4\,i}{\sqrt{-1-h}\sqrt{1-h}\,(1-3h+2h^2)}\Big]-$$

$$3\sqrt{\frac{-1-h}{-1+h}}\,h^3\sqrt{-1-2h-h^2}\,\mathrm{Log}\Big[-\frac{4\,i}{\sqrt{-1-h}\sqrt{1-h}\,(1-3h+2h^2)}\Big]+$$

$$\sqrt{\frac{-1-h}{-1+h}}\,h^4\sqrt{-1-2h-h^2}\,\mathrm{Log}\Big[-\frac{4\,i}{\sqrt{-1-h}\sqrt{1-h}\,(1-3h+2h^2)}\Big]-$$

$$\sqrt{-1+h}\,h\sqrt{\frac{1-h}{1+h}}\sqrt{1+h}\sqrt{1-h^2}\,\mathrm{Log}\Big[-\frac{4\,i}{\sqrt{-1+h}\sqrt{1+h}\,(1+3h+2h^2)}\Big]$$

$$2\sqrt{-1+h}\,h^2\sqrt{\frac{1-h}{1+h}}\sqrt{1+h}\sqrt{1-h^2}\,\mathrm{Log}\Big[-\frac{4\,i}{\sqrt{-1+h}\sqrt{1+h}\,(1+3h+2h^2)}\Big]-$$

$$\sqrt{-1+h}\,h^3\sqrt{\frac{1-h}{1+h}}\sqrt{1+h}\sqrt{1-h^2}\,\mathrm{Log}\Big[-\frac{4\,i}{\sqrt{-1+h}\sqrt{1+h}\,(1+3h+2h^2)}\Big]-$$

$$\sqrt{\frac{-1-h}{-1+h}}\,\pi\,\mathrm{Log}\Big[\frac{\sqrt{1-h}+\sqrt{1-h}\,h-i\,h\sqrt{1+h}}{\sqrt{1-h}\,(1+h)}\Big]+$$

$$\sqrt{\frac{-1-h}{-1+h}}\,h\,\pi\,\mathrm{Log}\Big[\frac{\sqrt{1-h}+\sqrt{1-h}\,h-i\,h\sqrt{1+h}}{\sqrt{1-h}\,(1+h)}\Big]+$$

$$\sqrt{\frac{-1-h}{-1+h}}\,h^2\,\pi\,\mathrm{Log}\Big[\frac{\sqrt{1-h}+\sqrt{1-h}\,h-i\,h\sqrt{1+h}}{\sqrt{1-h}\,(1+h)}\Big]-$$

$$\sqrt{\frac{1-h}{1-h}}\,h^3\,\pi\,\mathrm{Log}\Big[\frac{\sqrt{1-h}+\sqrt{1-h}\,h-i\,h\sqrt{1+h}}{\sqrt{1-h}\,(1-h)}\Big]+$$

$$\sqrt{\frac{1-h}{-1-h}}\,\pi\,\mathrm{Log}\Big[\frac{\sqrt{1-h}+\sqrt{1-h}\,h-i\,h\sqrt{1+h}}{\sqrt{1-h}\,(1+h}\Big]-$$

$$
\sqrt{\frac{-1-h}{-1+h}}\ h\,\pi\,\mathrm{Log}\Big[\frac{\sqrt{1-h}+\sqrt{1-h}\ h+i\,h\sqrt{1+h}}{\sqrt{1-h}\ (1+h)}\Big]-
$$

$$
\sqrt{\frac{-1-h}{-1+h}}\ h^2\,\pi\,\mathrm{Log}\Big[\frac{\sqrt{1-h}+\sqrt{1-h}\ h+i\,h\sqrt{1+h}}{\sqrt{1-h}\ (1-h)}\Big]+
$$

$$
\sqrt{\frac{-1-h}{-1+h}}\ h^3\,\pi\,\mathrm{Log}\Big[\frac{\sqrt{1-h}+\sqrt{1-h}\ h+i\,h\sqrt{1+h}}{\sqrt{1-h}\ (1-h)}\Big]-\sqrt{\frac{1-h}{1+h}}\ \pi\,\mathrm{Log}\Big[\frac{-i\,h+\sqrt{1-h^2}}{\sqrt{1-h^2}}\Big]-
$$

$$
h\sqrt{\frac{1-h}{1+h}}\ \pi\,\mathrm{Log}\Big[\frac{-i\,h+\sqrt{1-h^2}}{\sqrt{1-h^2}}\Big]+h^2\sqrt{\frac{1-h}{1+h}}\ \pi\,\mathrm{Log}\Big[\frac{-i\,h+\sqrt{1-h^2}}{\sqrt{1-h^2}}\Big]+
$$

$$
h^3\sqrt{\frac{1-h}{1+h}}\ \pi\,\mathrm{Log}\Big[\frac{-i\,h+\sqrt{1-h^2}}{\sqrt{1-h^2}}\Big]+\sqrt{\frac{1-h}{1+h}}\ \pi\,\mathrm{Log}\Big[\frac{i\,h+\sqrt{1-h^2}}{\sqrt{1-h^2}}\Big]+
$$

$$
h\sqrt{\frac{1-h}{1+h}}\ \pi\,\mathrm{Log}\Big[\frac{i\,h+\sqrt{1-h^2}}{\sqrt{1-h^2}}\Big]-h^2\sqrt{\frac{1-h}{1+h}}\ \pi\,\mathrm{Log}\Big[\frac{i\,h+\sqrt{1-h^2}}{\sqrt{1-h^2}}\Big]-
$$

$$
h^3\sqrt{\frac{1-h}{1+h}}\ \pi\,\mathrm{Log}\Big[\frac{i\,h+\sqrt{1-h^2}}{\sqrt{1-h^2}}\Big]\Big]\Big)\Big/\left(36\sqrt{1-h}\ (-1+h)\ (1+h)^{3/2}\right)
$$

The interpretation and simplification of this expression is in hand.

```
In[43]:= Plot3D[a / 4 h^2, {a, 0, Pi / 9}, {h, 0.1, 1}, PlotPoints → 20]
```

Graph.44

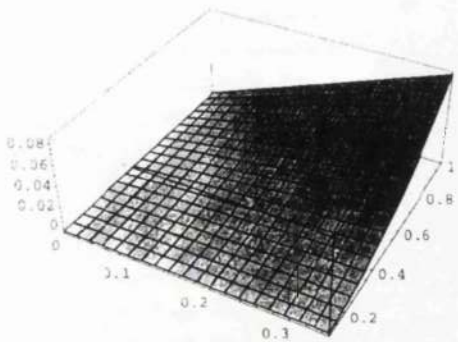


```
Out[43]= - SurfaceGraphics -
```

```
In[1]:= 9 + 9

Out[1]= 18

In[2]:= z = x + I y

Out[2]= x + ı y

In[3]:= ComplexExpand[z]

Out[3]= x + ı y

In[4]:= x + i y
        c = 1

In[8]:= h = 1

Out[8]= 1

In[27]:= Z = r Exp[I q]

Out[27]= r

        u = 100

In[30]:= x = r Cos[q]
         y = r Sin[q]

Out[30]= r

Out[31]= 0

In[29]:= Exp[I q]

Out[29]= 1

In[32]:= q =

Syntax::tsntxi : "q =" is incomplete; more input is needed.

                q =

In[32]:= q

Out[32]= 0

In[33]:= Unset[q]

In[34]:=
         q

Out[34]= q

In[28]:=
         ComplexExpand[Z, {Z}]

Out[28]= ı Im[r] + Re[r]
```

Ground Effect on Flow About Spinning Cylinder

Potential Flow past rotating cylinder in ground effect

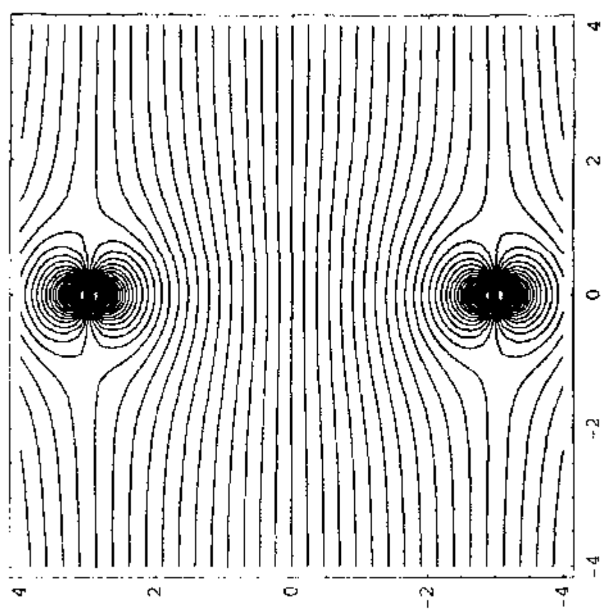

fig.4.2

Cylinder without rotation in ground effect. Three diametres above the ground.

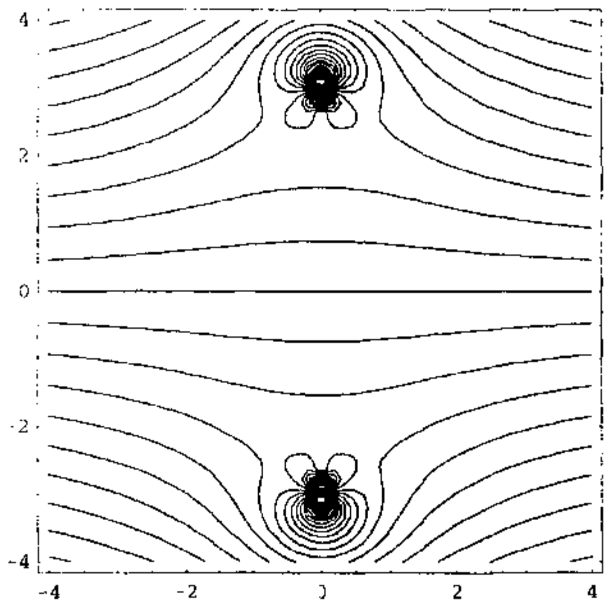

This is the effect of a small rotation. Vortex strength equals 0.3.

fig.43

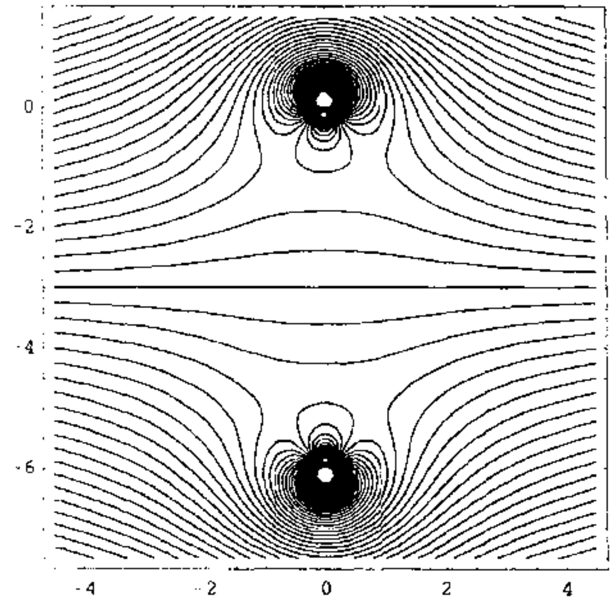

This is the effect of a low rotation.

fig.44

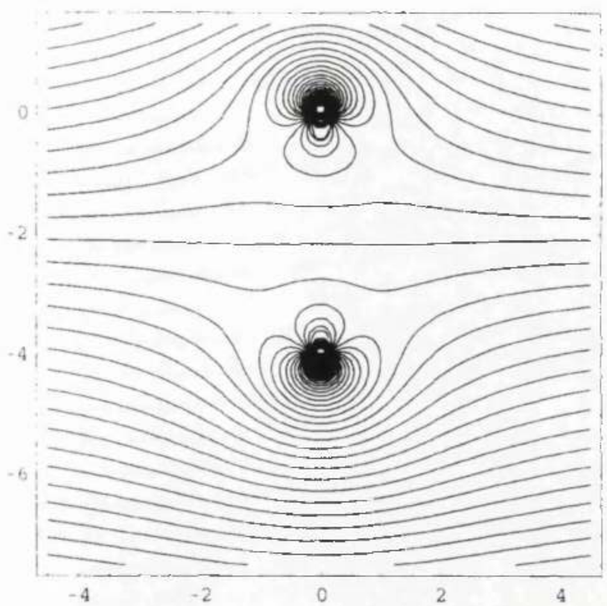

the following two illustrations are

fig.45

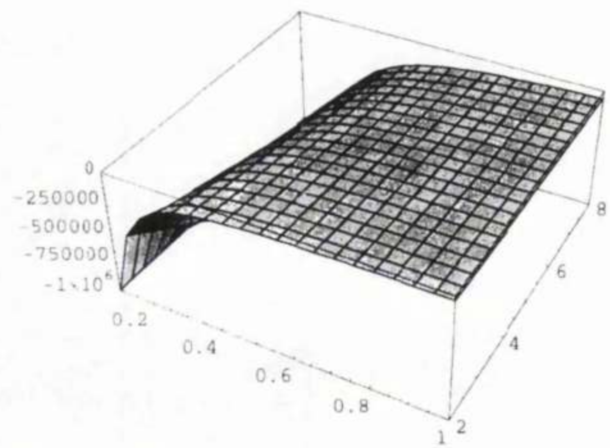

This illustration indicates the contribution to drag at the singularity at the centre of the cylinder.

graph.45

```
In[97]:= a = 1
         q = 0
         Plot3D[
           Im[1/(a^2 h^3 (a^2 - 4 h^2)^3) (5000 (i a^12 - 12 i a^10 h^2 + 48 i a^8 h^4 - 64 i a^6 h^6 + 768 i a^6 h^6 -
               3072 i a^4 h^8 + 4096 i a^2 h^10 - a^10 h v + i a^10 h v + 12 a^8 h^3 v + 24 i a^8 h^3 v -
               48 a^6 h^5 v - 256 i a^6 h^5 v + 64 a^4 h^7 v + 1024 i a^4 h^7 v - 2048 i a^2 h^9 v + 1024 i h^11 v -
               2 i a^8 h^2 v^2 + 40 i a^6 h^4 v^2 - 256 i a^4 h^6 v^2 + 640 i a^2 h^8 v^2 - 512 i h^10 v^2))],
           {h, .1, 1}, {v, 2, 8}, PlotPoints -> 20]

Out[97]= 1
Out[98]= 0
Out[99]= - SurfaceGraphics -
```

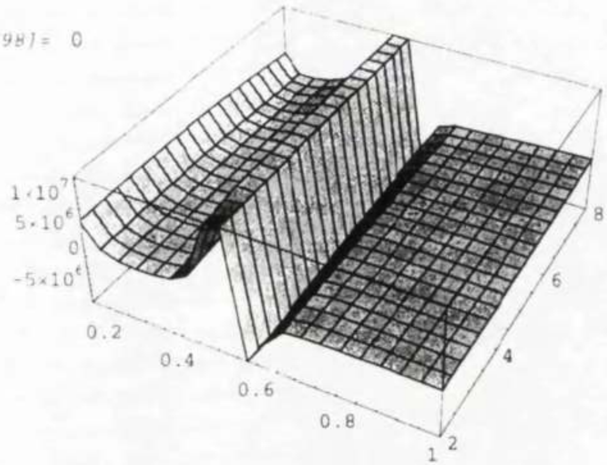

graph.46

This illustration indicates the contribution to lift at the singularity at the centre of the cylinder.

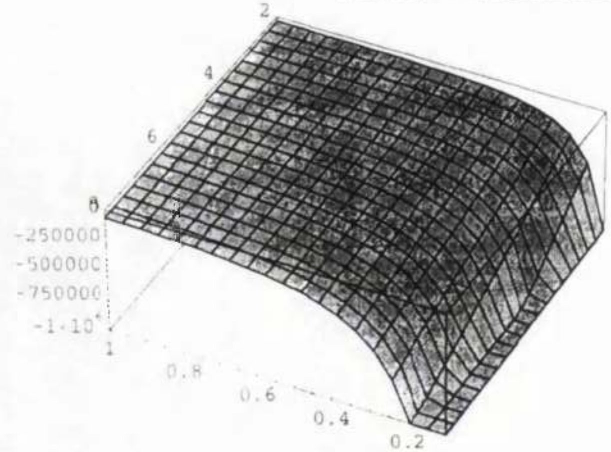

graph.47

This illustration indicates the contribution to drag at the singularity at the centre of the cylinder.

```
In[100]:= a = 1
          q = 0
          Plot3D[
            Im[1/(a^2 h^3 (a^2 - 4 h^2)^3) (5000 (i a^12 - 12 i a^10 h^2 + 48 i a^8 h^4 - 64 i a^6 h^6 + 768 i a^6 h^6 -
              3072 i a^4 h^8 + 4096 i a^2 h^10 - a^10 h v + i a^10 h v + 12 a^8 h^3 v + 24 i a^8 h^3 v -
              48 a^6 h^5 v - 256 i a^6 h^5 v + 64 a^4 h^7 v + 1024 i a^4 h^7 v - 2048 i a^2 h^9 v + 1024 i h^11 v -
              2 i a^8 h^2 v^2 + 40 i a^6 h^4 v^2 - 256 i a^4 h^6 v^2 + 640 i a^2 h^8 v^2 - 512 i h^10 v^2))],
            {h, .1, 1}, {v, 2, 8}, PlotPoints → 20, ViewPoint -> {-6, 12, 10}]

Out[100]= 1

Out[101]= 0
```

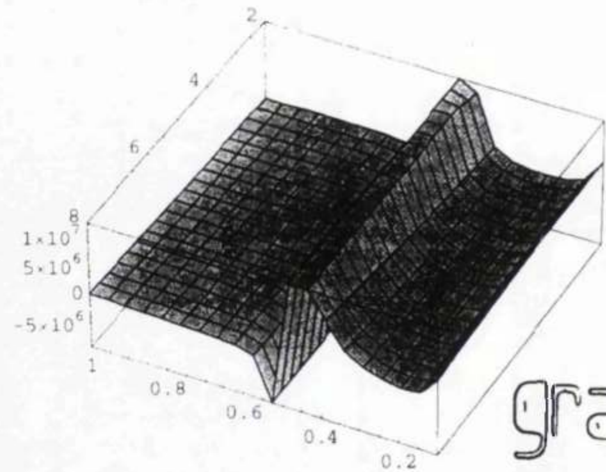

graph.48

```
Out[102]= - SurfaceGraphics -
```

This illustration indicates the contribution to lift at the singularity at the centre of the cylinder.

CFD

C.F.D ANALYSIS METHOD

4.1 OVERVIEW OF COMPUTATIONAL METHOD ADOPTED

The aim of this project was to analyze two different types of aerofoil profiles using CFD analysis. The most basic shaped wing is known to be the NACA 0012 and due there being adequate information available on it, it seemed logical to commence my CFD analysis on this profile. The second was the S-shaped profile. This incorporates the Munk M6R2 over the upper portion and the CJ-5 over its lower portion. The S-shaped profile was chosen due to all new designs being based on this fairly new concept which has an increased effectiveness and has been proven to be of more use in surface effect vehicles.

From the above mentioned book, it was found through numerical simulations for steady flow past the wings at high Reynolds numbers, with turbulence, by a finite volume method, that, for high cambered profile, increase in lift was significant. The stability, however, was very poor. The S-shaped profile not only acquired excellent lift stability but also had a moderate lift coefficient.

Although the Japanese are known to be further ahead with their studies on Wing-In-Surface Effect vehicles, the general information provided to and known by the British public interested in this field is incredibly scarce.

It may be that if more information, however vague and general, on this subject were to be made available to the public that more people would, in fact, be intrigued by W.I.S.E. craft and wish to study the subject in greater detail. Perhaps, even, to the extent of constructing a passenger liner for commercial use

Although my personal knowledge is limited, compared to what others may know, this thesis is aimed at not only persuading others to follow and continue this work but also to provide knowledge which they, otherwise, may not have known. For this reason it is not continued directly from the work of others, such as the book named above. Instead, an

initial step back was taken, allowing information on low Reynolds number steady flows to be analyzed, creating a firmer base from which to work.
[Ref: 62 - 65, 68 - 71]

4.2 INTRODUCTION

WISE (Wing-In-Surface Effect) craft are high-speed vehicles which are based on the advantageous aerodynamic phenomena present when in ground effect. This is especially the case, during their take-off procedure which is facilitated by the great L/D (lift to drag ratio) present. The term 'Surface Effect' is adopted because it describes all surfaces, whether ground or water.

In order for W.I.S.E. craft to be introduced in the passenger-carrying field of transportation, the study of wing profiles is both inevitable and essential. This is primarily due to WISE craft being a unique concept, unlike present sea going transportation vehicles, which do not include the wing concept in their design characteristics.

Although numerous methods have been used to study the aerodynamics of wings in ground effect such as the 'moving belt' technique, the 'boundary layer' method, the panel method, CFD simulation and many more, it has been proven to be incredibly difficult but highly important to compare the lift, drag and moment coefficients with α (the angle of attack) as well as with h/c (the height to chord ratio). For this reason, as well as the increase in WISE craft numbers over the years it is believed to be of great importance to analyze these characteristics using numerical simulation techniques based on CFD (Computational Fluid Dynamics) programs.

It may be noted that a vast amount interest has been shown in and research carried out on the stability of WISE craft. It has been found that together with reduction of h/c, the center of pressure, which is present on the underside of the wing, moves forward. This results in the nose of the craft moving upwards as the height between the wing and the surface decreases. It is for this reason that numerous WISE craft adopt a large tail plane concept resulting in an increase in stability. Unfortunately the tail planes do not increase the lift, but do however decrease the L/D ratio of the wings. This causes a great disadvantage and is the reason why Russia commenced study on the S shaped aerofoil. It was said that by giving the aerofoil an S shape at its ends its stability would increase.

Although results for the S shaped aerofoil have been obtained through practical experience as well as by experiments involving the upper section of such wing profiles it was believed that this project would result in providing numerical data on the subject. It should also describe in detail the forces exerted on the wing profiles during all stages of take-off.

4.3-FLUENT INPUT REQUIREMENTS

The analysis of the following topic has been carried out using the following subdivisions, namely;

History of WIGs - involving the Database,

The CFD analysis-involving the Gambit and Fluent 5 program, and

The Experimental tests.

4.3.1 CFD ANALYSIS USING GAMBIT AND FLUENT PROGRAMMES

This section of the report analyses a CFD problem involving wings in ground effect. Computational Fluid Dynamics programmers used were the Gambit and the, Fluent 5 programmes.

A frequently used aerofoil section in wing-in-ground effect craft, is the S-shaped aerofoil. Prior to commencing simulation of this aerofoil section over still water and then uneven ground conditions, it was thought essential to verify the programme's capabilities by primarily modelling the NACA 0012 section over ground and then over still water. This was carried out in order to acquire solutions, which could be compared with existing results and hence validated.

The simulations of the NACA 0012 over still water were carried out in order to observe variations in lift, drag, momentum coefficients, turbulence and indications of wave patterns created at low altitudes of flight.

Following this introduction to the problem, which included background information on aerofoil sections and described the CFD Fluent program, it goes on to analyse aerofoil sections studied during the analysis. It gives details of the strategy behind the numerous input requirements of gambit, such as the mesh generation process, the boundary

conditions involved, the Fluent 5 program creation of solver input files and information on the running of solutions given prior to the solver outputs having been attained.
Due to the involvement of five different angles of attack, namely 0, 2,5, 7.5 and 10 degrees varying with five different h/c values, namely 1.5,1,0.75,0.5 and 0.25, it was possible to show positive or negative contribution to the aerodynamics involved around the aerofoil.

4.3.2 GRID GENERATION

Due to CFD results being dependent on the grid formation of the model, it is very important that a correct grid generation be adopted. It is for this reason that a triangular meshing process was used to model the aerofoil sections under investigation. The grids were structured and had a spacing of 0.04 units. The meshing process was carried out as a pre-processing operation on Gambit. Once the pre-processing operations came to an end, the file could then be exported from Gambit and entered in to Fluent 5.

Fluent has the ability to work with both structured and unstructured grid generations. The main difference between the two types of grid generations is in the form of data structure, which describes the meshes in the most appropriate manner. A structured mesh of triangles or quadrilaterals incorporating the use of co-ordinates and connectivities which naturally map into the elements of a matrix. This means that the location of each point may be found with ease.

The main advantage of a structured grid lies in its computational efficiency since there is no requirement for the solver to refer to a connectivity table at each iteration. This resulted in a more effective outcome.

4.4 Overview of Physical Model in FLUENT

Fluent accommodates for an extensive scope of incompressible, and compressible, laminar and turbulent fluid flow problems. Fluent is capable of modelling various complex geometrical configurations.

A vital component of Fluent programming is the necessity to obtain a sturdy and exact turbulence model prior to commencing iteration. This is especially the case for turbulence models. There are turbulence models available in the Fluent Tutorial Guide covering a wide spectrum of examples and requiring little or no modification. Particular attention has been allocated to near-wall accuracy through the use of extended wall functions and Ronal models.

4.4.1 Continuity and Momentum Equations

FLUENT solves conservation equations for mass and momentum. For flows involving heat transfer or compressibility, an additional equation for energy conservation is solved.

4.4.1 The Mass Conservation Equation

The equation for conservation of mass or continuity equation is as follows:

$(\delta\rho/\delta\tau) + \delta/\delta XI(pui) = Sm$

This is the general format of the mass conservation equation, which is also dependable in the case of incompressible flows. Sm is the mass added to the continuous phase from the diffused second phase due to phenomena such as the vaporisation of liquid droplets and any other user-defined sources.

For 2D axisymmetric geometries, the continuity equation is given by:

$(\delta\rho/\delta\tau) + \delta/\delta x(\rho u) + \delta/\delta r(\rho v) + \rho v/r =$

Where;

x is the axial co-ordinate,

r is the radial co-ordinate,

u is the axial velocity, and

v is the radial velocity.

4.5 Momentum Conservation Equations

Conservation of momentum in the I direction in an inertial (non-accelerating) reference frame is described by [8]

$\delta/\delta\tau(\rho ui) + \delta/\delta xi(\rho uivj) = - \delta p/\delta xi + \delta\tau ij/\delta xj + \rho gi + Fi$ (8.2-3) from book

Where;

p is the static pressure,

tij is the stress tensor (described below), and

ρgi and Fi are the gravitational body force and external body.

Fi also accommodates for other model-dependant source terms such as porous-media and user-defined sources.

The stress tensor tij is given by

$\tau ij = [\mu\ (\delta ui/\delta xj + \delta uj/\delta xi)] - 2/3(\mu\ \delta ul/\delta xl)\ \delta ij$ (8.2-4) from book

Where μ is the molecular velocity and the second term on the right hand side is the effect of volume dilation.

For 2D axisymmetric geometries, the axial and radial momentum conservation equations are given by

$\delta/\delta\tau\ (\rho u) + 1/r\ \delta/\delta x\ (\ r\rho uu\ ) + 1/r\ \delta/\delta r\ (\ r\rho vu\ )$

$= - \delta \rho/\delta x + 1/r\, \delta/\delta x\, [r\mu\, (2\delta u/\delta x - 2/3\, (V.v))] + 1/r\, \delta/\delta r\, [r\mu\, (2\delta u/\delta r + \delta v/\delta x)] + Fx$

(8.2-5) from book

And

$\delta/\delta\tau\, (\rho v) + 1/r \delta/\delta x\, (r\rho uv) + 1/r\, \delta/\delta r\, (r\rho vv)$

$=-\delta p/\delta r + 1/r\, \delta/\delta x\, [r\mu\, (\delta v/\delta x - \delta u/\delta r)] + 1/r\, \delta/\delta r\, [r\mu\, (2\delta v/\delta r - 2/3\, (V.v)]$

$-2\mu v/r^2 + 2/3\, \mu/r\, (V.v) + \rho w^2/r + Fr$

(8.2-6) from book

Where

$V.v = \delta u/\delta x + \delta v/\delta r + v/r$ (8.2-7) from book

and w is the swirl velocity.

4.6 Time-Dependent Simulation

The FLUENT programme also has the ability to resolve equations for conservation of mass, momentum, energy, and species, as well as various other scalar equations in time-dependent form. It is for this reason that it may be stated that FLUENT has the required ability to simulate a variety of time-dependent problems.

When one desires to solve steady-state phenomena, which are inclined to becoming unstable, activating time dependence is regarded as an additional aid tool. Integration of the time dependent equations also regularly assists one in obtaining a steady-state result.

Temporal Discretisation- In FLUENT the time-dependent equations have to be discretised in both space and time. The spatial discretisation for the time-dependent equations is equivalent to the steady state problem. It entails the integration of all the individual terms in the differential equations over a time step dt. Insights on s are located in section 8.9.1 from the 'Fluent' User Guide manual'.

Iterations- Fluent resolves the time-dependent equations using implicit formulation. For this reason, it is vital that iterations be carried out at each time step. This panel, when exposed by the user, allows a maximum value to be appointed for the number of iterations essential at distinct time steps. When the convergence characteristics are discovered prior to this number of iterations being fulfilled, the solution will advance to the proximate time step.

The time step size is the scope of DT. For the modelling of transient cases with higher accuracy, it is vital to allocate DT a value which is at least one order of magnitude less than the smallest time constant indicated. This is the reason for choosing 1e-07 value for all cases under investigation in this report. They were then reduced systematically as the time-step constants decreased.

4.7 Turbulence Modelled

Turbulent flows are known for their spasmodic velocity domains. These irregularities amalgamate transported quantities such as energy, momentum, and species concentration, and additionally result in the fluctuation of these transported quantities.

Due to these irregularities having the ability of being small scale and high frequency, they are not computationally economical. However, the precise governing equations may be time-averaged, ensemble averaged, or otherwise controlled to eliminate all small scales, consequently becoming a transformed set of equations which are economical to simulate. It may also be stated that the altered equations embody supplementary variables, which are unknown. Turbulence models are therefore required to determine these variables.

FLUENT provides a variety of turbulent cases, which may be detected in section 9.1 of the Fluent users Guide. With regard to the problems investigated in this report, it was thought vital to select the ***Reynolds Stress Model***. This was deduced through trial and error, as other initially adopted models did not provide a good enough method to resolve such problems. The ***Reynolds Stress Model*** utilises a several equations, (5 equations are used), compared to other methods employing as little as one equation. Although this resulted in a more time consuming method it proved to be of greater accuracy.

4.8 The Reynolds Stress Model

The Reynolds stress model (RMS) is the most intricate turbulence model available in FLUENT. The RMS closes the Reynolds-averaged Navier-Stokes equations by solving transport equations for the Reynolds stresses along with an equation for the dissipation rate. This results in four additional transport equations being required in 2D and seven additional equations in 3D.

Due to the RMS model taking into account streamline curvature, swirl, rotation, and swift variations in the rate of strain adopting a highly rigorous method, unlike the one or two-equation models, it has greater potentiality to attain a legitimate solution to convoluted flows. However, the fidelity of the RMS predictions is still limited by the closure assumptions engaged in modelling various terms in the transport equation for the Reynolds stresses.

This procedure involves calculation of each Reynolds stress, ui'uj', using differential transport equations. The individual Reynolds stresses are then used to obtain closure of the Reynolds-averaged momentum equation. This action involves the exact momentum equations being multiplied by a fluctuating property, the product then being Reynolds-averaged.

When relating the Reynolds Stress the following equations are adopted:

The Reynolds Stress Transport Equation
The Turbulent Diffusive Transportation Equation
The Linear pressure-Strain Equations
The Low-Re Equation
Equations for a Quadratic Pressure-Strain Model
The Turbulent Kinetic Energy Equations
Equations involving Dissipation Rate
Equation for the modelling of Turbulent Viscosity

Equations incorporating boundary conditions for Reynolds Stresses

When one adopts the RMS model for solving turbulence problems, FLUENT transmits the equation residuals for the individual Reynolds stress transport equations to a data file. One has the ability to programme convergence criteria to the Reynolds stress residuals: normalised residuals in the range of 1×10^{-3} in most cases states a converged solution. However, one may be required to apply rigorous convergence criteria (below 1×10^{-4}) in order to assure total convergence. More information on the criterion adopted for the problems examined in this project are clearly stated further in this report.
Previously stated equations together with detailed information on each, may be obtained in section 9.5 of the Fluent Users Guide.

4.9 Near-Wall Treatment For Wall-Bounded Turbulent Flows

Pressures affect turbulent flows in a dramatic manner. The no-slip condition must be satisfied at the wall boundaries. This phenomenon ultimately affects the mean velocity field. This affects an additional characteristic, namely turbulence, in a non-trivial manner. In close proximity to the wall viscous damping decreases tangential velocity oscillations, while kinematics blocking lessens normal oscillations. However, turbulence is drastically altered due to the creation of turbulent kinematic energy caused by tremendous gradients in the mean velocity located at the outer region of the wall. Exact description of the flow in the near-wall region ultimately results in accurate predictions of wall-bounded turbulent flows.

In the cases under investigation in this report, the aerofoil sections were located between two walls. It was for this reason that careful thought was allocated to the previous section. One was placed at the top 1.5 m above the lower wall region when modelling the aerofoil sections over ground and 2 m when modelling the flow around the aerofoil sections over water surfaces.

In the problems being examined in this report, ***The Non-equilibrium Wall Functions*** were chosen as a means of better simulation. The key elements in the non-equilibrium wall functions are as follows:

Launder and Spalding's log-law for Mean Velocity is sensitised to pressure gradient effects.

The two-layer-based concept is adopted to compute the budget of turbulent kinetic energy in the wall-neighbouring cells.

Although some illustrations of this process are included in APPENDIX 'A', more detailed information may be found on the topic in section 9.7 of the Fluent Users Guide Manual.

4.10 Solution Strategies for Turbulent Flow Simulation

The length of individual cells of the mesh (modelled on Gambit) were chosen to be 0.04 units in length. It is vital to ensure that the mesh is fine to better calculate the variables around the whole flow field, however the Wall Functions involved require the mesh to be neither too fine nor too coarse. Prior to commencing the cases, mesh designs were thoroughly investigated. Some of the designs were incapable of being generated, a few were unable to run on the Fluent programme and others, which were too coarse, were incapable of providing adequate results. The majority of problems were caused at the interface region between the air and the water surface in the multiphase cases. It was for this reason that this specific mesh type was chosen. This mesh design proved to be sufficiently effective as well as less complicated resulting in less computational time on Fluent.

During this exercise close detail was paid to section 9.10 of the Fluent Users Guide, which relates to Mesh Generation techniques, accuracy and convergence. If further information is required on these topics please relate to the section mentioned.

4.10.1 Multiphase flow models

There are three models available in the Fluent programme for simulating flow irregularities.

The Volume Of Fluid (VOF) model,

The Cavitation Model, and

The Algebraic Slip Mixture Model.

For the investigation of the cases involved in this report, the VOF model was adopted for reasons explained below.

The VOF model is a Fixed Grid Technique designed for multiphase cases where the position of the interface amid the fluids is of interest. In the VOF model, a single set of Momentum Equations is communal to all fluids present and the Volume Fraction of individual fluids in each computational cell is followed throughout the zone.

For supplementary phases added to the model, a volume fraction of the phase in the computational cell is introduced. In each control volume, the volume fraction of all phases, sum to unity. The characteristic properties and variables in each given cell are either true of the phases or representative of a mixture of the phases, depending upon the Volume Fraction values.

Component Phases in each control volume determine the form of the transport equations.
A single Momentum Equation is solved throughout the zone investigated.
A set of Transport Equations is solved when turbulence properties are present in the flow field.

Additional information on the above, as well as ways in which interpolation may be carried out near the interface, is given, in detail, in section 15.2 of the Fluent Users Guide. Please refer to this section for further information.

4.11 PRESSURE DISTRIBUTION ON THE WATER SURFACE.

It may be noted when referring to APPENDIX 'A', that, when the height h is very small, i.e. 0.25, the front and back leading and trailing edge sections of the aerofoil experience a lower pressure distribution which results in a slight increase in the height of the water surface. However, directly below the wing the pressure is increased causing the water surface to deform downwards. This may be read in the FLUENT Users Manual that the positive pressure below the wing was caused by the positive pressure created by the power surface of the wing, and that the negative pressure of the water surface was created by the negative pressure of the upper surface of the wing.

It is due to the smooth and curved shape of the aerofoil that a smooth harmonic wave is made unlike in a 'static aircushion' effect, which produces a sudden height difference forward and aft of the craft.

The information obtained on the pressure distribution over the water surface is not sufficiently detailed to encourage pursuit of further study on this topic at this moment in time. Nevertheless, the possible results of such a study would be highly informative and helpful. It could be investigated in the future either by myself or by others interested in such a subject.

Directions on how to use the programmes is located in Appendix 'A'.

EXAMPLES OF INFORMATION ATTAINED ON FLUENT

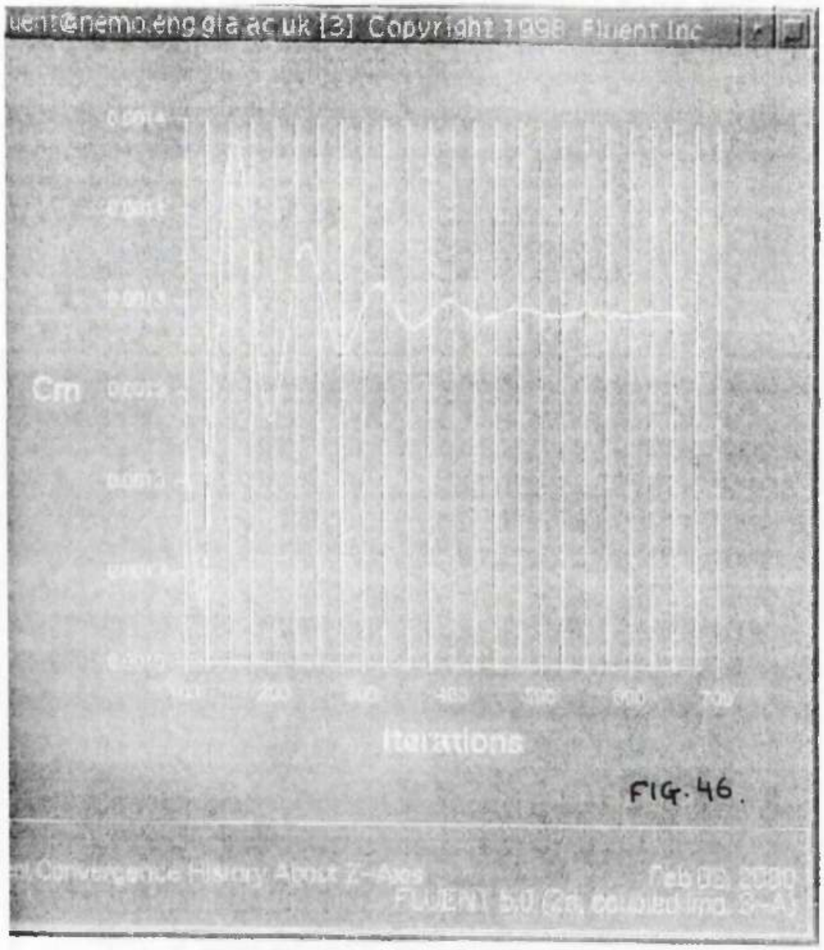
uent@nemo.eng.gla.ac.uk [3] Copyright 1998 Fluent Inc
Cm
200
300
700
Iterations
Convergence History About Z-Axis
Feb 03, 2000
FLUENT 5.0 (2d, coupled imp, 3-A)

FIG. 46.

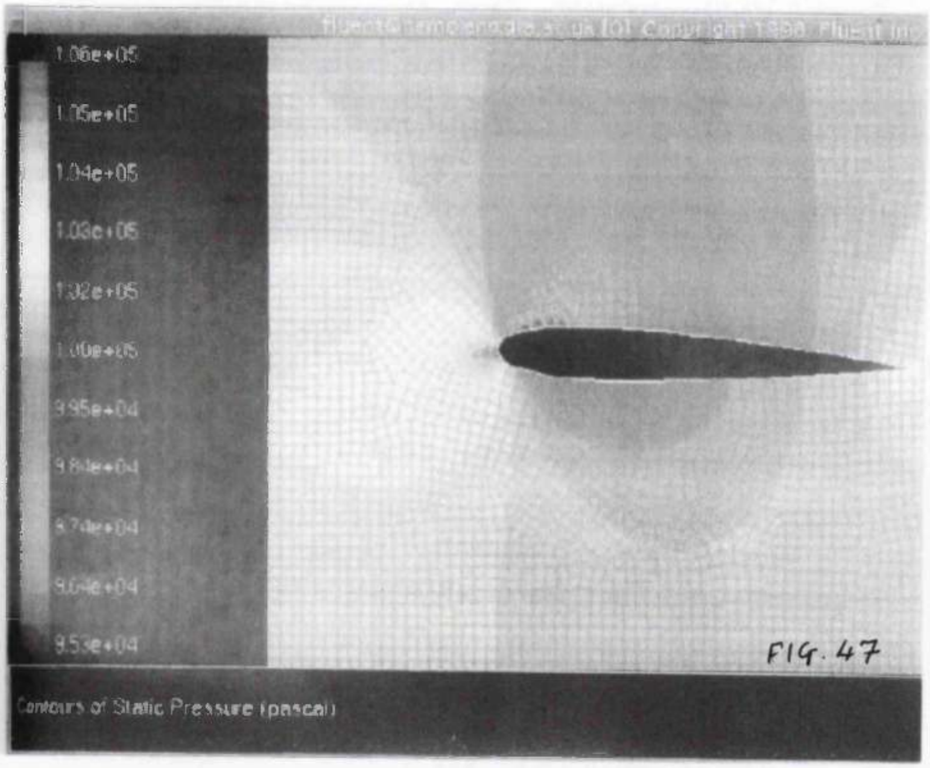
fluent5 (2d, segregated, ske) Copyright 1998 Fluent Inc
1.06e+05
1.05e+05
1.04e+05
1.03e+05
1.02e+05
1.00e+05
9.95e+04
9.84e+04
9.74e+04
9.64e+04
9.53e+04
Contours of Static Pressure (pascal)

FIG. 47

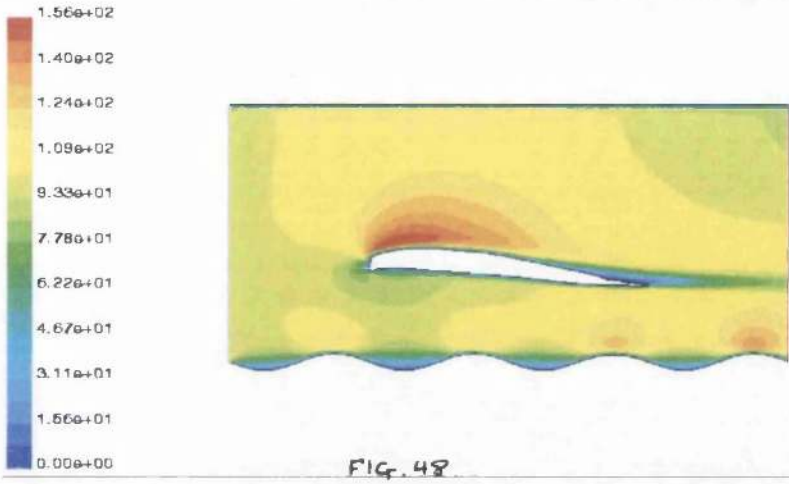

FIG. 48

Contours of Velocity Magnitude (m/s) (Time=2.2174e+01) Jun 04, 2000
FLUENT 5.0 (2d, segregated, RSM, unsteady)

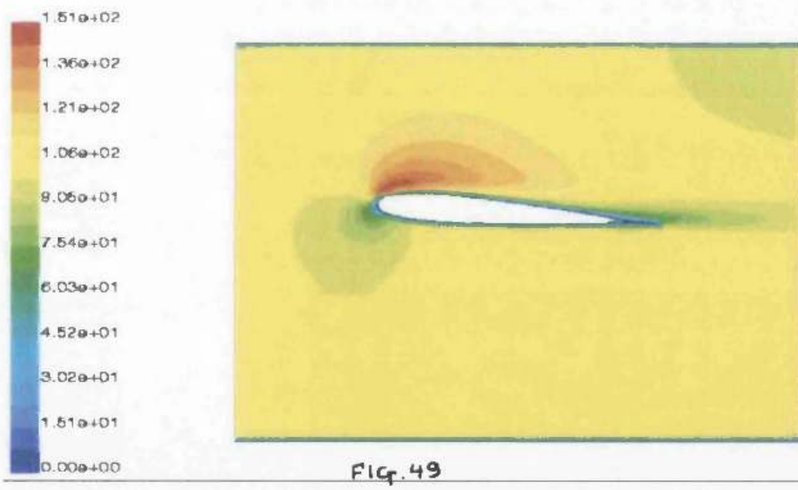

FIG. 49

Contours of Velocity Magnitude (m/s) (Time=8.6168e-01) Apr 11, 2000
FLUENT 5.0 (2d, segregated, lam, unsteady)

FIG. 50.

Contours of Static Pressure (pascal) (Time=2.2174e+01) Jun 04, 2000
FLUENT 5.0 (2d, segregated, RSM, unsteady)

RESULTS ATTAINED USING C.F.D. PROGRAMMES IN TABULATED AND GRAPHICAL FORMAT

NACA 0012 - Aerofoil-OVER GROUND

Cd values only

a

h	0	2	5	7.5	10
1.50					0.086234
1.00				0.06671	
0.75			0.15982		
0.50		0.029377			
0.25	0.028822				

TABLE 1

Cl values only

a

h	0	2	5	7.5	10
1.50					1.0285
1.00				0.92178	
0.75			0.69928		
0.50		-0.21265			
0.25	-0.8414				

TABLE 2

Cm values only

a

h	0	2	5	7.5	10
1.50					-0.22375
1.00				-0.18241	
0.75			-0.03609		
0.50		0.023336			
0.25	0.1262				

TABLE 3

cd		cl		cm
0		0		0
0		0		0
0		0		0
0		0		0
0.028822		-0.8414		0.1262
0		0		0
0		0		0
0		0		0
0.029377		-0.21265		0.023336
0		0		0
0		0		0
0		0		0
0.15982		0.69928		-0.03609
0		0		0
0		0		0
0		0		0
0.06671		0.92178		-0.18241
0		0		0
0		0		0
0		0		0
0.086234		1.0285		-0.22375
0		0		0
0		0		0
0		0		0
0		0		0

TABLE 4

NACA 0012 - Aerofoil-STILL WATER

Cd values only

h	a: 0	2	5	7.5	10
1.50	0.017169	0.019346	0.03446	-0.18969	
1.00	0.012408	0.019841	0.036658	0.068605	
0.75	0.018859	0.020617	0.031603	0.073714	
0.50	0.021735	0.021865	0.037706	0.081461	
0.25	0.042237	0.012408	0.040862	0.095695	

TABLE 5

Cl values only

h	a: 0	2	5	7.5	10
1.50	-0.015029	0.233585	0.627858	0.86567	
1.00	-0.059039	0.233379	0.48707	0.97065	
0.75	-0.108695	0.230043	0.38321	0.98994	
0.50	-0.252227	0.194882	0.787912	1.1143	
0.25	-0.907056	-0.059071	0.94841	1.5706	

TABLE 6

Cm values only

h	a: 0	2	5	7.5	10
1.50	-9.26E-05	-0.057311	-0.137762	-0.18969	
1.00	0.004914	-0.058846	-0.1269	-0.18799	
0.75	0.010187	-0.061696	-0.12207	-0.19307	
0.50	0.02736	-0.0627	-0.175944	-0.20425	
0.25	0.118582	0.004921	-0.20345	-0.2355	

TABLE 7

cd	cl	cm
0.017169	-0.015029	-9.26E-05
0.012408	-0.059039	0.004914
0.018859	-0.108695	0.010187
0.021735	-0.252227	0.02736
0.042237	-0.907056	0.118582
0.019346	0.233585	-0.057311
0.019841	0.233379	-0.058846
0.020617	0.230043	-0.061696
0.021865	0.194882	-0.0627
0.012408	-0.059071	0.004921
0.03446	0.627858	-0.137762
0.036658	0.48707	-0.1269
0.031603	0.38321	-0.12207
0.037706	0.787912	-0.175944
0.040862	0.94841	-0.20345
-0.18969	0.86567	-0.18969
0.068605	0.97065	-0.18799
0.073714	0.98994	-0.19307
0.081461	1.1143	-0.20425
0.095695	1.5706	-0.2355
0	0	0
0	0	0
0	0	0
0	0	0
0	0	0

TABLE 8

S-shaped over curved ground

Cd values only

h \ a	0	2	5	7.5	10
1.50	0.041426	0.037245	0.044284	0.065931	0.11001
1.00	0.040742	0.035018	0.044559	0.074175	0.20868
0.75	0.041362	0.034996	0.047741	0.071427	0.57114
0.50	0.042198	0.034033	0.04745	0.076134	0.22404
0.25	0.04728	0.038865	0.04562	0.12658	0.33224

TABLE 9

Cl values only

h \ a	0	2	5	7.5	10
1.50	0.28724	0.55056	0.86187	1.1201	1.1396
1.00	0.30925	0.60614	0.98046	1.0734	1.3418
0.75	0.33274	0.6581	0.9493	1.2961	1.9919
0.50	0.34468	0.69665	1.1398	1.3557	2.0987
0.25	0.30834	0.68021	1.0476	0.12093	2.1701

TABLE 10

Cm values only

h \ a	0	2	5	7.5	10
1.50	-0.05469	-0.11158	-0.19423	-0.25518	-0.24875
1.00	-0.0543	-0.12493	-0.21407	-0.23423	0.11468
0.75	-0.06261	-0.1353	-0.21174	-0.28596	0.11164
0.50	-0.07149	-0.15231	-0.25399	-0.30944	-0.28571
0.25	-0.09673	-0.20319	-0.33213	-0.55727	-0.40058

TABLE 11

	cd	cl	cm	h	h/c	
0	0.041426	0.28724	-0.05469	1.50	14.42209	0.75
	0.040742	0.30925	-0.0543	1.00	13.17445	0.50
	0.041362	0.33274	-0.06261	0.75	12.43073	0.38
	0.042198	0.34468	-0.07149	0.50	12.24266	0.25
	0.04728	0.30834	-0.09673	0.25	15.33372	0.13
2	0.037245	0.55056	-0.11158	1.50	6.76493	
	0.035018	0.60614	-0.12493	1.00	5.777213	
	0.034996	0.6581	-0.1353	0.75	5.317733	
	0.034033	0.69665	-0.15231	0.50	4.885236	
	0.038865	0.68021	-0.20319	0.25	5.713677	
5	0.044284	0.86187	-0.19423	1.50	5.13813	
	0.044559	0.98046	-0.21407	1.00	4.544704	
	0.047741	0.9493	-0.21174	0.75	5.029074	
	0.04745	1.1398	-0.25399	0.50	4.163011	
	0.04562	1.0476	-0.33213	0.25	4.354716	
7.5	0.065931	1.1201	-0.25518	1.50	5.886171	
	0.074175	1.0734	-0.23423	1.00	6.910285	
	0.071427	1.2961	-0.28596	0.75	5.510917	
	0.076134	1.3557	-0.30944	0.50	5.615844	
	0.12658	0.12093	-0.55727	0.25	104.6721	
10	0.11001	1.1396	-0.24875	1.50	9.653387	
	0.20868	1.3418	0.11468	1.00	15.55224	
	0.57114	1.9919	0.11164	0.75	28.67313	
	0.22404	2.0987	-0.28571	0.50	10.67518	
	0.33224	2.1701	-0.40058	0.25	15.30989	

TABLE 12

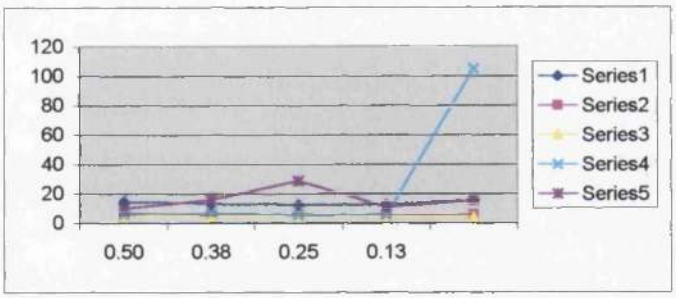

GRAPH 54

cd values

for 0 angle of attack

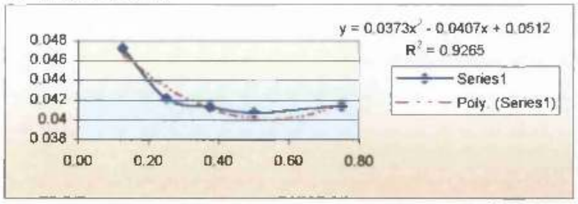

GRAPH 55

for 2 angle of attack

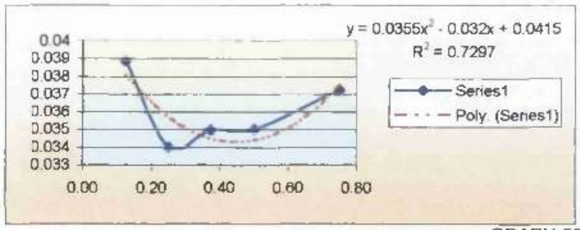

GRAPH 56

for 5 angle of attack

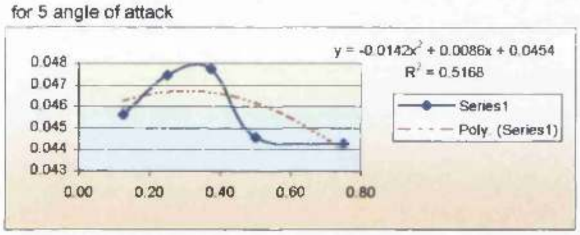

GRAPH 57

for 7.5 angle of attack

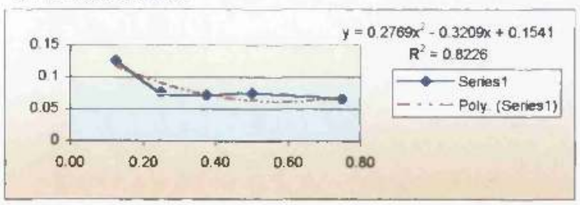

GRAPH 58

for 10 angle of attack

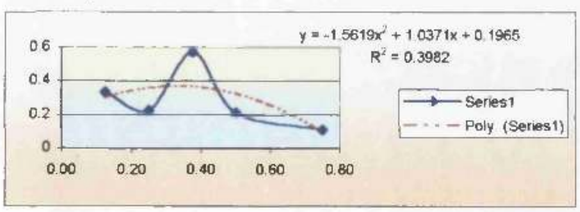

GRAPH 59

cl values

for 0 angle of attack

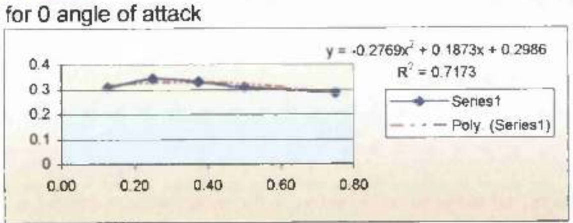

GRAPH 60

for 2 angle of attack

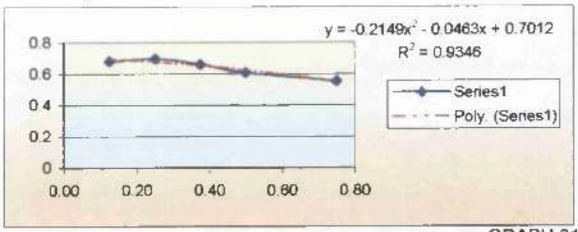

GRAPH 61

for 5 angle of attack

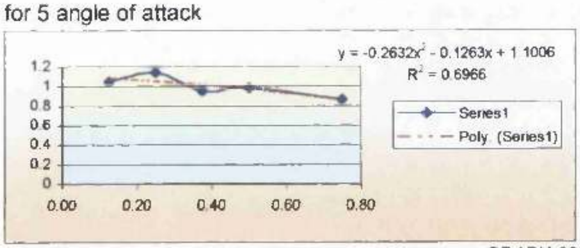

GRAPH 62

for 7.5 angle of attack

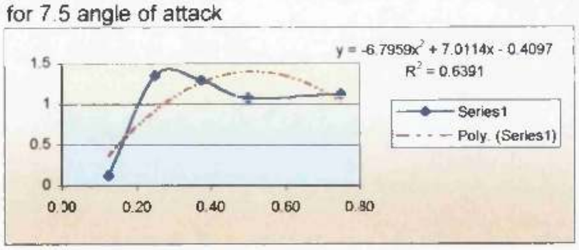

for 10 angle of attack

GRAPH 63

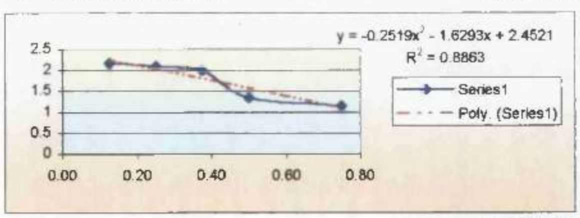

GRAPH 64

cm values

for 0 angle of attack

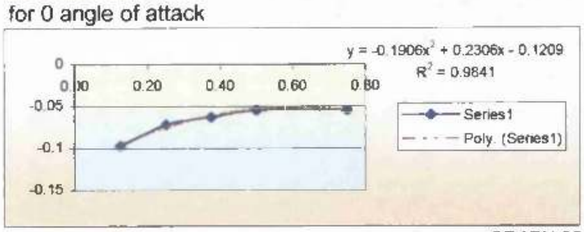

GRAPH 65

for 2 angle of attack

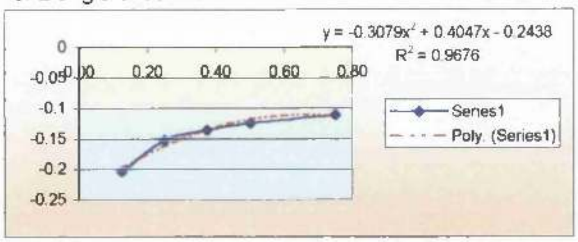

GRAPH 66

for 5 angle of attack

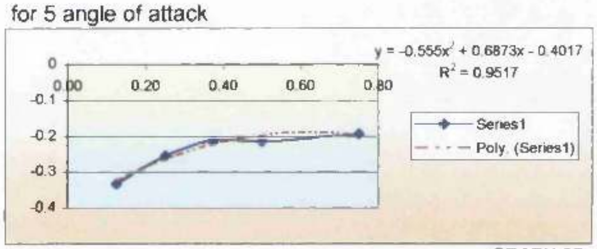

GRAPH 67

for 7.5 angle of attack

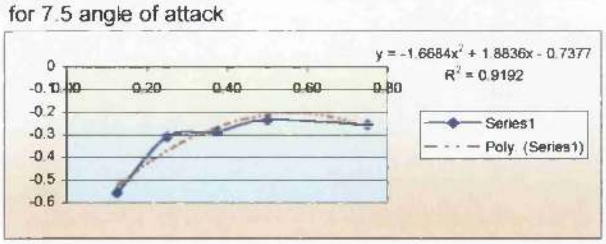

for 10 angle of attack

GRAPH 68

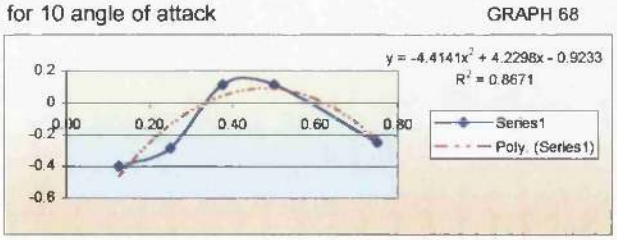

GRAPH 69

S-shaped over still water

Cd values only

a

h	0	2	5	7.5	10
1.50	0.040975	0.03818	0.046736	0.073696	0.10807
1.00	0.040598	0.035468	0.04582	0.068686	0.10724
0.75	0.03972	0.034798	0.045735	0.085898	0.16291
0.50	0.038358	0.031415	0.045229	0.10355	0.21126
0.25	0.036509	0.0275	0.057833	0.15045	0.36733

TABLE 13

Cl values only

a

h	0	2	5	7.5	10
1.50	0.28468	0.55673	0.8566	0.94699	1.0376
1.00	0.32357	0.60402	1.0107	1.158437	1.2916
0.75	0.31343	0.66068	1.0183	1.159099	1.3195
0.50	0.37769	0.72033	1.1847	1.3115	1.642
0.25	0.40805	0.87006	1.4109	1.9227	2.8111

TABLE 14

Cm values only

a

h	0	2	5	7.5	10
1.50	-0.0537	-0.10914	-0.18968	-0.19524	-0.22699
1.00	-0.05691	-0.1195	-0.21375	-0.25781	-0.28488
0.75	-0.05337	-0.13125	-0.21675	-0.23259	-0.23536
0.50	-0.06545	-0.14397	-0.24382	-0.24771	-0.25579
0.25	-0.08465	-0.1781	-0.26444	-0.26793	-0.19579

TABLE 15

	cd	cl	cm	h		h/c
	0.040975	0.28468	-0.0537	1.50	14.39335	0.75
	0.040598	0.32357	-0.05691	1.00	12.5469	0.50
0	0.03972	0.31343	-0.05337	0.75	12.67269	0.38
	0.038358	0.37769	-0.06545	0.50	10.15595	0.25
	0.036509	0.40805	-0.08465	0.25	8.947188	0.13
	0.03818	0.55673	-0.10914	1.50	6.857902	
	0.035468	0.60402	-0.1195	1.00	5.871991	
2	0.034798	0.66068	-0.13125	0.75	5.266998	
	0.031415	0.72033	-0.14397	0.50	4.361196	
	0.0275	0.87006	-0.1781	0.25	3.160702	
	0.046736	0.8566	-0.18968	1.50	5.455989	
	0.04582	1.0107	-0.21375	1.00	4.533492	
5	0.045735	1.0183	-0.21675	0.75	4.491309	
	0.045229	1.1847	-0.24382	0.50	3.81776	
	0.057833	1.4109	-0.26444	0.25	4.099015	
	0.073696	0.94699	-0.19524	1.50	7.782131	
	0.068686	1.158437	-0.25781	1.00	5.929229	
	0.085898	1.159099	-0.23259	0.75	7.410786	
	0.10355	1.3115	-0.24771	0.50	7.895539	
	0.15045	1.9227	-0.26793	0.25	7.824934	
	0.10807	1.0376	-0.22699	1.50	10.41538	
	0.10724	1.2916	-0.28488	1.00	8.30288	
10	0.16291	1.3195	-0.23536	0.75	12.34634	
	0.21126	1.642	-0.25579	0.50	12.86602	
	0.36733	2.8111	-0.19579	0.25	13.06713	

TABLE 16

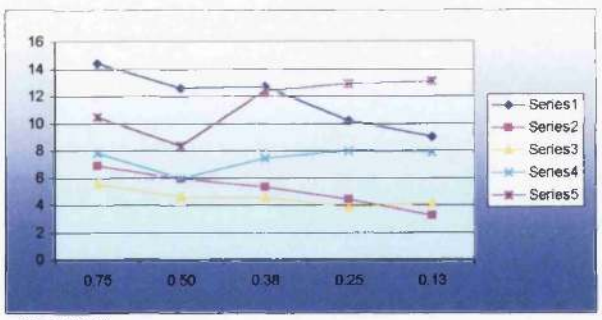

OR -0.19644

GRAPH 70

cd values

for 0 angle of attack

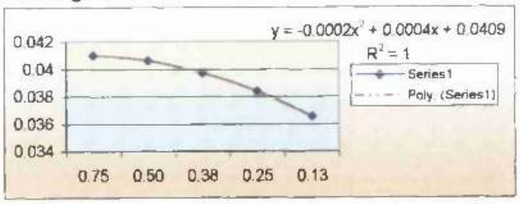

GRAPH 71

for 2 angle of attack

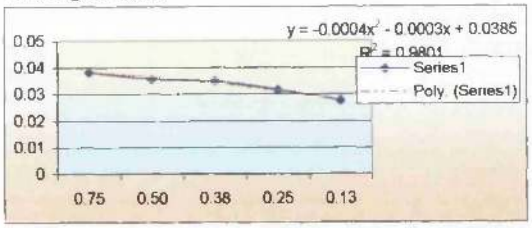

GRAPH 72

for 5 angle of attack

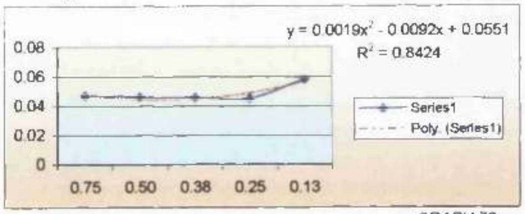

GRAPH 73

for 7.5 angle of attack

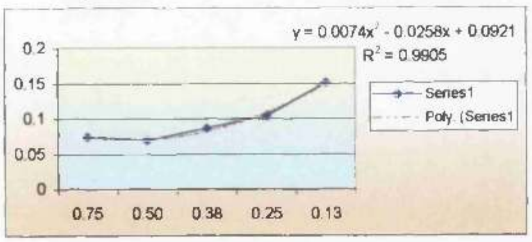

GRAPH 74

for 10 angles of attack

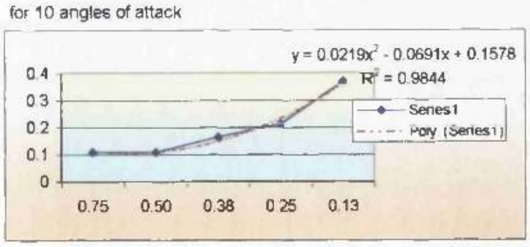

GRAPH 75

cf values

for 0 angle of attack

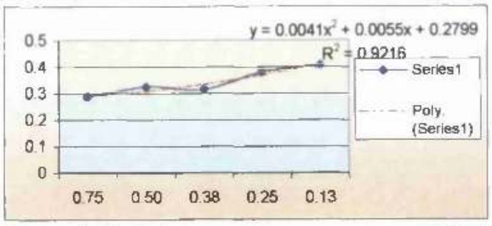

GRAPH 76

for 2 angle of attack

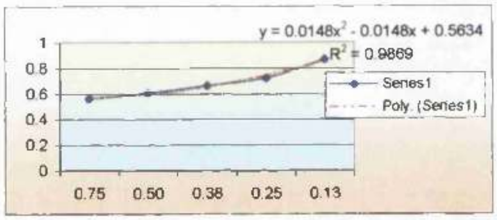

GRAPH 77

for 5 angle of attack

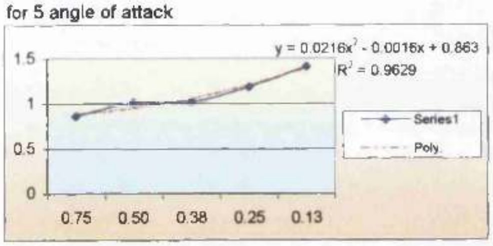

GRAPH 78

for 7.5 angle of attack

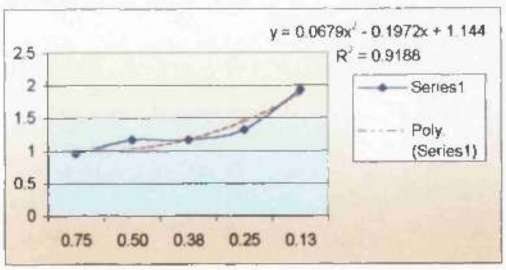

GRAPH 79

for 10 angles of attack

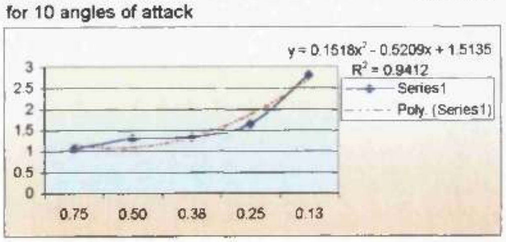

GRAPH 80

cm values

for 0 angle of attack

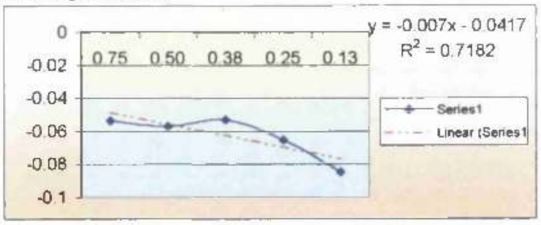

for 2 angle of attack

GRAPH 81

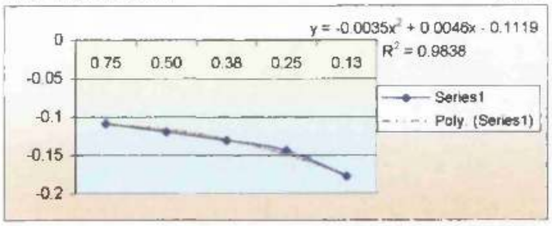

GRAPH 82

for 5 angle of attack

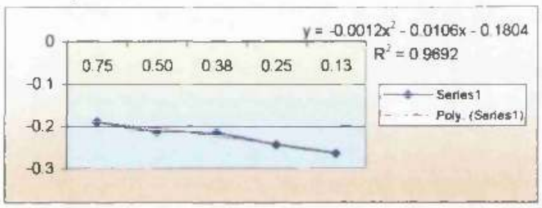

for 7.5 angle of attack

GRAPH 83

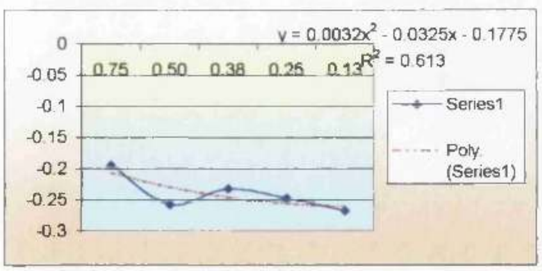

GRAPH 84

for 10 angles of attack

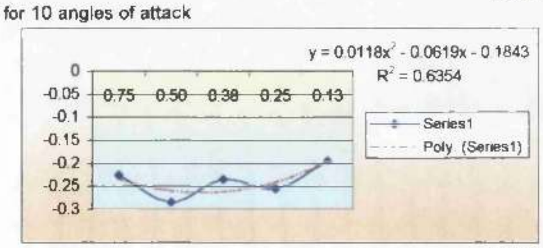

GRAPH 85

All Cd

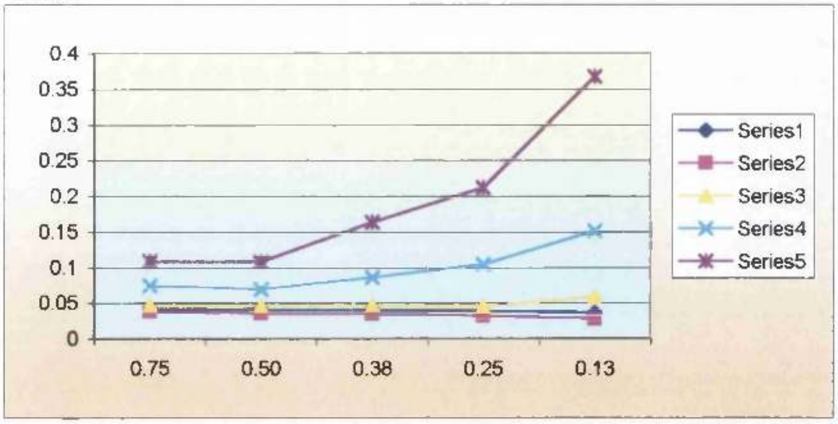

GRAPH 86

All Cl

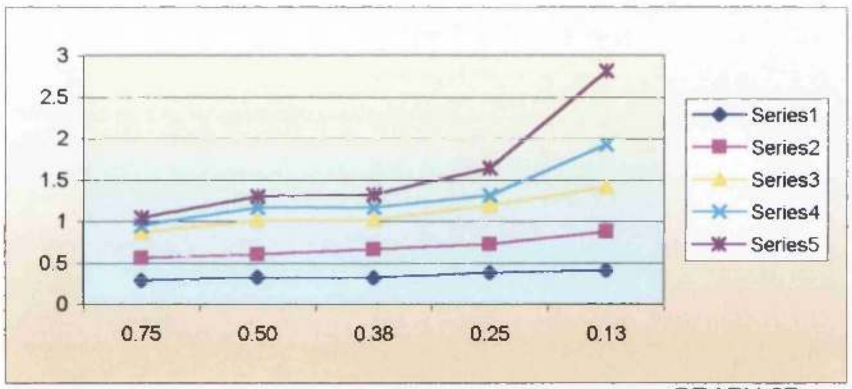

GRAPH 87

All Cm

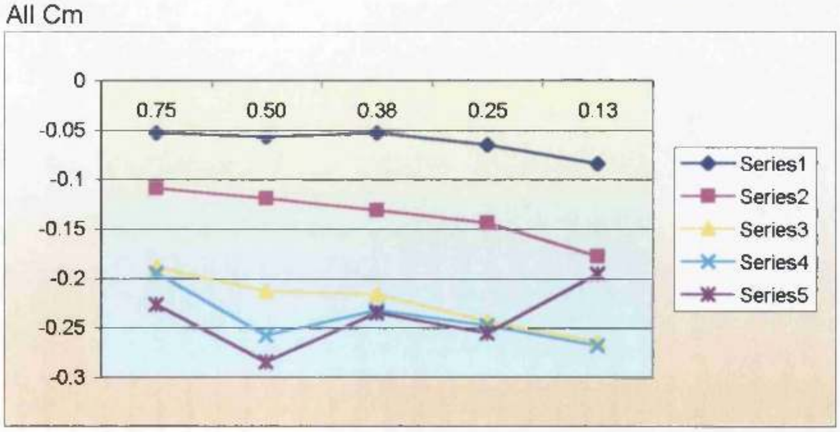

GRAPH 88

S-Shaped over peak (curved ground)

Cd values only

h \ a	0	2	5	7.5	10
1.50	0.03305	0.0427	0.03176	0.042	0.0672
1.00	0.03743	0.01592	0.00898	0.02658	0.04946
0.75	0.04159	0.01976	0.02254	0.00761	0.04265
0.50	0.04508	0.01389	0.01752	0.02291	0.02743
0.25	0.04031	0.01124	0.01324	0.01695	0.06435
0.125	0.01017	-0.0412	-0.0951	-0.0962	0.28011

TABLE 17

Cl values only

h \ a	0	2	5	7.5	10
1.50	0.21082	0.18803	0.72162	0.58275	0.68051
1.00	0.08584	0.38607	0.62789	0.71695	0.82932
0.75	0.06117	0.23515	0.62616	0.65827	0.61
0.50	0.07929	0.14626	0.53695	0.72871	0.6094
0.25	-0.4127	0.18564	0.5396	0.43392	1.59
0.125	-0.8957	-0.5575	-0.4196	-0.0339	0.28011

Cm values only

TABLE 18

h \ a	0	2	5	7.5	10
1.50	-0.5251	-0.0525	-0.1805	-0.168	-0.1907
1.00	-0.0443	-0.1189	-0.1949	-0.2205	-0.1786
0.75	-0.0407	-0.1082	-0.1847	-0.2288	-0.2209
0.50	-0.0373	-0.1069	-0.178	-0.2317	-0.2599
0.25	-0.0505	-0.1232	-0.1986	-0.0235	-0.0424
0.125	-0.0854	-0.2243	-0.3595	-0.4423	-0.2392

TABLE 19

	cd	cl	cm	h	h/c	
0	0.03305	0.21082	-0.5251	1.50	0.75	15.68
	0.03743	0.08584	-0.0443	1.00	0.50	43.60
	0.04159	0.06117	-0.0407	0.75	0.38	67.99
	0.04508	0.07929	-0.0373	0.50	0.25	56.85
	0.04031	-0.4127	-0.0505	0.25	0.13	-9.77
	0.01017	-0.8957	-0.0854	0.13	0.0625	-1.14
2	0.0427	0.18803	-0.0525	1.50		22.71
	0.01592	0.38607	-0.1189	1.00		4.12
	0.01976	0.23515	-0.1082	0.75		8.40
	0.01389	0.14626	-0.1069	0.50		9.49
	0.01124	0.18564	-0.1232	0.25		6.05
	-0.0412	-0.5575	-0.2243	0.13		7.38
5	0.03176	0.72162	-0.1805	1.50		4.40
	0.00898	0.62789	-0.1949	1.00		1.43
	0.02254	0.62616	-0.1847	0.75		3.60
	0.01752	0.53695	-0.178	0.50		3.26
	0.01324	0.5396	-0.1986	0.25		2.45
	-0.0951	-0.4196	-0.3595	0.13		22.67
7.5	0.042	0.58275	-0.168	1.50		7.21
	0.02658	0.71695	-0.2205	1.00		3.71
	0.00761	0.65827	-0.2288	0.75		1.16
	0.02291	0.72871	-0.2317	0.50		3.14
	0.01695	0.43392	-0.0235	0.25		3.91
	-0.0962	-0.0339	-0.4423	0.13		283.81
10	0.0672	0.68051	-0.1907	1.50		9.87
	0.04946	0.82932	-0.1786	1.00		5.96
	0.04265	0.61	-0.2209	0.75		6.99
	0.02743	0.6094	-0.2599	0.50		4.50
	0.06435	1.59	-0.0424	0.25		4.05
	0.28011	**0.28011**	**-0.2392**	0.13		100.00

TABLE 20

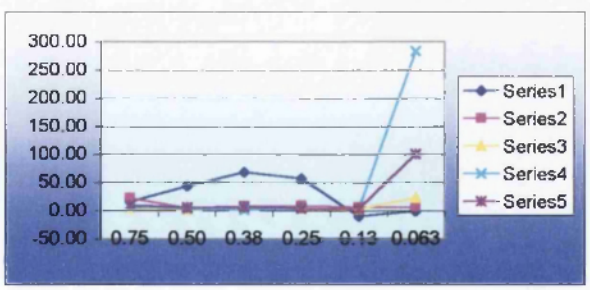

GRAPH 89

cd values

for 0 angle of attack

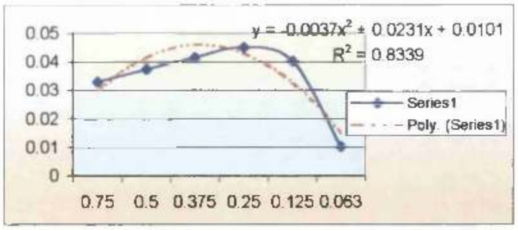

for 2 angle of attack

GRAPH 90

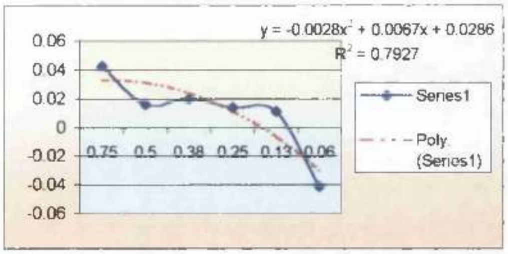

for 5 angle of attack

GRTAPH 91

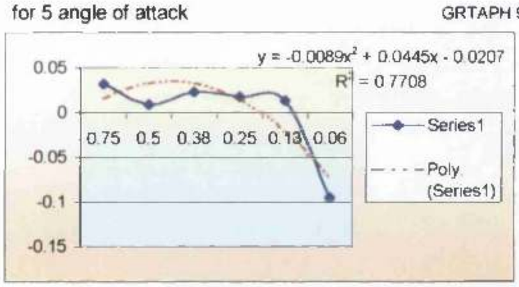

GRAPH 92

for 7.5 angle of attack

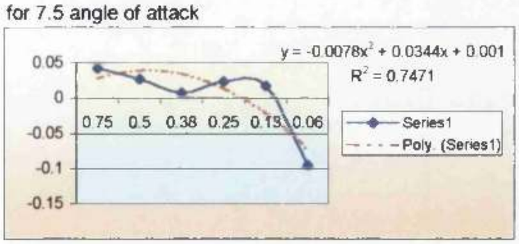

for 10 angle of attack

GRAPH 93

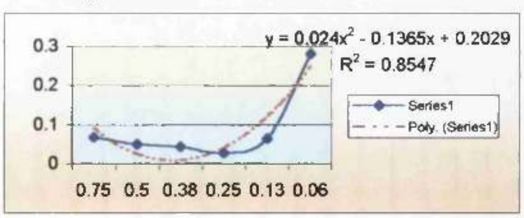

GRAPH 94

cl values

for 0 angle of attack

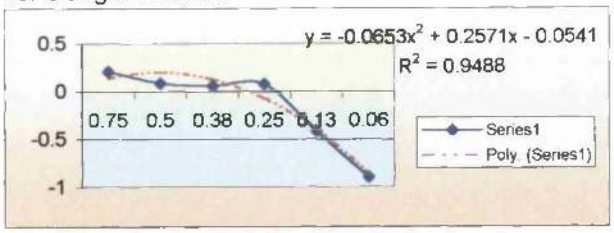

GRAPH 95

for 2 angle of attack

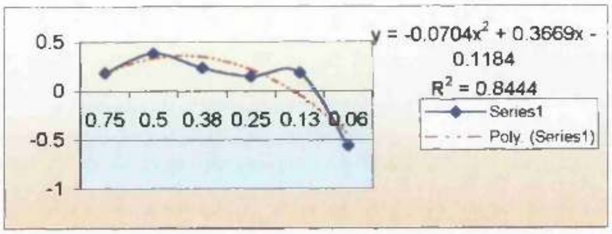

GRAPH 96

for 5 angle of attack

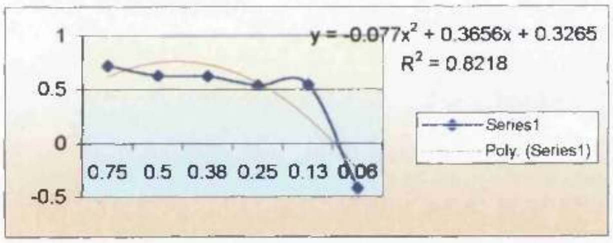

GRAPH 97

for 7.5 angle of attack

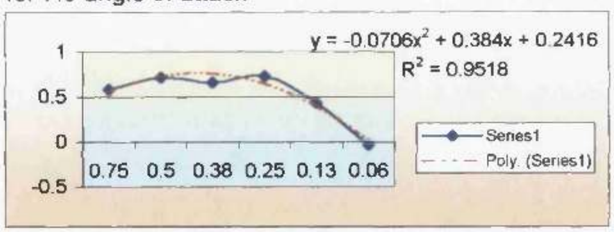

GRAPH 98

for 10 angle of attack

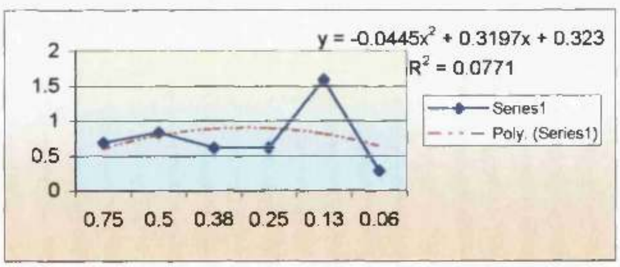

GRAPH 99

cm values

for 0 angle of attack

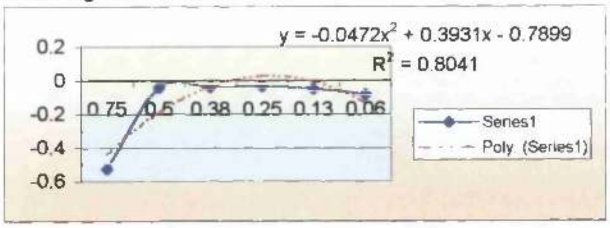

GRAPH 100

for 2 angle of attack

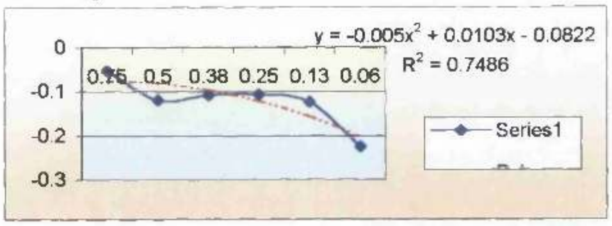

GRAPH 101

for 5 angle of attack

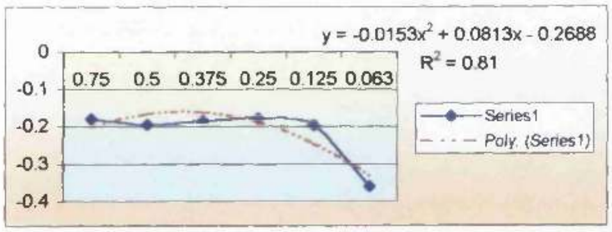

GRAPH 102

for 7.5 angle of attack

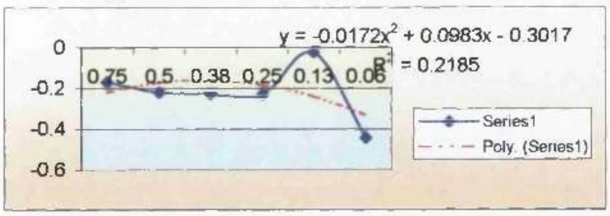

GRAPH 103

for 10 angle of attack

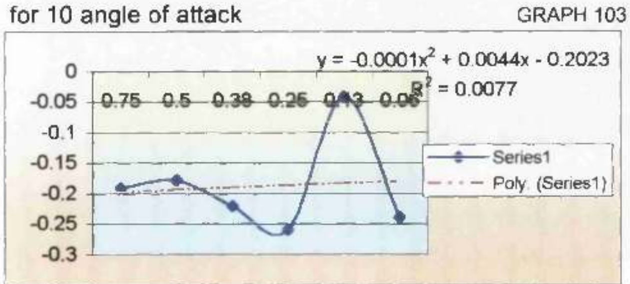

GRAPH 104

All Cd

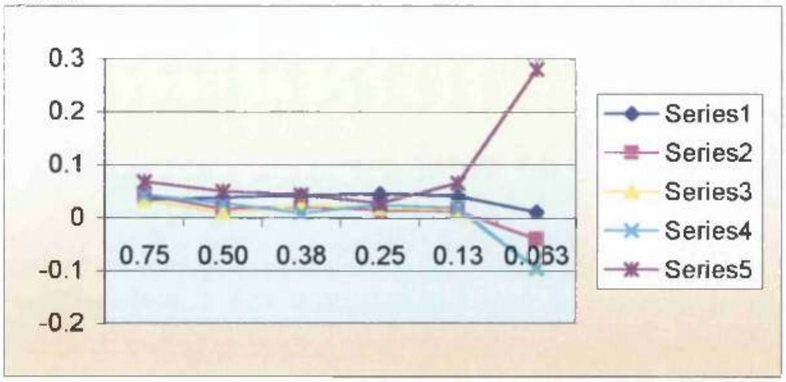

GRAPH 105

All Cl

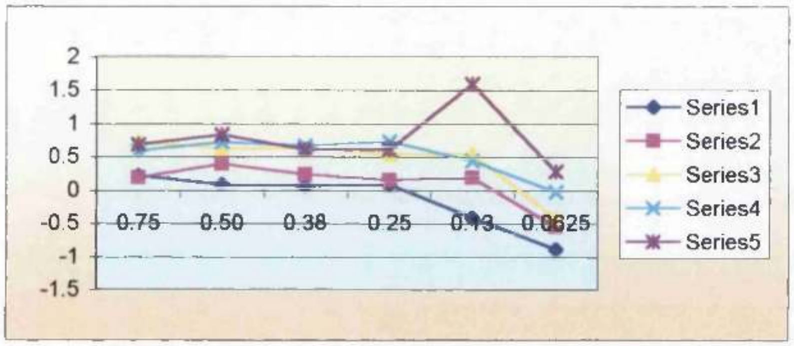

GRAPH 106

All Cm

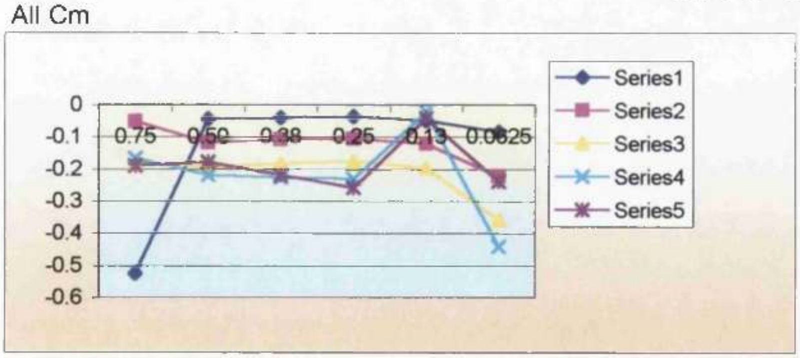

GRAPH 107

S-shaped over trough (over ground)

Cd values only

h \ a	0	2	5	7.5	10
1.50	0.0378	0.03837	0.0505	0.07763	0.15769
1.00	0.03936	0.04276	0.05956	0.08583	0.14527
0.75	0.03166	0.04482	0.06501	0.09642	0.14552
0.50	0.04213	0.04742	0.073	0.10534	0.16763
0.25	0.04507	0.05167	0.08156	0.12105	0.19216
0.125	0.0475	0.05455	0.08824	0.12798	0.21112

TABLE 21

Cl values only

h \ a	0	2	5	7.5	10
1.50	0.40625	0.73442	1.0748	1.1732	1.089
1.00	0.44648	0.81743	1.1588	1.344	1.2635
0.75	0.50773	0.86398	1.2451	1.3886	1.4053
0.50	0.55222	0.91348	1.3169	1.496	1.461
0.25	0.58436	1.0129	1.4595	1.654	1.6586
0.125	0.61717	1.0351	1.5711	1.7407	1.7909

TABLE 22

Cm values only

h \ a	0	2	5	7.5	10
1.50	-0.05753	-0.11342	-0.20044	-0.23346	-0.14423
1.00	-0.058	-0.11594	-0.20312	-0.25087	-0.21703
0.75	-0.06797	-0.11744	-0.2084	-0.24886	-0.24532
0.50	-0.06204	-0.11879	-0.21291	-0.25684	-0.23287
0.25	-0.0688	-0.12494	-0.22462	-0.26812	-0.24409
0.125	-0.06831	-0.12735	-0.23117	-0.27539	-0.246

TABLE 23

	cd	cl	cm	h	h/c	
0	0.0378	0.40625	-0.05753	1.50	0.75	9.3051
	0.03936	0.44648	-0.058	1.00	0.50	8.8158
	0.03166	0.50773	-0.06797	0.75	0.38	6.2354
	0.04213	0.55222	-0.06204	0.50	0.25	7.6292
	0.04507	0.58436	-0.0688	0.25	0.13	7.7119
	0.0475	0.61717	-0.06831	0.125	0.0625	7.6956
2	0.03837	0.73442	-0.11342	1.50		5.2251
	0.04276	0.81743	-0.11594	1.00		5.2315
	0.04482	0.86398	-0.11744	0.75		5.1875
	0.04742	0.91348	-0.11879	0.50		5.1915
	0.05167	1.0129	-0.12494	0.25		5.1013
	0.05455	1.0351	-0.12735	0.125		5.2696
5	0.0505	1.0748	-0.20044	1.50		4.6989
	0.05956	1.1588	-0.20312	1.00		5.1400
	0.06501	1.2451	-0.2084	0.75		5.2212
	0.073	1.3169	-0.21291	0.50		5.5432
	0.08156	1.4595	-0.22462	0.25		5.5884
	0.08824	1.5711	-0.23117	0.125		5.6164
7.5	0.07763	1.1732	-0.23346	1.50		6.6169
	0.08583	1.344	-0.25087	1.00		6.3859
	0.09642	1.3886	-0.24886	0.75		6.9439
	0.10534	1.496	-0.25684	0.50		7.0414
	0.12105	1.654	-0.26812	0.25		7.3186
	0.12798	1.7407	-0.27539	0.125		7.3522
10	0.15769	1.089	-0.14423	1.50		14.4803
	0.14527	1.2635	-0.21703	1.00		11.4974
	0.14552	1.4053	-0.24532	0.75		10.3551
	0.16763	1.461	-0.23287	0.50		11.4736
	0.19216	1.6586	-0.24409	0.25		11.5857
	0.21112	1.7909	-0.246	0.125		11.7885

TABLE 24

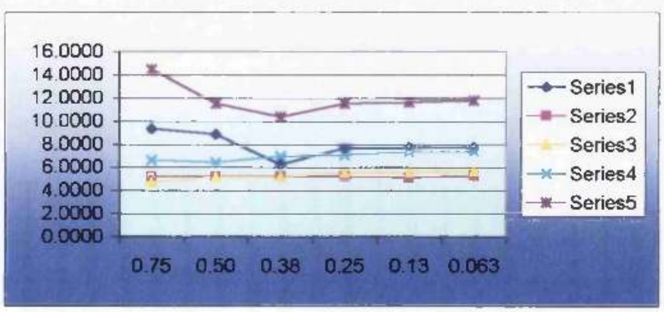

GRAPH 108

cd values

for 0 angle of attack

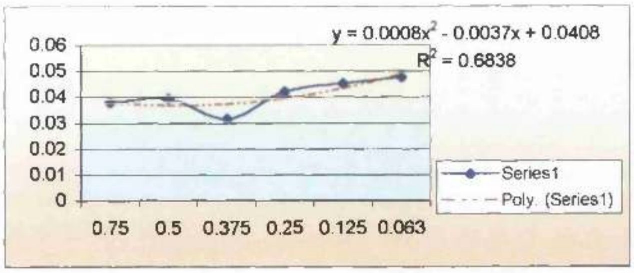

for 2 angle of attack

GRAPH 109-S1

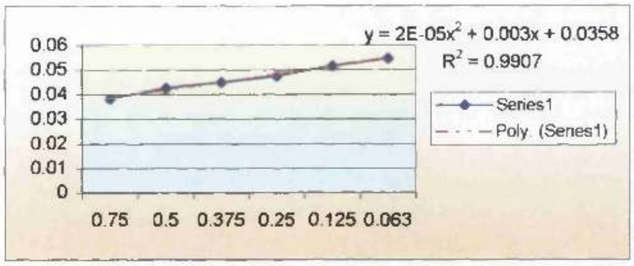

for 5 angle of attack

GRAPH 109-S2

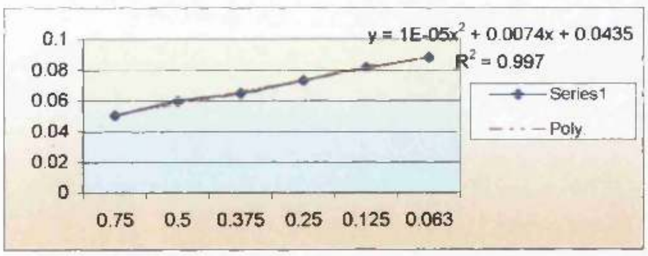

GRAPH 109-S3

for 7.5 angle of attack

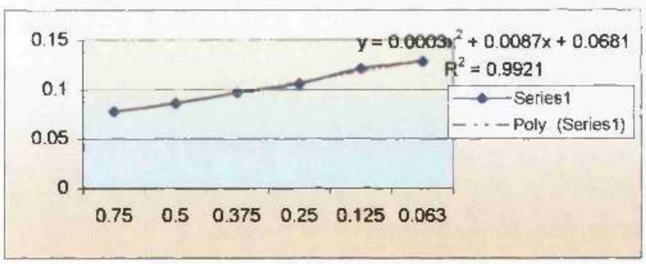

GRAPH 109-S4

for 10 angle of attack

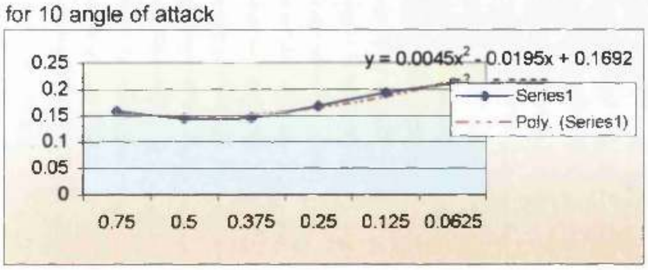

GRAPH 109-S5

cl values

for 0 angle of attack

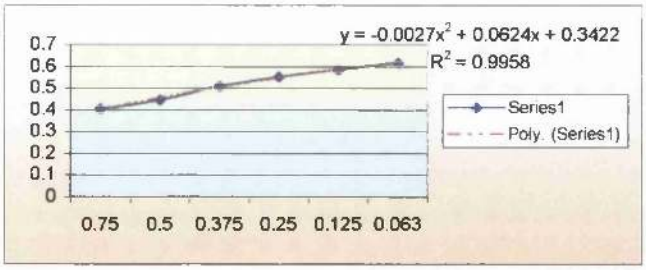

GRAPH 110-S1

for 2 angle of attack

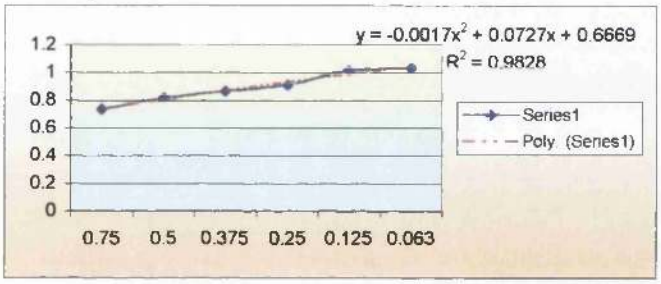

for 5 angle of attack

GRAPH 110-S2

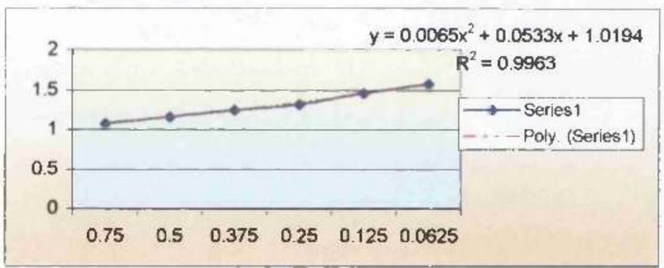

GRAPH 110-S3

for 7.5 angle of attack

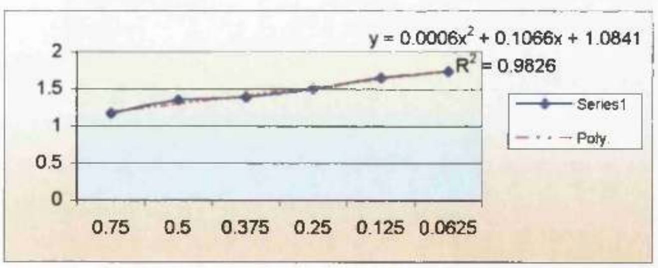

GRAPH 110-S4

for 10 angle of attack

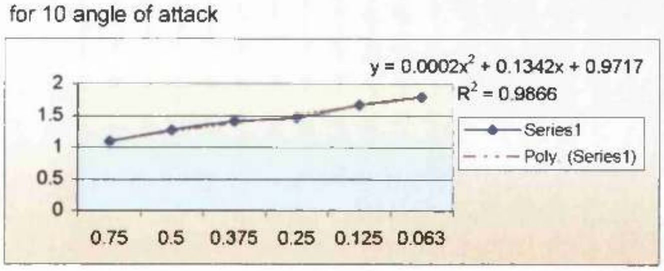

GRAPH 110-S5

cm values

for 0 angle of attack

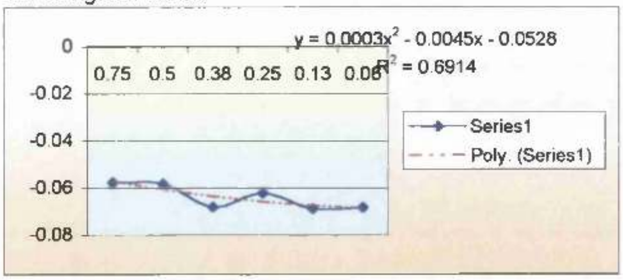

GRAPH 111-S1

for 2 angle of attack

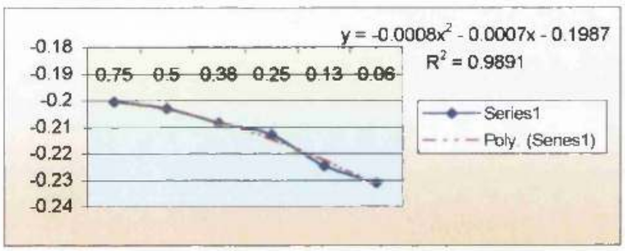

GRAPH 111-S2

for 5 angle of attack

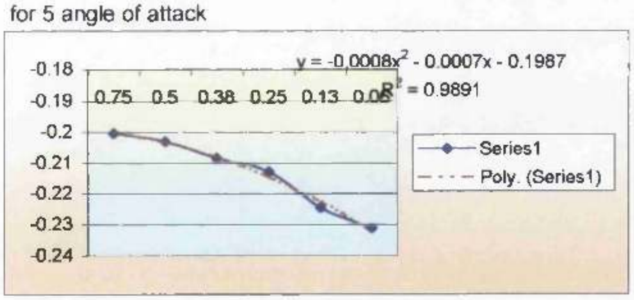

GRAPH 111-S3

for 7.5 angle of attack

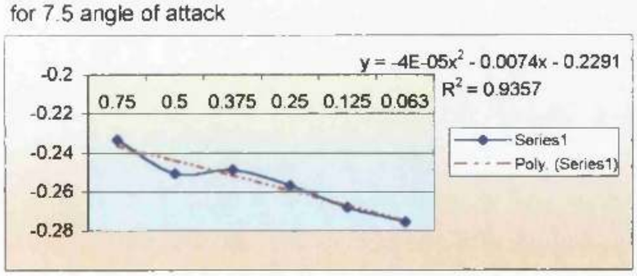

GRAPH111-S4

for 10 angle of attack

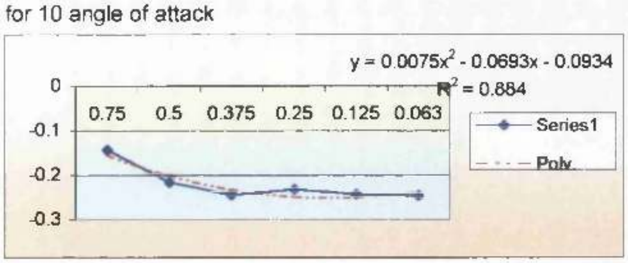

GRAPH 111-S5

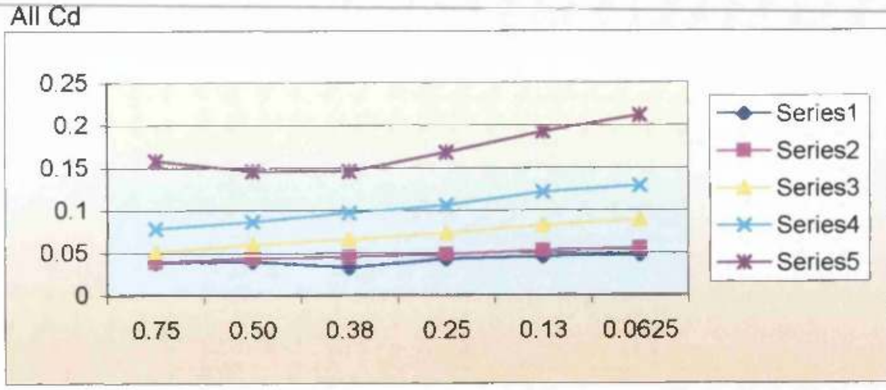

GRAPH 109 S1-5 B

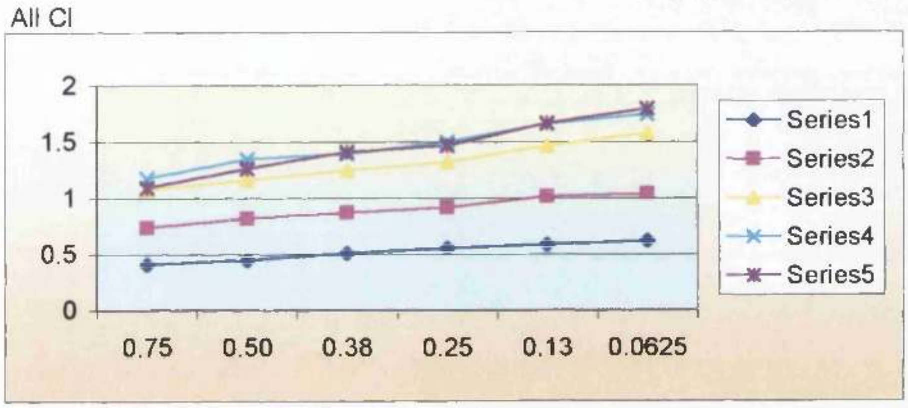

GRAPH 110 S1-5 B

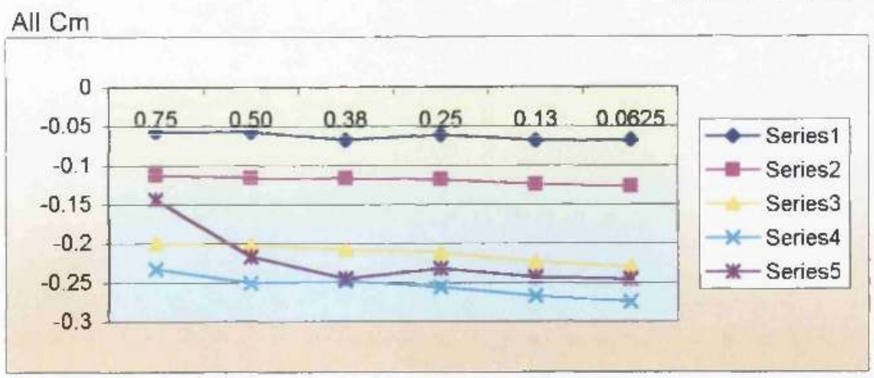

GRAPH 111 S1-5 B

cd values of the S-shaped aerofoil at 0 angle of attack

1.50	0.03305	0.0378	0.04098	0.04143
1.00	0.03743	0.03936	0.0406	0.04074
0.75	0.04159	0.03166	0.03972	0.04136
0.50	0.04508	0.04213	0.03836	0.0422
0.25	0.04031	0.04507	0.03651	0.04728

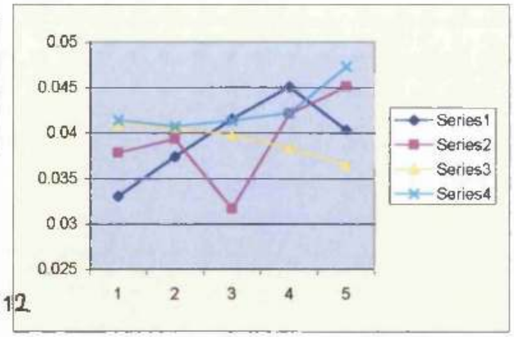

GRAPH 112

cd values of the S-shaped aerofoil at 2 angle of attack

1.50	0.0427	0.03837	0.03818	0.03725
1.00	0.01592	0.04276	0.03547	0.03502
0.75	0.01976	0.04482	0.0348	0.035
0.50	0.01389	0.04742	0.03142	0.03403
0.25	0.01124	0.05167	0.0275	0.03887

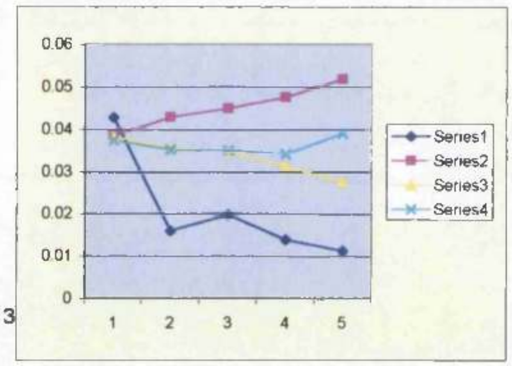

GRAPH 113

cd values of the S-shaped aerofoil at 5 angle of attack

1.50	0.03176	0.0505	0.04674	0.04428
1.00	0.00898	0.05956	0.04582	0.04456
0.75	0.02254	0.06501	0.04574	0.04774
0.50	0.01752	0.073	0.04523	0.04745
0.25	0.01324	0.08156	0.05783	0.04562

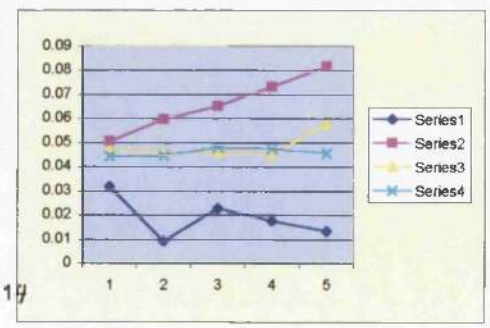

GRAPH 114

cl values for 2 angle of attack of an s-shaped aerofoil

1.50	0.18803	0.73442	0.55673	0.55056	1.50
1.00	0.38607	0.81743	0.60402	0.60614	1.00
0.75	0.23515	0.86398	0.66068	0.6581	0.75
0.50	0.14626	0.91348	0.72033	0.69665	0.50
0.25	0.18564	1.0129	0.87006	0.68021	0.25

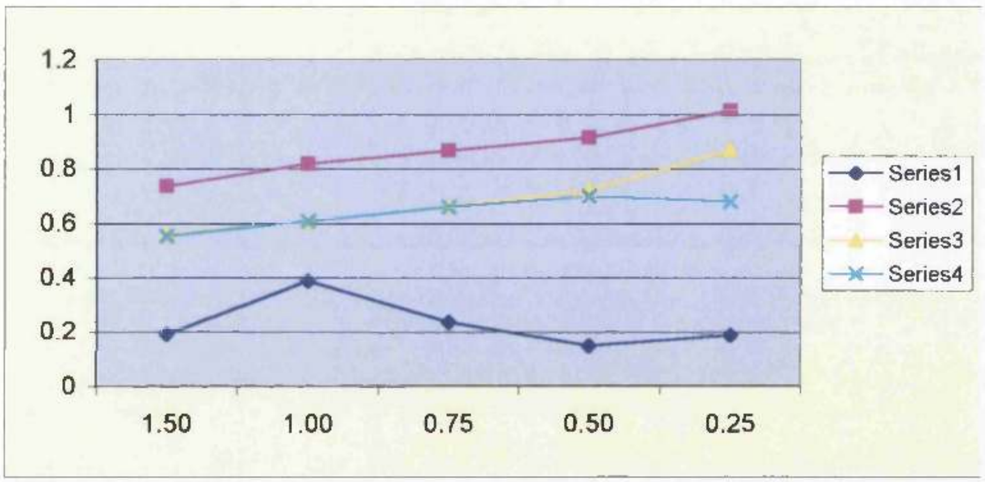

GRAPH 117

5.0 ANALYSIS OF RESULTS

The following section is comprised of all the analytical data obtained from the Fluent program. A section discussing the various graphs precedes each graphical representation and should be referred to for all information purposes.

In previous years numerous WISE craft operated using pilots trial and error processes in order to find suitable heights and angles of attack at which to either take off at or land. It is believed that the following information although incredibly detailed will prevent further accidents occurring through pilot error. The best suited and worse angles of attack at which to fly at are stated and described below. This information would allow a pilot of a WISE craft to fly safely at optimum height to chord ratios and angles of attack.

5.1 NACA OVER STILL WATER

With close reference to the previous graphs in this section, the following has been noted. At zero angle of attack, no lift is produced for the NACA 0012 aerofoil. As the angle of attack increases, so does the Lift Coefficient Cl. The first column indicates that although, there is no lift for this aerofoil at zero degrees, there is still a significant decrease in Cl as the height to chord ratio, h/c decreases.

At 2 degrees angle of attack and for 5 degrees it is noted that between h/c values of 0.75 and 0.38, one notes a decrease in the value of Cl as h/c decreases. However, as h/h decreases further between 0.38 and 0.13, a significant increase in Cl is noted. This is due to the pressure increase below the lower section of the aerofoil together with the angle of attack as the height between the aerofoil and the water surface decreases.

At 7.5 degrees angle of attack, one notes an increase in the value of Cl as h/c decreases. Again this is due to there already being a significant Cl value initially at h =1.5m, this together with the decrease in h/c produces an increase in pressure as the aerofoil reduces height, producing this overall increase in the lift coefficient Cl, and hence lift. At 10 degrees angle of attack, which on its own produces significant lift, together with the pressure build up below the aerofoil as the h/c values decreases, an overall increase in the value of Cl, hence lift is produced.

Therefore, it may be stated that from 2 degrees angle of attack at h/c = 0.38, as either or both the angle of attack increases or the value of h/c decreases, the value of Cl increases, producing increased Lift. Hence, it could be said, that if a NACA 0012 aerofoil section was to take off from still water its h value (i.e. the distance between the lower section of the aerofoil and the water surface), for a chord length of 2m should be 0.75m and it should have a minimum angle of attack of 2 degrees, when travelling at a speed of 100 metres per second, in order to produce some sort of, although little, lift.
It should therefore not even attempt to take off if the h/c value is less than 0.38 and the angle of attack is less than 2 degrees.

With reference to the individual graphs of the Cl values at different angle of attack, it is reinstated that the previously mentioned statements are correctly interpreted. In addition to this it may be noted that not only are the R^2 values close to 1 (specifically for 7.5 degrees, where $R^2 = 0.9428$, and for 10 degrees, where $R^2 = 0.9311$), but that the chart and equations (2nd Order Polynomial Equations), together with the corresponding trend lines of the graphs, describe the change in Cl in a similar manner to the line joining the points for each series.

This is particularly the case for 7.5 degrees angle of attack. It may be noted that for this reason, these equations could be used to find additional points between the h/c values of 0.75 and 0.13 as well as predict additional points outside this range. However, care must be taken, as forecasts could be invalid in reality. This information or advice, not only applies to this subtopic but to all forthcoming information.

As may be seen, either from the tables or from individual graphical representations, the overall angles of the lines (for all except from the 2 degrees angle of attack graph) increases as the h/c values decreases. Thus indicating that the drag coefficient Cd increases as the distance between the lower surface of the aerofoil and the water surface decreases. Both for zero and for ten degrees angle of attack, the equations of the second order polynomial trendlines are very similar to the lines through the points. It may be noted that the R^2 values are incredibly close to 1, specifically 0.9576 and 0.9919 respectively, resulting in an incredibly similar trendline to the actual line joining the points. Therefore, if it were desired to find additional information either for values between $0.13<h/c<0.75$ or outside this range, the equations denoted may be used.

Although different equations are adopted for 5 and 7.5 degrees angle of attack, it may be noted that due to a decrease of Cd at h/c = 0.38 for 5 degrees the R^2 term is 0.6493. In addition to this, due to a low Cd value at h/c = 0.75 for 0.75 degrees, the R^2 term is 0.8693. Due to the decrease of Cd at 0.13 when at 2 degrees $R^2 = 0.7467$. Even in these cases, although the equations themselves should not be used for further information, the lines through the points (not the trendlines) may be used for approximate solutions.

Although the graphical representations of the Cm values are known to go up and down, resulting in an inaccurate prediction, it is believed that some of the trendline equations could be used for a prediction of further information, which would be of some accuracy. This is especially the case for trendlines with equations which have R^2 terms greater than 0.9.

For example for 0 degrees angle of attack, it may be seen that the overall trend indicates an increase in Cm as h/c decreases, resulting in instability. The R^2 term of this graphical representation is 0.9405, meaning that the equation for the trendline could be used for further information. This is also the case for 5,7.5 and 10 degrees angle of attack, where the respective R^2 terms are 0.9867, 0.9867 and 0.9327 respectively. With the R^2 for 7.5 degrees being the best trendline representation of points, resulting in quite an accurate equation for additional information.

However, due to the great change in the 2 degree graph for Cm, it is not advised to use this equation as a source of further information. However with close reference to known data, a close approximation could be made using the line joining the points for information on $0.13 < h/c < 0.75$. Both the 5 and 7.5 degree graphs for Cm, indicate a decrease in the Cm value as the h/c values decrease result in better stability. However for the 10 degree Cm graph as the h/c values decrease the Cm values increase resulting in instability which, may be due to high angle of attack and turbulence at the trailing edge.

It may therefore be noted that, for all angles of attack, as the h/c values decrease the Cd values increase. However, with regard to the Cm graphs, although for 0 and 2 degree the aerofoil becomes greatly unstable when close to $h/c = 0.13$, which could be due to the small angles producing little to no lift.
For 10 degrees, Cm, once again increases as h/c decreases due to the large angle of attack close to the still water surface producing an increased pressure build up on the lower surface of the aerofoil, as well as high turbulence at the trailing edge which corresponds to drag.

However for 5 and especially 7.5 degrees, a decrease in Cm is present as h/c decreases, resulting in better stability. For this reason and with close reference to the Cl, Cd and Cm results, as a final conclusion, it is true that 5 and 7.5 degrees produce better ground effect, lift and have a decreased instability, especially when in close proximity to the water surface

Referring to the Cl, Cd and Cm graphs, which show all five series together. Where series 1, 2, 3, 4 and 5 represent 0, 2, 5, 7.5 and 10 degrees angles of attack respectively, for values between the range of $h/c = 0.13$ and 0.75 it may be noted that all series, apart from 10 degrees, intersect at $h/c = 0.48$, where the corresponding Cl value is around 0.25, however series 5 intersects series 4 at around $h/c = 0.43$, where Cl is approximately just over 0.5. Series 5 intersects series 1 at around $h/c = 0.44$, where Cl is just under 0.5. Series 5 intersects series 2, where h/c is around 0.45 and Cm is around 0.375. Finally series 5 intersects series 3 when h/c is equal to approximately 0.45 and the value of Cm is around 0.34.

Nevertheless, point (0.48,0.25) is the most common and it may therefore be stated that for all series apart from series 5, an angle of attack of around 0.48 degrees corresponds to the same value of Lift Coefficient Cl, which is around 0.25.

For values where h/c is less than 0.5, it is best to use 0 degrees angle of attack, for $0.44 < h/c < 0.5$ it is best to use 7.5 degrees angle of attack, for $h/c > 0.45$ best to use 10 degrees angle of attack.

With regard to the Cd values for all five series shown on the one graphical representation, it may be stated that for values of $h/c > 0.5625$, it is best to use series 4 and for values of $h/c < 0.5$ best to use series 5.

Finally, looking at all five Cm series together on the one graphical representation, one may note that there are two intersections occurring. One intersection occurs at $h/c = 0.5$, where Cm is just below -0.05 for all series apart from series 5 (which represents the 10 degree angle of attack) and another intersection occurs at $h/c = 0.19$ where the value of Cm is approximately -0.2. For $h/c < 0.19$, it is best to use 2 degrees angle of attack, for $0.19 < h/c < 0.41$.For $0.41 < h/c < 0.5$ it is therefore best to use 7.5 degrees and for $0.5 < h/c < 0.75$, best to use 0 degrees angle of attack.

5.2 NACA 0012 OVER FLAT GROUND

Five programs were run for this case, this was due to there being no requirement for the information apart from its use as verification to the Fluent programme's capabilities. However, there was a similarity between the majority of points for the NACA 0012 over ground, with the equivalent points over still water.

The following programs were run; h/c = 0.13 with a = 0 ; h/c = 0.25 with a = 2 ; h/c = 0.38 with a = 5 ; h/c = 0.5 with a = 7.5 and finally h/c = 0.75 with a = 10. Where h/c is the height to chord ratio and a is the angle of attack. This was thought to be better than having the angle of attack increase as the h/c decreased, mainly due to turbulence which is created causing drag and instability.

With regard to the Cl graph shown, series 1 represents the programmes run for over flat ground. These results were then compared to the equivalent points for NACA 0012 over still water. This is represented by series 2. A second order polynomial equation has been allocated for series 1 and 2 which, describes their trendline. R^2 has also be stated, this indicates the accuracy between the actual series lines and the trendline. The closer R^2 is to 1, the higher the accuracy between the two lines, which results in the 2nd Order Polynomial Equation being a good prediction method for values either within the range covered or outside it.

It is noted that due to series 1 and series 2 being similar, the trendline has an R^2 term with a value of 0.9854. This means that an approximate value of either NACA0012 over water or ground for an increasing angle of attack as the h/c values increase, with reference to the already found points. If a better approximation is required then care must be taken and either series 1 or 2 must be used individually depending on the required information. However, in both cases Cl increases as the angle of attack increases and the value of h/c increases.

With regard to the Cd graph shown, there is a drastic increase in Cd while over ground, at h/c = 0.38 and a = 5, the line joining those five points of series 1 may be inaccurate. With regard to series 2, although Cd decreases as h/c and a decrease (simultaneously), the two series lines are of a similar nature (i.e. overall both decreasing in Cd as h/c decreases) there trendline has an RE2 term equal to 0.9606 resulting in an equation which together with close comparison to each series could provide an approximate solution of further points/information if required.

Now with regard to the Cm graph, due to the two series having slight variation of values, the trendline best describes series 1 rather than both series 1 and 2. The RE2 term however is 0.9646 resulting in a good approximation of values or further information for series 1 by using the 2nd Order Polynomial Equation describing the trendline, this together with close comparison to series 1 its self could provide a close approximation of solutions. Overall, the graph does show an increase of Cm (instability) as h/c decreases together with a simultaneous decrease of angle of attack.

5.3 S-SHAPED OVER STILL WATER

With regard to the individual Cl graphs for the S-shaped aerofoil over still water, unlike the NACA0012 aerofoil section, the S-shaped aerofoil is specially designed to work in harmony with ground effect. It is for this reason, and due to its curved design that for all cases of angle of attack, as h/c decreases from 0.75 to 0.13 the Cl values increase producing increased lift as ground effect is adopted. In addition to this a 2nd Order Polynomial Equation describing the trendline and an R^2 term is indicated for all cases. Due to there being a close similarity between the trendline and each series, the R^2 terms are all greater than 0.9, resulting in equations being a good method of predicting additional, although approximate solutions to each problem. It may be noted that, by referring to the individual Cl graphs, as the angle of attack increases so does the value of Cl. Once again the closer the R^2 terms are to 1, the more accurate the equation of the trendline, resulting in a good approximation method of attaining a solution.

Now referring to the Cl graph of all series together, one notes that the higher the angle of attack as h/c decreases, the better. The higher the series number i.e. series 5, the steeper its curve. For this reason it is best to use higher angles of attack such as 10 degrees, when close to the surface i.e. h/c = 0.13, in order to achieve a maximum value of Cl.

With close reference to the individual Cd graphs, one notes that 0 and 2 degrees angle of attack, as h/c decreases the value of Cd decreases. In both cases the R^2 term is incredibly close to 1, specifically, $R^2 = 1$ and $R^2 = 0.9801$ respectively, resulting in an excellent trendline and 2nd Order Polynomial Equation which, may be used for further information.

As the angle of attack is increased to 5 degrees, Cd increases as h/c decreases. Once again, it is noted that the R^2 terms are once again close to 1. (Although for 5 degrees the R^2 term is equal to 0.8424, four out of five points lie on the trendline with one just a bit lower, even this equation could be used with good approximate results, if care was taken and comparisons to known results was made.

For 7.5 degrees $R^2 = 0.9905$, this results in an excellent trendline and equation, which could be used for further information. For 10 degrees $R^2 = 0.9844$, here two of the points lie just off the trendline and hence if the equation was used care must be taken and reference to previous points must be made.

With regard to the Cd graph showing all the series together one notes that, with the exception of series 1 and 2, they follow a similar pattern to the Cl graphs. The greater the angle of attack the greater the steepness of the graph, hence producing a greater Cd value as the angle of attack increases inversely to the h/c values. (i.e. h/c decreases). Hence, although 10 degrees at h/c = 0.13 gives the highest Cl value, it also gives the highest Cd value. In addition to this information a graph representing the Cl/CD value is made available for the reader for further information, although not analysed in this section. However, the following point is made; For an S-shaped aerofoil over still water, best CD/CL *100 vs h/c, for 0.25 and under use 7.5 degrees for 0.25 and over use 5 degrees.

With regard to the individual Cm graphs, from 0 degrees at h/c = 0.75 to 10 degrees at h/c = 0.25, as both the angle of attack and h/c decrease, so does the Cm value. In other words better stability is gained when the angle of attack is 7.5 degrees and the h/c value is 0.25. Although instability increases for 10 degrees at h/c = 0.13 to reach a value close to that of 2 degrees at h/c = 0.13, the worst Cm value is reached at 0 degrees angle of attack where h/c = 0.75, producing an unstable circumstance. However, it should be noted that Cm increases as h/c increases and the angle of attack decreases.

For this reason and also by taking into account all Cd, Cl and Cm values for the S-shaped aerofoil over still water, one may state that it is at its best when flying at 10 degrees when h/c = 0.13 where the instability is at its lowest.

S-SHAPED OVER TROUGH (curved ground to simulate 8:1 waves).

Thirty programmes were run for the S-shaped aerofoil over a wavy solid boundary, which were designed in such a manner as to represent waves in a water surface. For this reason, they had a ratio of 8:1 and were placed at h/c values of 0.75, 0.5, 0.3, 0.25, 0.13 and 0.0625, the shape of the wavy boundary allowed the aerofoil to get closer to the surface. The trough was placed directly below the centre of the aerofoil. However, once again, the angles of attack remained the same, specifically 0,2,5,7.5, and 10.

As may be seen from the individual Cl graphs for all angles of attack, as h/c decreases Cl increased to reach a maximum value. All points increased in harmony with each other, this is noted due to the trendline R^2 terms all having a value greater than 0.9, once again the closer this value is to 1 the better the approximation gained from the provided equation of the trendline, which would be used for further information.

Referring to the Cl graph which includes all Cl series, indicates that the highest Cl values are reached by series 5 which is 10 degrees angle of attack, and series 4 which is 7.5 degrees angle of attack. The highest being series 4 for h/c > 0.315 and series 5 for h/c < 0.315, especially when under 0.13. The lowest Cl values were attained for series 1, which is for 0 degrees angle of attack.

Now with regard to the individual Cd graphs one notes that, apart from that of 0 degrees angle of attack which has an R^2 term with a value of 0.6838, all the rest have R^2 terms greater than 0.96. Thus resulting in trendlines similar to the actual series lines joining the points, as well as resulting in adequate equations suitable for further use as methods of producing additional approximate information.

Overall all series, and hence trendlines indicate an increase in Cd, as h/c decreases. When referring to the Cd graph which, includes all series, one notes that the highest value of Cd is reached by series 5 at Cd = 0.21112, which works out at around 26.7 % of its Cl value. However one should note that its lowest percentage for Cd/Cl * 100 is attained for 7.5 degrees angle of attack at h/c = 0.75. However, this is not in extreme ground effect.

Regarding the individual Cm graphs one notes that, for all values, Cm decreases as h/c decreases. Also, apart from 0 degrees, which has an R^2 value of 0.6914 and 10 degrees which has an R^2 value of 0.884, 2, 5 and 7.5 degrees all have R^2 values greater than 0.9, resulting in adequate trendlines, and trendline equations which when dealt with carefully and compared to actual line, can be a good method of finding an approximate solution.

Referring to the Cm graph, which includes all series, one notes that the lowest Cm value indicates that instability is reached at 7.5 degrees angle of attack when the aerofoil is in extreme ground effect at h/c = 0.0625, and the worst is reached, in other words the most unstable or highest Cm, by 0 degrees angle of attack at h/c = 0.75

Referring to the Cd/Cl * 100 vs h/c graph, we note that both 2 and 5 degrees are appropriate to provide lift and have the least Cd percentage value. Therefore best to use 2 or 5 degrees when just taking off.

With regard to the Cl graph, which is comprised of all 5 series, we note that the highest value of Cl is reached when a=0 and h/c = 0.13. Other than this, the second highest is reached when a = 10 and h/c = 0.5. One may note that (approximately / overall) as the angle of attack increases Cl increases and apart from a = 10 and h/c = 0.13 as h/c decreases Cl decreases.

With regard to the individual graphs of Cd, 0 and 10 degrees, have the highest R^2 terms with 0.9 < RE2 > 0.8. The rest however, have $0.7 < R^2 < 0.8$. For 0 degrees Cd increases before it decreases, this occurs once h/c passes 0.25 and tends toward 0.0625. However, for the rest, as h/c decreases Cd also decreases.

Regarding the Cd graph, which includes all series, we note that the highest Cd value is reached by 10 degrees at h/c 0.0625 and the lowest Cd values are reached by both 5 and 7.5 degrees.

With reference to the Cd/Cl * 100 vs h/c graph we notice that, taking into account the lift vs time at take off and hence angle of attack, the best angles for just after take off are between h/c values of 0.0625 and 0.13. Once over h/c of 0.13 it is best to use 0 degrees, then for values up to h/c = 0.44 it is best to use 5 degrees. For values over this it is best to use 7.5 degrees.

THE SINGULAR GRAPHICAL REPRESENTATION BELOW EACH TABLE ARE THE Cd/Cl GRAPHS.

With regard to the Cd/Cl *100 graph indicated in figure !!!, throughout h/c best to use 5 degrees for best CD/CL *100 vs h/c

5.5 COMPARISON OF S-SHAPED AERFOIL

The graphical representations, which follow in this section, represent the Cd, Cl and Cm values of the s-shaped aerofoil. The reader must note that the numbers ranging from 1 – 5 on the x – axis, represent the blue numbers (the height) from 1.5 – 0.25 respectively. For all cases series 1 represents values over peak, series 2 over trough, series 3 over still water and series 4 over curved ground. The following graphs have not been discussed further as they are self-explanatory. Please refer to them for further information.

6.0 DISCUSSION OF CFD

6.1 GENERAL

Two-Dimensional Computational Fluid Dynamics Analysis of Wings In ground Effect and assessment on lift, drag and momentum coefficients resulting in a Three-Dimensional Turbulence model of efficiency and instability.

The analysis of the following topic has been carried out using the following subdivisions, namely;

- *History of Wigs- involving the Database,*
- *Analysis of Potential Flow On Ground Effect By Image Methods,*
- **The CFD analysis-involving the Gambit and Fluent 5 program, and**
- **Plans For The Experimental Tests In The Future**

6.2 Database:

A database of WIG craft was comprised. This allowed statistical analysis of WIG characteristics to be carried out. With the use of specific attributes of previous WIG designs a new design could then be comprised. During this procedure, it was noted that the S-shaped aerofoil section was a very common wing configuration in the design of Ekranoplans. In addition to this, it was noted that although wing designs varied according to Characteristic requirements, the fuselage shape did not alter. It was for this reason that it was brought to my attention than the fuselage shape could be changed in order to be more aerodynamic and efficient.

Due to the S-shaped aerofoil being of excellent shape for ground effect flight it was thought possible to alter the fuselage shape into an approximate S-shaped design. It was for this reason that the following study concentrated on the S-shaped aerofoil.

It is believed that once adequate information has been aquired through the course for this thesis on the S-shaped section, that further studies incorporating the aerofoil shape as part of the fuselage as well as the wing sections could be pursued by either myself or others intrigued by WISE designs.

6.3 Potential Flow:

There are several cases of Potential Flow which were examined. This study took place in order to gain a better understanding of the flows around aerofoil sections such as those examined in this thesis.

- Potential Flow Past a Cylinder at Various Heights
    - Without Circulation
    - With Circulation
- Flow Past a Source Sink Pair Aligned into the Flow For A Range Of Heights
- Flow Past An Oblique Series Of Vorticies Approximating A Flat Plate At Incidence

Flow Past A Doublet - Vortex Model Of An Aerofoil Where The Doublet Size Varies In Such A Manner To Match The Projected Foil Blockage For An Angle Of Attack Corresponding To The Vortex Strength.

- **Analyse The Foil Itself Using CFD**

6.4 CFD:

Although difficult, it is vital to compare lift, drag and moment coefficients with both α (the angle of attack) as well as h/c (the height to chord ratio). For this reason, as well as the increase in WISE craft over the years it is believed of great importance to analyze these characteristics using numerical simulation techniques based on CFD programs. It is hoped to describe all forces exerted on wing profiles while analyzing all stages of take-off. The aim of this section was to analyze two different types of airfoil profiles using CFD. The NACA 0012 due to there being adequate information available on it, (it seemed logical to commence my CFD analysis on this profile) and the S-shaped profile, (which incorporates the Munk M6R2 over the upper portion and the CJ-5 over its lower portion). This was due to all new designs being based on this fairly new concept which has an increased effectiveness and has been proven to be of more use in surface effect vehicles.

Details of the strategy behind the numerous input requirements of the Gambit program, such as the mesh generation process, the boundary conditions involved have been studied as well as the Fluent 5 program creation of solver input files and information on the running of solutions given prior to the solver outputs attained. Due to the involvement of five different angles of attack, namely 0,2,5,7.5 and 10 degrees varying with five different h/c values, namely 1.5,1,0.75,0.5 and 0.25, a positive or negative contribution to the aerodynamics involved around the airfoil could then be produced. Statistical analysis on the outcomes would then take place, resulting in effective results. Examples of the types of programs run are shown below, the LHS is NACA0012 over still water and the RHS for S-shaped over curved ground simulating waves. These are two cases from 150.

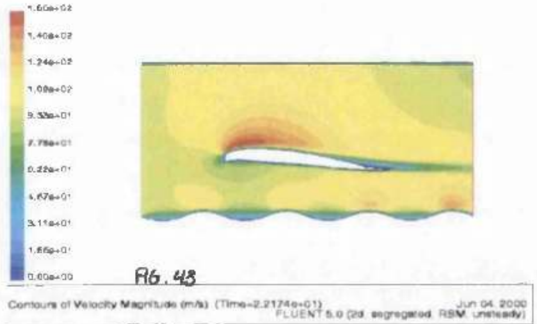

FIG. 48

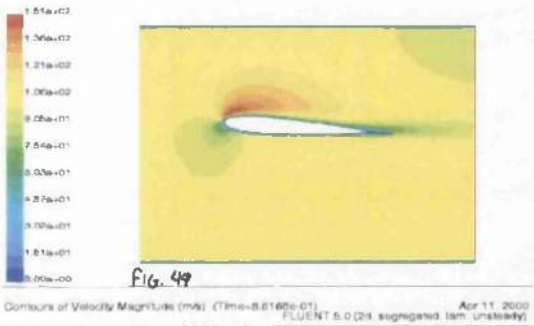

FIG. 49

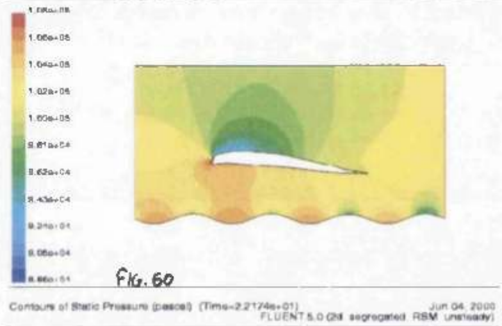

FIG. 50

Although numerous methods have been used to study the aerodynamics of wings in ground effect such as the 'moving belt' technique, the 'boundary layer' method, the panel method, CFD simulation and many more, it has been proven to be incredibly difficult but highly important to compare the lift, drag and moment coefficients with α (the angle of attack) as well as with h/c (the height to chord ratio). For this reason, as well as the increase in WISE craft numbers over the years it is believed to be of great importance to analyze these characteristics using numerical simulation techniques based on CFD (Computational Fluid Dynamics) programs.

7.0 VERIFICATION

Prior to commencing simulation of the S-shaped aerofoil section, it was essential to verify the 'FLUENT' programmes capabilities by modelling the NACA 0012 section over ground and over still water. This was carried out in order to acquire solutions, which were then compared with existing results and thus validated. It was for this reason that various methods of analysis in [Section 3] were exampined.

The simulations of the NACA 0012 over curved ground and still water were carried out in order to observe variations in lift, drag and momentum coefficients, turbulence and stability/instability.

Due to the involvement of five different angles of attack, namely 0,2,5,7.5,10 degrees varying with five different height to chord ratios, namely 1.5,1te tool for verificatin ,0.75,0.5,0.25, it was possible to simulate the aerodynamics around the aerofoil section.

Although the NACA 0012 aerofoil was not designed for In Ground Effect flight (I.G), purposes but for Out Of Ground Effect (O.G), it nevertheless provided an adequate tool for validation purposes.

The simulation proved that for a chord to height ratio less than 0.38 with an angle of attack between 2 and 10 degrees, pressure below the aerofoil section increased as either the height to chord ratio decreased or the angle of attack increased. The results were as expected.

Even though, for purposes of this study it is not imperative to know the graph equations and the R squared terms for the NACA 0012, this information is provided in order to aid the readers understanding of the simulations.

7.1 S-SHAPED AEROFOIL

A Frequently used aerofoil section for WISE craft is the S-shaped aerofoil. Although complicated due to its asymmetrical configuration, it provides valuable information when studied. What was noted during the simulation procedures was the following;

- $h/c < 0.25$ or $h/c = 0.25$ use $a=7.5$ degrees.
- $h/c > 0.25$ or $h/c = 0.25$ use $a=10$ degrees.

8.0 CONCLUSION OF CFD

Changes in wing resistance near the ground are important for the more accurate determination of the conditions in the taking off and landing of an airplane. It has been found that the wing resistance diminishes on approaching the ground, while the lift increases somewhat, thereby making the lift-drag ratio more favourable.

The results which were found through Computational Dynamics were of great importance to both the aerodynamic knowledge gained on the S-shaped aerofoil section, as well as proving the aerofoils efficiency for ground effect flight. It could therefore be adopted as a design for a fuselage as well as for the wing sections allowing improved aerodynamic efficiency and stability. In addition to this, knowledge on the aerodynamic characteristics of such an aerofoil section allowed flight the detection of stable and safe flight paths to be chosen for future reference.

The information which was gathered may be briefly summarised in the following section;

Due to all WISE craft primarily having to take-off at zero angle of attack, in order to gain speed before increasing the angle of attack the initial stage of take-off is level. Once the required speed is attained (depending on the size and capabilities of the craft), the craft should gradually increase its angle of attack to 7.5 degrees until the height to chord ratio of 0.25 is reached. This angle of attack should then be followed by a maximum angle of attack of 10 degrees is reached. This would allow a stable and efficient take-off procedure without instability hazards.

Graph trendlines are provided and analysed in the previous section (section 5) allowing further predictions to be made. This information is intended to enlighten the reader and be adopted by pilots of WISE craft in order to attain a safe take-off, landing and cruising procedure.

9.0 CONCLUDING REMARKS

9.1 GENERAL

The aim of this study was to predict the aerodynamic characteristics for fuselage design in future propositions and optimum flight paths WISE craft should follow in order to prevent accidents caused either by high angles of attack or by wrong take-off procedures. This was attained by simulating a commonly used aerofoil in the WISE sector, the S-shaped aerofoil, using 'GAMBIT' and 'FLUENT 5' Computational Fluid Dynamics Programmes and assessing the lift, drag and momentum coefficients. A three-dimensional turbulence model of efficiency and instability was then attained and analysed,

9.2 DATABASE

In order for the simulations to commence the History of WISE craft was studied, this allowed a database of WISE craft to be constructed, which includes design specifications on sizing and characteristic qualities to be listed suitable for quick reference. An analysis of this information was conducted in order to attain trendline equations for guidance to further designs.

Numerous trends relating the main dimensions as well as characteristics such as the speed, range, weight, payload, fuel etc. have been provided. This information may be found in section 1.4 in the form of tables, graphical representations and equations. This will ultimately aid in the future of WISE designs and WISE forecasting.

Once the graphs and equations have been used to attain the desired WISE dimensions, speed, range and other characteristics, further analysis may be made using the information provided in section 2 on the WISE Design Aspects such as the aerofoil shape, engine requirements and many more to fulfil the design specifications.

9.3 CFD

Once the background of WISE designs was achieved, a method of simulation was chosen. In order for this to take place further research was inevitable on previous methods of analysis on WISE craft. This incorporated Flow Computation Techniques, Theoretical Analysis, Experimental Methods, Numerical Calculations and Computational Analysis, which may be found in section 3.

Following this research, further study followed on the chosen 'GAMBIT' and 'FLUENT' programmes. This allowed simulations of the NACA 0012 to take place for verification purposes prior to simulation on the S-shaped aerofoil.

> For Verification purposes, Methods of Analysis were studied and Computational Analysis took place in the form of Potential Flow Models On Ground Effect by the Image Methods.

Due to CFD results being dependent on the grid formation of the model, it is very important that a correct grid generation be adopted. It is for this reason that a triangular meshing process was used to model the aerofoil sections under investigation. The grids were structured and had a spacing of 0.04 units. The meshing process was carried out as a pre-processing operation on Gambit. Once the pre-processing operations came to an end, the file could then be exported from Gambit and entered in to Fluent 5.

A vital component of Fluent programming is the necessity to obtain a sturdy and exact turbulence model prior to commencing iteration. This is especially the case for turbulence models. There are turbulence models available in the Fluent Tutorial Guide covering a wide spectrum of examples and requiring little or no modification. Particular attention has been allocated to near-wall accuracy through the use of extended wall functions and Ronal models.

In FLUENT the time-dependent equations have to be discretised in both space and time. The spatial discretisation for the time-dependent equations is equivalent to the steady state problem. It entails the integration of all the individual terms in the differential equations over a time step dt

Fluent resolves the time-dependent equations using implicit formulation. For this reason, it is vital that iterations be carried out at each time step. This panel, when exposed by the user, allows a maximum value to be appointed for the number of iterations essential at distinct time steps. When the convergence characteristics are discovered prior to this number of iterations being fulfilled, the solution will advance to the proximate time step.

FLUENT provides a variety of turbulent cases, which may be detected in section 9.1 of the Fluent users Guide. With regard to the problems investigated in this report, it was thought vital to select the ***Reynolds Stress Model***. This was deduced through trial and error, as other initially adopted models did not provide a good enough method to resolve such problems.

For the cases under investigation, the graphics windows were activated for Residuals, Cl, Cd and Cm values. Due to the indicated value for the forces being vague, which was not accurate enough, the graphics windows were used to indicate a rough approximation of the solution in order to observe its overall trends. However the individual files of the forces were opened before an accurate solution to several decimal places was achieved.

ANALYSIS

Once all information from simulations was attained through the 'FLUENT' programme, tables were constructed of all numerical information attained and graphs followed with trendline equations. Analysis of this information allowed prediction of lift paths to take place and discussions made.

This thesis is intended to provide the reader with further information in order to increase ones capacity of knowledge on the WISE sector and influence further analysis on this sector.

FUTURE EXPERIMENTAL ANALYSIS

Experiments in the form of a truck traveling at various speeds with a scaled down model of a WIG mounted on the top would take place. Boththe fuselage and wing sections would have the approximate shape of the S-shaped aerofoil section. This would allow verification of results previously attained to take place, as well as provide additional information on external disturbances such as gusts to be analyzed. This could obtain a better feel of the movements and dynamic forces required in the take-off procedure.

UNIVERSITY
of
GLASGOW

Two-Dimensional Computational Fluid Dynamics Analysis of Wings In Ground Effect and Assessment on lift, drag and momentum coefficients resulting in a Three-Dimensional Turbulence model of efficiency and instability.

By
Elizabeth Ford
9504789

supervisor
Dr R.C McGREGOR

Vol. 2 of 2

POSTGRADUATE STUDIES (MSc)
Department of MECHANICAL ENGINEERING
DATE – JUNE 2001

REFERENCES

1. A Force In Being?. By B. Day. Sea Power. 1980 (Nov). Vol.23. pp. 34-40.
2. A New Computational Method for the Hydrodynamic Performance of Hydrofoil Craft. By F van Malree. 1997. Fast'97. Pp291-297.
3. A New method For Analysing the Seakeeping of Multi-Hull Ships. By D. Kring and P. D. Sclavounos. . First International Conference on Fast Sea Transport, Trondheim, June 1991, Fast'91. Vol. 1. pp. 429-444.
4. A nonlinear unsteady One - Dimensional Theory for Wings In Extreme Ground Effect. By E. O. Tuck. Journal of Fluid Mechanics. 1980. Vol. 98. Part 1. pp 33-47.
5. A Parametric Analysis Of A Flying Wing Configuration In Extreme Ground Effect. By K. V. Rozhdestvensky and S. Kubo. Internat. Workshop of Ekranoplans and Very Fast Craft Held at the Universtity of New South Wales, Australia. December 1996. Pp 78-96.
6. A Possible Maritime Future for Surface Effect Craft in the U. K. By C. B. Betts and B. R. Clayton. Proceedings on Ram Wing and ground Effect Craft. The Royal Aeronautical Society. 19th May 1987.
7. A Production Model of WIG as a High Speed Marine Craft: "Marine Slider; μ sky-2". By S. Kubo, T. Matsubara, T. Matsuoka and T. Kawamura. First International Conference on Fast Sea Transport, Trondheim, June 1991, Fast'91. Vol. 1. pp. 607-622.
8. A Review of Current Technical Knowledge Necessary to Develop Large Scale Wing-In-Surface Craft. By S. F. Hooker. AIAA-89-1497-CP.
9. A Simulation Study on the Maneuverability of a 105 - passenger Hovercraft. By I. Yoshino and H. Yagi. Journal of Naval architects of Japan. Vol 174. Pp365-375. (Japanese)
10. A Study Of The Efficiency Of The Wing-In-Ground-Effect Concept. By A. H. Day. Proceedings of the Workshop on 21st Century Flying Ships. 1995. Pp 1-22.
11. A Study on a WIG with Upper - Surface Blowing (USB) PAR. By R. Murao, T. Hori and T. Tsukada. RINA. International Conference on Wing-in-Ground-Effect Craft (WIGs). 4 and 5 December 1997. London. Pp 1-9.
12. A Study on Motion Characteristics of WISES Under Disturbances. By Y. Minami and T. Fuwa. Transactions Soc. Naval Architects of West Japan. Aug. 1997. N94. pp 43-53.(Japanese).
13. A Study on Numerical Schemes For More Accurate and Efficient Computations of free - ssurface Flows by Finite Difference Method. By A. Lungu and Kazu-hiro Mori. Journal of The Society of Naval Architectsof Japan. Vol. 173. Pp 9-17.
14. A Study On The Conceptual Design of Wing-in-Surface Effect Ships. By T. Fuwa et al. The 6th International Symposium on Practical Design

of Ships and Mobile Units. September 17-22 1995. PRADS'95. Pp1735-1746.

15. Aerodynamic Characteristics of a Large Number of Aerofoils tested in the Variable-Density Wind Tunnel. By R. M. Pinkerton and h. Greenberg. National Advisory Committee for Aeronautics. Report No. 628. 1938.
16. Aerodynamic Design of Wing In Ground Effect Craft. By Thomas Kuhmstedt and Gerd Milbradt. 1995. Fast'95. Pp597-608.
17. Aerodynamic Scheme of Ekranoplane Optimization with Reference to new Areas of Application. By A. V. Nebylov and E. T. Zhigalko. NATO Announcement of the Applied Vehicles Technology Panel. Symp. On Fluid Dynamics problems of Vehicles Operating Near Or In The Air-Sea Interface. Amsterdam, Netherlands. 5-8 Oct. 1998.
18. Aerodynamic Technology - the role of aerodynamic technology in the design and development of modern combat aircraft. By T. McMichael et al. Aeronautical Journal . December 1996. Pp 411-424.
19. Aerofoil Ground effect Revisited. By C. Coulliette and A. Plotkin. Aeronautical Journal. February 1996. pp 65-74.
20. Aero-Marine Design and Fluing Qualities of Floatplanes and Flying-Boats. By D. Stinton. Aeronautical Journal, March 1987.
21. An Analytic Solution For Two - and Three - Dimensional Wings In Ground Effect. By Sheila E. Widnall and Thomas M. Barrows. Journal of Fluid Mechanics. 1970. Vol. 41. Part 4. pp. 769-792.
22. An Effective Mathematical Model Of The Flow Past Ekranoplan With Small Endplate Tip clearances In Extreme Ground Effect. By K. V. Rozhdestvensky. Proceedings International Workshop 21st Century Flying Ships, University Of New South Wales, Australia. Pp155-177.
23. An Experimental Technique For Accurate Simulation Of The Flow Field For Wing-In-Surface-Effect Craft. By A. Sowdon and T. Hori. Aeronautical Journal. June/July 1996. Pp 215-222.
24. An Operational Evaluation Of The Hydrofoil Concept in United States Coast Guard Missions. By R. E. Williams. 2nd International Conference on Hovering Craft Hydrofoils Advanced transit Systems. Amsterdam 17-20 May 1976.
25. An Outline of Conceptual Design and feasibility Analysis of a Flying Wing Configuration on the Basis of Extreme Ground Effect Theory. By S. Kubo and Kirill V. Rozhdestvensky. 1997. Fast'97. pp 503-510.
26. Analysis of the Efficiency of an Ekranocat: A Very - High - Speed Catamaran with Aerodynamic alleviation. By L. J. Doctors. RINA. International Conference on Wing-in-Ground-Effect Craft (WIGs). 4 and 5 December 1997. London. Pp 1-16.
27. Analysis of Vehicles With Wings Operating In Ground Effect. By h. V. Borst. AIAA Paper 79-2034.1979.
28. Application of the Slender Monohull to High Speed Container Vessels. By H. Sipila and A. Brown. 1997. Fast'97. Pp247-249.

29. Applications of Modern Hydrodynamics to Aeronautics. National Advisory Committee for Aeronautics. Report No. 116. Washingto Government Printing Office. 1921.
30. Aspects of Hydrofoil Design; With Emphasis on Hydrofoil Interaction in Calm Water. By H. J. B. Morch and K. J. Minsaas. . First International Conference on Fast Sea Transport, Trondheim, June 1991, Fast'91. Vol. 1. pp. 143-162.
31. Assessment of Load Alleviation Devices Installed on a Power-Augmented…etc By E. F. McCabe, David W. Taylor Naval Ship Research and Development Centre, Report ASCD 383. 1997.
32. Calculation of Free-Surface Flows generated by Planning Carfts, By T. Hino, N. Hirata and T. Hori. . First International Conference on Fast Sea Transport, Trondheim, June 1991, Fast'91. Vol. 1. pp. 317-330.
33. Channel Corrections for Model Experiments With hydrofoils. By K. Koushan and C. F. L. Kruppa. 1997. Fast'97. pp299-305.
34. Characteristic Features of Ekranoplan. Sudostroenei Jnl. 1995.pp6 - 8. Rozhedestvensky.
35. Characteristic Study of Two - Dimensional Wings in Surface Effect by CFD. By H. Akimoto, S. Kubo and H. Ikeda. Journal of Naval Architects of Japan. Vol 184. pp47-54. (Japanese).
36. Comparison of a Cargo Catamaran with Conventional Seaborn and Airborn Transportation. By A. Kraus and A. Naujeck. . First International Conference on Fast Sea Transport, Trondheim, June 1991, Fast'91. Vol. 1. pp. 293-308.
37. Computational and Experimental Studies of Wings In Ground Effect Craft and WIG Effect Craft. By H. H. Chung, I. R. Park, K. H. Chung and M. S. Shin. Proceedings Workshop on Ekranoplans and Very Fast Craft. Sydney, Australia. 1996. Pp 38-59.
38. Concept Exploration and Assessment of Alternative High-Speed Ferry Types. By A. F. Molland, T. Karayanis and P. R. Couser. 1997. Fast'97. pp77-84.
39. Concept Of a Large Surface Effect Ship for Fast Ocean Transport by D. w. Czimmek, B. H. Schaub. . First International Conference on Fast Sea Transport, Trondheim, June 1991, Fast'91. Vol. 1. pp. 35-52
40. Conceptual Basas of WIG Craft Building; Ideas, Rreality and Outlooks. By E. A. Aframeev. NATO Announcement of the Applied Vehicles Technology Panel. Symp. On Fluid Dynamics problems of Vehicles Operating Near Or In The Air-Sea Interface. Amsterdam, Netherlands. 5-8 Oct. 1998.
41. Conceptual Design Study Of Power Augmented Ram Wing In Ground Effect Aircraft. By J. W. Moore. AIAA Aircraft Systems Technology Conference. AIAA-78-1466. 1978. Pp 1-13.
42. Crtical Review of Design Philosaphies for recent Transport WIG Effect Vehicles. By S. Ando. Transaction Japan Society Aeronautical Space Sciences. 1990. Vol. 33. Part 99. pp28-40.

43. Description of Hull Form and Evaluation of Ship Performance (2nd report) - Relation between hull form and propulsive performance. Journal of the Society of Naval Architects of Japan. Vol 184. Pp561-567. (Japanese).
44. Design Philosophy of PAR-WIG for Commuter Transport. By S. Ando. RINA. International Conference on Wing-in-Ground-Effect Craft (WIGs). 4 and 5 December 1997. London.pp1-20.
45. Design, Trial and Operation of "Hong Xiang" Ferry. By L. Hu. First International Conference on Fast Sea Transport, Trondheim, June 1991, Fast'91. Vol. 1. pp. 529-540.
46. Development of a Wing In Ground Effect Craft Marine Slider: μ SKY-1 As A High Speed Craft. By Syozo Kubo et al. 4th Pacific Congress Marine Sciences Technology. 1990. Volume 1. Part 1. pp 220-227.
47. Development of High speed Craft With Aero - Hydrodynamic Support. By m. A. Basin and R. Latorre. 1997. Fast'97. pp85-89.
48. Development of IMO Safety Requirements for a new high Speed Seagoing transportation-WIG Craft - Present State. By Alexander I. Bogdanov. 1995. Fast'95. pp.631-639.
49. Early History taken from: An Early Historical Review of WIG vehicles by R. G. Ollila, from "Acollection of Technical papers by AIAA/SNAME Advanced Marine Vehicles Conference, Oct. 2 - 4 1979.Maryland.
50. Economy and Speed in Comercial Operations by B. Foss. . First International Conference on Fast Sea Transport, Trondheim, June 1991, Fast'91. Vol. 1. pp. 259-276.
51. EKRANOPLAN: A High-Speed Marine vehicle of a New Type. By V. Chubikov, V. Pashhin, V. Treshchevsky and A. Maskalik. First International Conference on Fast Sea Transport, Trondheim, June 1991, Fast'91. Vol. 1. pp. 641-648.
52. Ekranoplan: A High - Speed Marine Vehicle of a New Type. By Dr. V. Chubikov et al. 1991. Fast'91. pp 641-648.
53. Endless - Belt Techniques For Ground Simulation. By Thomas R. Turner. NASA SP-116. 1966. pp 435-446.
54. Evaluation of a Power-Augmented-Ram Wing Operating Free in Heav…etc. By F. H. Krause. David Taylor Naval Ship Research and Development Centre. ASED 385.1977.
55. Evaluation and Quantification of HSC Safety for Approval and Operational Purposes. By P. Werenskiold. 1997. Fast'97. pp521-523.
56. Fast Ferry Interantional, April 1990, November 1991, June 1993.
57. Flow Computation for Three-Dimensional Wing in Ground Effect using multi-Block technique. By Nobuyuki Hirata. Journal of the Society of Naval Architects of Japan. Vol.177. pp 49-57. 1995.
58. Fluent "User's Guide Volume 2". Fluent Incorporated. 1998.
59. Fluent "User's Guide Volume 3". Fluent Incorporated. 1998.
60. Fluent "User's Guide Volume 4". Fluent Incorporated. 1998.

61. Fluent "User's Guide Volume 5". Fluent Incorporated. 1998.
62. Fluid mechanics; Volume 6 of Course of Theoretical Physics by L. D. Landau and E. M. Lifshitz.
63. Free Surface Effect on Characteristics of Two - Dimensional Wing. By K. Kataoka, J. Ando and K. Nakatake. Ransactions West Japan Society of Naval Architects. 1992. Vol.83. pp21-30. (Japanese).
64. Gambit 1 "Command reference Guide" Fluent Incorporated. 1998.
65. Gambit 1 "Modeling Guide" Fluent Incorporated. 1998.
66. Gambit 1 "Tutorial Guide" Fluent Incorporated. 1998
67. Ground Effect - Theory and Practice. By E. Pistolesi. N.A.C.A. Technical Memorandum No. 828. (Updated in 1975). Pp 1-40.
68. Haracteristic Features of Ekranoplan. By Kirill V. Rozhdestvensky. Sudostroenie Journal. 1995. pp. 45-48.
69. Heavy, Long-Haul Operations Using The Air-Sea Interface. By Dr. D. Stinton. RINA. International Conference on Wing-in-Ground-Effect Craft (WIGs). 4 and 5 December 1997. London. Pp 1-18.
70. High Speed Over Water, Ideas from the Past, the Present and Future by R. L. Trillo. First International Conference on Fast Sea Transport, Trondheim, June 1991, Fast'91. Vol. 1. pp. 17-34
71. High Speed vessels in the USA - An Introduction to the United States' Regulatory Environment. By LCDR Ronald Lokites and Chris B. McKesson. 1997. Fast'97. pp571-579.
72. Historical Review of WIG Vehicles. By R. G. Ollila. Journal of Hydronauics. 1980. Vol 14. Part 3. Pp65-76.
73. History and development of the "Aerodynamic Ground Effect craft" (A G E C) With Tnadem Wings. By G. W. Jorg. Proceedings on Ram Wing and ground Effect Craft. The Royal Aeronautical Society. 19th May 1987.
74. How Far How Fast? By P. Dorey. 2nd International Conference on Hovering Craft Hydrofoils Advanced transit Systems. Amsterdam 17-20 May 1976.
75. Hybird Hydrofoil Technology – An Overview. By J. R. Meyer. First International Conference on Fast Sea Transport, Trondheim, June 1991, Fast'91. Vol. 1. pp. 623-640.
76. Hydroaviation. By S. F. Hooker et al. International High Performance Marine Vehicle Conference. HPMV 92. 1992. WS1-8.
77. Hydrodynamic Design of Fast Ferries by the Concept of Super-Slender Twin Hull. By R. Sato, H. Nogami, Y. Shirose, A. Ito, H. Miyata, k. Masaoka, E. Kamal, and Y. Tsuchiya. . First International Conference on Fast Sea Transport, Trondheim, June 1991, Fast'91. Vol. 1. pp. 523-528.
78. Hydrodynamical Characteristics of a Ekranoplane Wing Flying near the Wavy Sea Surface. By V. G. Byelinskyy, P. I. Zinchuk. NATO Announcement of the Applied Vehicles Technology Panel. Symp. On Fluid Dynamics problems of Vehicles Operating Near Or In The Air-Sea Interface. Amsterdam, Netherlaands. 5-8 Oct. 1998.

79. Hydrodynamics by Horacle lamb.
80. Interaction Forces between Twin Hulls of a Catamaran Advancing in Waves (Part 1) By M. Kashiwagi. Journal of Naval Architect of Japan Vol. 173. pp119-131. (Japanese)
81. Interaction Forces between Twin Hulls of a Catamaran Advancing in Waves (Part 2) By M. Kashiwagi. Journal of Naval Architect of Japan Vol. 174. Pp181-190.(Japanese)
82. International High-Performance Vehicles Conference Papers 2-5 November 1988. Shanghai, China. The Chinese Society of Naval Architecture and Marine Engineering.
83. Introduction and Use of Future Transport Systems By F. T. Barwell. 2nd International Conference on Hovering Craft Hydrofoils Advanced transit Systems. Amsterdam 17-20 May 1976.
84. Investigation of a Three - Dimensional Power - Augmented RAM Wing in Ground Effect. By N. Hirata et al. 35th Aerospace and Science Exhibit. Jan. 1997. AIAA 97-08022. pp 1-11.
85. Investigation of Dynamic Ground Effect. By Ray Cung Chang and Vincent U. Muirhead. Proceedings of the 1985 NASA Amens Research Center's Ground - Effects Workshop. California. August 1985. Pp 363-394.
86. Investigation of the Static Lift Capability of a Low Aspect-Ratio Wing Operating in a Powered ground-Effect Mode. By J. K. Huffman and C. M. Jackson Jr. NASA TM X-3031. 1974.
87. Janes High Speed Marine Craft and Air Cushion Vehicles, 1983.
88. Janes High Speed Marine Craft and Air Cushion Vehicles, 1989.
89. Janes High Speed Marine Craft and Air Cushion Vehicles, 1991.
90. Janes High Speed Marine Craft and Air Cushion Vehicles, 1993.
91. Janes Surface Skimmers. (Hovercraft and Hydrofoils). 1973 - 74. By Roy McLeavy. Pp27.
92. Janes High Speed Marine Craft and Air Cushion Vehicles, 1994.
93. Janes Surface Skimmers Hovercraft and Hydrofoils 1973-74.
94. Large Wing-In-Ground Effect Transport Aircraft. By R. H. Lang, J. W. Moore.
95. Longitudinal Stability of Ekranoplans and Hydrofoil Ships. By V. Korolyov. NATO Announcement of the Applied Vehicles Technology Panel. Symp. On Fluid Dynamics problems of Vehicles Operating Near Or In The Air-Sea Interface. Amsterdam, Netherlands. 5-8 Oct. 1998.
96. Long-Range High-Speed catamaran Passenger Ship Desing. By K. S. Min. First International Conference on Fast Sea Transport, Trondheim, June 1991, Fast'91. Vol. 1. pp. 591-606.
97. Market Focused Design Strategy: Viable Transport System or Flight of Fancy?. By. G. K. Taylor. RINA. International Conference on Wing-in-Ground-Effect Craft (WIGs). 4 and 5 December 1997. London. Pp. 1-10.
98. Matched Asymptotics In Aerodynamics Of WIG Vehicles. By K. V. Rozhdestvensky. Proceedings of the International Society on High

Performance Marine Conference Exhibit. -HPMV '92. 1992. June 24-27. PPWS17-27.

99. McGraw-Hill Series In Aeronautical and Aerospace Engineering 'Low-Speed Aaerodynamics From Wing Theory to Panel Method' By Katz and Plotkin. 1991.

100. Mesh generation for Aerospace Applications. By N. P. Weatherill. Sadhana. Vol. 16. Part 1. June 1991. Pp 1-45. (Printed in India).

101. Motions and Added Resistance of Surface Effect Ships Sailing in Waves. By J. C. Moulijn. Dept. of Marine technology, Delft University. NE. NATO Announcement of the Applied Vehicles Technology Panel. Symp. On Fluid Dynamics problems of Vehicles Operating Near Or In The Air-Sea Interface. Amsterdam, Netherlaands. 5-8 Oct. 1998.

102. Near Surface vehicles The Next Breakthrough or the Niche Cul de Sac?. By G. H. Fuller. RINA. International Conference on Wing-in-Ground-Effect Craft (WIGs). 4 and 5 December 1997. London. Pp1-11.

103. New Method for Improvement of Performance and Seakeeping Characteristics of High – Speed Craft. By A. Ponomarev. First International Conference on Fast Sea Transport, Trondheim, June 1991, Fast'91. Vol. 2. pp. 1029-1038

104. Nonlinear Aerodynamics of Ekranoplan in Strong Ground Effect. By Kirill V. Rozhdestvensky. 1995. Fast'95. pp.521-630.

105. Numerial Study on the Aerodynamic Characteristics of a Three - Dimensional power - Augmented Ram Wing in Ground Effect. By N. Hirata. Journal of the Society of Naval Architects of Japan. Vol. 179. Pp31-39.

106. Numerical Analysis of 3 -D WIG Advancing Over Still Water Surface. By N. Mizutani. Journal of the Society of Naval Architects of japan. Vol. 174. pp35-46. (Japanese).

107. Numerical Investigation Of Nonlinear Unsteady Aerodynamics Of The WIG Vehicle. By N. V. Kornev and V. K. Treshkov. Proc. Symp. HPMV-92. 1992. Pp205-215.

108. Numerical Investigation on Wave reduction by Wings Attached to Hull. By Seung - Myun Hwangbo et al. Journal of the Society of Naval architects of Japan. Vol 177. Pp41-48.

109. Numerical Simulation of Wing in Ground Effect Craft "Marine Slider; μ sky-1" as a High Speed boat. By S. Kubo, T. Matsuoka and T. Kawamura. Proc. 4th Pacific Cong. Marine Sci. Tech., Vol. 1. pp. 220-227. 1990.

110. Numerical Simulation of Wing In Ground Effect. By T. Kawamura and S. Kubo. 3rd International Symposium on Computational Fluid Dynamics.1989. pp 1037-1042.

111. Numerical Study on 3-Dimensional Power - Augmented ram Wing in Ground Effect. By Seung - Hyun Kwag.Proc. 7th International offshore Polar Engineer Conference. USA. 1997. pp 704-711.

112. On Innovation in Aerodynamics. By M. G. Hall. Aeronautical Journal. December 1996. Pp 463-470.

113. On the Design of Stable Ram Wing Vehicles. By R. W. Staufenbiel. Symp. Proc. Ram Wing and Ground Effect Craft. Pp. 110-136. 1987.

114. On the Desiogn of Stable ram Wing vehicles. By R. W. Staufenbiel. Proceedings on Ram Wing and ground Effect Craft. The Royal Aeronautical Society. 19th May 1987.

115. On the Drag for a Sidewall ACV Over Calm Water. By R. C. McGregor. 2nd International Conference on Hovering Craft Hydrofoils Advanced transit Systems. Amsterdam 17-20 May 1976.

116. On the Hydrodynamics Coefficients of High Speed Vessels with Vertical motions. By Forng - Chen Chiu, Shiann - Jorng Horng and Chun - Tsung Wang. Journal of Naval Architects of Japan Vol. 177. Pp231-241. (Japanese).

117. On The Question of Influence…. By K. V. Rozhdestvensky. ACAD SCI USSR. 1980. Pp142-148. (In Russian).

118. Operating the PT150 Hydrofoil. By Johs. Presthus. 2nd International Conference on Hovering Craft Hydrofoils Advanced transit Systems. Amsterdam 17-20 May 1976.

119. Operational Conciderations. By N. H. Cross. RINA. International Conference on Wing-in-Ground-Effect Craft (WIGs). 4 and 5 December 1997. London.pp 1-4.

120. Optimal Takeoff Performance of a Vectored Thrust Aircraft. By G. Avanzini and G. de Matteis. Aeronautical Journal. August/September 1995. Pp 275-281.

121. Performance Analysis of Wing In Ground Effect Craft. By Ho-Hwan Chun et al. RINA. International Conference on Wing-in-Ground-Effect Craft (WIGs). 4 and 5 December 1997. London.pp1-12.

122. Performance Analysis of Wing-in-Ground Effect Craft. By Ho-Hwan Chung et al. RINA. International Conference on Wing-in-Ground-Effect Craft (WIGs). 4 and 5 December 1997. London. Pp 1-13.

123. Preliminary Design Of A 20 Passenger PARWIG Craft and Construction of a 1/10 Scale Radio Controlled Model. By. H. H. Chung, C. H. Chang, K. J. Paik and S. I. Chang. 1997. Fast'97. Pp513-518.

124. Progress Report on Aerodynamic Analysis of a Surface Piercing Hydrofoil-Controlled Wing-In-Ground Effect SEABUS Configuration. By C. M. van Beek, B. Oskam and G. Fantacci. NATO Announcement of the Applied Vehicles Technology Panel. Symp. On Fluid Dynamics problems of Vehicles Operating Near Or In The Air-Sea Interface. Amsterdam, Netherlands. 5-8 Oct. 1998.

125. Ram Wings – A Future? By J. m. l. Reeves. Proceedings on Ram Wing and ground Effect Craft. The Royal Aeronautical Society. 19th May 1987.

126. Recent Advances in Wing-in-Ground Effect Vehicle Technology. By R. W. Gallington, H.Rr. Chaplin, H. Krause, J. A. Miller and J. C. Pemberton. AIAA/SNAME Advanced Marine Vehicles Conf. Pp78-874. 1976.
127. Review of Research on High Speed Marine Vehicles. The High - Speed Marine Committee. Final Report and Recommendations to the 20th ITTC. pp363-413.
128. Revised Classification Requirements for the Design and Construction of the Latest Generation of High Speed Ferries. By R. Curry, T. W. Grove and A. Mak. 1997. Fast'97. pp 524-535.
129. RFB Research and Development in WIG Vehicles. AIAA –89-1495-CP.
130. Roll Damping Due to Lift Effects On High Speed Monohhulls. By J. J. Blok and A. B. Aalbers. First International Conference on Fast Sea Transport, Trondheim, June 1991, Fast'91. Vol. 2. pp. 1331-
131. Safety on Fast Sea Transport. By H. helmersen and p. Werenskiold. First International Conference on Fast Sea Transport, Trondheim, June 1991, Fast'91. Vol. 2. pp. 1349.
132. Seakeeping Analysis of Surface Effect Ships. By D. E. Nakos, A. Nestegard, T. Ulstein and P. D. Sclavounos. . First International Conference on Fast Sea Transport, Trondheim, June 1991, Fast'91. Vol. 1. pp. 413-428.
133. Seakeeping of Foilcatamarans by S. Falch. . First International Conference on Fast Sea Transport, Trondheim, June 1991, Fast'91. . Vol. 1. pp. 209-222.
134. SES 500 – Fincantieri - Design Criteria, by A. Cordano and L. De Martini. . First International Conference on Fast Sea Transport, Trondheim, June 1991, Fast'91. Vol. 1. pp. 179-198.
135. Simulation of The Interaction Between Aerodynamics and Vehicle Dynamics In General Unsteady Ground Effect. By D. T. Mook and A. O. Nuhalt. AIAA-89 Intersociety Advanced Marine Vehicles Conference. 1989. Pp 430-438.
136. Simulation on Viscous Flow around Two -Dimensional Power - Augmented Ram Wing in Ground Effect. By N. Hirata. Journal of Naval architects of Japan. Vol 174. pp 47-53. (Janpanese).
137. Simulation Study on the Behaviour of Wing-In-Surface Effect ships. By Takeshi Fuwa, Nobuyuki hirata, Yosimasa Minami and Masahiro Yamaguchi. 1995. Fast'95. pp 609-620.
138. Simulation Study On The Behaviour of Wing-in-Susrface Effect Ships. By T. Fuwa, N. Hirata, Y. Minami and m. Yamaguchi. 1995. Fast'95. Pp 609-621.
139. Single jet - Induced Effects on Small - Scale Hover Data in Ground Effect. By D. B. Levin and D. A. Wardwell. Journal of Aircraft. Vol. 34. No. 3. May - June 1997. Pp 400-456.
140. Some Conciderations on Rules and regulations for Fast Sea Transportation in Japan. By K. Ogawa. First International Conference

on Fast Sea Transport, Trondheim, June 1991, Fast'91. Vol. 2. pp. 1293-1296

141. Some Military Applications of Small Hovercraft. By G. W. Shepherd. 2nd International Conference on Hovering Craft Hydrofoils Advanced transit Systems. Amsterdam 17-20 May 1976.

142. Some Stability Problems of Ground Effect Wing Vehicles in Forward Motion. By P. E. Kumar. Aero. Quart. Vol. 23. pp. 41-52. 1972.

143. Some Thoughts On Power - Augmented - Ram Wing - in - Ground (PAR - WIG) Effect Vehicle. By S. Ando. Transatlantic Japan Society Aero. Space Science. 1988. Volume 31. Pp29-47.

144. State-of-the-Art and Perspectives of Development of Ekranoplans in Russia. By K. V. Rozhdestvensky and D. N. Synitsin. 1993. Fast'93. Part 2. Pp 1657-1670.

145. State-of-the-Art of Research on Aerodynamics and Hydrodynamics of Ekranoplans. By A. I. Maskalik, K. V. Rozhdestvensky and D. N. Sinitsyn. NATO Announcement of the Applied Vehicles Technology Panel. Symp. On Fluid Dynamics problems of Vehicles Operating Near Or In The Air-Sea Interface. Amsterdam, Netherlands. 5-8 Oct. 1998.

146. Study on Aerodynamic Characteristics of Wing in ground Effect. By T. nagamatsu et al. Journal Kansai Society of Naval Architects of Japan. No. 218. September 1992. pp145-153. (Japanese)

147. Synthetic Aspects of Transport Ecomony and Transport \vehicle Performance with Reference to High Speed Mrine Vehicles. By S. Akagi. . First International Conference on Fast Sea Transport, Trondheim, June 1991, Fast'91. Vol. 1. pp. 277-292.

148. Taking Advantage of Surface Proximity Effects With Aero-Marine vehicles. By R. L. Trillo, Symp. Proceedings on Ram Wing and ground Effect Craft. The Royal Aeronautical Society. 19th May 1987.

149. Tandem Airfoil Flairboats (TAF) The first ownstable aerodynamic Ground Effect Craft (AGEC) qualified and suitable for passenger traffic and leasure-boats. By G. W. Jorg. RINA. International Conference on Wing-in-Ground-Effect Craft (WIGs). 4 and 5 December 1997. London. Pp 1-3.

150. The "Swordfish" type hydrofoil: Design Criteria and Operational Experience. By M. Baldi. 2nd International Conference on Hovering Craft Hydrofoils Advanced transit Systems. Amsterdam 17-20 May 1976.

151. The Aerodynamics of Ram Wing Vehicles For Application to high Speed Ground Transportation. By Timothy M. Barrows and Sheila E. Widnall. 8th Aerospace and Science Meeting, New York. AIAA paper No. 70-142.1970. pp 1-11.

152. The Aerodynamics of the Unconventional Air Vehicles of A. Lippisch, H. V. Borst and Associates Wayne, Pennsylvania 1980.

153. The Concept of Heavy Ekranoplane Use for Aerospace Plane Horizontal Take-off and Landing. By N. Tomita et al. RINA. International Conference on Wing-in-Ground-Effect Craft (WIGs). 4 and 5 December 1997. London.pp1-11.

154. The Current Level of Power-Augmented-Ram Wing Technology. By F. H. Krause, et al. of AIAA Paper 78.32174.3/85. 1978.

155. The Design and Operating Features of Vosper Thornycraft Skirts. By R. Dyke. 2nd International Conference on Hovering Craft Hydrofoils Advanced transit Systems. Amsterdam 17-20 May 1976.

156. The Essentials Of Fluid Dynamics by Dr. L. Prandtl

157. The Hoverwing Technology - Bridge Between WIG and ACV. By H. Fischer and K. Matjasic. RINA. International Conference on Wing-in-Ground-Effect Craft (WIGs). 4 and 5 December 1997. London. Pp 1-11

158. The Hoverwing Technology ; The Bridge between WIG and ACV. By H. Fisher and K. Matjasic. NATO Announcement of the Applied Vehicles Technology Panel. Symp. On Fluid Dynamics problems of Vehicles Operating Near Or In The Air-Sea Interface. Amsterdam, Netherlands. 5-8 Oct. 1998.

159. The Hydrodynamic Lift Effect on the Stability and on the Banking Angle of the Fast Crafts. By M. Simeone. . First International Conference on Fast Sea Transport, Trondheim, June 1991, Fast'91. Vol. 1. pp. 331-346.

160. The Lerge Conercial Hydrofoil and its Limits in Size and Speed. By Baron Hanns Von Schertel. 2nd International Conference on Hovering Craft Hydrofoils Advanced transit Systems. Amsterdam 17-20 May 1976.

161. The Naval Architect 1973.

162. The Power Augmented-Ram Wing In Ground Effect Concept as an Airborn Amphibious Quick Reaction… etc. By C. E. Heber, Jr.,et al.AIAA Paper 81-2077. 1981.

163. The Prediction of Resistance of Surface Effect Ships. By H. Oehlmann and J. C. Lewthwaite. First International Conference on Fast Sea Transport, Trondheim, June 1991, Fast'91. Vol. 2. pp. 693-708.

164. The Pressure Distribution On Two - Dimensional Wings Near The Ground. By J. A. Bagley. Aero. Res. Courc. R. & M. No. 3238. 1961. Pp 1-40.

165. The Ram - Wing Surface Effect Vehicle: Comparison of One - dimensional Theory with Wind - Tunnel and free Flight Results. By Captain R. W. Gallington et al. Hovering Craft Hydrofoil. 1972. Pp10-19.

166. The Ram-Wing Surface Effect Vehicle; Comparison of One-Dimenssional Theory with Wind Tunnel and Free Flight |Results. By R. W Gallington, M. K M. K. Miller, and W. D. Smith. Hovering Craft and Hydrofoil, pp. 10-19. 1972.

167. The Role of WIG Effect Vehicles In The Transport Industry. Fast Ferry International. April 1990.
168. The Sixth International Conference High Speed Surface Craft Conference. 14-15 1988.
169. The Theory pf Thin Wings in Subsonic flow. By S. M. belotserkovskii. Translated from Russian. (Plenum Press. New York. 1967.
170. The Very High Speed Surface Peircing WIG Vessel IRF-01. By S. Roccotelli, G. Fantacci. T. Giublesi, M. Bogliardi and Alenia. NATO Announcement of the Applied Vehicles Technology Panel. Symp. On Fluid Dynamics problems of Vehicles Operating Near Or In The Air-Sea Interface. Amsterdam, Netherlands. 5-8 Oct. 1998.
171. Theoretical Analysis of Dynamics of a WIG Vehicle in Extreme ground Effect. By K. V. Rozhdestvensky. NATO Announcement of the Applied Vehicles Technology Panel. Symp. On Fluid Dynamics problems of Vehicles Operating Near Or In The Air-Sea Interface. Amsterdam, Netherlaands. 5-8 Oct. 1998.
172. Theory Of Power Augmented ram Lift At Zero Forward Speed. By R. W. Gallington and H. R. Chaplin. DTNSRDC Report ASCD 365. 1976. Pp 1-8.
173. Thickness-Induced Lift on a Thin Aerofoil in Ground Effect. By a. Plotkin and C. G. Kennell. AIAA Journal. Vol. 19. No. 11. November 1981. Pp 1484-1486.
174. Unsteady Effects of Camber On The Aerodynamic Characteristics Of A Thin Aerofoil Moving Near the Ground. By M. F. Zedan and A. O. Nuhait. Aeronautical ournal. November 1992. Pp 343-350.
175. USSR research and Design Efforts in the development of Marine Ekranoplans and Their Transportation Capability in various Water areas. By L. D. Volkov, V. M. Pashin et al. Internal Society High Performance Marine Vehicle Conference. Exhibit Arlington U. S. A. 1992. WS60-65.
176. Virtual Testing of Navigational Safety of Wing-In-Ground Effect Vehicles. By K. V. Rozhdestvensky. RINA. International Conference on Wing-in-Ground-Effect Craft (WIGs). 4 and 5 December 1997. London.pp1-6.
177. VT.2 – 100 Ton Amphibious Hovercraft. By A. E. Bingham. 2nd International Conference on Hovering Craft Hydrofoils Advanced transit Systems. Amsterdam 17-20 May 1976.
178. WIG (Ekranoplane) As A Transport Vessel and Sport Craft. By M. Basin. RINA. International Conference on Wing-in-Ground-Effect Craft (WIGs). 4 and 5 December 1997. London. Pp 1-13.
179. WIG Safety - A Classifcation Society Point of View. By Karsten Fach and Ulf Petersen. RINA. International Conference on Wing-in-Ground-Effect Craft (WIGs). 4 and 5 December 1997. London. Pp 1-12.

180. . Wind Tunnel Test Results For Eight and Twenty Passenger Class Wing-in-Ground Effect Ships. By Myung-Soo Shin et al. 1997. Fast'97, pp.565-570.

181. Wing Resistance Near The Ground. By C. Wieselberger. National Advisory Committee For Aeronautics Technical Memorandum No.77. 1922.(Updated in 1975).

182. Wing resistance near The Ground. By C. Wieselsberger. NACA TM-77. 1992. Pp 1-8.

183. Wing-In-Ground-Effect Craft. By R. Trillo. Jane's High Speed Marine Craft. 1992-1993 (June) pp 381-394.

184. Wing-In-Surface-Effect Ferries: The Imminent Future Of Ultra-Fast Ferries is Off The Water. By W. J. Greene. RINA. International Conference on Wing-in-Ground-Effect Craft (WIGs). 4 and 5 December 1997. London.pp1-10.

185. WISES Design Method and Their Application. By T. takahashi and T. Fuwa. Journal Kansai Society of Naval Architects of Japan. Vol.222. September 1994. pp183-190. (Japanese).

186. On some Problems of Fluid with a Free Surface, ASME Jnl. Of Fluid Mechanics. By Dobrovolskaya,Vol. 36 Part 4, pp805 - 829.

187. The Wave Resistance of an Air - Cushion Vehicle in Steady and Accelerated Motion, By Doctors, L. J. and Sharma, S. D., Journal of Ship Research, Vol. 16, No. 4, pp.248 - 260.

188. The Use of Pressure Distribution to model the Hydrodynamics of Air - Cushion Vehicles and Surface - Effect Ships, Proc. HPMV'92 Conference and Exhibit, ASNE, Flagship Section, Arlington, VA, pp. SE56 - SES72.

189. On Seakeeping of Conventional and High - Speed Vessels, by Faltinsen, O., 15th Georg Weinblum Lecture, Journal of Ship Research, June, 1993.

190. The Administration's Role in the Development and Implementation of Safety Standards for High - Speed Craft. By Graham, W. A., Proceedings, IMAS 91 - High Speed Marine Transportation, Sydney, Australa, pp 243 - 253.

191. Agnes 200: an Outline for a Future Surface Effect Ship, By Guezou, J. P., Letty, P., and Picart, Y. P., IMAS 91 - High Speed Marine Transportation, 1991, Sydney Australia.

192. Dynamics and Hydrodynamics of Surface Effect Ships. By Kaplan, R., Bentson, J., and Davies, s., Transactions of SNAME Spring Meeting /STAR Symposium. Pittsbyrg. 1981. Vol. 89, pp. 211 - 248.

193. A Collection of Simplified Fied Equations for SES Design, Procs, HPMV'92 Conference anad Exhibit, By McKensson, C,. C. B. ASNE Flagship Section, Arllington VA, pp SES73 - SES 83.

194. High - Speed Craft Operational Performance and Limitations, By Werenskiold, P., 3rd Conference on High Speed Marine Craft.

Norwegian Society of Chartered Engineers, Kristiansand, Norway. 1990.

195. Dynamic Response Of An Air - Cushion Lift Fan. By Sullivan, P. A., Gosselin, f and Hinchey, M, J., Proceedings, hpmv'92, conference and Exhibits, ASNE, Flagship Section, Arlington, VA, 1192, pp ACV39 - ACV47.

APPENDIX A

Raketa-2

picture:

FLHRO-PB

picture: Flying Dragon Ltd

G-35

picture: Radacraft

Navion

picture:

TAF VIII-2 Jörg IV

picture: G. Jörg

Volga-2

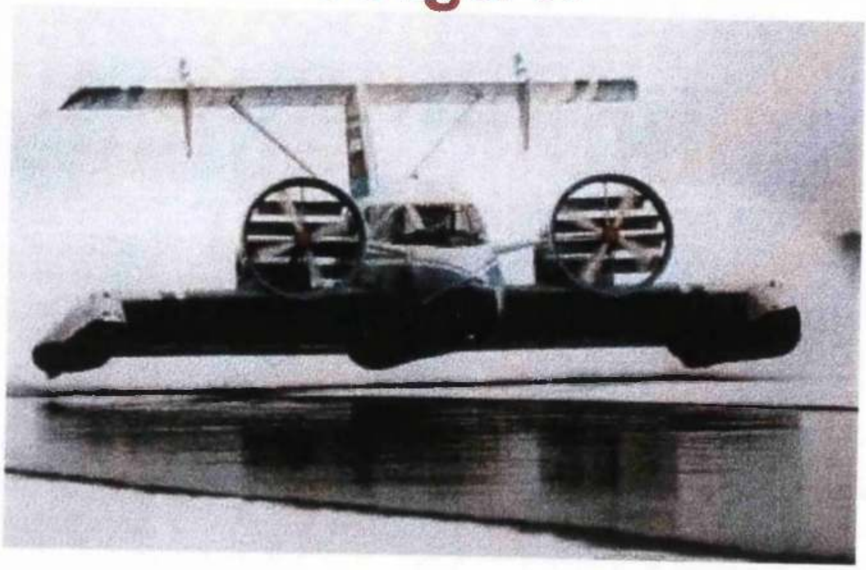

picture:

X-114

picture: RFB

WeberWIG

picture:

DY-806

picture: EvO, The WIG Page

UT

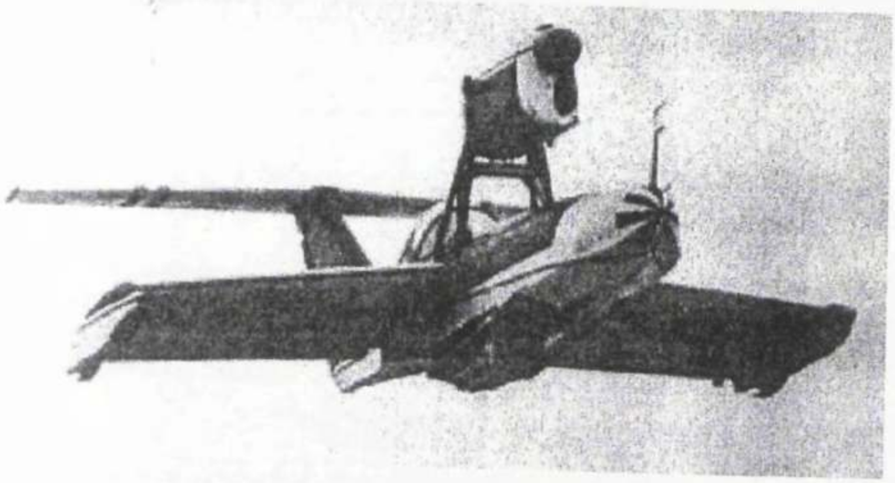

picture:

TAF VIII-5

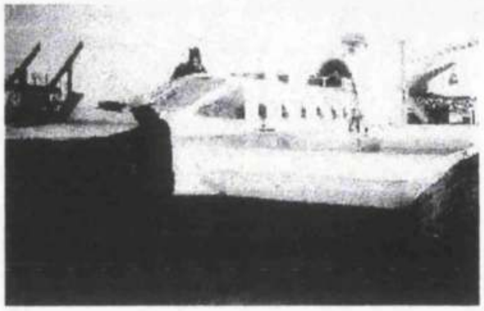

picture: G. Jörg

TAB VII Jörg I

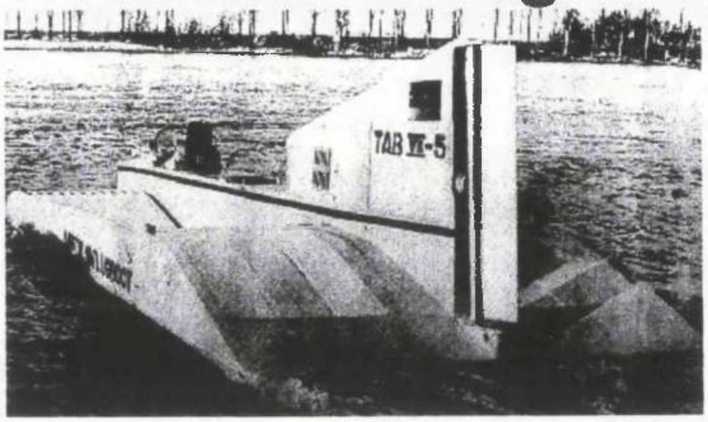

picture: G. Jörg

SM-11

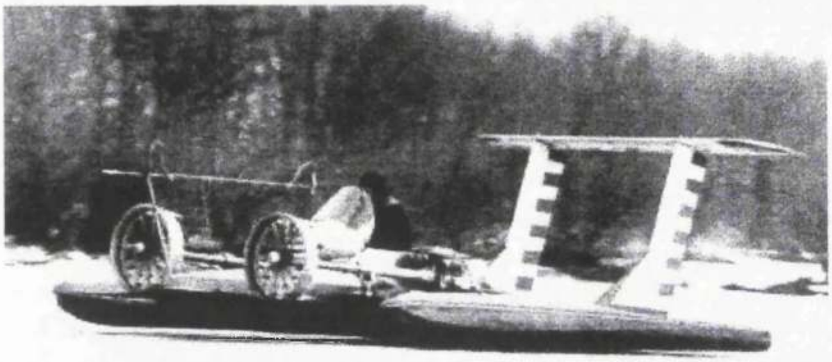

picture: A. Belyaev

SM-8

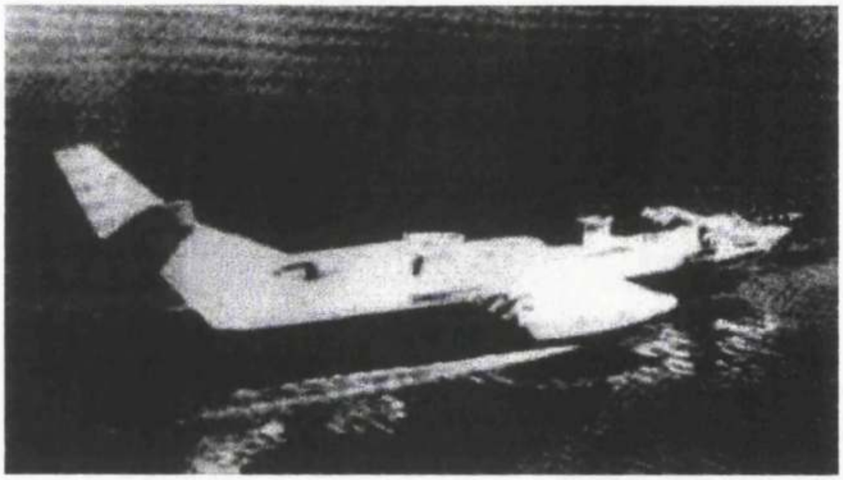

picture: A. Belyaev

Seawing 12

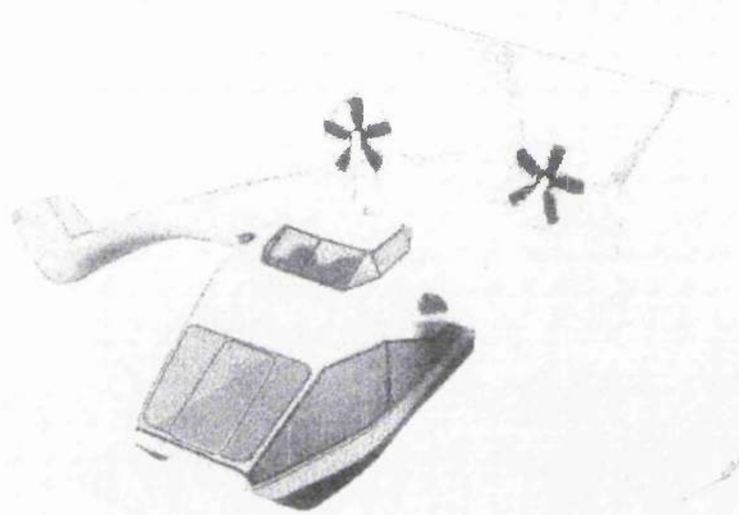

picture: Sea Wing

Seawing 05

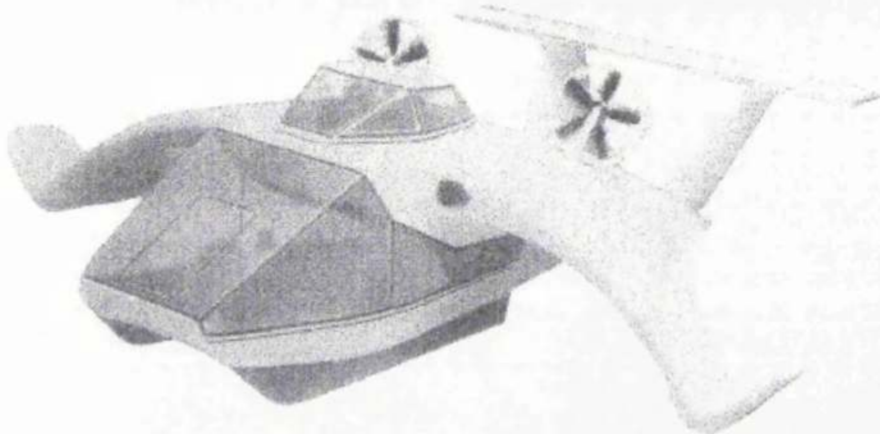

picture: Sea Wing

Rameses-1

picture:

OIIMF-2

picture:

KAG-3

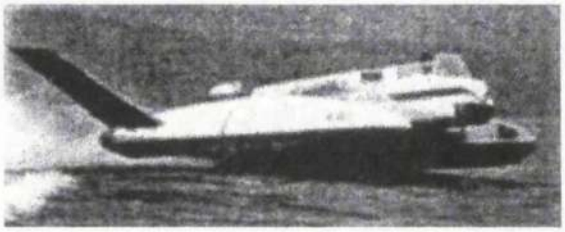

picture: Kawasaki

Hydroflyht future design

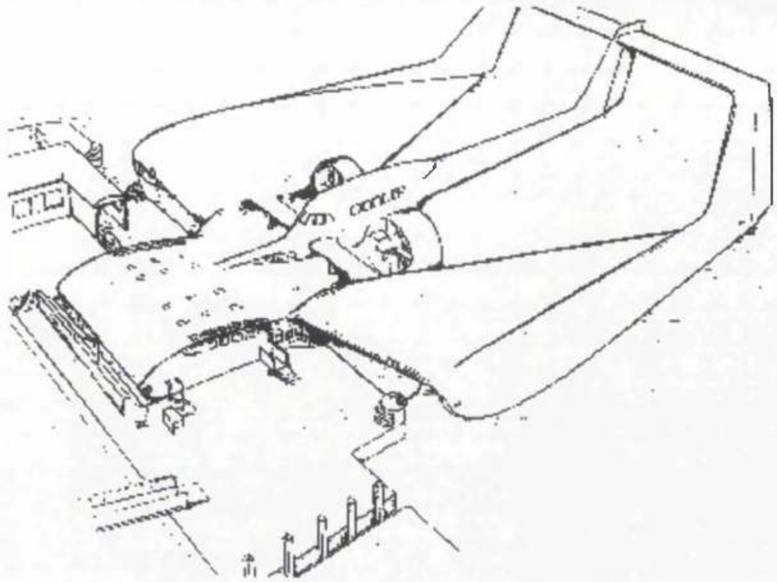

picture:

ESKA-1

picture:

Dickson's Ram Wing

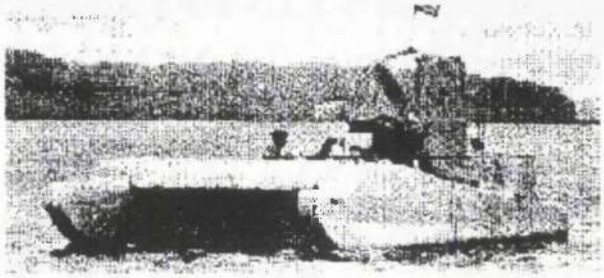

picture:

Beriev 1

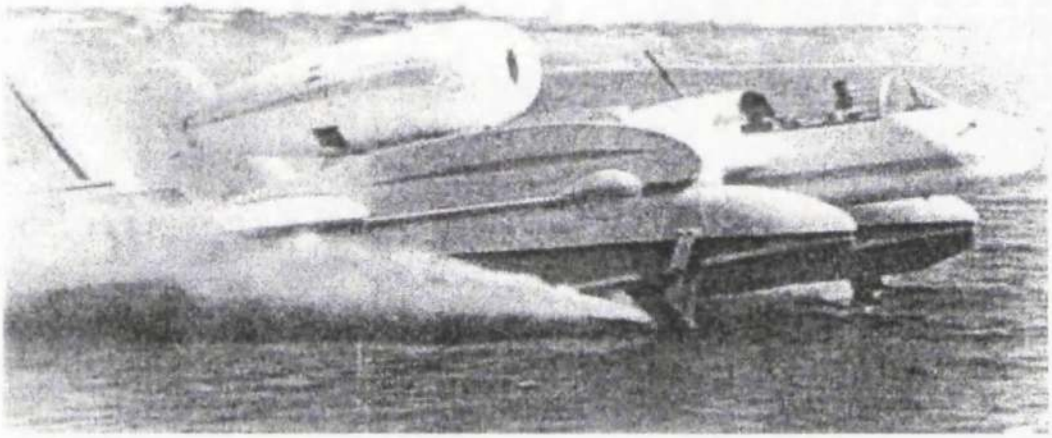

picture: Beriev

BEF-401

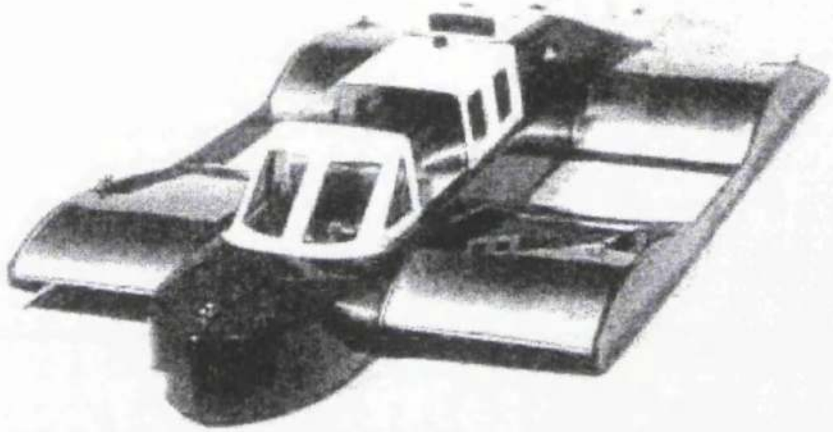

picture: Strahl

A90.150 Orlyonok

Photo: A. Belyaev

Lun

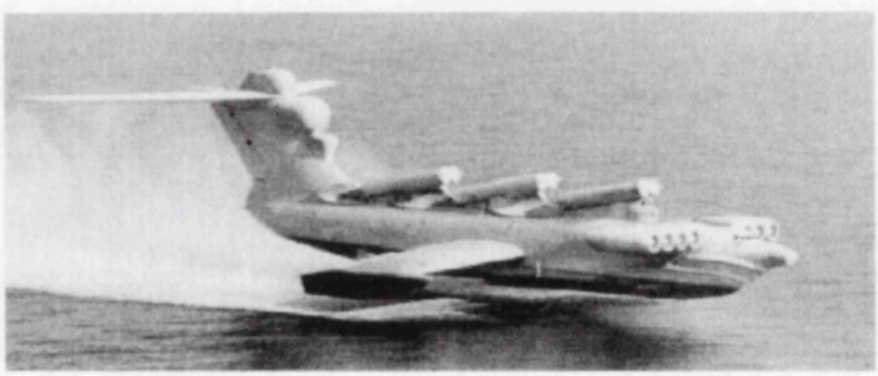

Photo: A. Belyaev

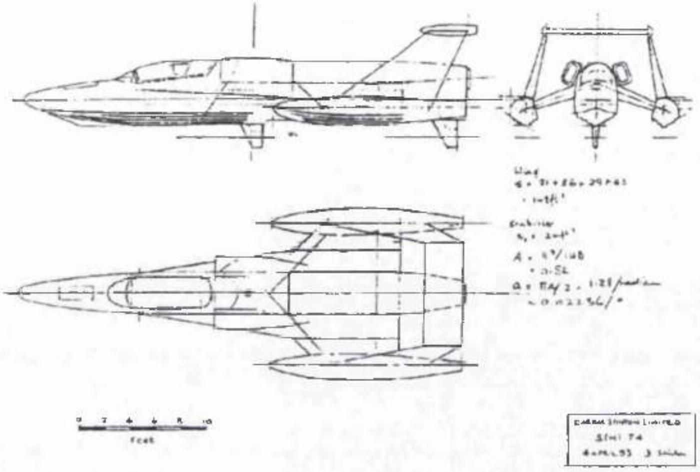

Fig. 6.5 Layout of ram wing project to reach transonic speeds above water, while hydro-stabilizer and rudder surfaces run in water. [illegible] (Author, courtesy of Royal Institution of Naval Architects, [illegible])

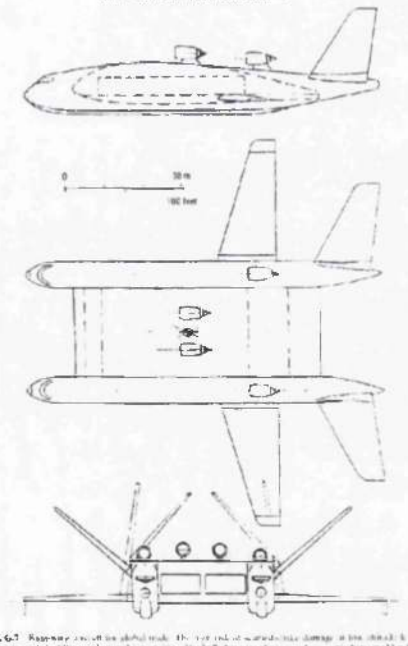

Fig. 6.7 [illegible]

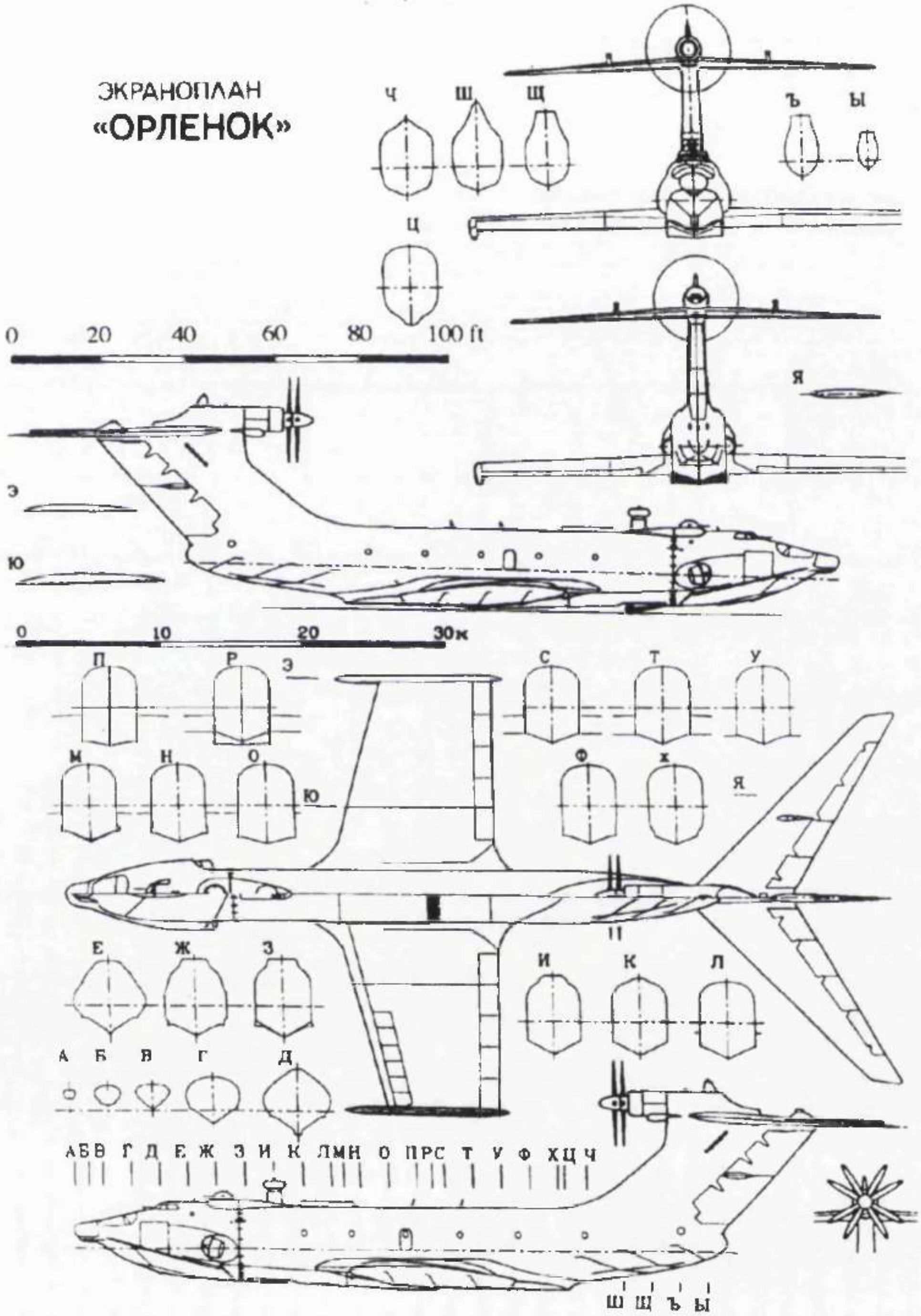

Fig. G.3 Russian Alexseyev Central Hydrofoil Design Bureau ekranoplan, Orlenok. Turbofan engine exhausts are deflected beneath the wings to provide cushion-lift, like a hovercraft, and thrust. The turbine contra prop is for propulsion. (After Russian aeromodeller's magazine, AX, *AeroXobbi* (1992).)

Volga-2

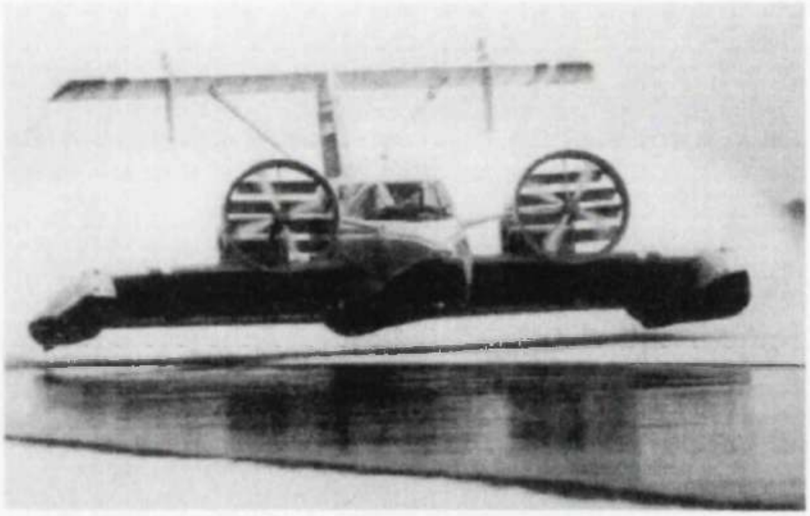

Photo: G. Theophile

The Volga-2 is an 8 passenger PAR-WIG vehicle, performance tests showed that the operating economics of this vehicle are comparable with existing hydrofoils. The flexible construction is of a light alloy with the use of balloon type structures in order to give the craft amphibious capabilities (snow and ice). The Volga can handle waves up to 0.5 m and can climb a 10% gradient on land. The Volga is powered by two VAZ-413 rotary engines of 95 kW each.

Raketa 2

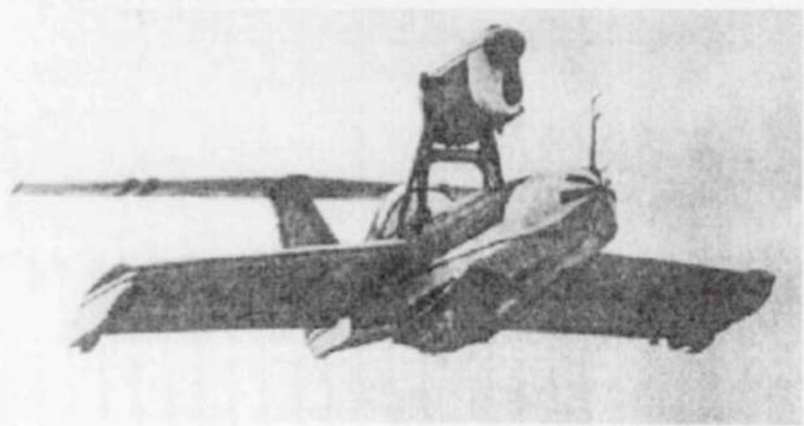

Photo: A. Belyaev

The WIG Page Datasheet no. 10

Beriev 1

from

Beriev

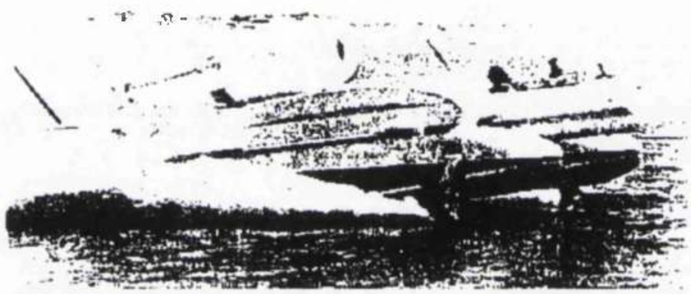

The Be-1 is a small test vehicle for exploring the stability and control of the VVA-14. The single seat test craft has two floats with a very low aspect ratio wing in between and small wings extending from the floats. The Be-1 is powered by a RU-19 turbojet that is mounted on the back of the wing. Starting aid is provided by surface piercing hydrofoils that are mounted on the floats. Apart from the floats the Be-1 is also equipped with a landing gear. The Be-1 was built in 1961 and the first flight from water was made in 1964

Technical data

Explanation of symbols

Pictures

Click on an image to enlarge

thumbnail	size (b)	picture by	description
	22456	Beriev	ashore
	24071	Beriev	rear view
	15881	Beriev	on foils

The WIG Page Datasheet no. 11

VVA-14

from

Beriev

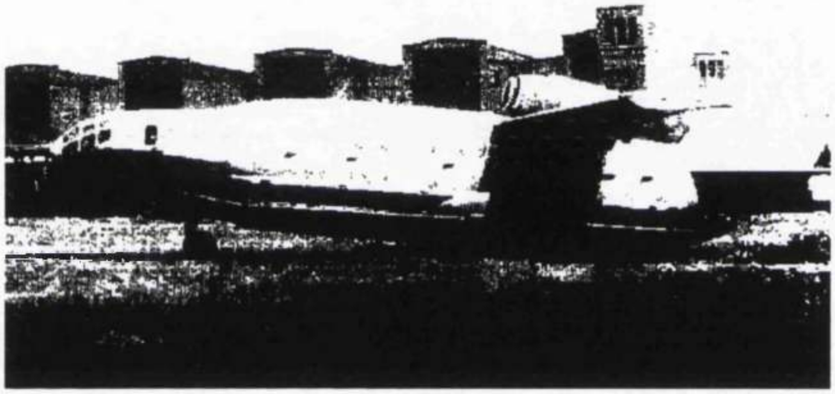

The VVA-14 is not a true WIG vehicle, since the ground effect is only a take off aid. The VVA-14 cruises at an altitude of 10 km. The first flight of the VVA-14 took place in 1972. Later the VVA-14 was fitted with inflatable pontoons for operation from water. The VVA-14 is powered by two D-30M turbofans mounted above the trailing edge of the central wing. The landing gear of the VVA-14 is borrowed from the Tu-22.

In 1976 a VVA-14 prototype was converted to a VVA-14M1P, the inflatable pontoons were replaced by rigid ones and two additional D-30M turbofans were installed at the nose of the vehicle. These engines blow in the cavity under the wing for PAR take off.

Technical data

l	26.00 m
b	30.00 m
W_{max}	52 t
V_{cr}	760 km/h
R	2450 km
Explanation of symbols	

Pictures

Click on an image to enlarge

Impression of the Skate 50-seat amphibious hoverferry

Artist's impression of an Orion type sidewall craft

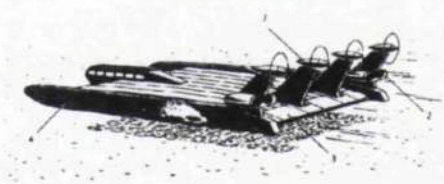

The Soviet giant wing-in-ground-effect machine has similar lines to the craft depicted above, it is believed. The main power plants (1) are thought to be gas-turbines rather than turboprops as shown, and the booster gas turbines (2) to accelerate the craft through hump to cruising speed are likely to have been moved to a forward position.

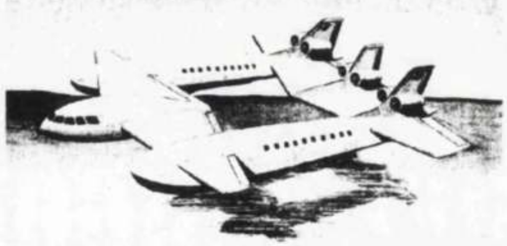

Impression of a new catamaran-hulled Ekranoplan research craft now under development in the Soviet Union. Designed for high speed long distance passenger services along the main Soviet rivers, it rides on a dynamic air cushion formed between its wings and the supporting surface below. Seats are provided for forty passengers in each of the twin hulls. Top speed is likely to be between 150-200 knots

NVA-60P

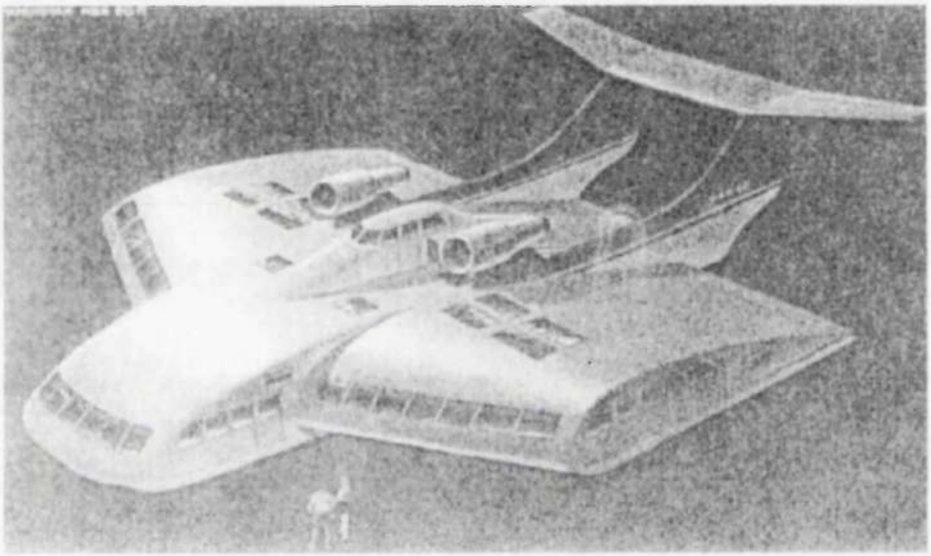

The NVA-30's twin 36 kN turbofans are mounted on top of the fuselage and the fuselage mounted lift fan is powered by a 5200 kW gasturbine. The NVA-60 can accomodate 200 passengers.

NVA-60P Technical Data	
Length	25.5 m
Width (span)	33.4 m
Max. take-off weight	60 ton
Payload	27 ton
Cruise speed	280 km/h

The WIG Page picture no. 1

A90.125 Orlyonok

picture: A. Belyaev

The WIG Page picture no. 22

Airfisch 1

picture: FF

The WIG Page picture no. 24

Airfisch 3

picture: FF

The WIG Page picture no. 28

Airfisch 8

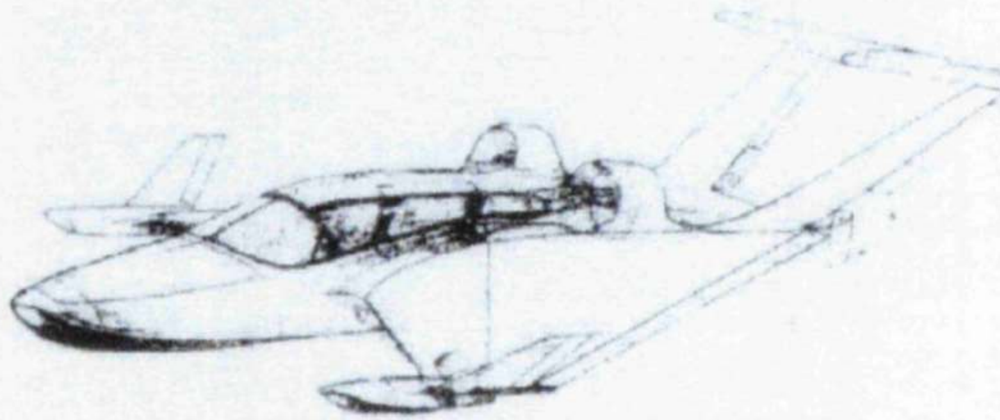

picture: FF

The WIG Page picture no. 30

Amphistar / Xtreme Xplore

picture: Amphistar USA

The WIG Page picture no. 29

AN-2E

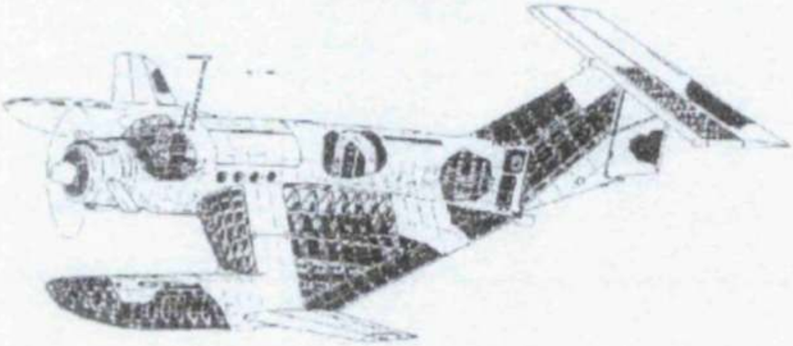

picture:

The WIG Page picture no. 43

CIST Lippisch type craft

picture:

The WIG Page picture no. 48

E-120

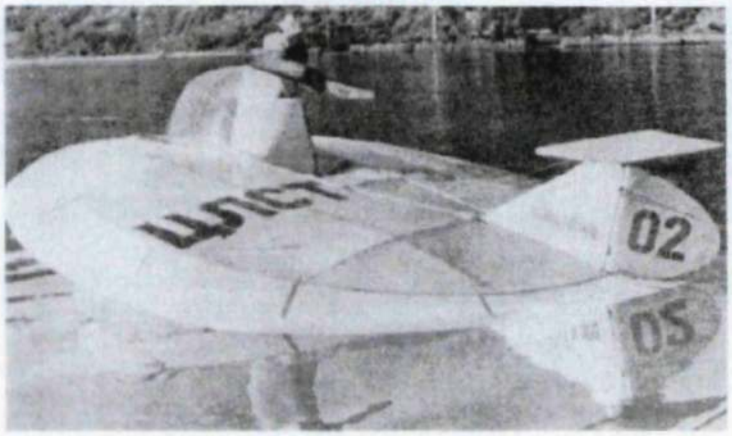

picture:

The WIG Page picture no. 49

ES-2

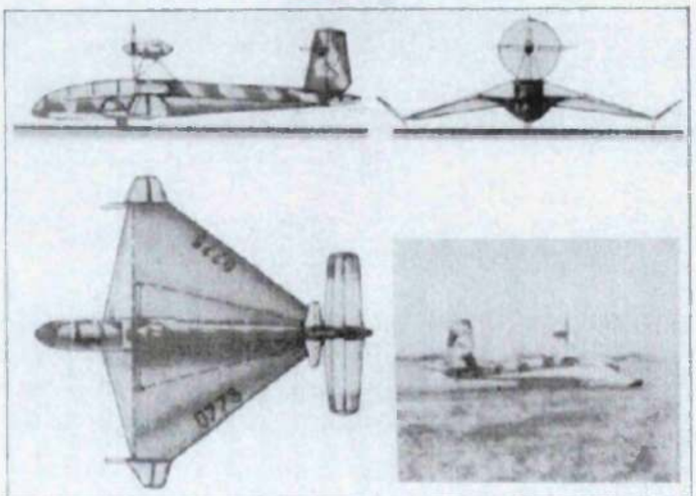

picture:

The WIG Page picture no. 55

ESKA-4

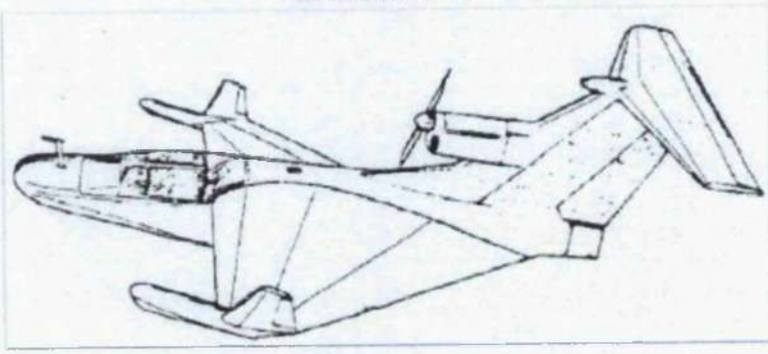

picture:

The WIG Page picture no. 79

Hoverwing 80

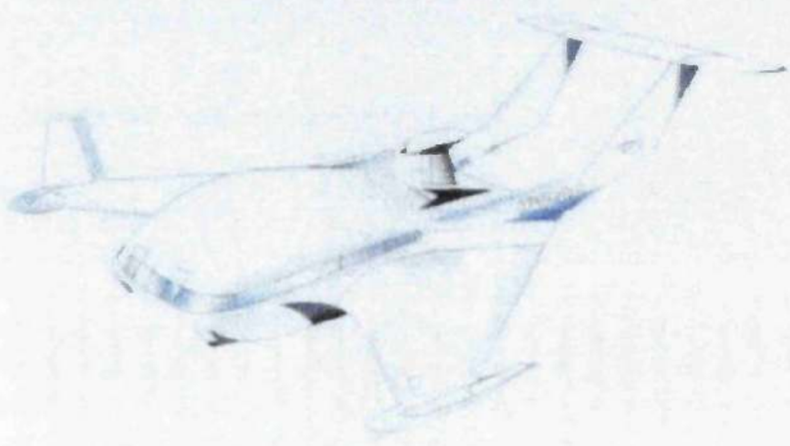

picture: FF

The WIG Page picture no. 306

FLHW-A

picture: Flying Dragon Ltd

The WIG Page picture no. 03

L-325

picture:

The WIG Page picture no. 89

KM

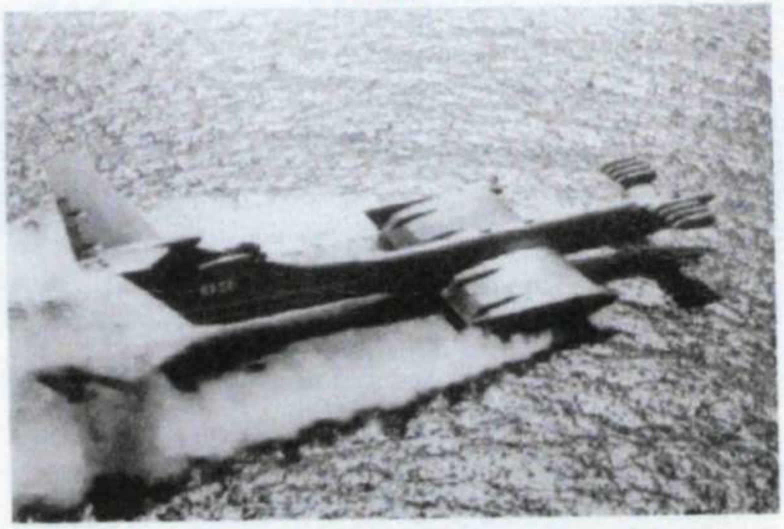

picture: A. Belyaev

The WIG Page picture no. 80

Icarus

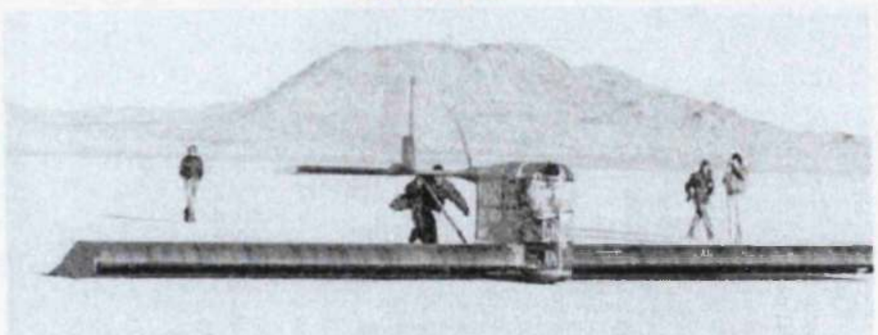

picture

The WIG Page picture no. 71

HW2VT

picture: FF

The WIG Page picture no. 64

Hydroflyht 5 seater

picture

The WIG Page picture no. 173

HP-6

picture: Wingship

The WIG Page picture no. 82

Ivolga

picture:

The WIG Page picture no. 123

SM-5

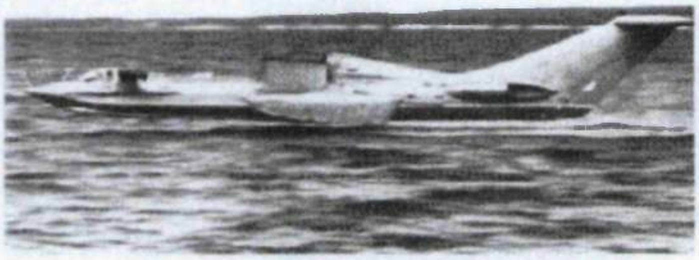

picture: A. Belyaev

The WIG Page picture no. 124

SM-6

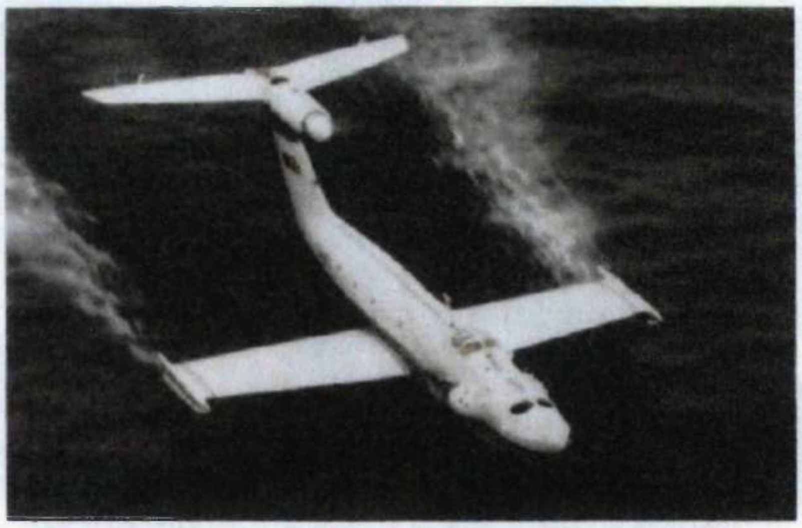

picture: A. Belyaev

The WIG Page picture no. 185

X-112

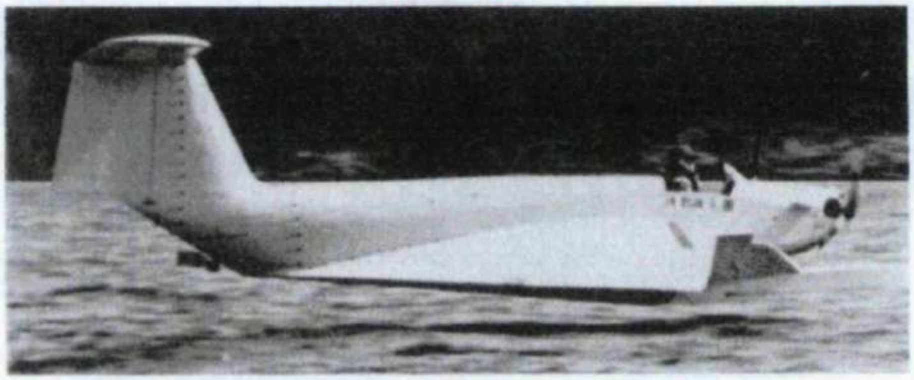

picture:

The WIG Page picture no. 190

X-113

picture:

The WIG Page picture no. 160

VT-01

picture: Techno Trans

The WIG Page picture no. 165

VVA-14

picture: Avico Press

The WIG Page picture no. 152

TY-1

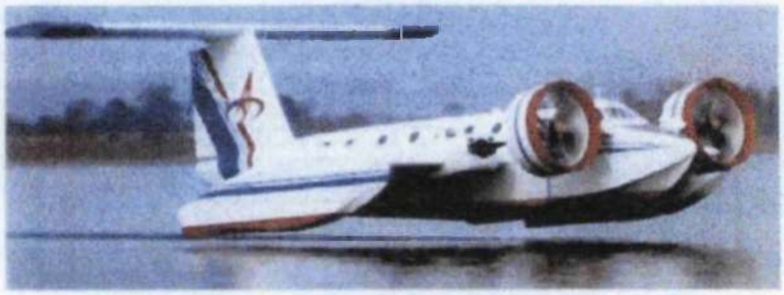

picture:

The WIG Page picture no. 154

Unknown

picture:

The WIG Page picture no. 139

Swan

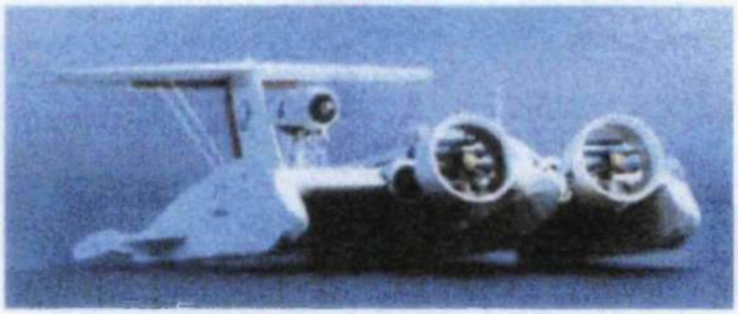

picture: Yun Liang

The WIG Page picture no. 146

TAF VIII-3 Jörg VI

picture: G. Jorg

The WIG Page picture no. 243

SM-9

picture: A. Belyaev

The WIG Page picture no. 118

SM-10

picture: A. Belyaev

The WIG Page picture no. 204

XTW-2

picture: CSSRC

The WIG Page picture no. 47

XTW-3

picture: CSSRC

The WIG Page picture no. 121

SM-3

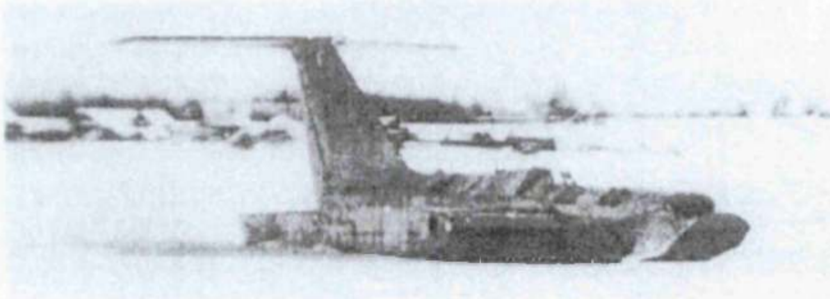

picture: A. Belyaev

The WIG Page picture no. 122

SM-4

picture: A. Belyaev

The WIG Page picture no. 117

SM-1

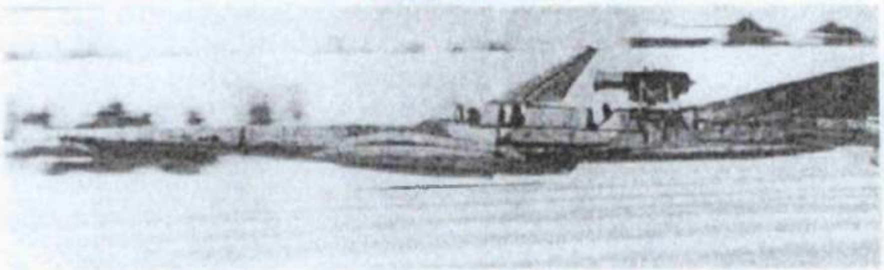

picture: A. Belyaev

The WIG Page picture no. 119

SM-2

picture: A. Belyaev

The WIG Page picture no. 129

Spasatel

picture: G. Theophile

The WIG Page picture no. 308

Pelican 6

picture: Orion Technologies

The WIG Page picture no. 109

NVA-30P

picture:

The WIG Page picture no. 112

PSI-575

picture:

APPENDIX B

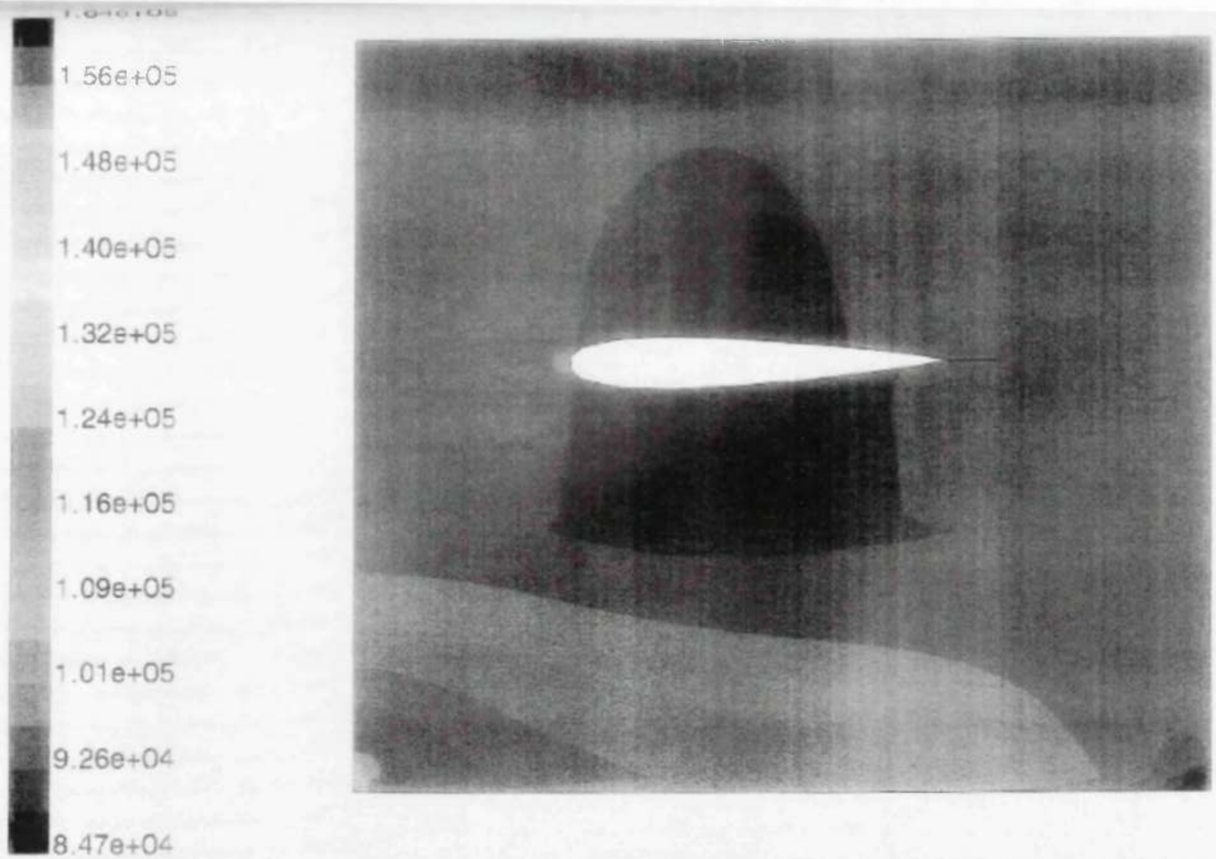

Contours of Static Pressure (pascal) (Time=6.1817e-01) Apr 25, 2000
FLUENT 5.0 (2d, segregated, RSM, unsteady)

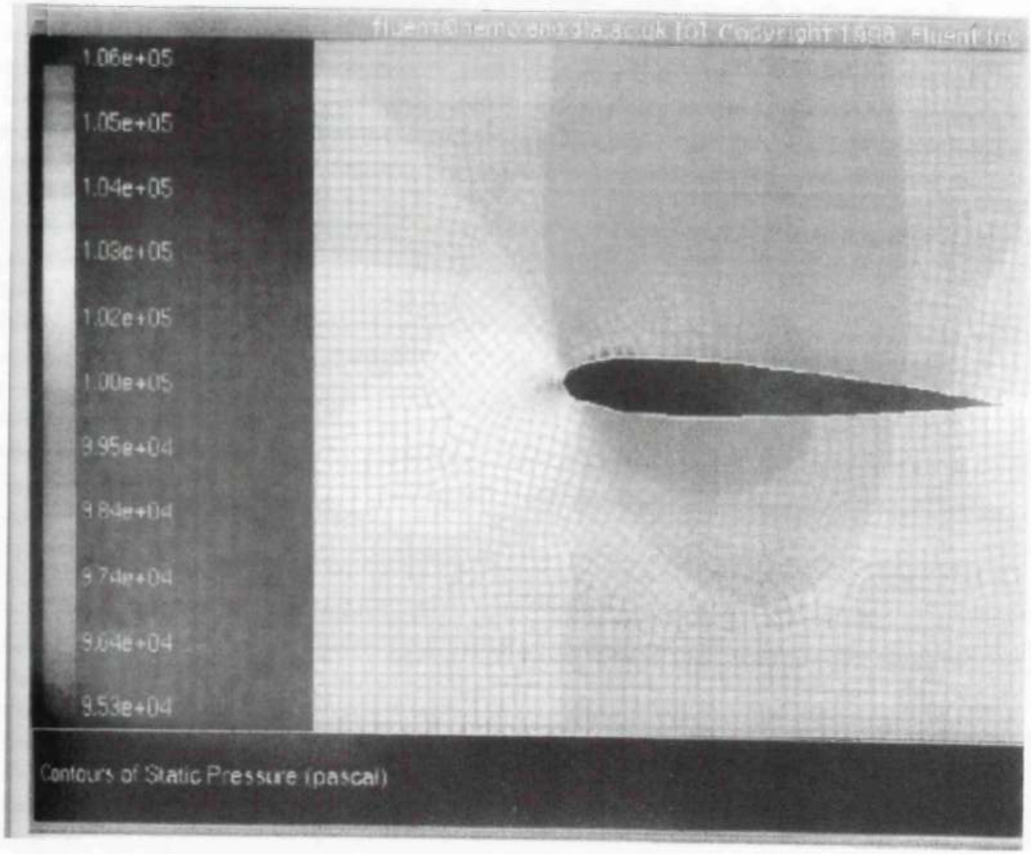
Copyright 1998, Fluent Inc
1.06e+05
1.05e+05
1.04e+05
1.03e+05
1.02e+05
1.00e+05
9.95e+04
9.84e+04
9.74e+04
9.64e+04
9.53e+04
Contours of Static Pressure (pascal)

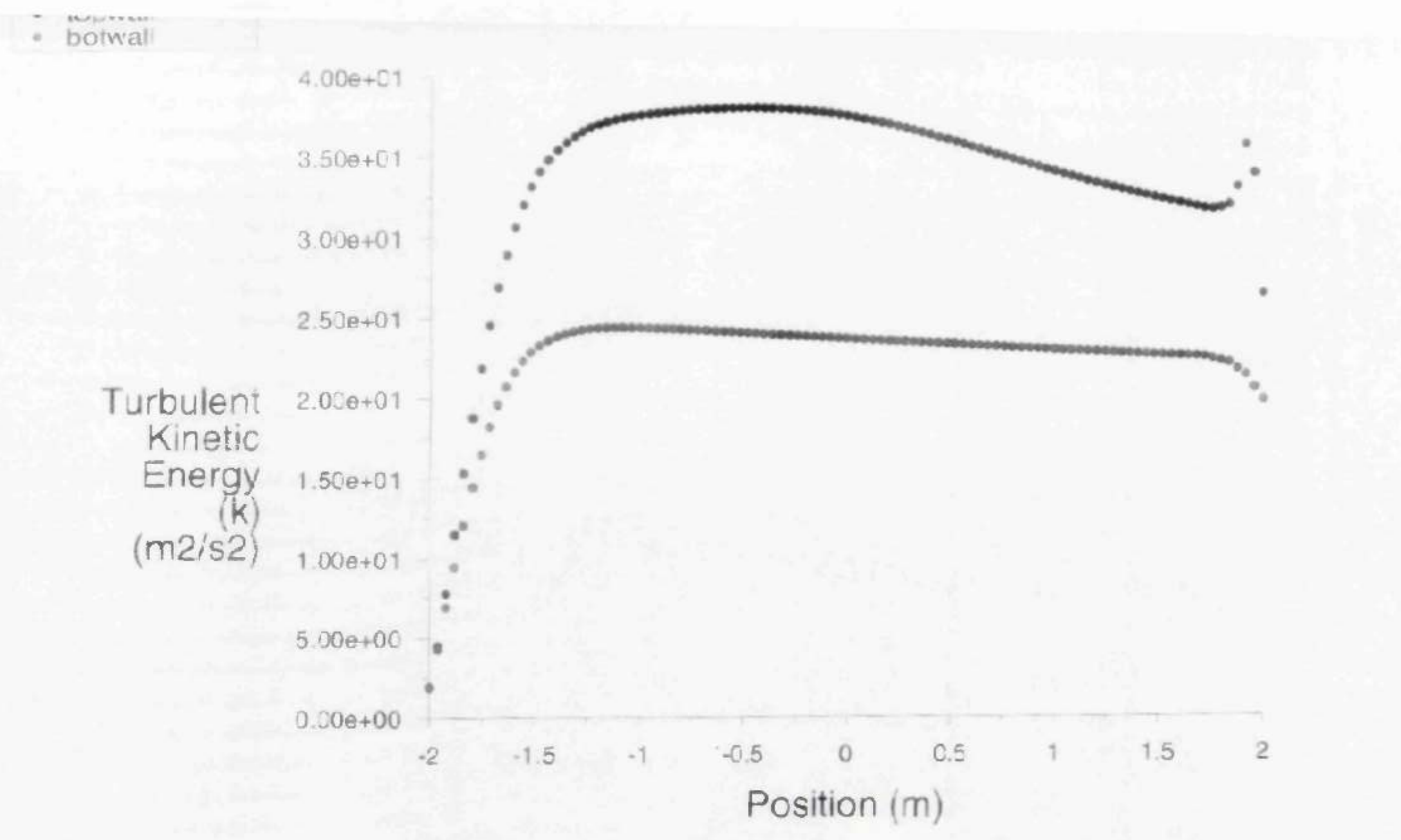

Turbulent Kinetic Energy (k) (Time=6.1817e-01) Apr 25, 2000
FLUENT 5.0 (2d, segregated, RSM, unsteady)

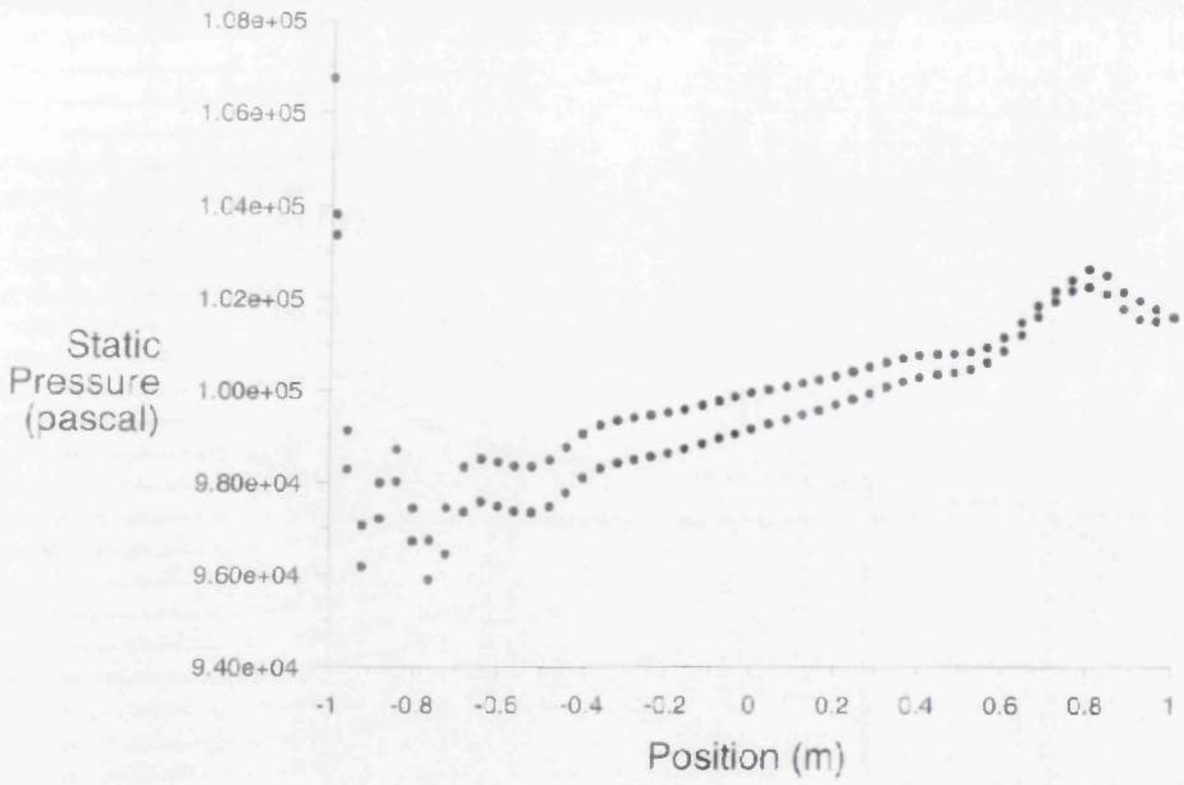

Static Pressure (Time=6.1817e-01)

Apr 25, 2000
FLUENT 5.0 (2d, segregated, RSM, unsteady)

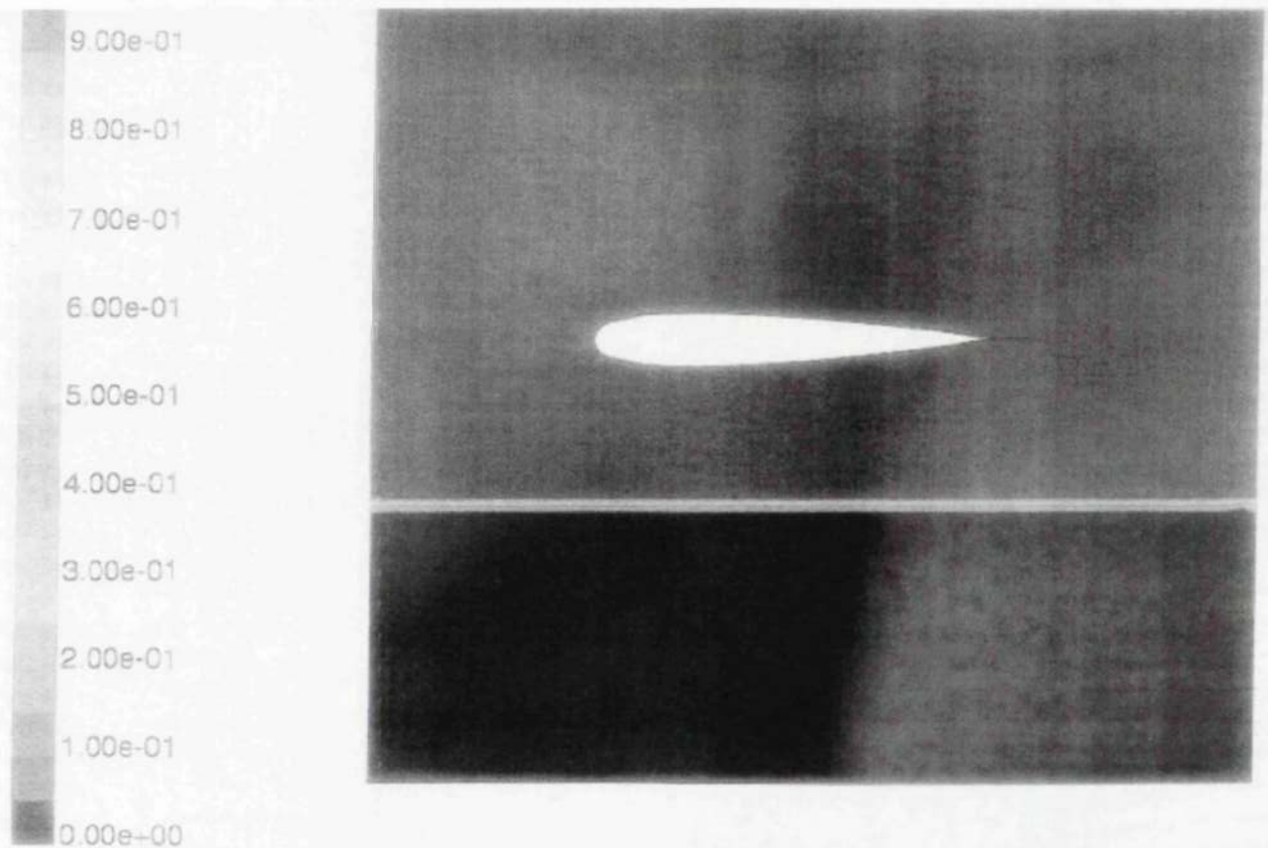

Contours of Volume fraction of air (Time=6.1817e-01) Apr 25, 2000
FLUENT 5.0 (2d, segregated, RSM, unsteady)

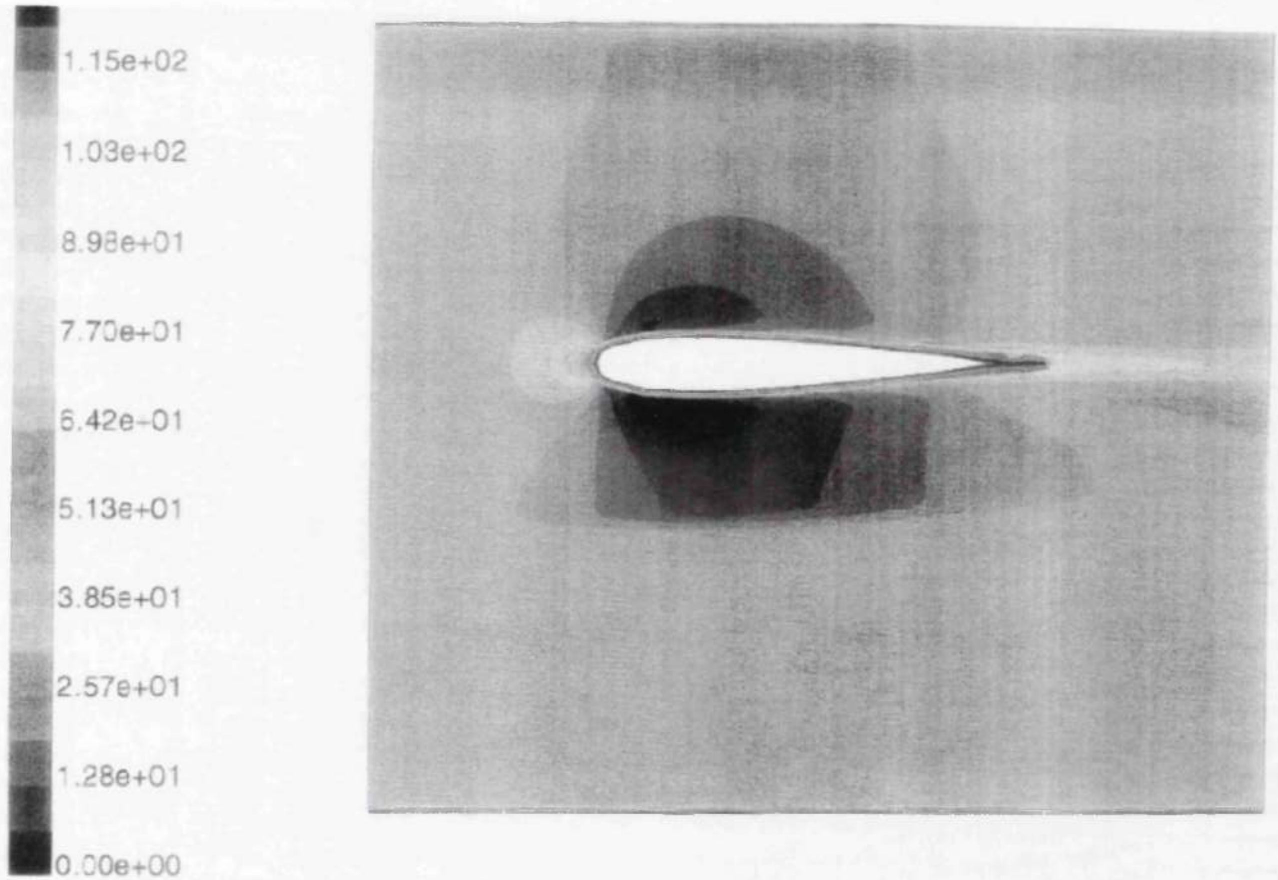

Contours of Velocity Magnitude (m/s) (Time=6.1817e-01) Apr 25, 2000
FLUENT 5.0 (2d, segregated, RSM, unsteady)

APPENDIX C

POTENTIAL FLOW ON GROUND EFFECT BY IMAGE METHOD.

APPENDIX C
SECTION A

STREAM FUNCTION WITHOUT WAKE

```
In[12]:= s = .2
Out[12]= 0.2

In[38]:= ComplexExpand[Exp[I q]]
Out[38]= Cos[q] + i Sin[q]
```

```
NSolve[
 u (1 + s (1 / Abs[z - c] - 1 / Abs[z + c] + 1 / Abs[z - c + 2 h I] - 1 / Abs[z + c + 2 h I])) == c - 1,
 {x, y}]
NSolve[D[(u z - u s (Log[z - c] - Log[z + c] + Log[z - c + 2 h I] - Log[z + c + 2 h I])), x] == 0,
 {x, y}]
NSolve[D[(u z - u s (Log[z - c] - Log[z + c] + Log[z - c + 2 h I] - Log[z + c + 2 h I])), y] == 0,
 {x, y}]
```

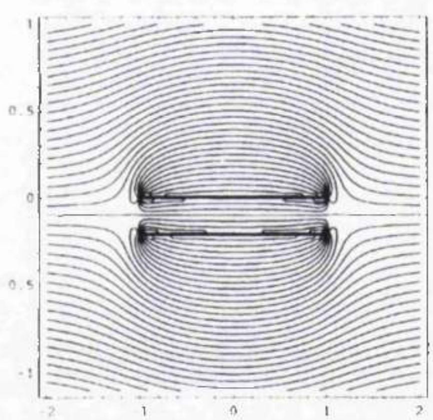

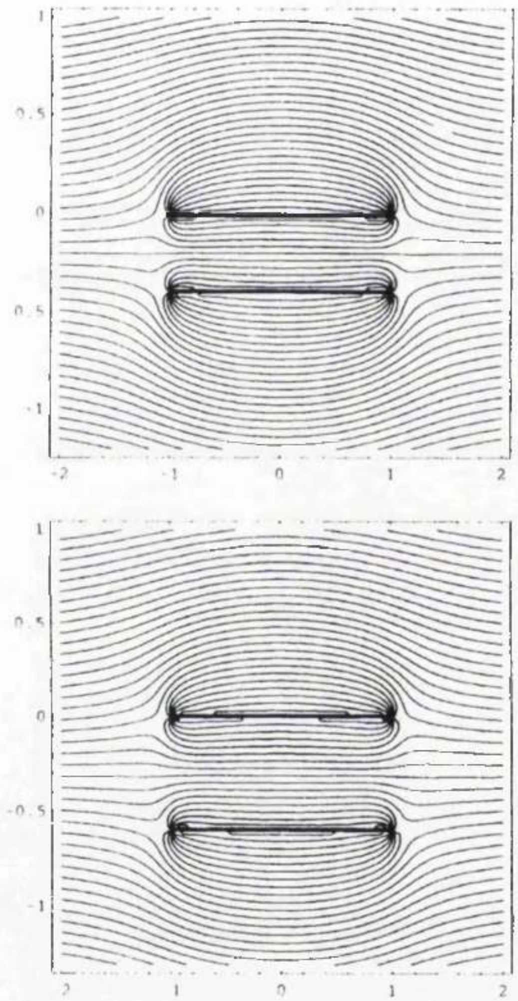
1
0.5
0
-0.5
-1
-2
-1
0
1
2
1
0.5
0
-0.5
-1
2
1
0
1
2

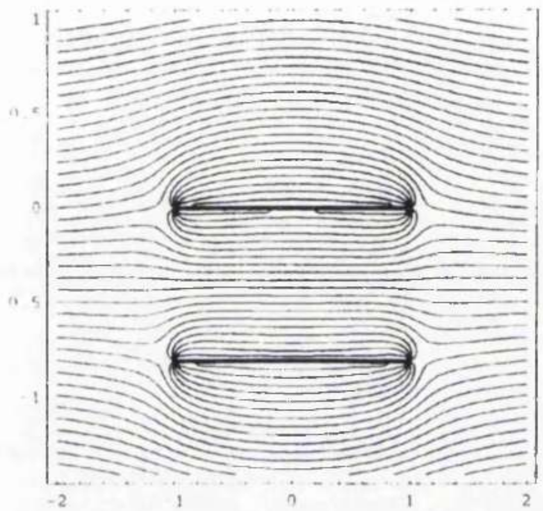

1
0.5
0
-0.5
-1
-2
-1
0
1
2

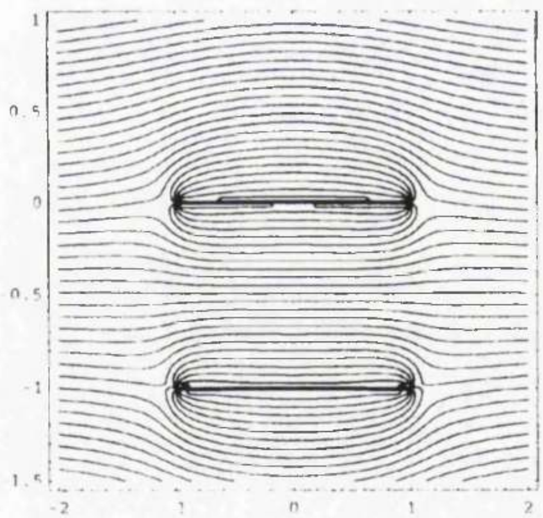

1
0.5
0
-0.5
-1
-1.5
-2
-1
0
1
2

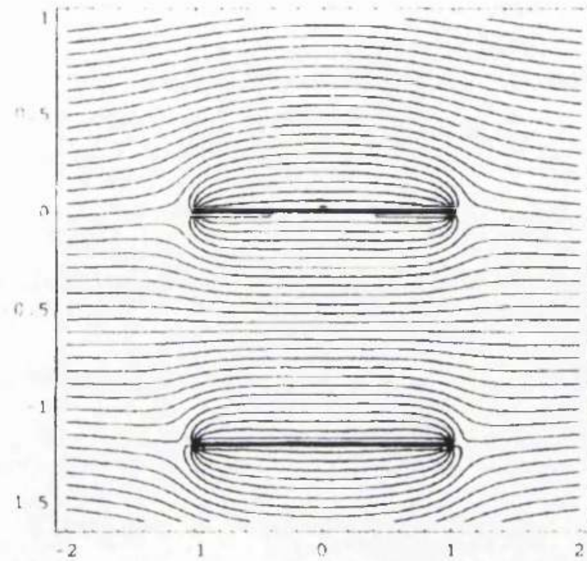
1
0.5
0
-0.5
-1
-1.5
-2
-1
0
1
2

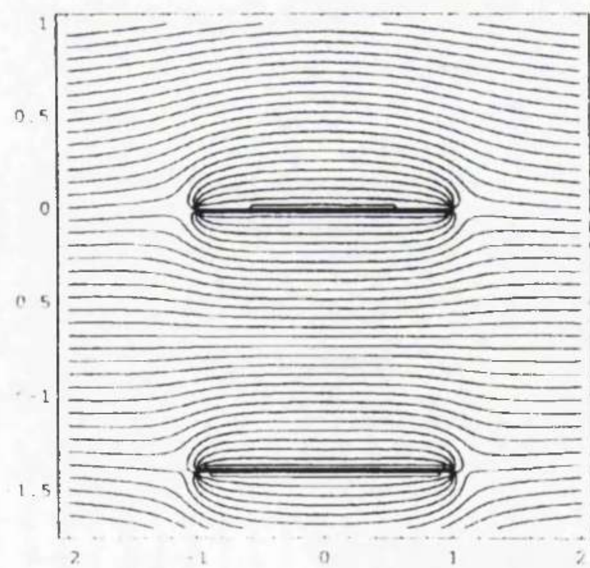
1
0.5
0
-0.5
-1
-1.5
-2
-1
0
1
2

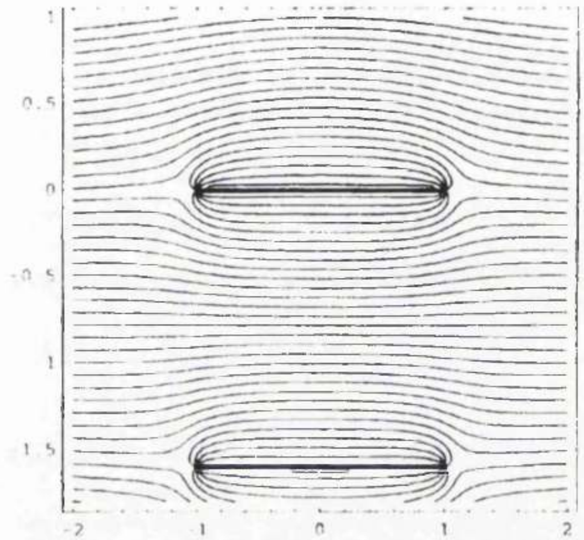
1
0.5
0
-0.5
1
-1.5
-2
-1
0
1
2

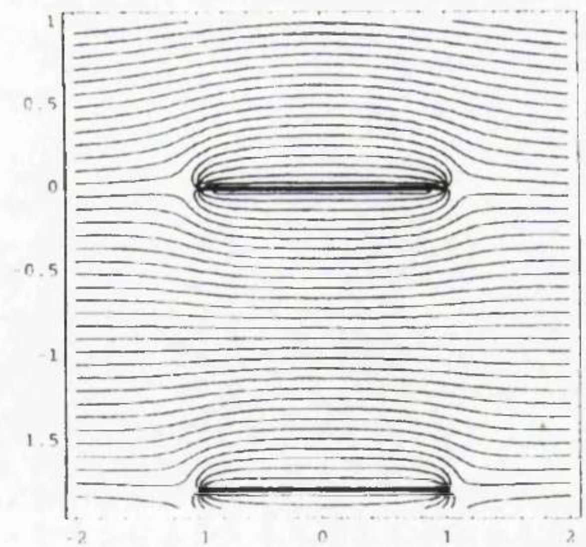
1
0.5
0
-0.5
-1
1.5
-2
1
0
1
2

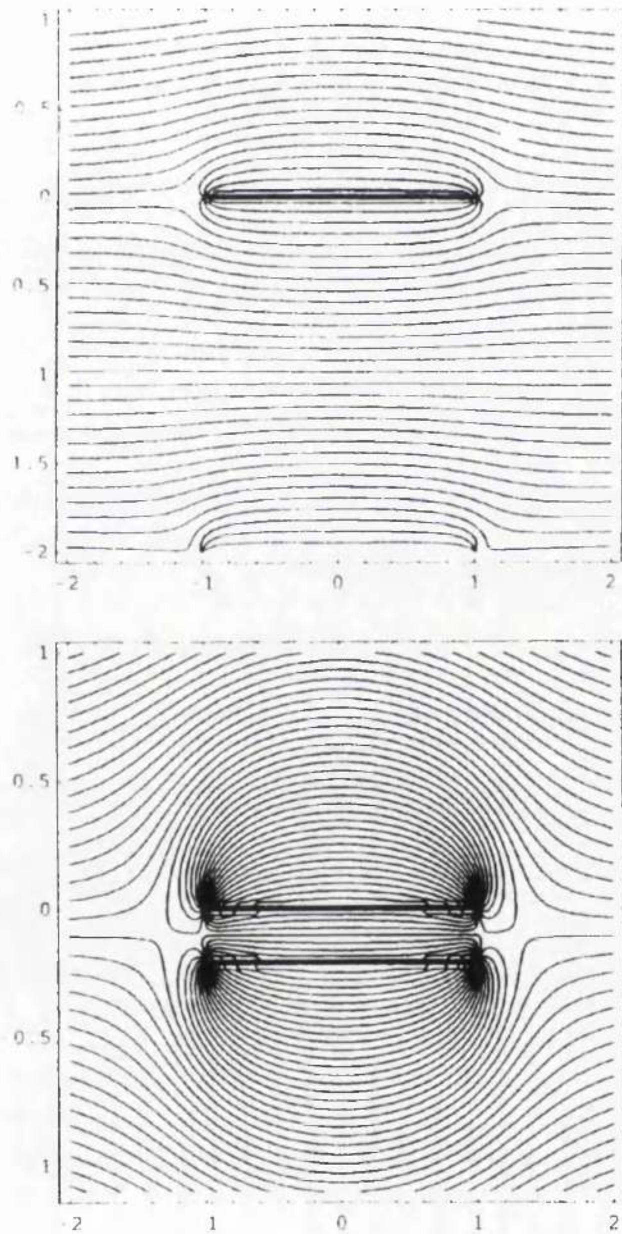

1
0.5
0
0.5
1
1.5
-2
-2
-1
0
1
2
1
0.5
0
0.5
1
2
1
0
1
2

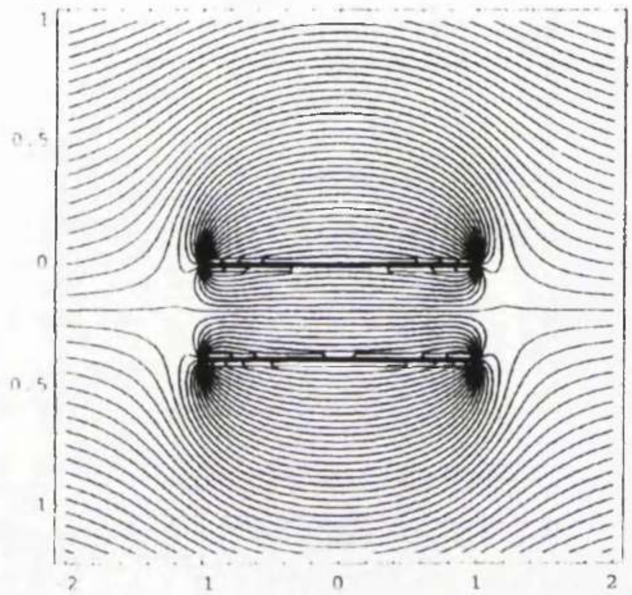
1
0.5
0
0.5
1
2
1
0
1
2

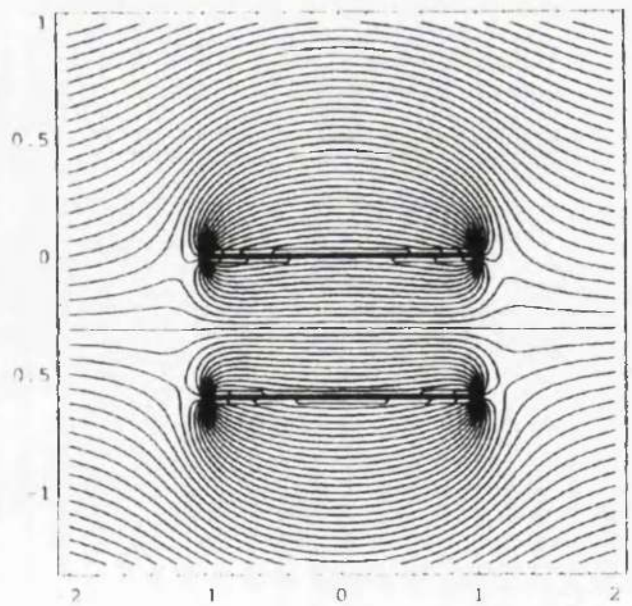
1
0.5
0
0.5
-1
2
1
0
1
2

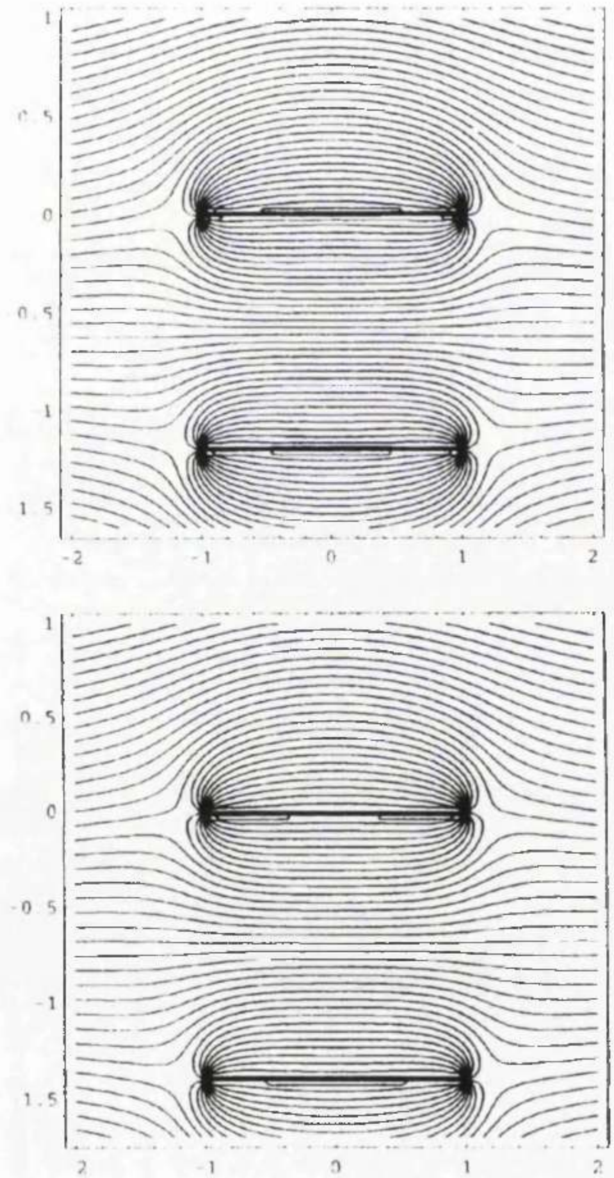
1
0.5
0
-0.5
-1
-1.5
-2
-1
0
1
2

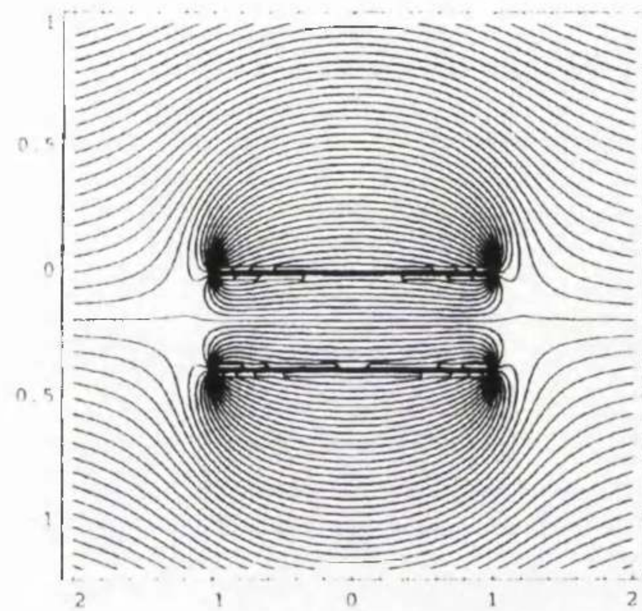

1
0.5
0
-0.5
-1
-2
-1
0
1
2

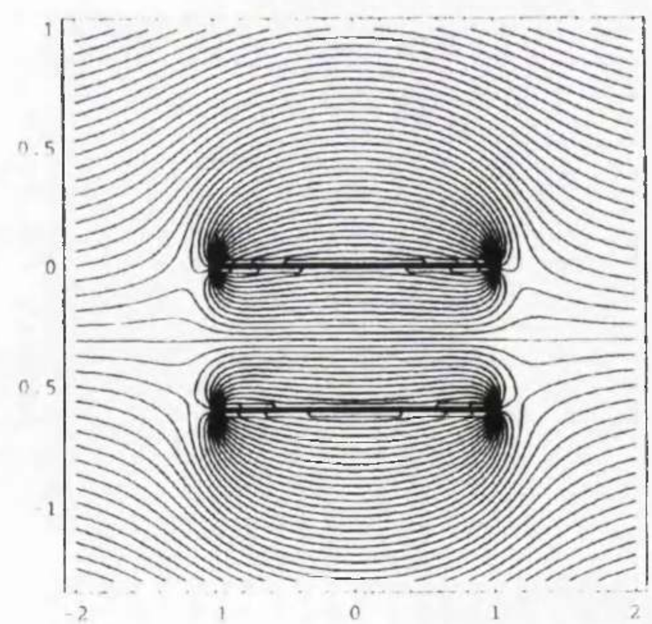

1
0.5
0
-0.5
-1
-2
-1
0
1
2

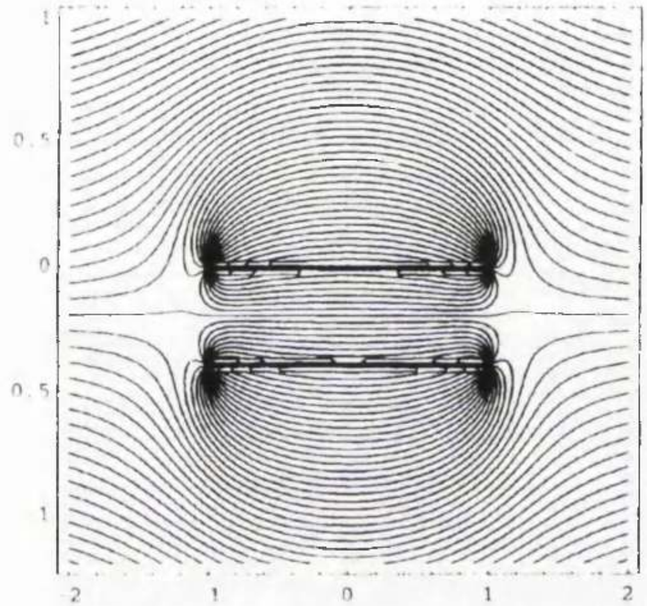
1
0.5
0
0.5
1
2
1
0
1
2

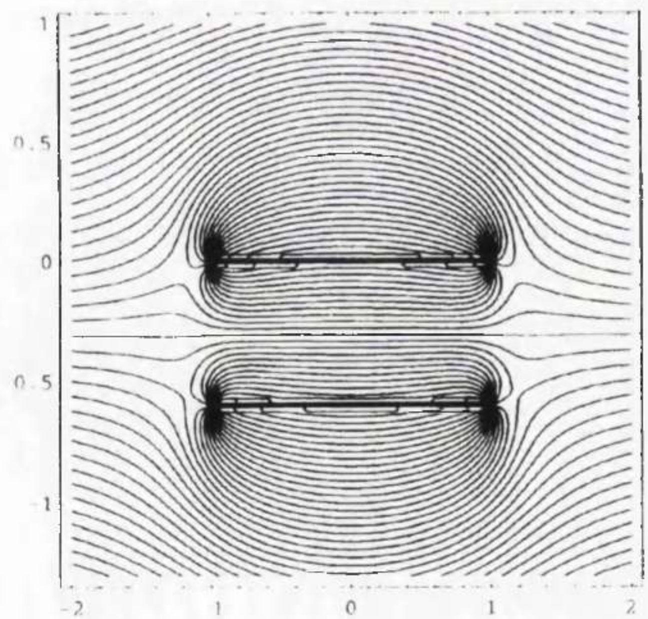
1
0.5
0
0.5
-1
-2
1
0
1
2

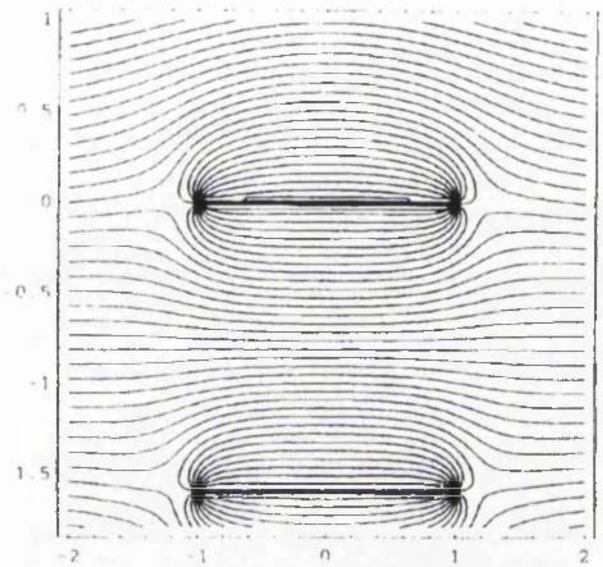
1
0.5
0
-0.5
-1
-1.5
-2
-1
0
1
2

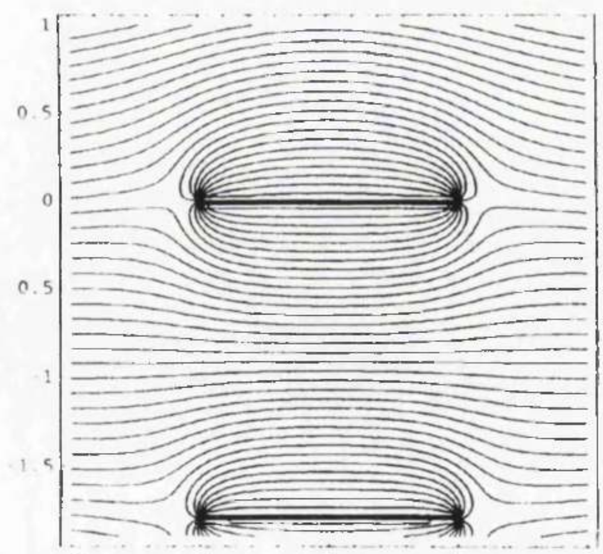
1
0.5
0
-0.5
-1
-1.5
-2
-1
0
1
2

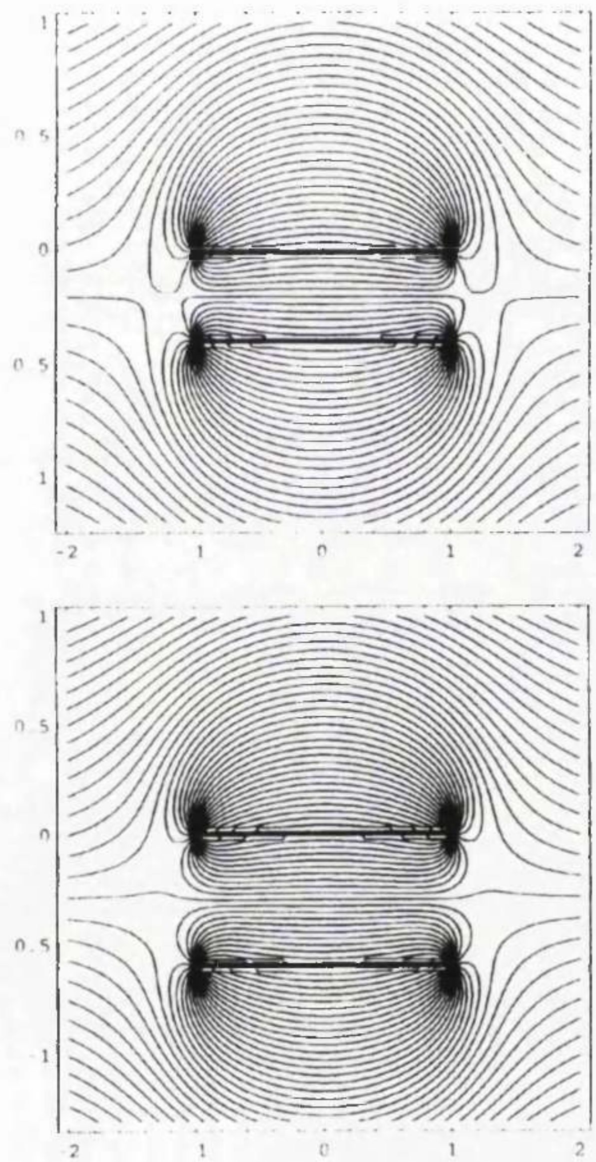
1
0.5
0
-0.5
-1
-2
-1
0
1
2
1
0.5
0
-0.5
-1
-2
-1
0
1
2

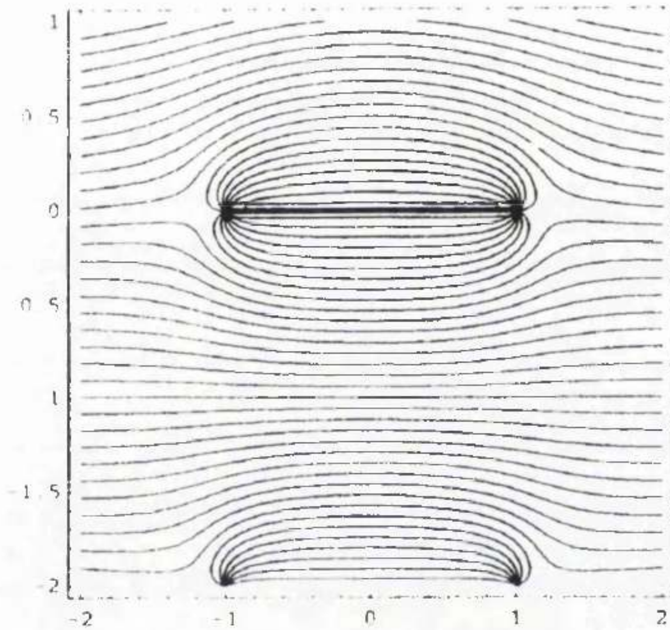
1
0.5
0
-0.5
-1
-1.5
-2
-2
-1
0
1
2

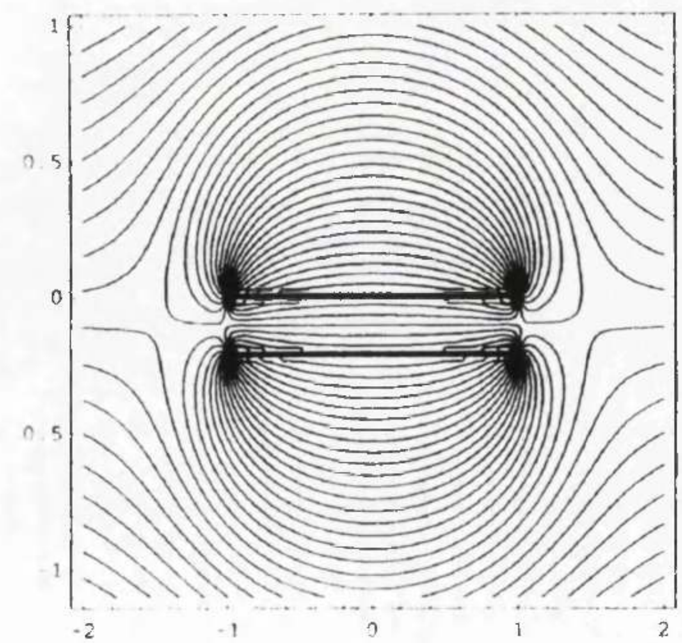
1
0.5
0
-0.5
-1
-2
-1
0
1
2

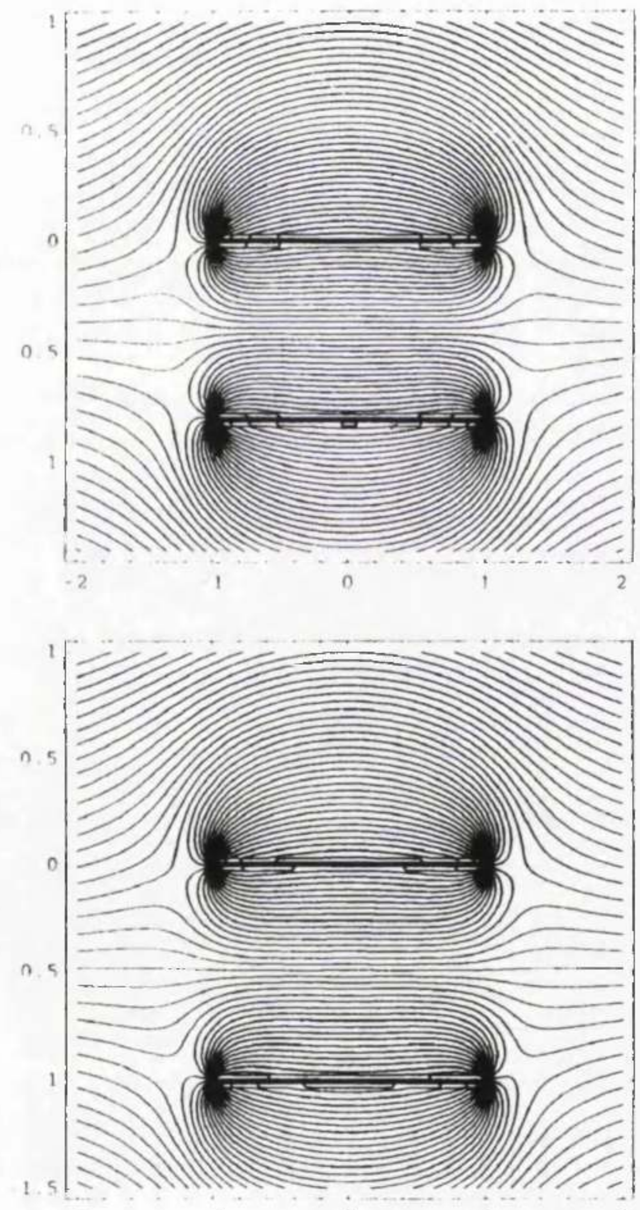

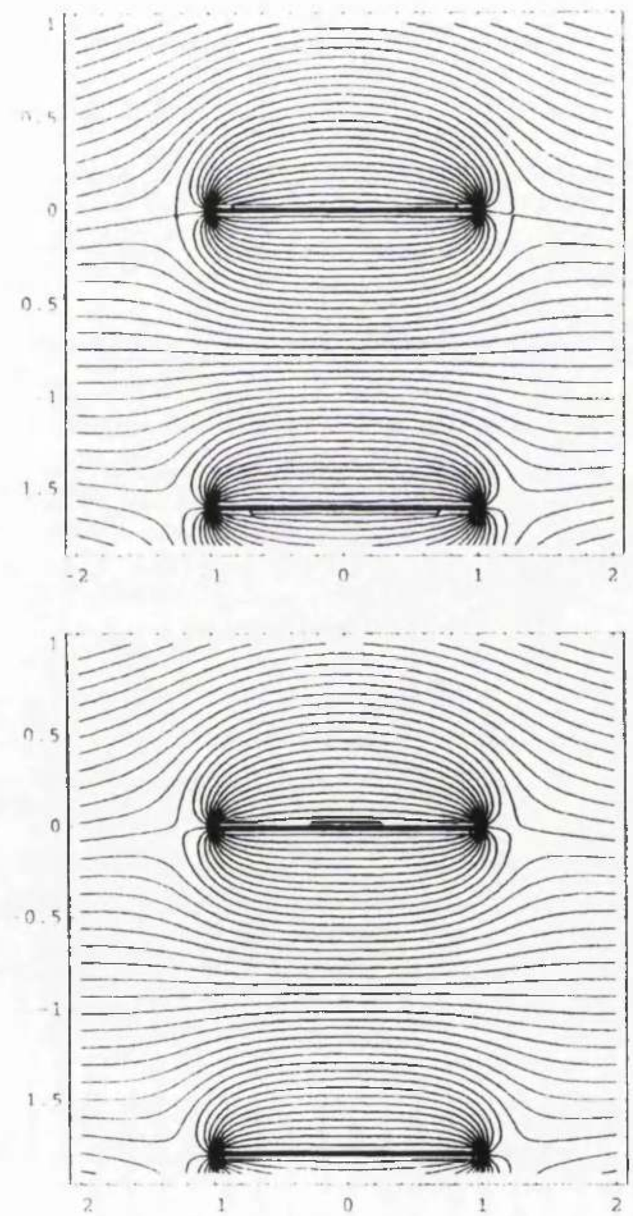

1
0.5
0
0.5
-1
1.5
-2
-1
0
1
2
1
0.5
0
-0.5
-1
1.5
2
1
0
1
2

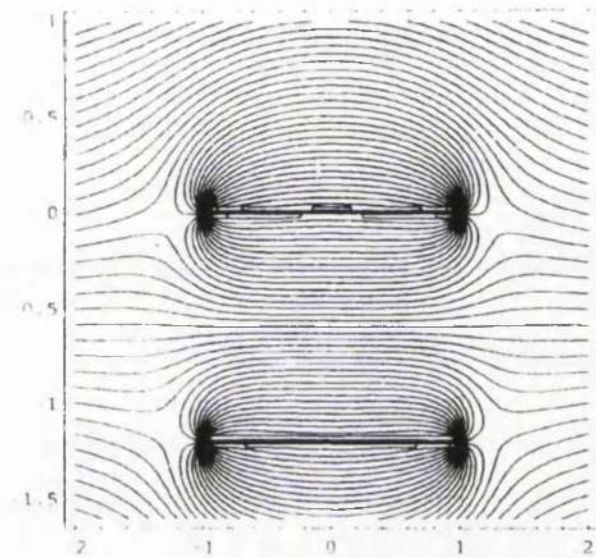

1
0.5
0
-0.5
-1
-1.5
-2
-1
0
1
2

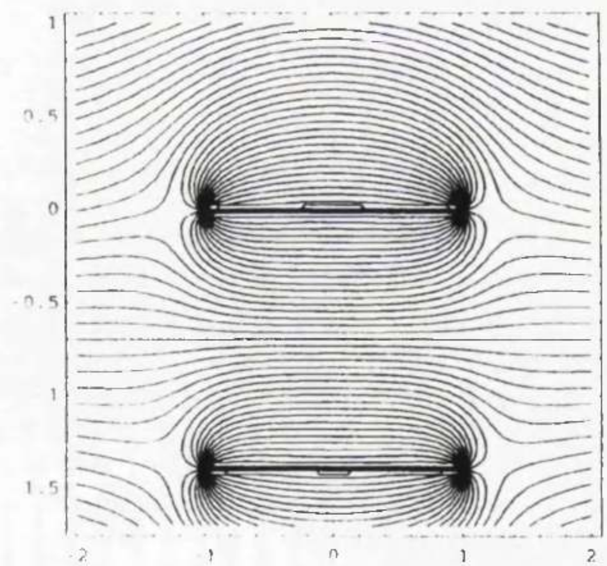

1
0.5
0
-0.5
-1
-1.5
-2
-1
0
1
2

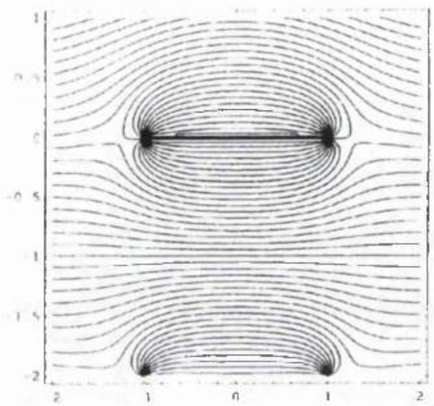

In[55]:=

```
Unset[h]
Unset[u]
Unset[s]
```

In[59]:=

```
u = 100
```

Out[59]= 100

In[60]:=

```
Do[Do[
  Plot3D[Im[Residue[
      (D[(u z - u s (Log[z - c] - Log[z + c] + Log[z - c + 2 h I] - Log[z + c + 2 h I])), x])^2
      , {r, c}]], {h, 0.1, 1}, {s, 0.1, 0.3}]
   Plot3D[Re[Residue[
      (D[(u z - u s (Log[z - c] - Log[z + c] + Log[z - c + 2 h I] - Log[z + c + 2 h I])), x])^2
      , {r, c}]], {h, 0.1, 1}, {s, 0.1, 0.3}], {h, 0.1, 1, 0.1}], {s, 0.1, 0.3, 0.1}]
```

APPENDIX C
SECTION B

SOURCE FUNCTION WITH WAKE

```
In[61]:= Do[Do[Do[ContourPlot[
        Im[u z - u s (Log[z - c] - 0.9 Log[z + c] + Log[z - c + 2 h I] - 0.9 Log[z + c + 2 h I])],
        {x, -2 c, 2 c}, {y, -h - c, c}, Contours → 41,
        PlotPoints → 120, ContourShading → False]
       Residue[(D[(u z - u s (Log[z - c] - 0.9 Log[z + c] +
               Log[z - c + 2 h I] - 0.9 Log[z + c + 2 h I])), x]) ^2
        , {z, c}], {h, 0.1, 1, 0.1}], {u, 60, 100, 80}], {s, 0.1, 0.3, 0.1}]
```

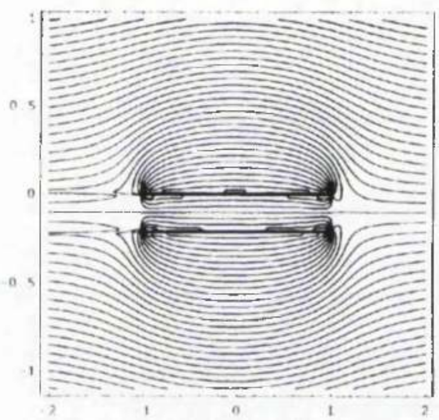

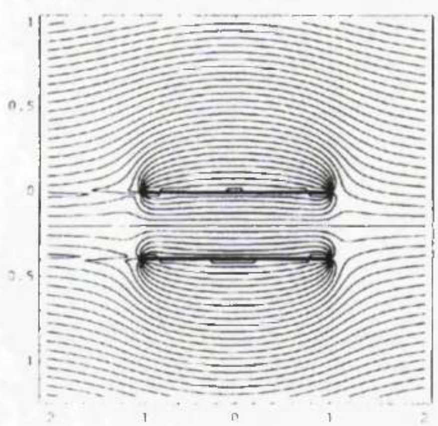

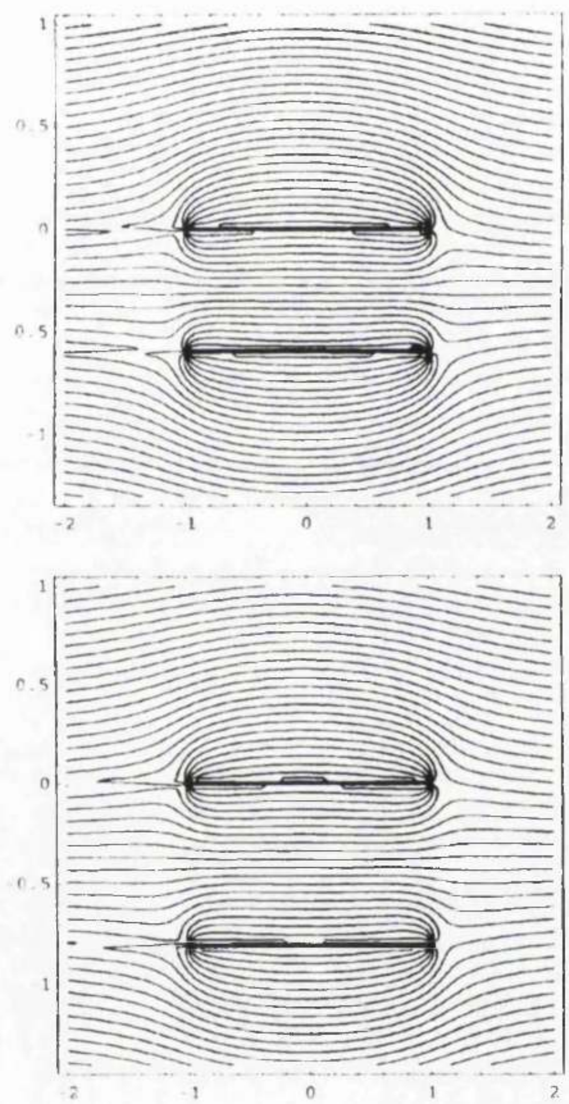
1
0.5
0
-0.5
-1
-2
-1
0
1
2
1
0.5
0
-0.5
-1
-2
-1
0
1
2

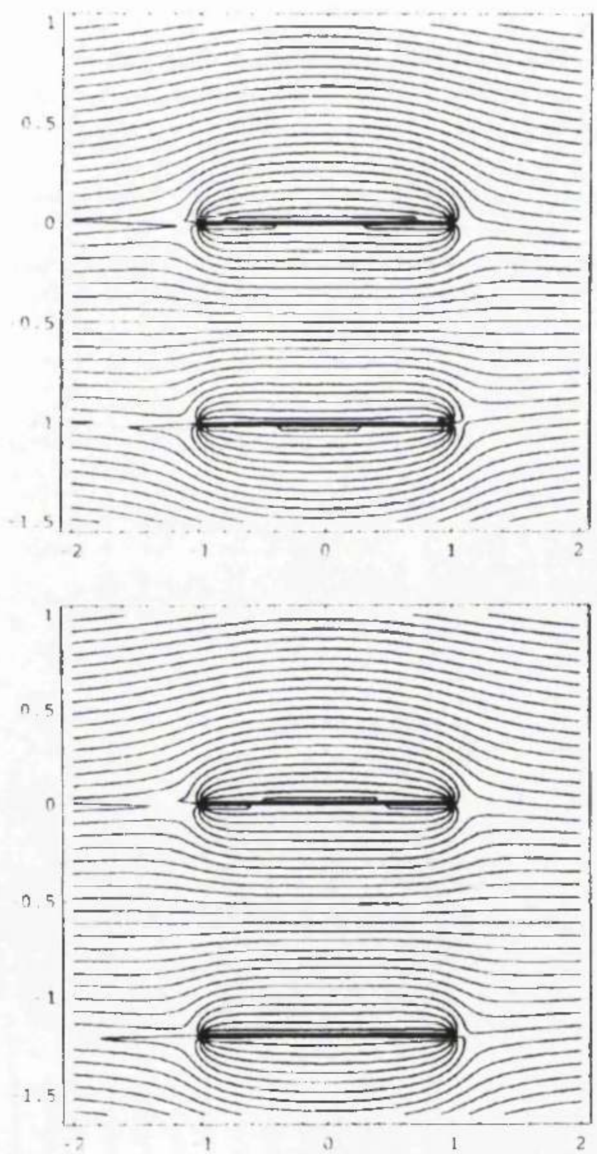
1
0.5
0
-0.5
-1
-1.5
-2
-1
0
1
2
1
0.5
0
-0.5
-1
-1.5
-2
-1
0
1
2

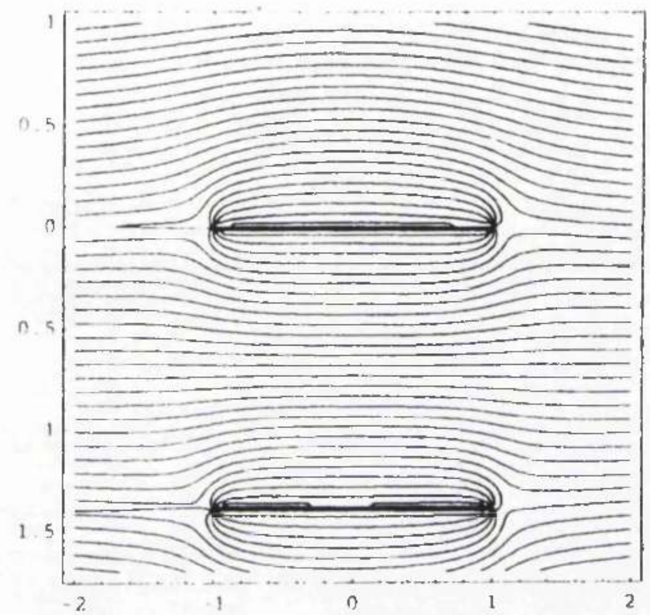
1
0.5
0
0.5
1
1.5
-2
-1
0
1
2

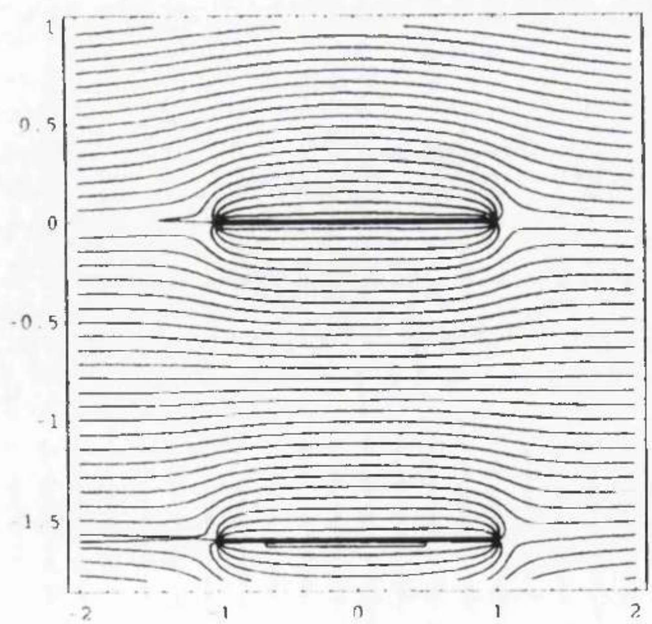
1
0.5
0
-0.5
-1
-1.5
-2
-1
0
1
2

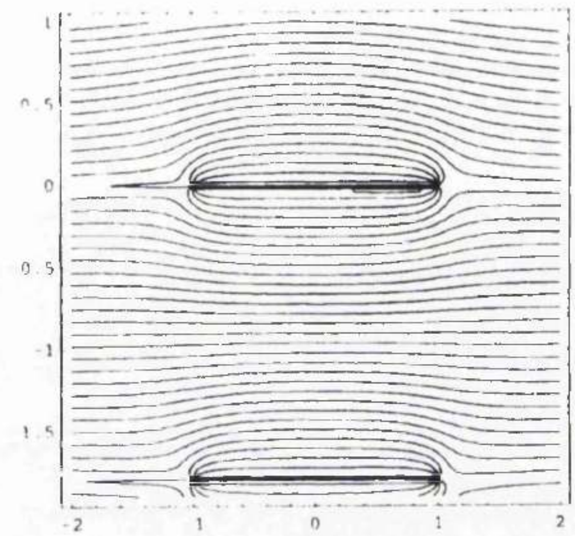

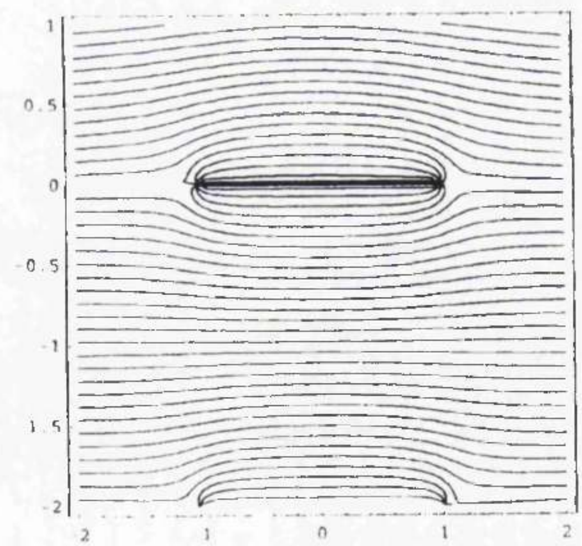

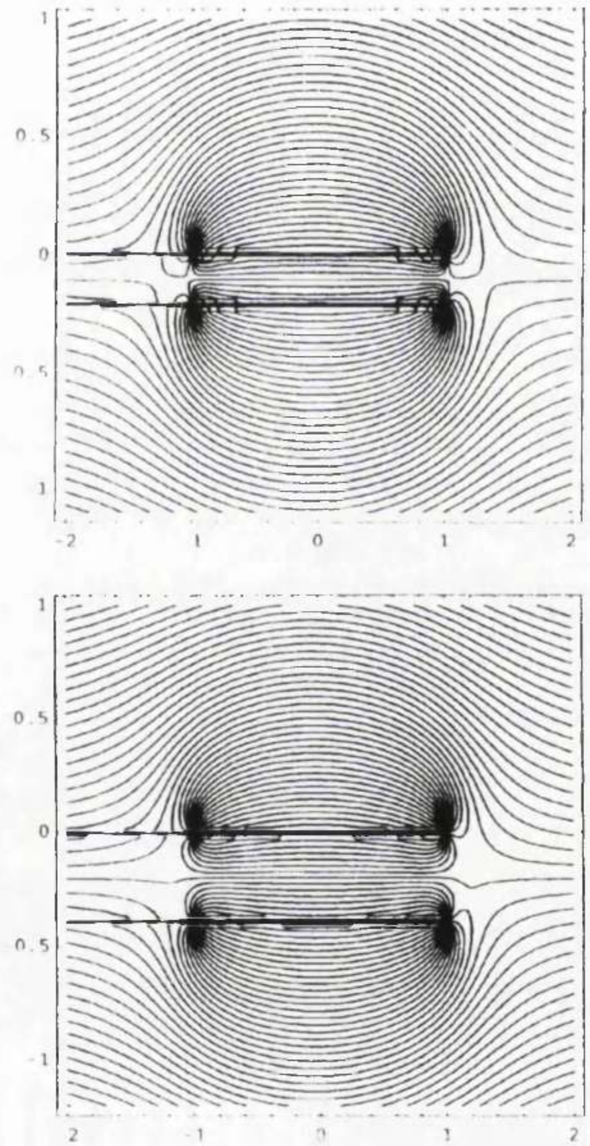

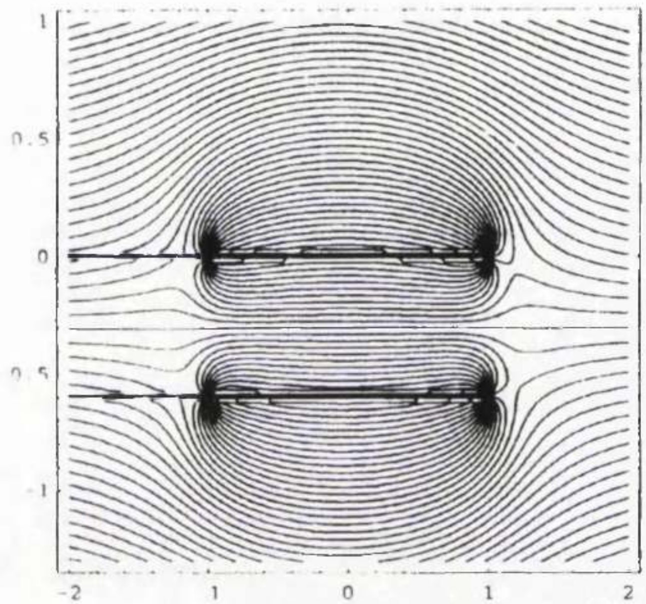

1
0.5
0
-1
-2
1
0
1
2

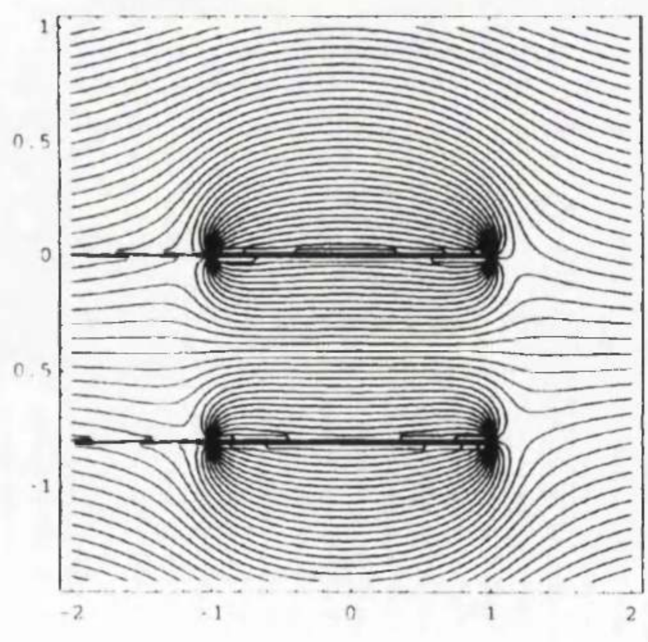

1
0.5
0
0.5
-1
-2
-1
0
1
2

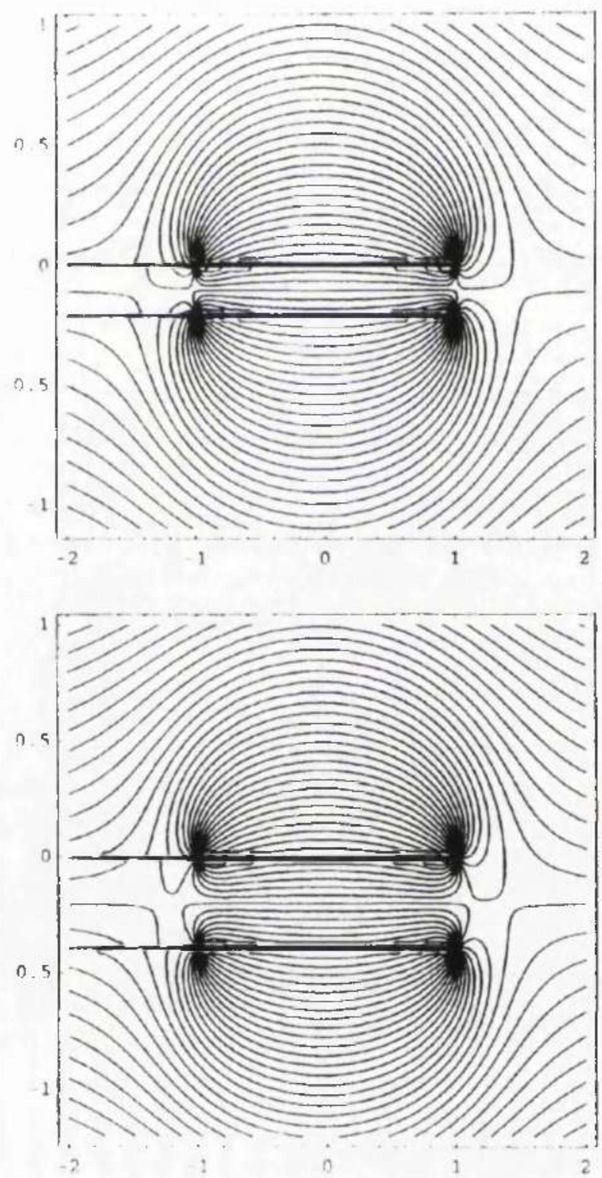
1
0.5
0
-0.5
-1
-2
-1
0
1
2
1
0.5
0
-0.5
-1
-2
-1
0
1
2

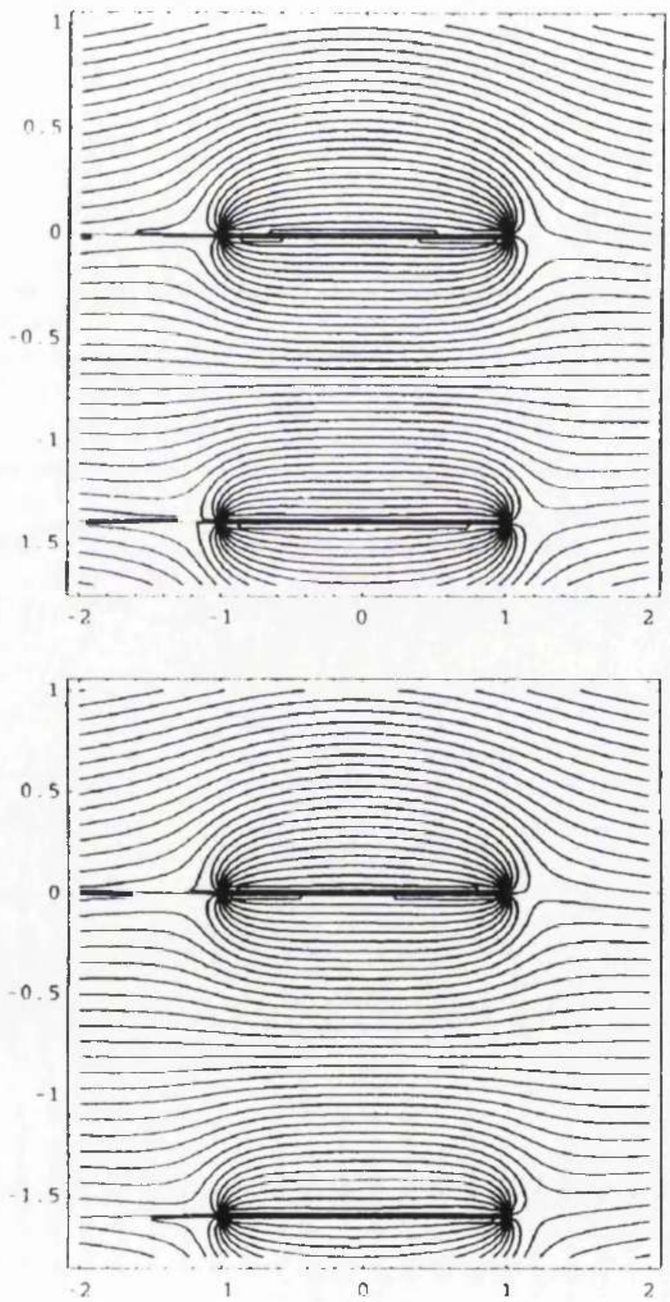

1
0.5
0
-0.5
-1
-1.5
-2
-1
0
1
2

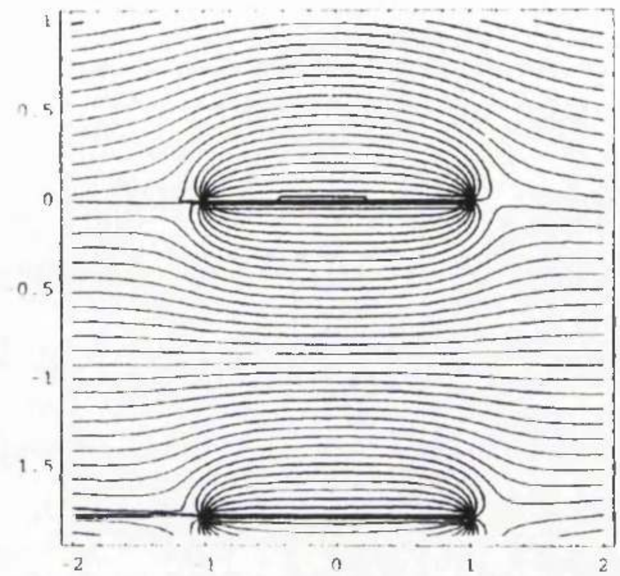

1
0.5
0
-0.5
-1
1.5
-2
-1
0
1
2

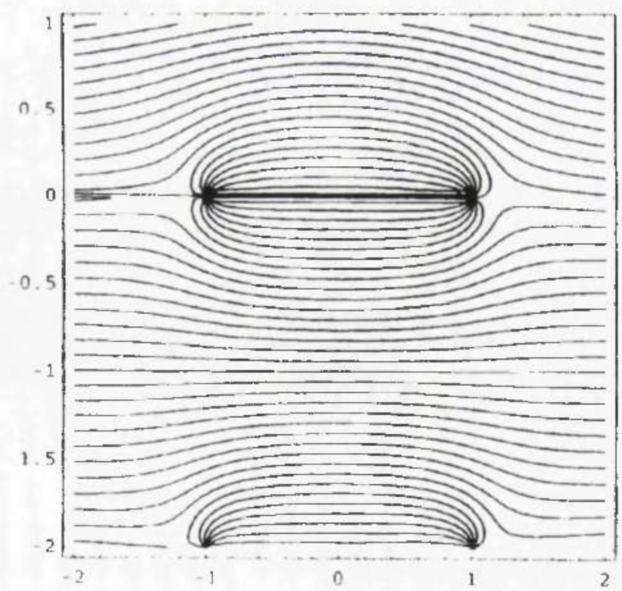

1
0.5
0
-0.5
-1
1.5
-2
-2
-1
0
1
2

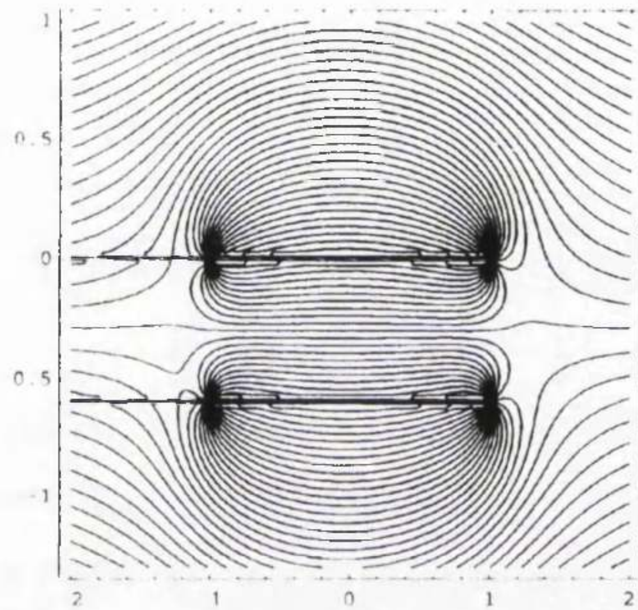
1
0.5
0
-0.5
-1
-2
-1
0
1
2

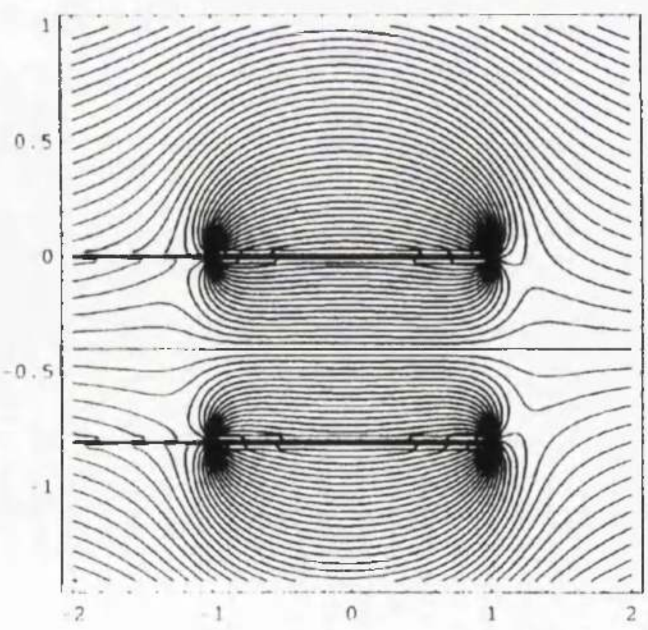
1
0.5
0
-0.5
-1
-2
-1
0
1
2

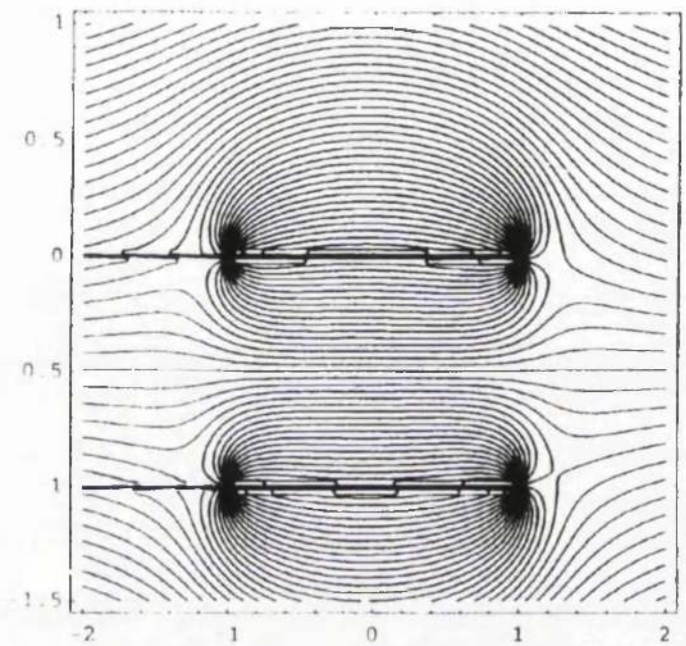

1
0.5
0
-0.5
-1
-1.5
-2
-1
0
1
2

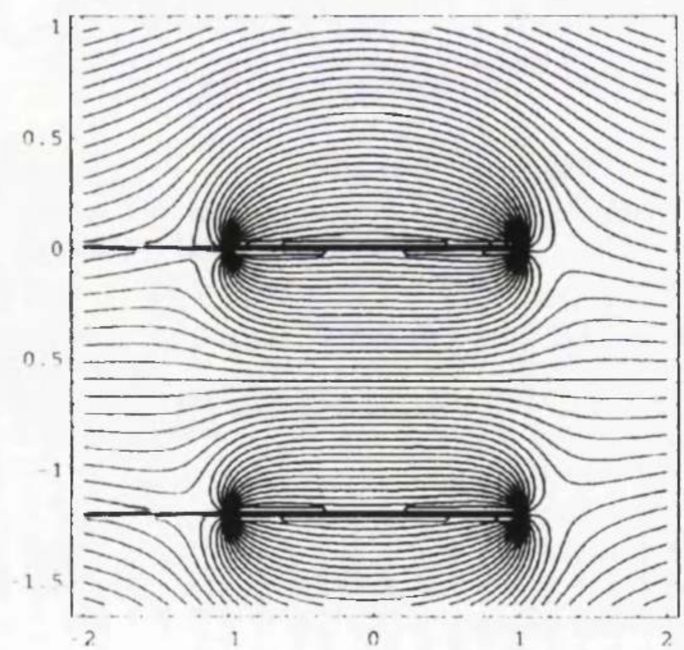

1
0.5
0
-0.5
-1
-1.5
-2
-1
0
1
2

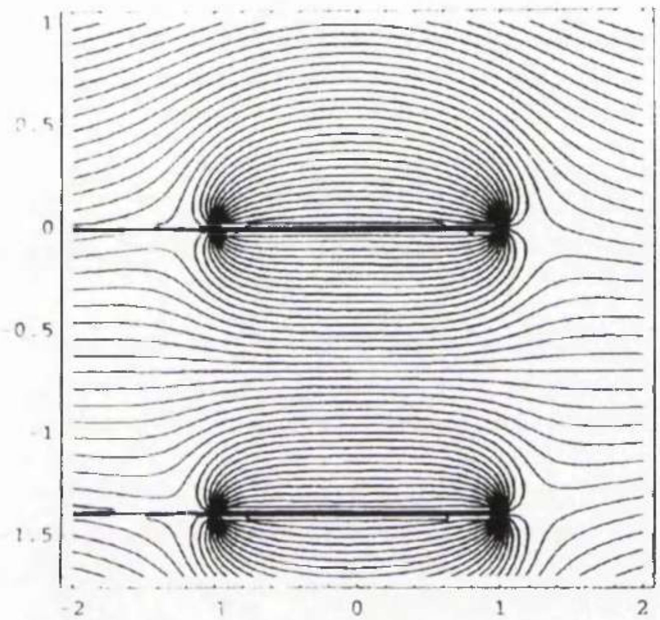
1
0.5
0
-0.5
-1
-1.5
-2
-1
0
1
2

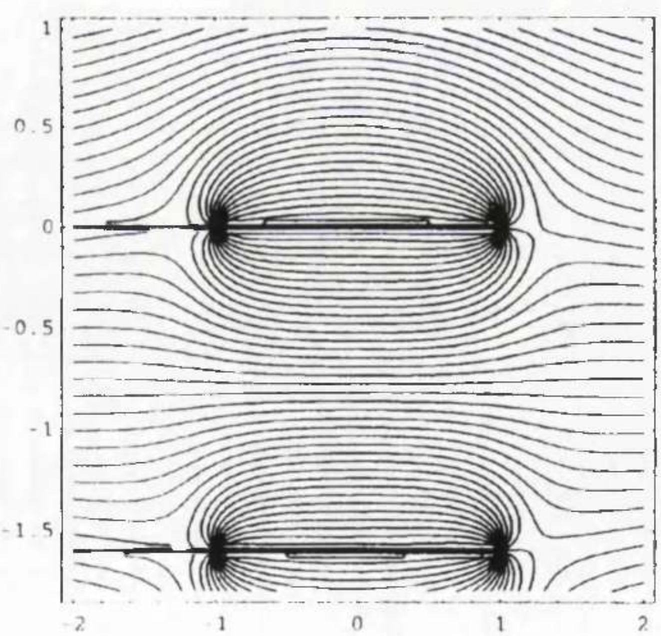
1
0.5
0
-0.5
-1
-1.5
-2
-1
0
1
2

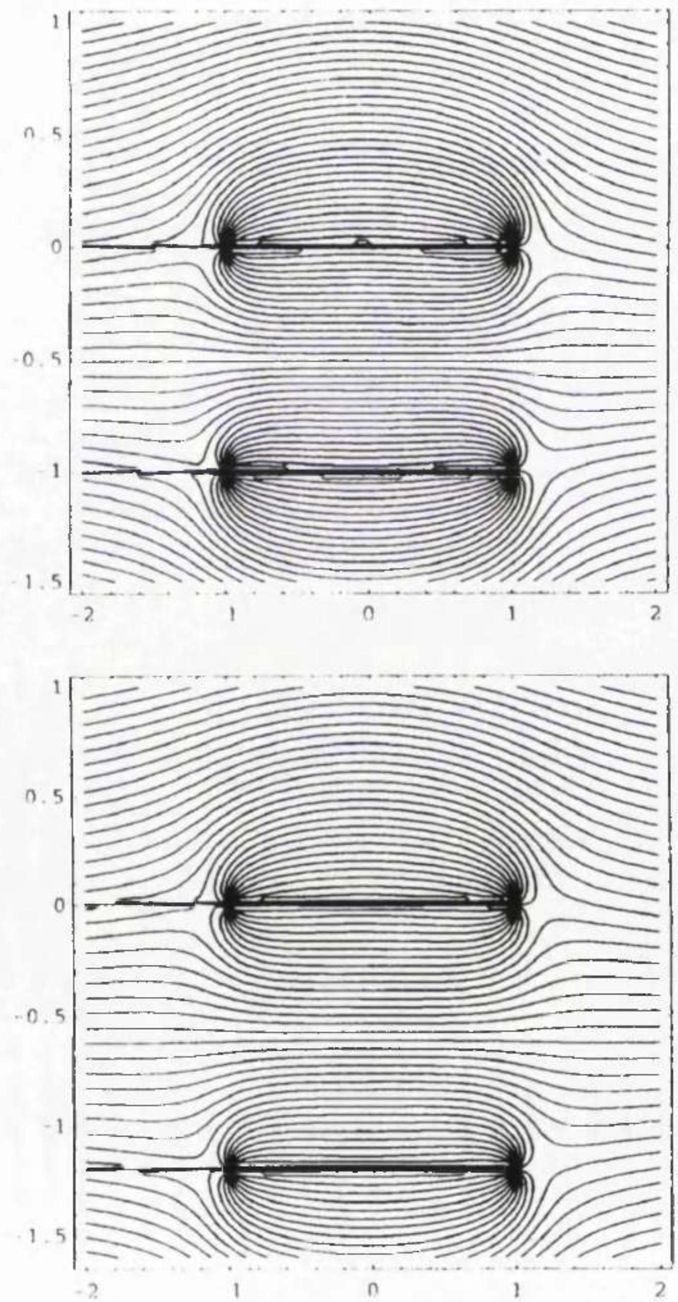

1
0.5
0
-0.5
-1
-1.5
-2
1
0
1
2
1
0.5
0
-0.5
-1
-1.5
-2
1
0
1
2

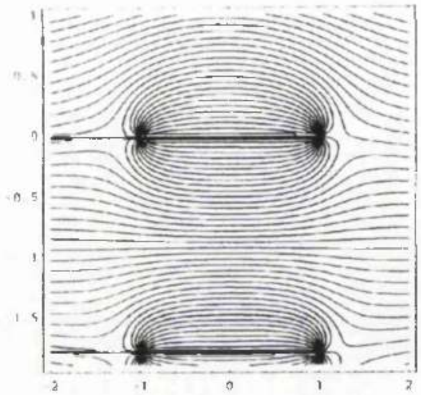

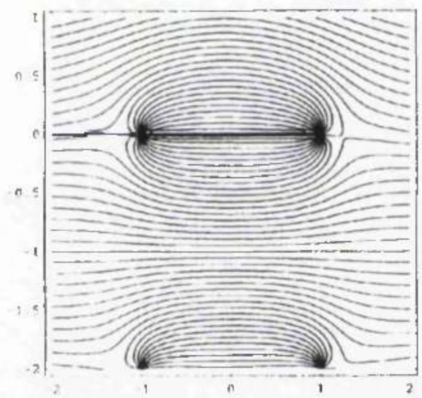

In[65]:=

```
Unset[u]
Unset[s]
Unset[h]
Residue[
 (D[(u z - u s (Log[z - c] - 0.9 Log[z + c] + Log[z - c + 2 h I] - 0.9 Log[z + c + 2 h I])), x])^
  2
 ,
 {z,
  c}]
```

Out[65]= [illegible] 128 [illegible] 384 h^3 [illegible] 384 [illegible] 128 [illegible]

64 [illegible]

[illegible] 76.8 [illegible] 96 h^3 [illegible] 166.4 [illegible] 57.6 [illegible]

APPENDIX C
SECTION C

SOURCE AND SINK WITHOUT WAKE GIVING LIFT AND DRAG

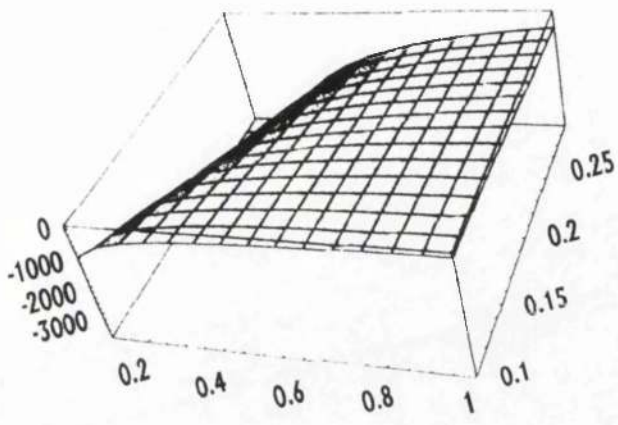
0
-1000
-2000
-3000
0.2
0.4
0.6
0.8
1
0.1
0.15
0.2
0.25

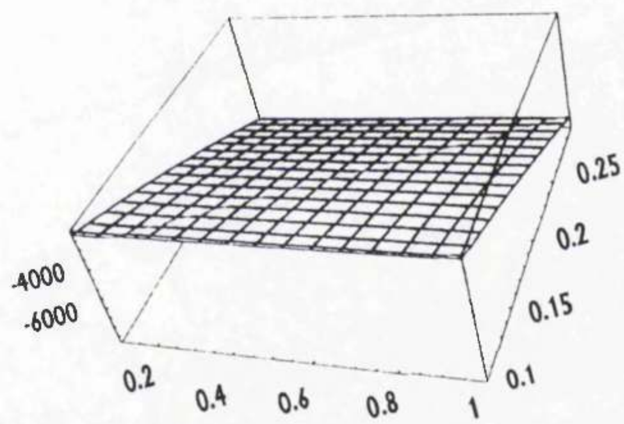
-4000
-6000
0.2
0.4
0.6
0.8
1
0.1
0.15
0.2
0.25

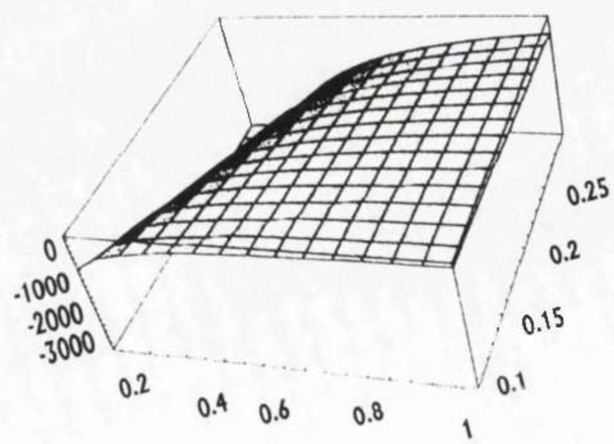
0
-1000
-2000
-3000
0.2
0.4
0.6
0.8
1
0.1
0.15
0.2
0.25

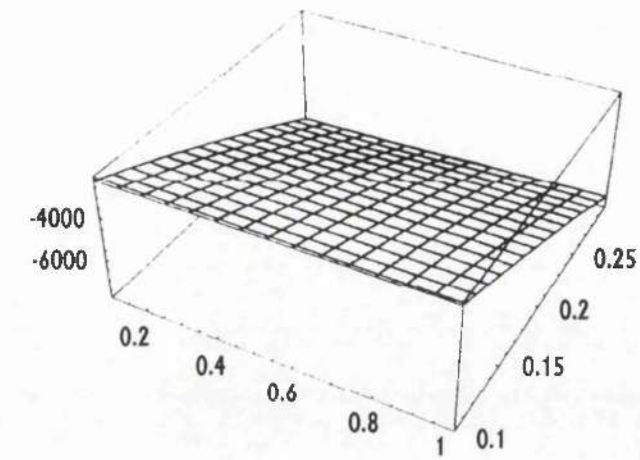
-4000
-6000
0.2
0.4
0.6
0.8
1
0.1
0.15
0.2
0.25

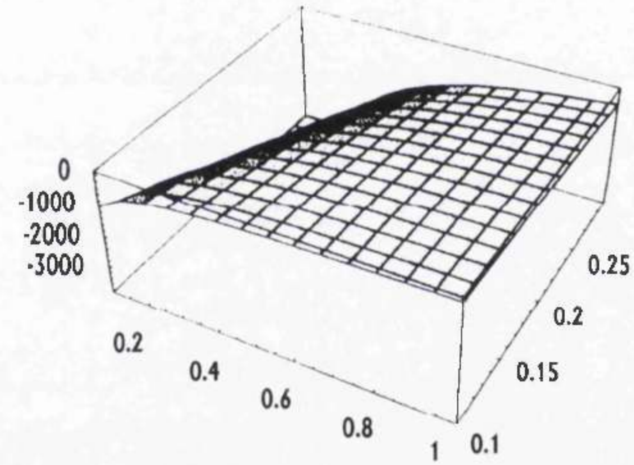
0
-1000
-2000
-3000
0.2
0.4
0.6
0.8
1
0.1
0.15
0.2
0.25

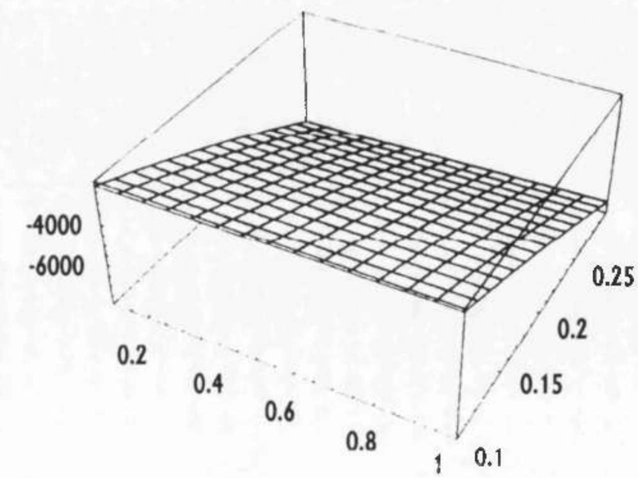
-4000
-6000
0.2
0.4
0.6
0.8
1
0.1
0.15
0.2
0.25

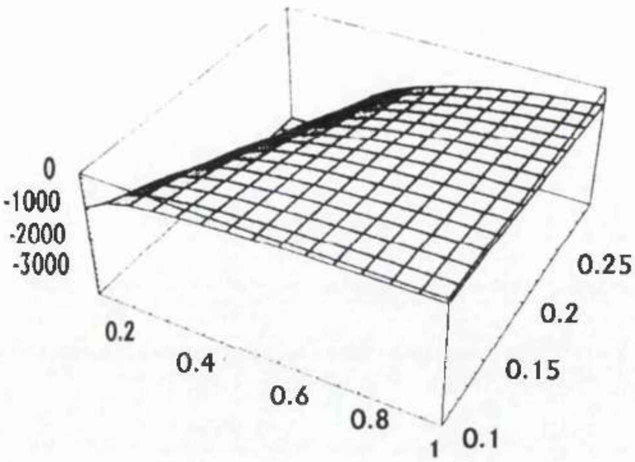
0
-1000
-2000
-3000
0.2
0.4
0.6
0.8
1
0.1
0.15
0.2
0.25

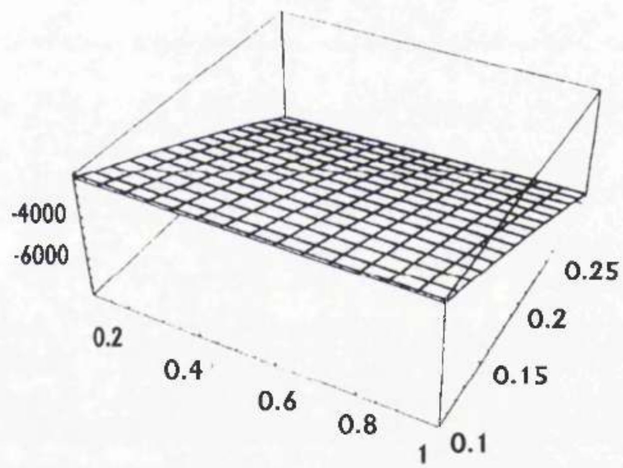
-4000
-6000
0.2
0.4
0.6
0.8
1
0.1
0.15
0.2
0.25

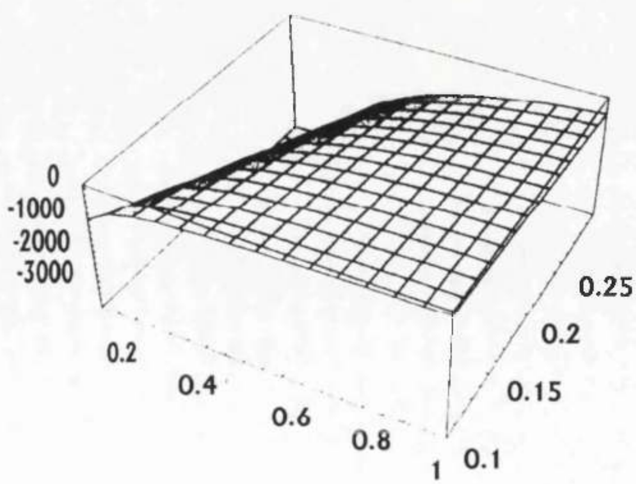
0
-1000
-2000
-3000
0.2
0.4
0.6
0.8
1
0.1
0.15
0.2
0.25

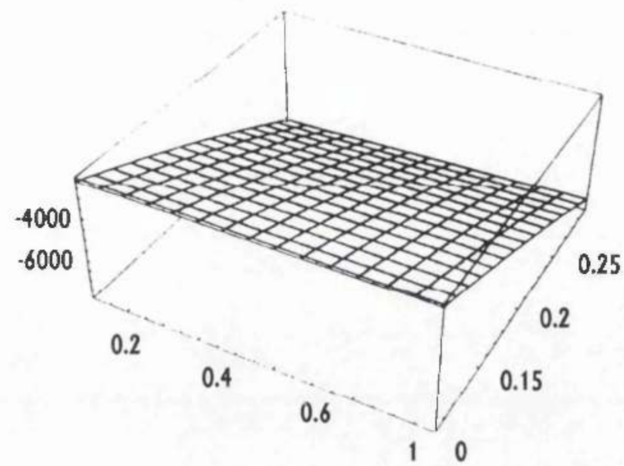
-4000
-6000
0.2
0.4
0.6
1
0
0.15
0.2
0.25

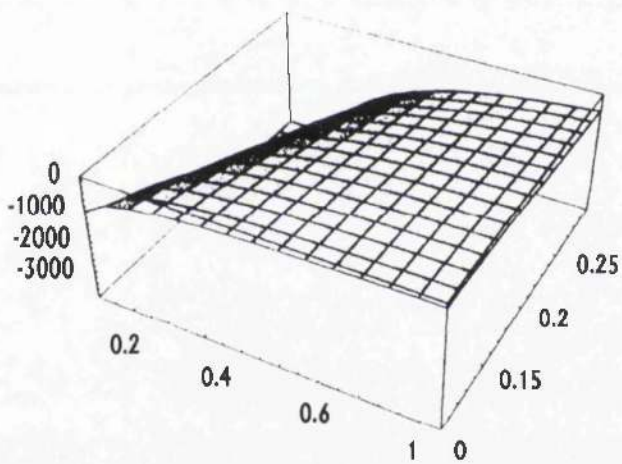
0
-1000
-2000
-3000
0.2
0.4
0.6
1
0
0.15
0.2
0.25

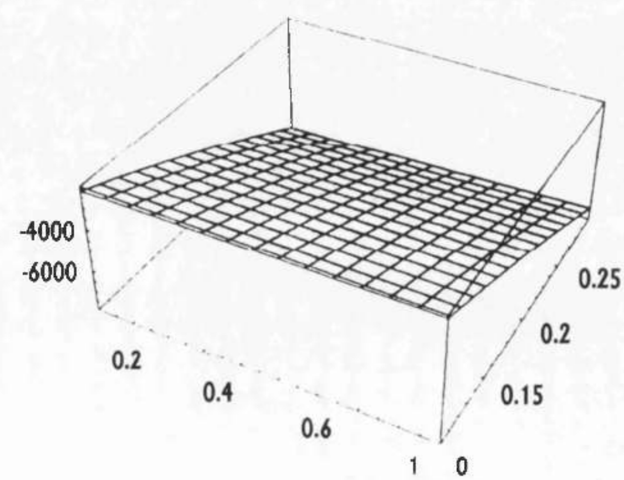
-4000
-6000
0.2
0.4
0.6
1
0
0.15
0.2
0.25

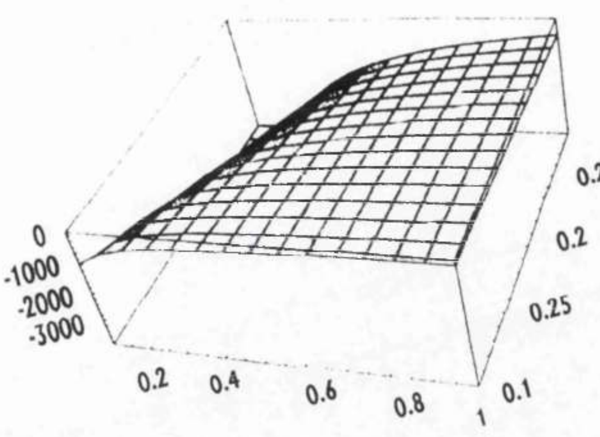
0
-1000
-2000
-3000
0.2
0.4
0.6
0.8
1
0.1
0.25
0.2
0.25

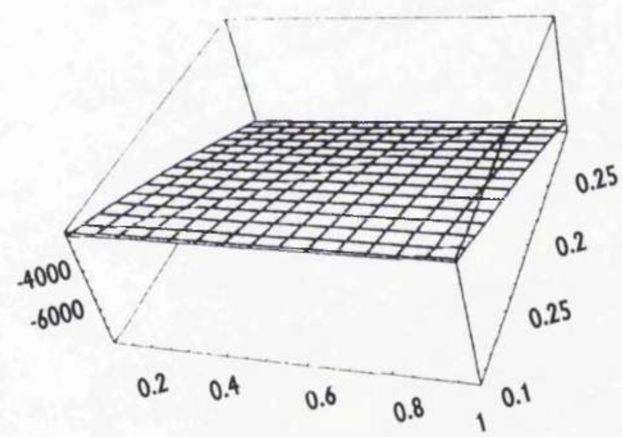
-4000
-6000
0.2
0.4
0.6
0.8
1
0.1
0.25
0.2
0.25

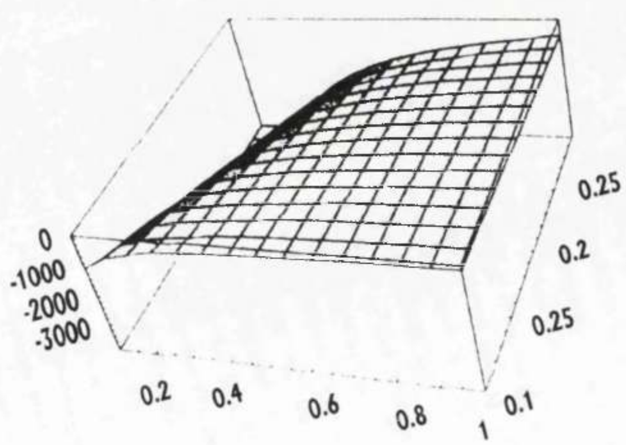
0
-1000
-2000
-3000
0.2
0.4
0.6
0.8
1
0.1
0.25
0.2
0.25

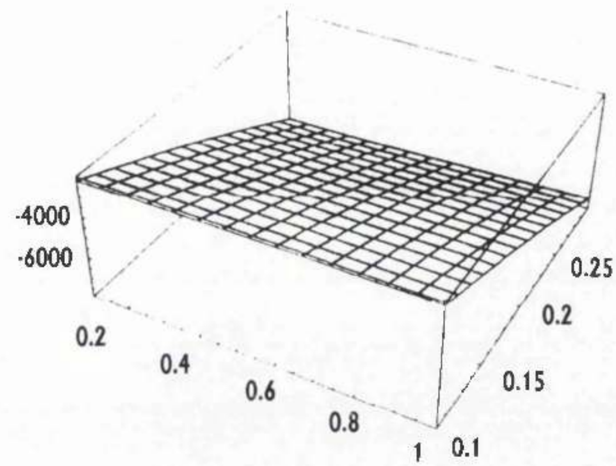
-4000
-6000
0.2
0.4
0.6
0.8
1
0.1
0.15
0.2
0.25

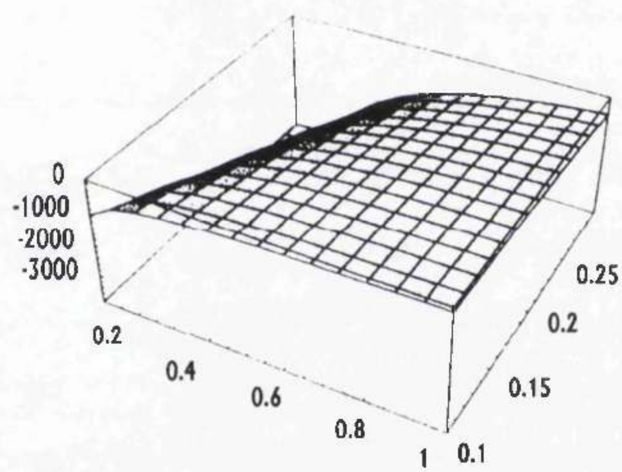
0
-1000
-2000
-3000
0.2
0.4
0.6
0.8
1
0.1
0.15
0.2
0.25

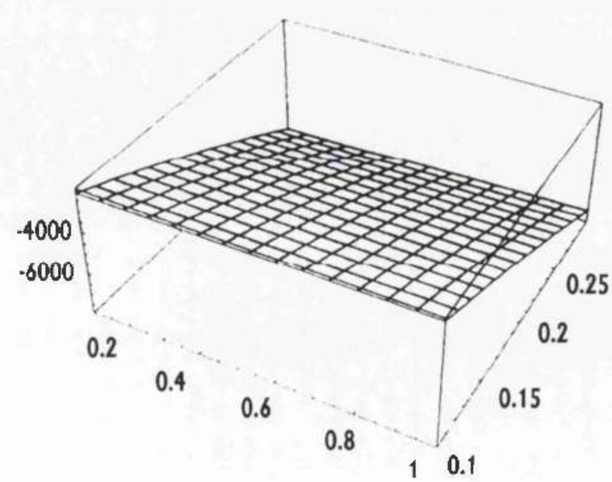
-4000
-6000
0.2
0.4
0.6
0.8
1
0.1
0.15
0.2
0.25

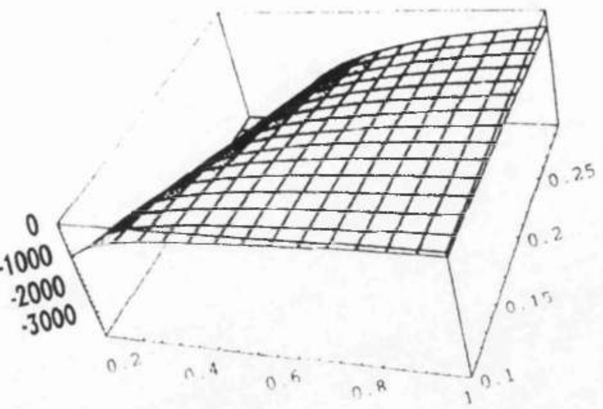
0
-1000
-2000
-3000
0.2
0.4
0.6
0.8
1
0.1
0.15
0.2
0.25

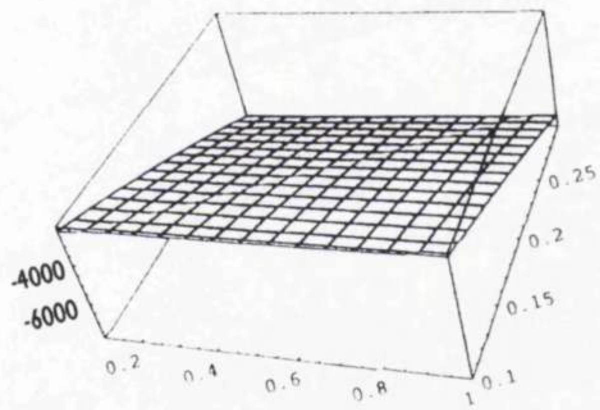
-4000
-6000
0.2
0.4
0.6
0.8
1
0.1
0.15
0.2
0.25

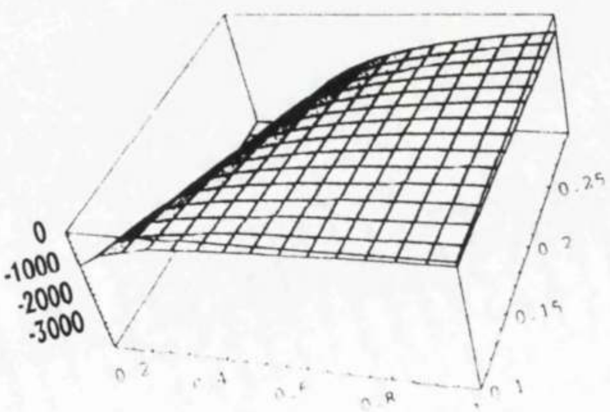
0
-1000
-2000
-3000
0.2
0.8
0.15
0.2
0.25

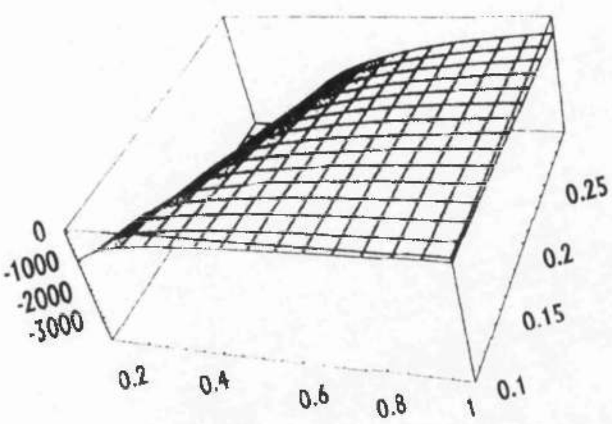
0
-1000
-2000
-3000
0.2
0.4
0.6
0.8
1
0.1
0.15
0.2
0.25

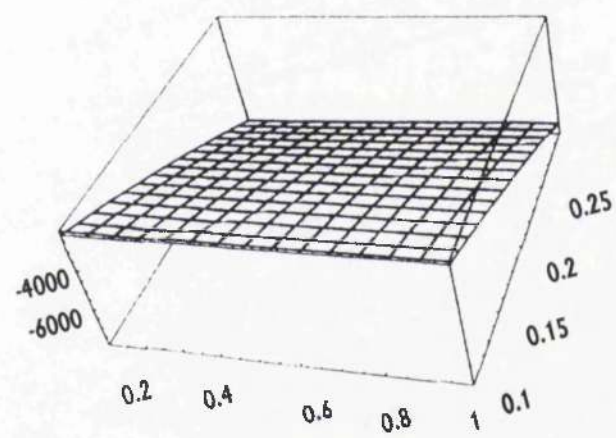
-4000
-6000
0.2
0.4
0.6
0.8
1
0.1
0.15
0.2
0.25

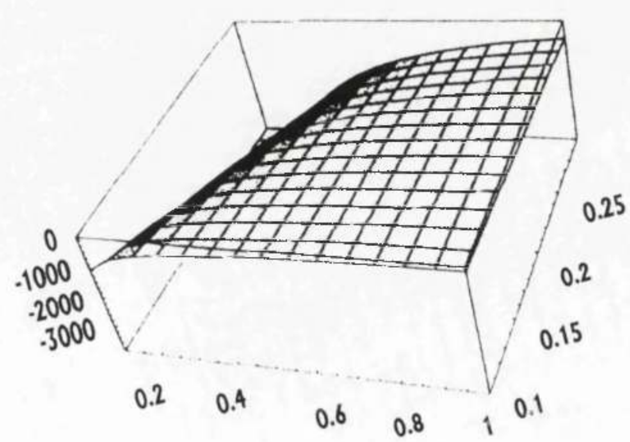
0
-1000
-2000
-3000
0.2
0.4
0.6
0.8
1
0.1
0.15
0.2
0.25

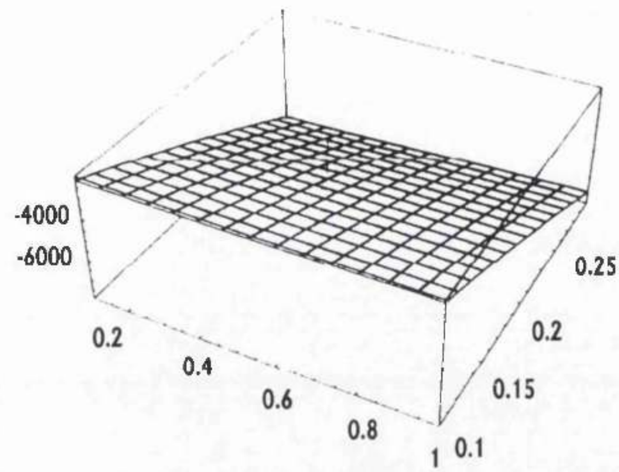
-4000
-6000
0.2
0.4
0.6
0.8
1
0.1
0.15
0.2
0.25
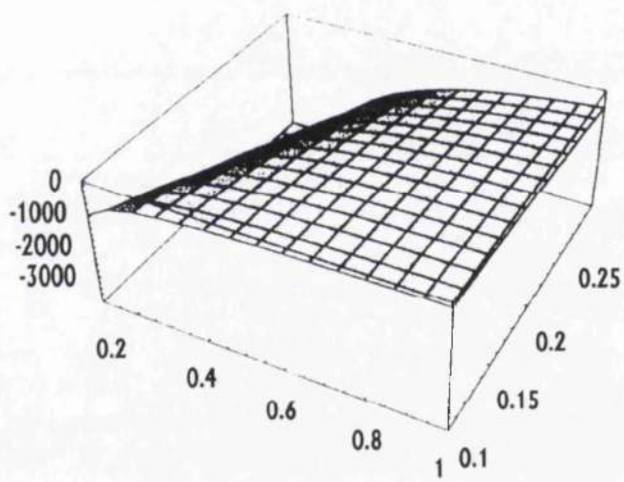
0
-1000
-2000
-3000
0.2
0.4
0.6
0.8
1
0.1
0.15
0.2
0.25
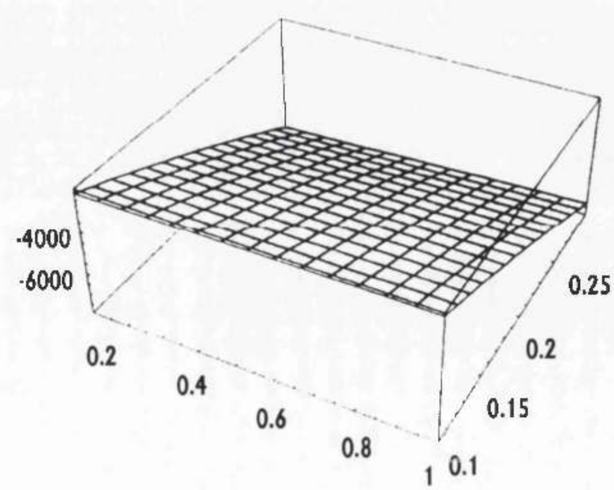
-4000
-6000
0.2
0.4
0.6
0.8
1
0.1
0.15
0.2
0.25

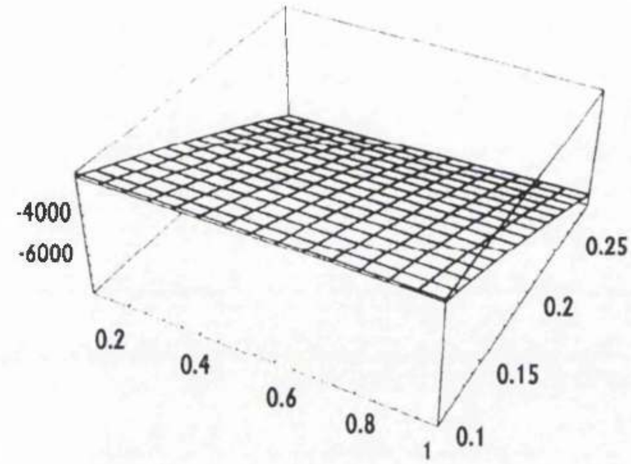
-4000
-6000
0.2
0.4
0.6
0.8
1
0.1
0.15
0.2
0.25

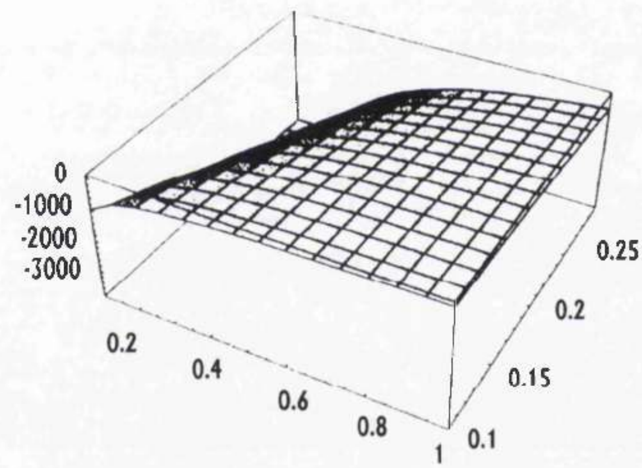
0
-1000
-2000
-3000
0.2
0.4
0.6
0.8
1
0.1
0.15
0.2
0.25

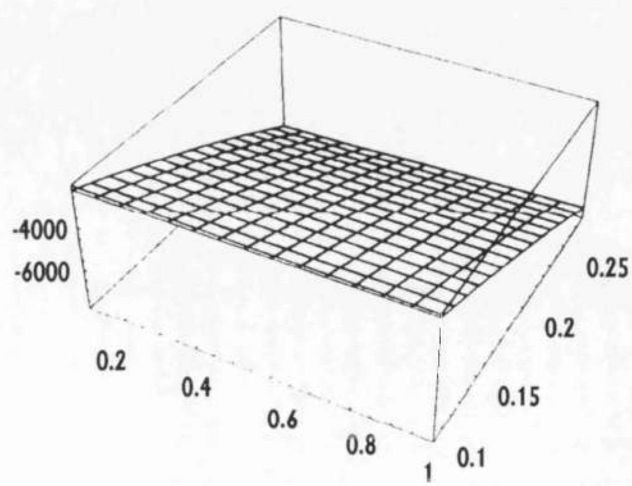
-4000
-6000
0.2
0.4
0.6
0.8
1
0.1
0.15
0.2
0.25

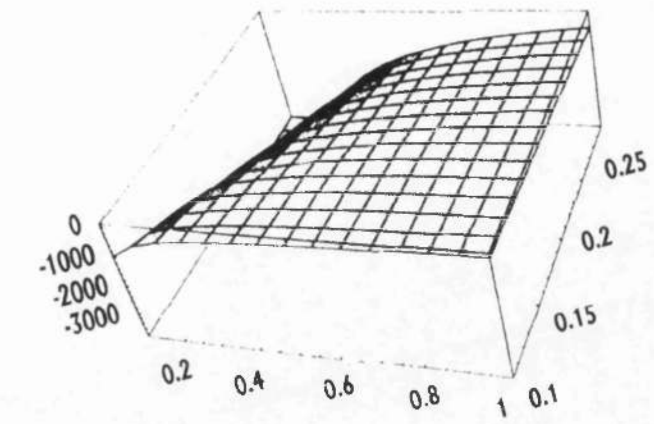
0
-1000
-2000
-3000
0.2
0.4
0.6
0.8
1
0.1
0.15
0.2
0.25

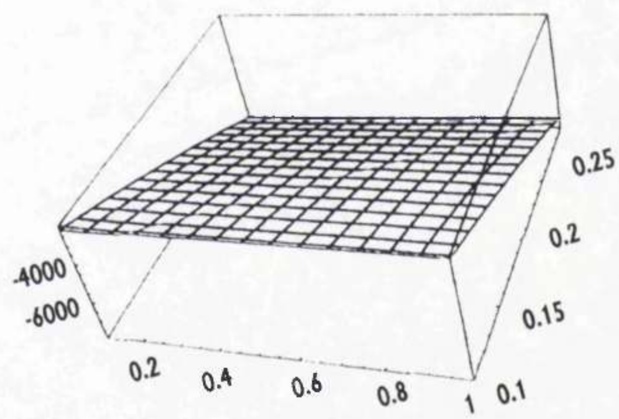
-4000
-6000
0.2
0.4
0.6
0.8
1
0.1
0.15
0.2
0.25

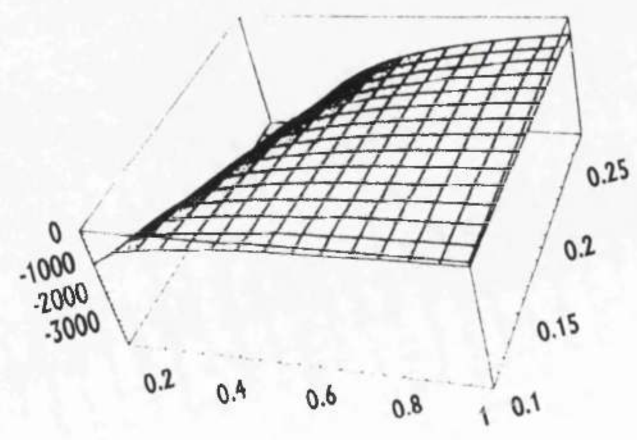
0
-1000
-2000
-3000
0.2
0.4
0.6
0.8
1
0.1
0.15
0.2
0.25

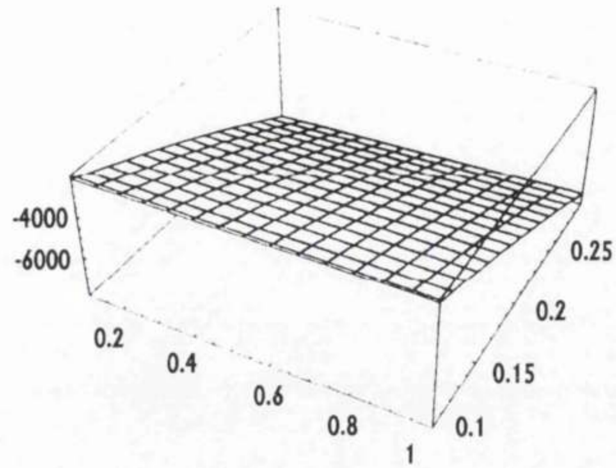
-4000
-6000
0.2
0.4
0.6
0.8
1
0.1
0.15
0.2
0.25

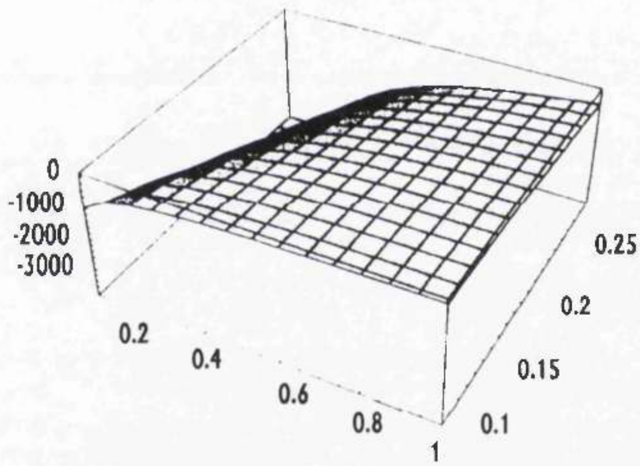
0
-1000
-2000
-3000
0.2
0.4
0.6
0.8
1
0.1
0.15
0.2
0.25

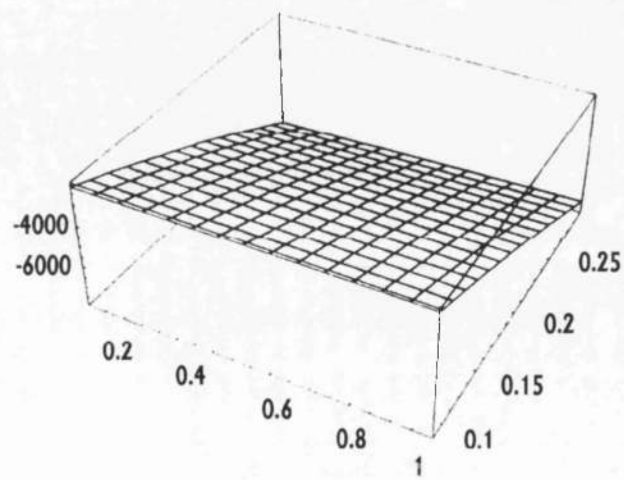
-4000
-6000
0.2
0.4
0.6
0.8
1
0.1
0.15
0.2
0.25

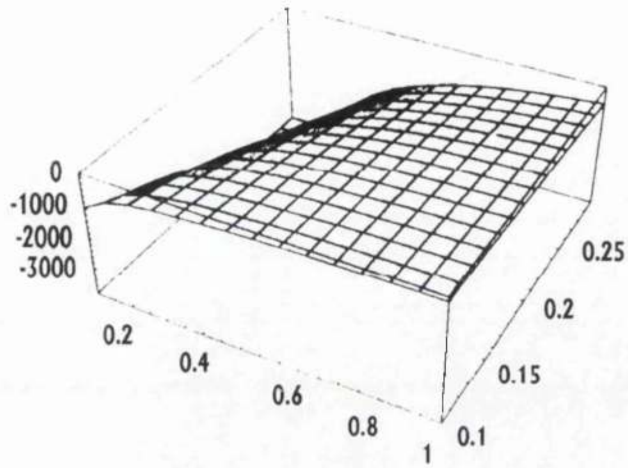
0
-1000
-2000
-3000
0.2
0.4
0.6
0.8
1
0.25
0.2
0.15
0.1

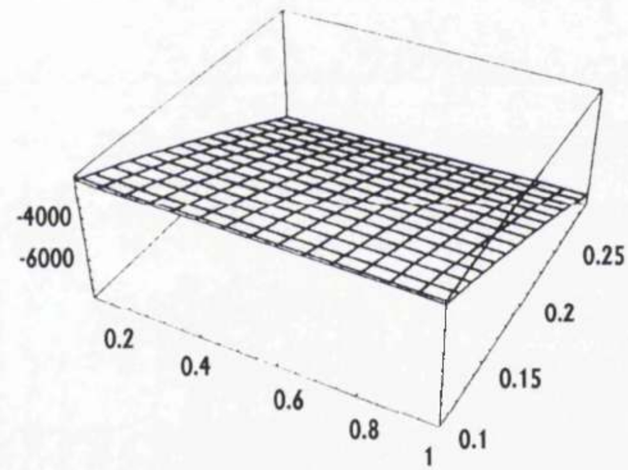
-4000
-6000
0.2
0.4
0.6
0.8
1
0.25
0.2
0.15
0.1

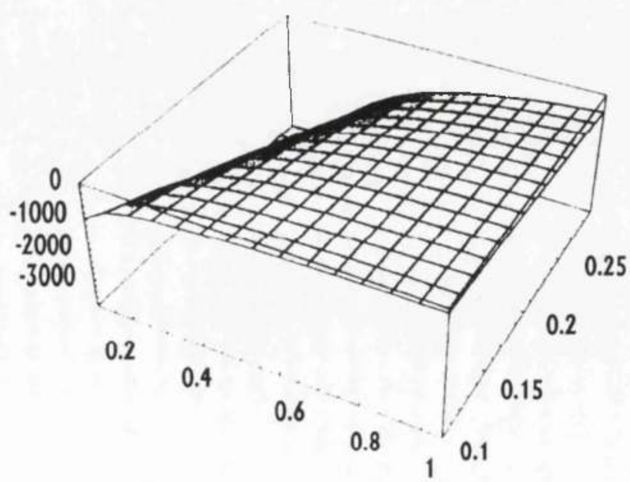
0
-1000
-2000
-3000
0.2
0.4
0.6
0.8
1
0.25
0.2
0.15
0.1

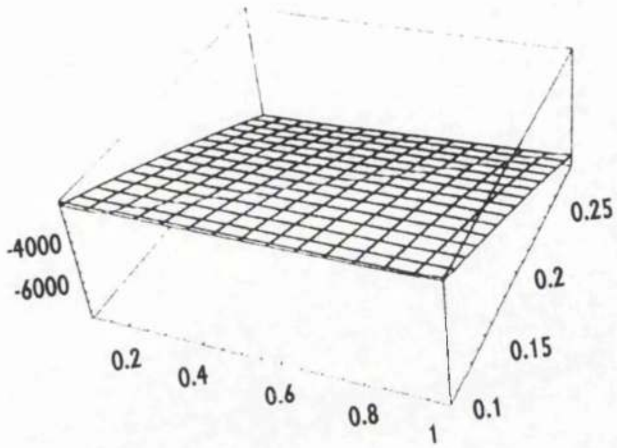
-4000
-6000
0.2
0.4
0.6
0.8
1
0.1
0.15
0.2
0.25

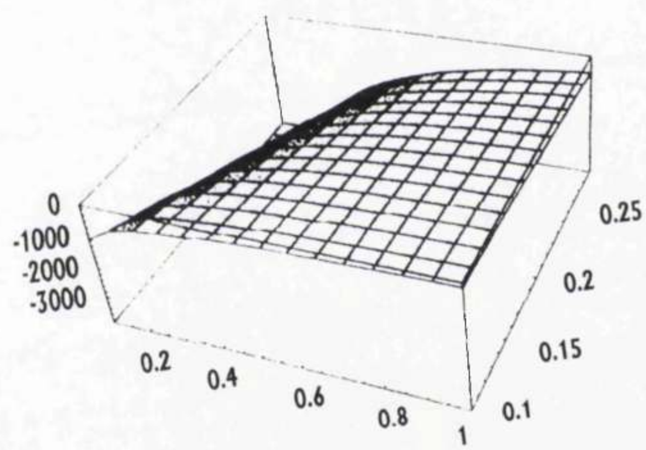
0
-1000
-2000
-3000
0.2
0.4
0.6
0.8
1
0.1
0.15
0.2
0.25

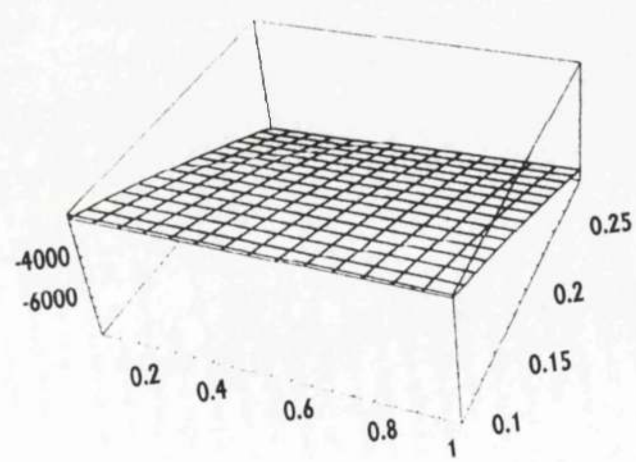
-4000
-6000
0.2
0.4
0.6
0.8
1
0.1
0.15
0.2
0.25

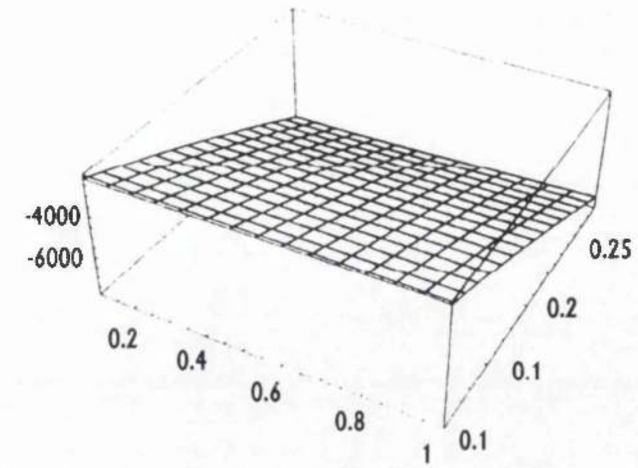
-4000
-6000
0.2
0.4
0.6
0.8
1
0.25
0.2
0.1
0.1

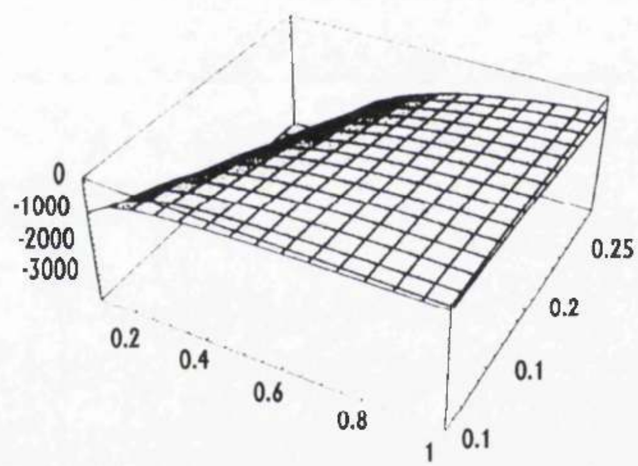
0
-1000
-2000
-3000
0.2
0.4
0.6
0.8
1
0.25
0.2
0.1
0.1

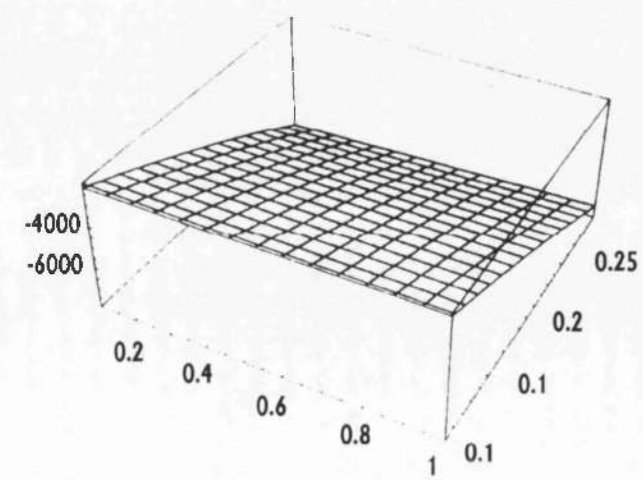
-4000
-6000
0.2
0.4
0.6
0.8
1
0.25
0.2
0.1
0.1

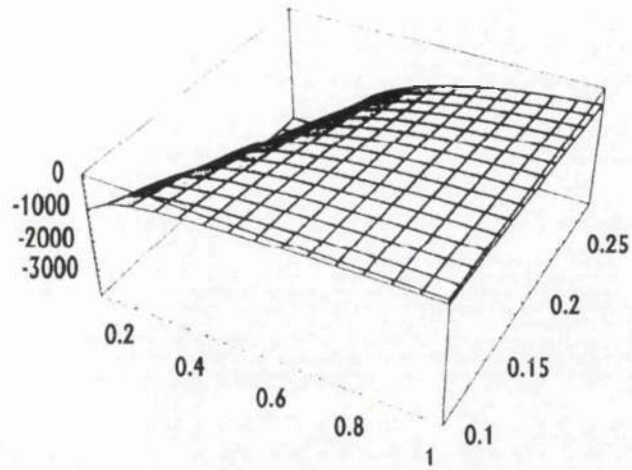
0
-1000
-2000
-3000
0.2
0.4
0.6
0.8
1
0.1
0.15
0.2
0.25

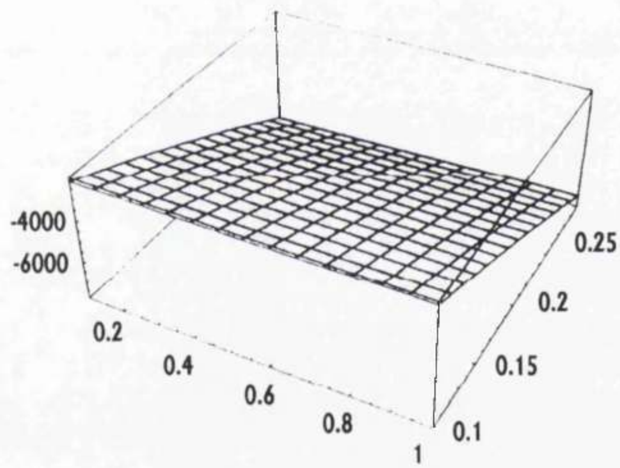
-4000
-6000
0.2
0.4
0.6
0.8
1
0.1
0.15
0.2
0.25

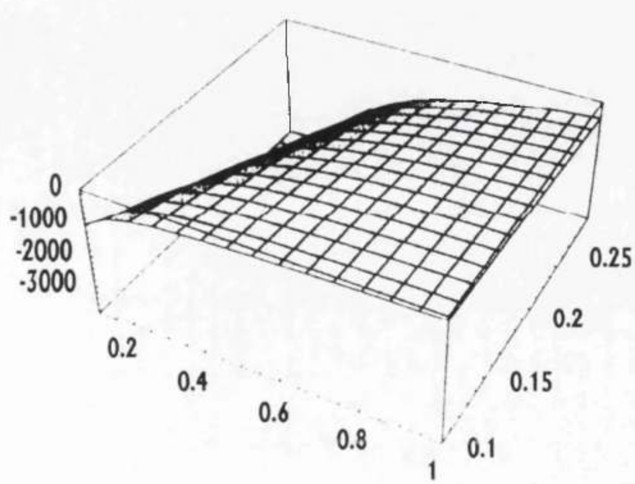
0
-1000
-2000
-3000
0.2
0.4
0.6
0.8
1
0.1
0.15
0.2
0.25

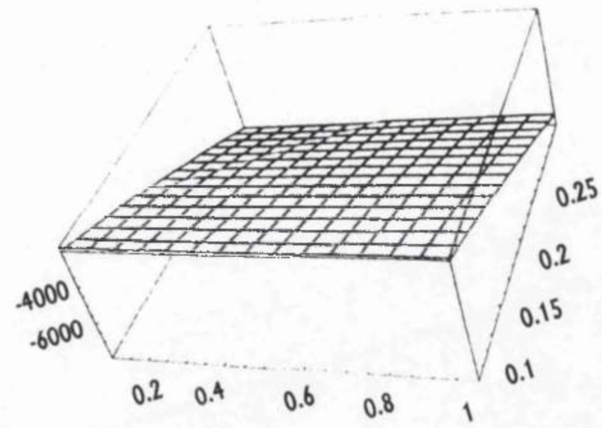
-4000
-6000
0.2
0.4
0.6
0.8
1
0.1
0.15
0.2
0.25

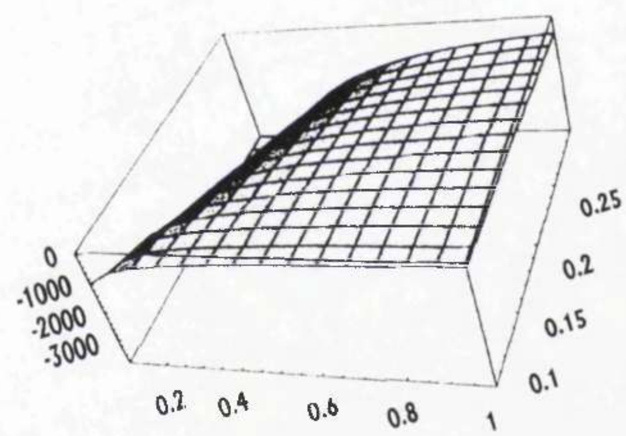
0
-1000
-2000
-3000
0.2
0.4
0.6
0.8
1
0.1
0.15
0.2
0.25

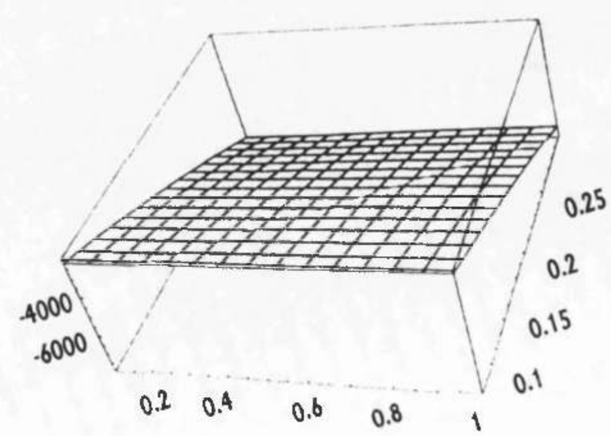
-4000
-6000
0.2
0.4
0.6
0.8
1
0.1
0.15
0.2
0.25

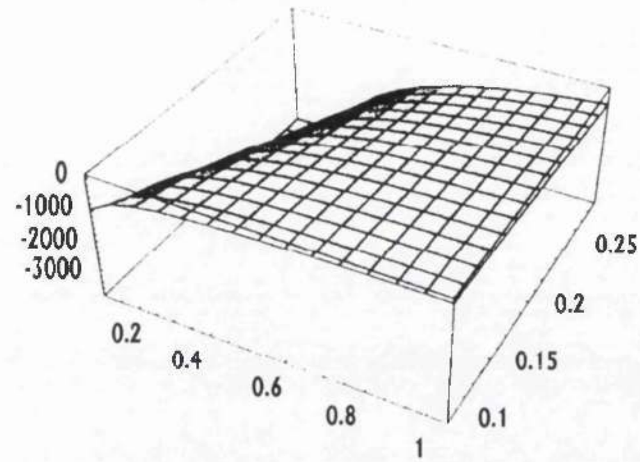
0
-1000
-2000
-3000
0.2
0.4
0.6
0.8
1
0.1
0.15
0.2
0.25

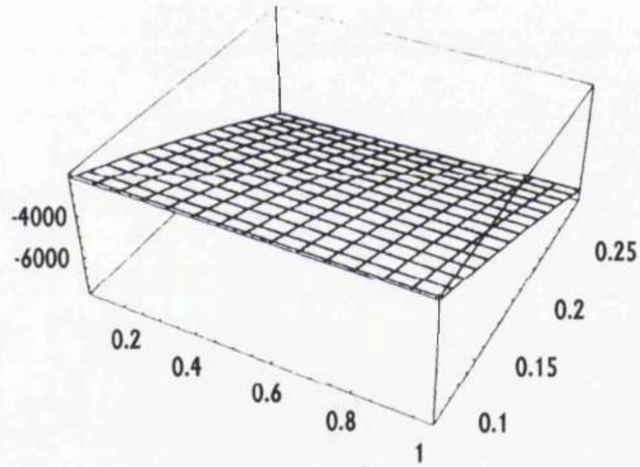
-4000
-6000
0.2
0.4
0.6
0.8
1
0.1
0.15
0.2
0.25

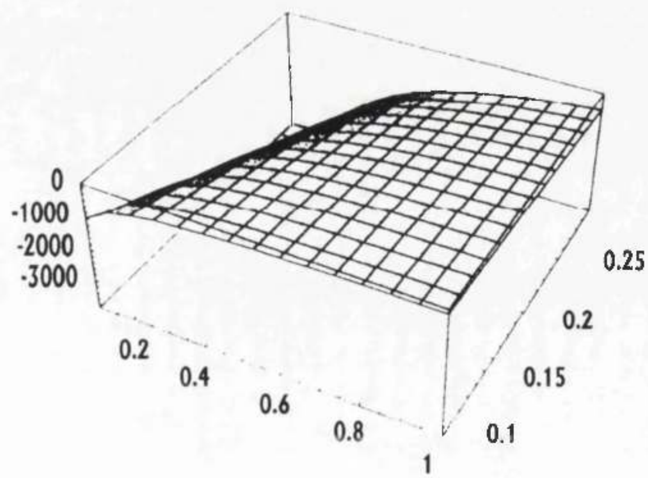
0
-1000
-2000
-3000
0.2
0.4
0.6
0.8
1
0.1
0.15
0.2
0.25

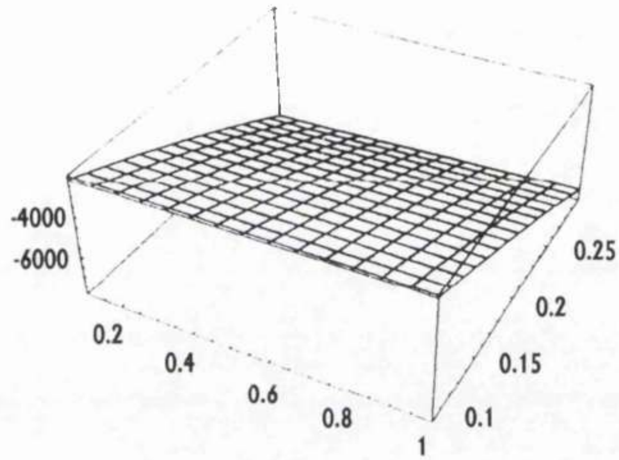

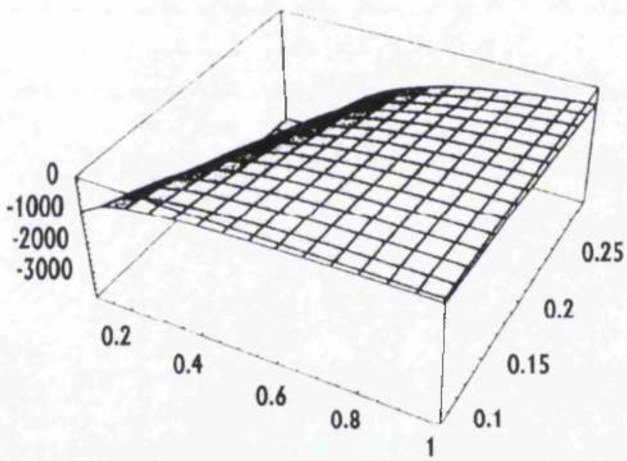

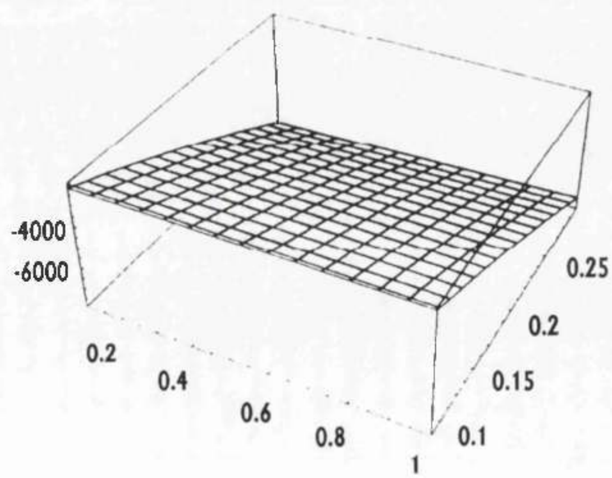

In (62)

s = 0.2

Out (62) = 0.2

D

SOURCE AND SINK WITH WAKE GIVING LIFT AND DRAG

```
In(63):- Do(
  Plot3D[Im[Residue[
      (D[(u z - u s (Log[z - c] - 0.9 Log[z + c] + Log[z - c + 2 h I] - 0.9 Log[z + c + 2 h I])),
         x]) ^ 2
      , {r, c}]], {h, 0.1, 1}, {s, 0.1, 0.3}]
   Plot3D[Re[Residue[
      (D[(u z - u s (Log[z - c] - 0.9 Log[z + c] + Log[z - c + 2 h I] - 0.9 Log[z + c + 2 h I])),
         x]) ^ 2
      , {r, c}]], {h, 0.1, 1}, {s, 0.1, 0.3}], {h, 0.1, 1, 0.1}]
```

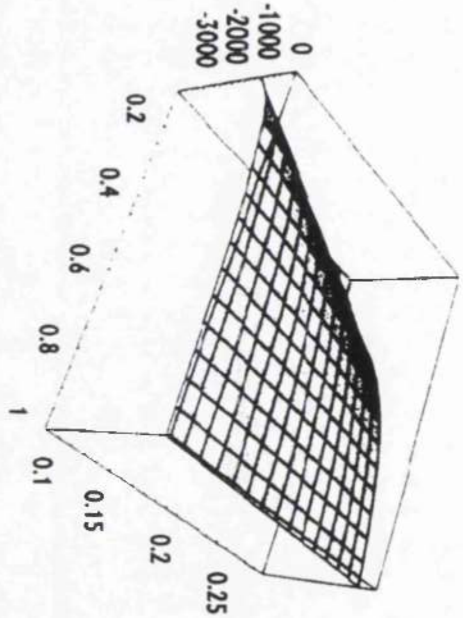

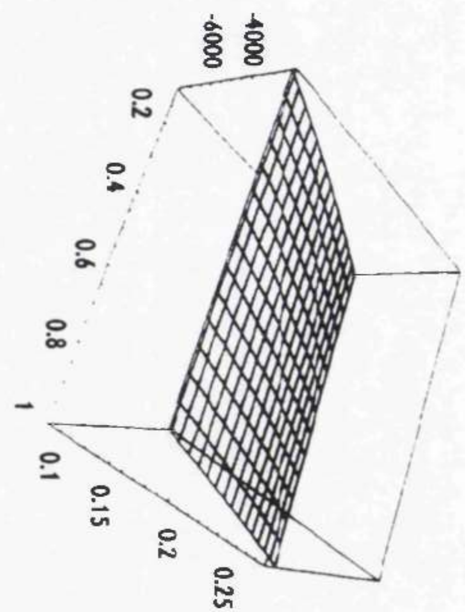

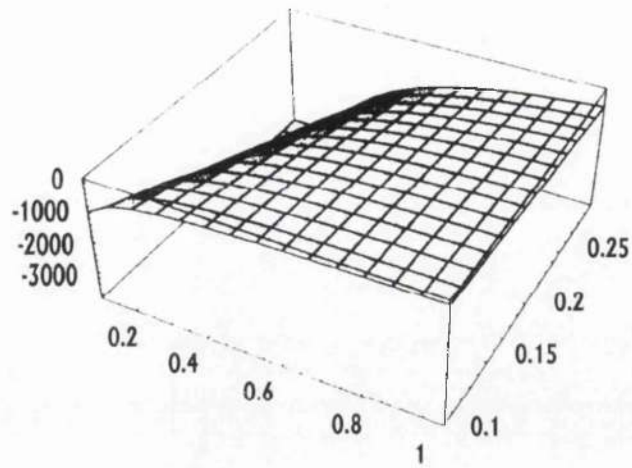
0
-1000
-2000
-3000
0.2
0.4
0.6
0.8
1
0.1
0.15
0.2
0.25

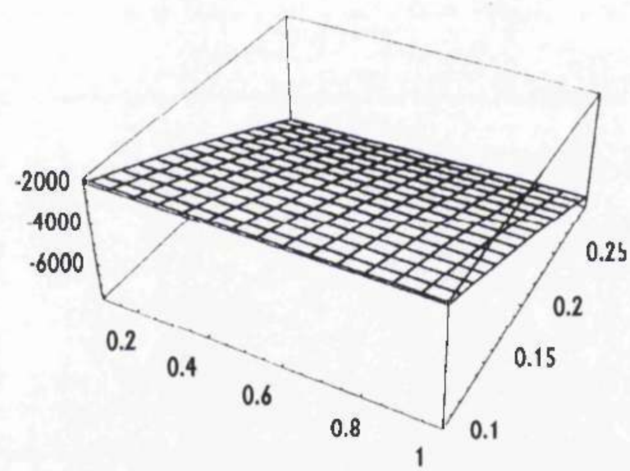
-2000
-4000
-6000
0.2
0.4
0.6
0.8
1
0.1
0.15
0.2
0.25

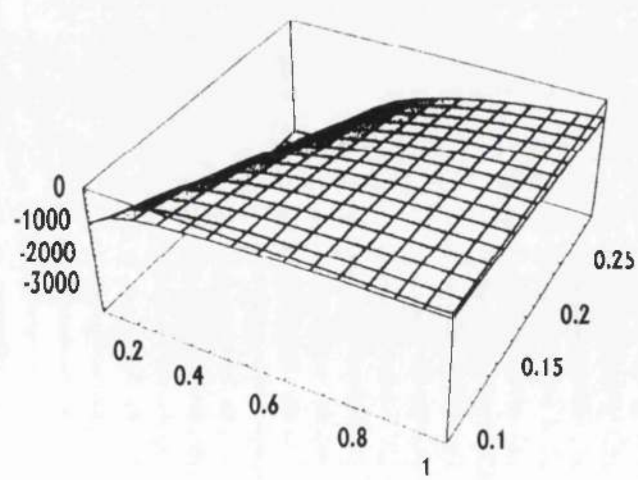
0
-1000
-2000
-3000
0.2
0.4
0.6
0.8
1
0.1
0.15
0.2
0.25

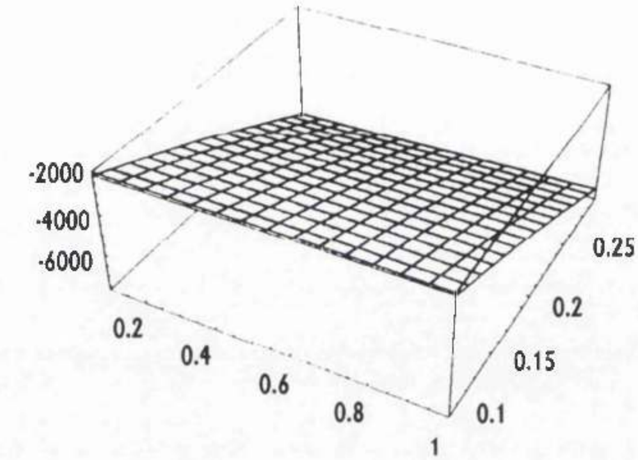
-2000
-4000
-6000
0.2
0.4
0.6
0.8
1
0.1
0.15
0.2
0.25

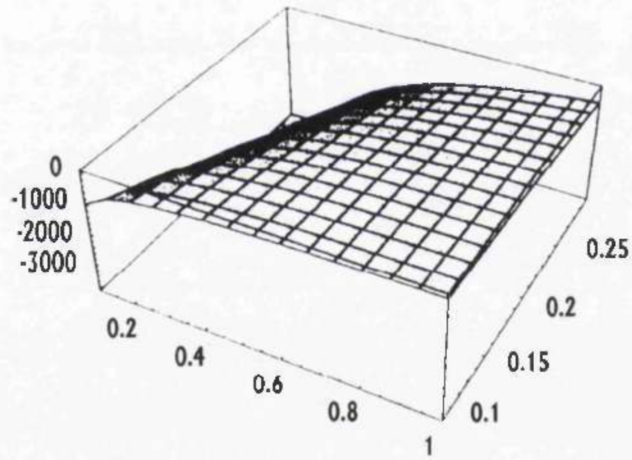
0
-1000
-2000
-3000
0.2
0.4
0.6
0.8
1
0.1
0.15
0.2
0.25

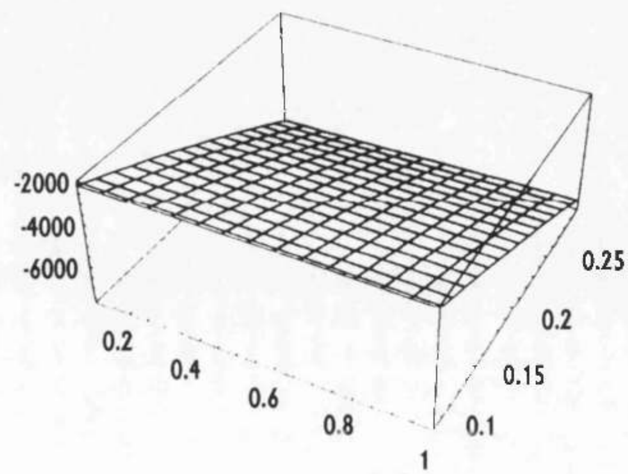
-2000
-4000
-6000
0.2
0.4
0.6
0.8
1
0.1
0.15
0.2
0.25

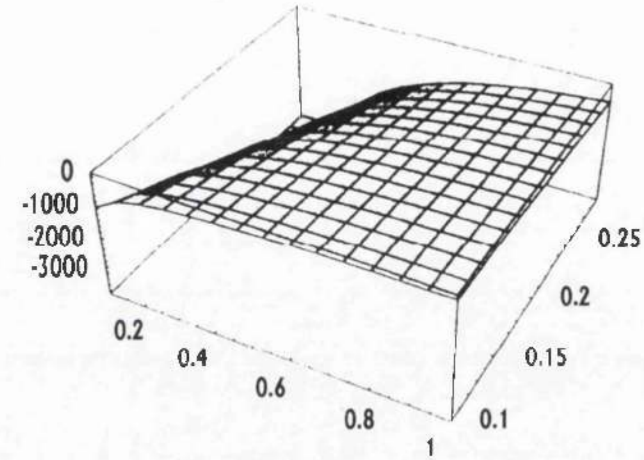
0
-1000
-2000
-3000
0.2
0.4
0.6
0.8
1
0.1
0.15
0.2
0.25

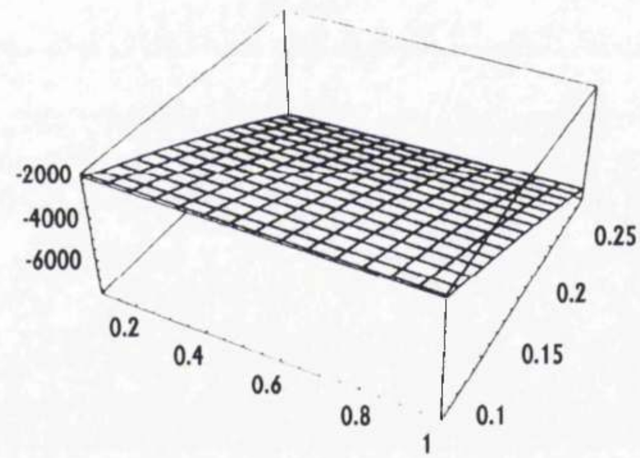
-2000
-4000
-6000
0.2
0.4
0.6
0.8
1
0.1
0.15
0.2
0.25

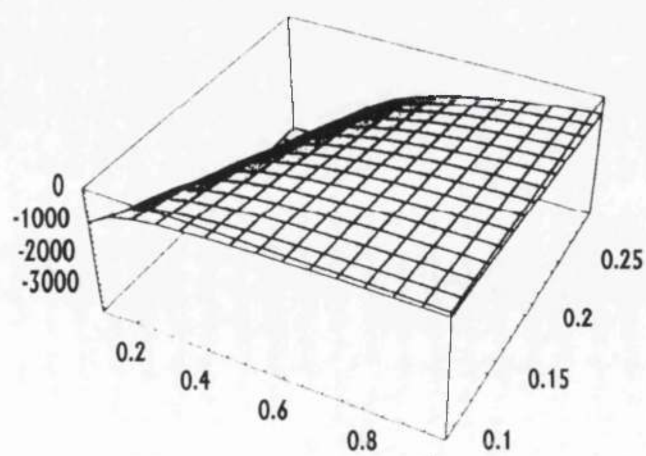
0
-1000
-2000
-3000
0.2
0.4
0.6
0.8
1
0.1
0.15
0.2
0.25

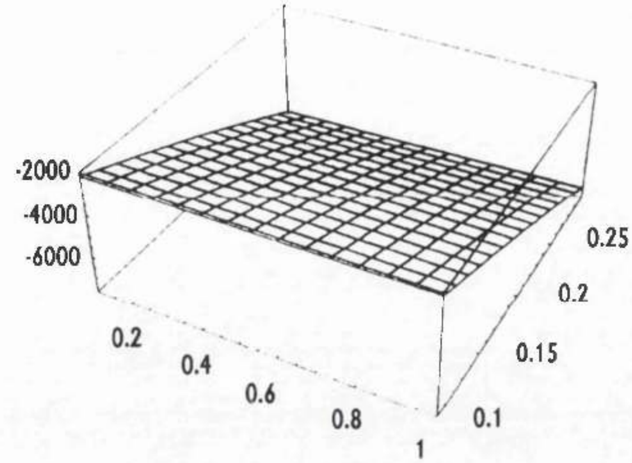
-2000
-4000
-6000
0.25
0.2
0.15
0.1
0.2
0.4
0.6
0.8
1

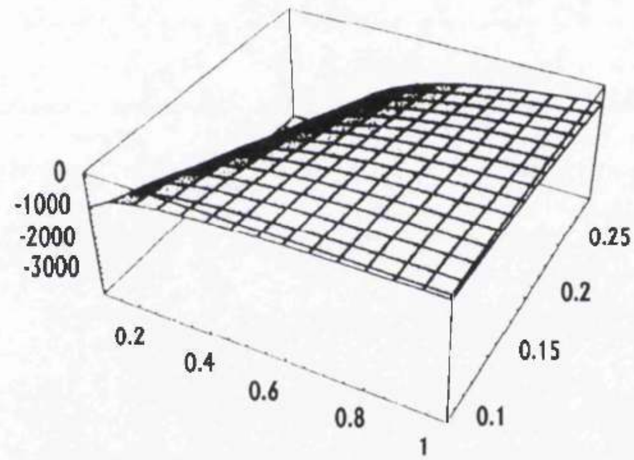
0
-1000
-2000
-3000
0.25
0.2
0.15
0.1
0.2
0.4
0.6
0.8
1

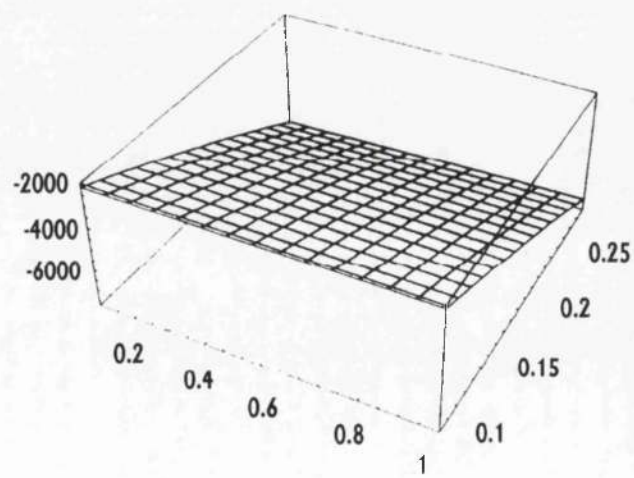
-2000
-4000
-6000
0.25
0.2
0.15
0.1
0.2
0.4
0.6
0.8
1

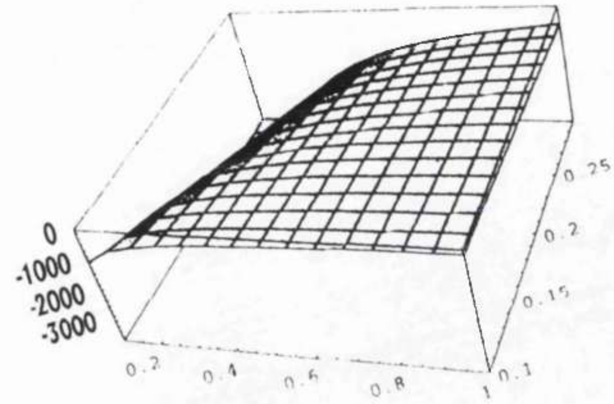
0
-1000
-2000
-3000
0.2
0.4
0.6
0.8
1
0.1
0.15
0.2
0.25

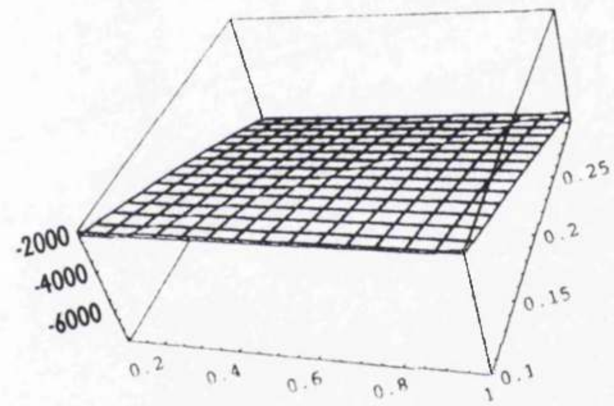
-2000
-4000
-6000
0.2
0.4
0.6
0.8
1
0.1
0.15
0.2
0.25

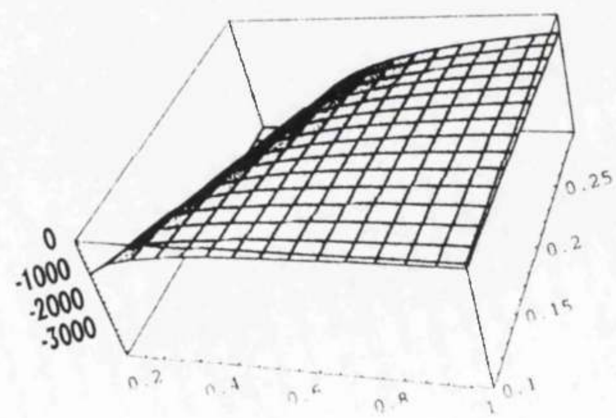
0
-1000
-2000
-3000
0.2
0.8
1
0.1
0.15
0.2
0.25

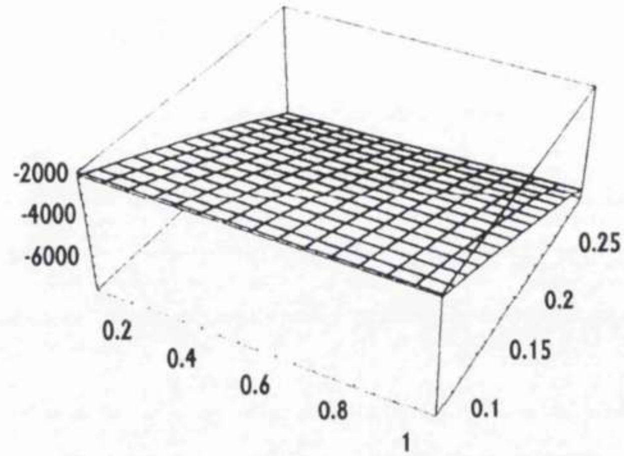
-2000
-4000
-6000
0.2
0.4
0.6
0.8
1
0.1
0.15
0.2
0.25

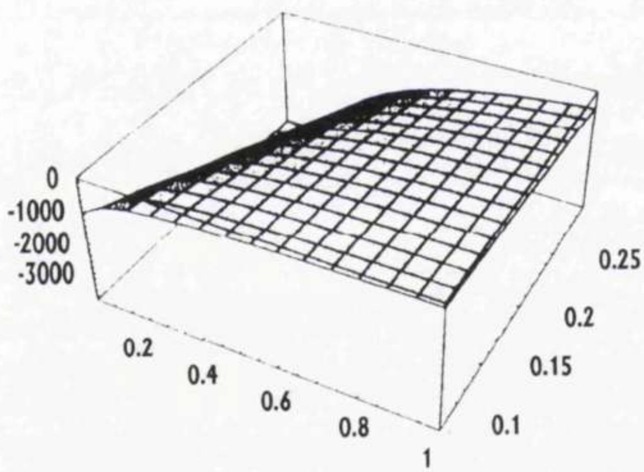
0
-1000
-2000
-3000
0.2
0.4
0.6
0.8
1
0.1
0.15
0.2
0.25

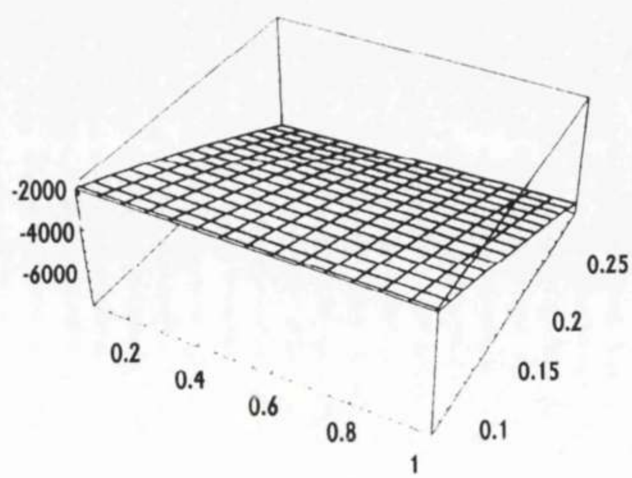
-2000
-4000
-6000
0.2
0.4
0.6
0.8
1
0.1
0.15
0.2
0.25